CANADIAN THESES ON MICROFICHE

I.S.B.N.

THESES CANADIENNES SUR MICROFICHE

National Library of Canada
Collections Development Branch

Canadian Theses on
Microfiche Service

Ottawa, Canada
K1A 0N4

Bibliothèque nationale du Canada
Direction du développement des collections

Service des thèses canadiennes
sur microfiche

NOTICE

The quality of this microfiche is heavily dependent upon the quality of the original thesis submitted for microfilming. Every effort has been made to ensure the highest quality of reproduction possible.

If pages are missing, contact the university which granted the degree.

Some pages may have indistinct print especially if the original pages were typed with a poor typewriter ribbon or if the university sent us a poor photocopy.

Previously copyrighted materials (journal articles, published tests, etc.) are not filmed.

Reproduction in full or in part of this film is governed by the Canadian Copyright Act, R.S.C. 1970, c. C-30. Please read the authorization forms which accompany this thesis.

THIS DISSERTATION
HAS BEEN MICROFILMED
EXACTLY AS RECEIVED

AVIS

La qualité de cette microfiche dépend grandement de la qualité de la thèse soumise au microfilmage. Nous avons tout fait pour assurer une qualité supérieure de reproduction.

S'il manque des pages, veuillez communiquer avec l'université qui a conféré le grade.

La qualité d'impression de certaines pages peut laisser à désirer, surtout si les pages originales ont été dactylographiées à l'aide d'un ruban usé ou si l'université nous a fait parvenir une photocopie de mauvaise qualité.

Les documents qui font déjà l'objet d'un droit d'auteur (articles de revue, examens publiés, etc.) ne sont pas microfilmés.

La reproduction, même partielle, de ce microfilm est soumise à la Loi canadienne sur le droit d'auteur, SRC 1970, c. C-30. Veuillez prendre connaissance des formules d'autorisation qui accompagnent cette thèse.

LA THÈSE A ÉTÉ
MICROFILMÉE TELLE QUE
NOUS L'AVONS REÇUE

NL-339 (r. 82/08)

Canada

National Library of Canada
Canadian Theses Division
Ottawa, Canada
K1A 0N4

Bibliothèque nationale du Canada
Division des thèses canadiennes

0-315-05962-1

53882

PERMISSION TO MICROFILM — AUTORISATION DE MICROFILMER

- Please print or type — Écrire en lettres moulées ou dactylographier

Full Name of Author — Nom complet de l'auteur
JOHN HAK-KEUNG CHOI

Date of Birth — Date de naissance
SEPT. 28, 1951

Country of Birth — Lieu de naissance
HONG KONG

Permanent Address — Résidence fixe
1006, 11147-82 AVE
EDMONTON

Title of Thesis — Titre de la thèse
Reactions of CCl($X^2\Pi$) with Alkynes, Silanes, Cyclic and Heterocyclic Compounds

University — Université
UNIVERSITY OF ALBERTA, EDMONTON

Degree for which thesis was presented — Grade pour lequel cette thèse fut présentée
Ph.D.

Year this degree conferred — Année d'obtention de ce grade
1981

Name of Supervisor — Nom du directeur de thèse
Dr. O.P. Strausz

Permission is hereby granted to the NATIONAL LIBRARY OF CANADA to microfilm this thesis and to lend or sell copies of the film.

The author reserves other publication rights, and neither the thesis nor extensive extracts from it may be printed or otherwise reproduced without the author's written permission.

L'autorisation est, par la présente, accordée à la BIBLIOTHÈQUE NATIONALE DU CANADA de microfilmer cette thèse et de prêter ou de vendre des exemplaires du film.

L'auteur se réserve les autres droits de publication; ni la thèse ni de longs extraits de celle-ci ne doivent être imprimés ou autrement reproduits sans l'autorisation écrite de l'auteur.

Date
Oct 14, 1981

Signature
John Choi

NL-91 (4/77)

THE UNIVERSITY OF ALBERTA

Reactions of CCl($X^2\Pi$) with Alkynes, Silanes, Cyclic and Heterocyclic Compounds

by

© John H. K. Choi

A THESIS

SUBMITTED TO THE FACULTY OF GRADUATE STUDIES AND RESEARCH
IN PARTIAL FULFILMENT OF THE REQUIREMENTS FOR THE DEGREE
OF DOCTOR OF PHILOSOPHY

DEPARTMENT OF CHEMISTRY

EDMONTON, ALBERTA

FALL 1981

THE UNIVERSITY OF ALBERTA

RELEASE FORM

NAME OF AUTHOR John H. K. Choi

TITLE OF THESIS Reactions of CCl($X^2\Pi$) with Alkynes, Silanes, Cyclic and Heterocyclic Compounds

DEGREE FOR WHICH THESIS WAS PRESENTED Doctor of Philosophy

YEAR THIS DEGREE GRANTED Fall 1981

Permission is hereby granted to THE UNIVERSITY OF ALBERTA LIBRARY to reproduce single copies of this thesis and to lend or sell such copies for private, scholarly or scientific research purposes only.

The author reserves other publication rights, and neither the thesis nor extensive extracts from it may be printed or otherwise reproduced without the author's written permission.

(SIGNED) ...John Choi...................

PERMANENT ADDRESS:

1006-11147 82 Avenue
Edmonton, Alberta

DATED ...October 5......1981

THE UNIVERSITY OF ALBERTA

FACULTY OF GRADUATE STUDIES AND RESEARCH

The undersigned certify that they have read, and recommend to the Faculty of Graduate Studies and Research, for acceptance, a thesis entitled Reactions of CCl($X^2\Pi$) with Alkynes, Silanes, Cyclic and Heterocyclic Compounds submitted by John H. K. Choi in partial fulfilment of the requirements for the degree of Doctor of Philosophy.

....
O. P. Strausz - Supervisor

P. Kebarle
....
P. Kebarle

Josef Takats
....
J. Takats

Dennis D. Tanner
....
D. D. Tanner

....
J. Gray - Physics

TN Bell
....
T. N. Bell -
External Examiner

Date October 5, 1981

Abstract

Rate constants have been measured for the gas-phase reactions of CCl($X^2\Pi$) with some inorganic compounds, saturated compounds, and representative series of alkynes, silanes, cyclic and heterocyclic compounds.

CCl was generated from the isothermal flash photolysis of dibromochloromethane in the presence of helium. The decay of CCl was monitored by kinetic absorption spectroscopy, by following the (Q_1 0,0) band of the $A^2\Delta \leftarrow X^2\Pi$ system at 277.7 nm. The rate constant, k_1, for the reaction of CCl with a substrate was derived from the increase in the observed decay rate of CCl, in the presence of a reactive substrate, relative to the background decay rate.

CCl is less reactive than CH, and consequently displays more selective behaviour towards the substrates. It is non-reactive towards H_2, primary and secondary C-H bonds, but inserts slowly into tertiary C-H bonds, and perhaps also reacts with C-Cl and N-H bonds.

It is concluded that the principal feature of the reactions with alkynes is cycloadditions to the acetylenic bonds since primary and secondary C-H bonds are relatively inert. The observation that k_1 increases with increasing alkylation of the substrates from $\sim 10^7$ to $\sim 10^{10}$ M^{-1} s^{-1}, and the linear correlation between log k_1 and ionization potential of the substrates, reveal the electrophilic nature of CCl. The few deviations from linearity observed with highly substituted alkynes can be ascribed to steric

hindrance. No isotope effect was detected upon deuteration of acetylene.

Reactions with silanes are, in general, quite rapid (k_1 $\sim$ 10^9 M^{-1} s^{-1}), and appear to be mainly restricted to Si-H bond insertion, since Si-C, Si-F, Si-Cl bonds were found to be non-reactive and reaction with Si-Si bonds is relatively slow. The electrophilic nature of CCl was again revealed in the increase/decrease of k_1 with the electron-donating/withdrawing substituent groups at Si, and in the linear relationship observed between log k_1 and ionization potential of the substrates. The reactivity of the silanes also correlates with other bond parameters such as stretching frequency and hydridic character of the Si-H bond.

A primary isotope effect was observed upon deuteration of the silanes, up to a factor of $\sim$ 2 depending on the reactivity of the Si-H bond.

The presence of the heteroatoms O and S greatly enhances the reactivity of saturated cyclic substrates (k_1 $\sim$ 10^9 M^{-1} s^{-1}) as compared to their inert hydrocarbon analogs. The nature of the interactions with the heteroatoms is still unclear, but probably involves ylide-type intermediates resulting in apparent C-heteroatom bond insertion products.

In general, substituted benzenes are quite reactive (k_1 $\sim$ 10^8 M^{-1} s^{-1}) as are aromatic systems containing heteroatoms (k_1 $\sim$ 10^9 M^{-1} s^{-1}). In the latter case, however, no correlation was observed between log k_1 and ionization potential; this was ascribed to the fact that the overall rate constant comprises two reactions, cycloaddition across the C=C bond, and reaction at the heteroatom site.

The reactivity of CCl is discussed in comparison with that of other electrophilic species such as $CH(X^2\Pi)$, $CBr(X^2\Pi)$, $CH_2(A^1A_1)$, $SiH_2(A^1A_1)$, $S(^3P)$ and $O(^3P)$.

Acknowledgments

The author is deeply grateful to Professor O. P. Strausz for his inspired guidance and constant support throughout the course of this work.

Special thanks are due to Dr. F. C. James for his invaluable assistance, and the members of the photochemistry group for many helpful discussions, especially Mr. A. Jodhan, for technical advice.

It is a pleasure to acknowledge the many services rendered by the staff of the Electronic Shop, especially Mr. E. Feschuk.

The author also thanks Dr. E. M. Lown for assistance in the preparation of this manuscript.

Finally, the assistance of Mr. D. S. Post in the typing of this thesis is much appreciated.

Table of Contents

Chapter Page

I. INTRODUCTION 1

A. CARBYNE CHEMISTRY 2

1. Nature of Carbynes 2

2. Electron Configuration and Term Symbols ..4

3. Transition Spectra 5

4. Generation of Carbynes 12

5. Reactions of Carbynes 27

B. FLASH PHOTOLYSIS 50

1. Flash Spectroscopy 50

2. Kinetic Spectrophotometry 51

C. AIM OF THE PRESENT INVESTIGATION 51

II. EXPERIMENTAL 54

A. APPARATUS 54

1. The Vacuum System 54

2. The Flash Photolysis System 56

3. Miscellaneous 68

B. OPERATIONAL PROCEDURES 73

1. The Vacuum System 73

2. Development of The Plates 75

C. Materials 76

III. RESULTS 83

A. SOURCE 83

B. ABSORPTION SPECTRUM OF $CCl(X^2\Pi)$ 83

C. RELATIONSHIP BETWEEN THE ABSORPTION PEAK

HEIGHT AND THE CCl($X^2\Pi$) CONCENTRATION 85

D. DETERMINATION OF THE BEER-LAMBERT COEFFICIENT γ 87

1. Full Cell Length *versus* Half Cell Length 87

2. Variation of Cell Length 88

E. The CCl($X^2\Pi$) DECAY 91

1. Determination of the Background Decay Rate Constant, k' 91

2. Effects of Flash Energy, Pressure of $CHClBr_2$ and Pressure of He on The Background Decay Rate Constant k' 93

3. Determination of the Pseudo-First Order Decay Rate Constant in the Presence of Substrate, k" 96

4. Determination of the Second Order Rate Constant for the Reaction of CCl with Various Substrates, k_1 97

IV. DISCUSSION 166

A. GENERATION OF CCl($X^2\Pi$) 166

B. REACTION WITH INORGANIC COMPOUNDS AND SOME SATURATED COMPOUNDS 169

C. REACTIONS WITH ALKYNES 174

D. REACTION WITH SILANES 187

E. REACTION WITH CYCLIC AND HETEROCYCLIC COMPOUNDS 205

V. CONCLUSIONS 222

Bibliography 229

Appendix A 240

B 244

List of Tables

Table | Page

I.1 Observed Carbyne Transitions and Their Corresponding Wavelengths in the U.V. Region 7

I.2 Potential Photochemical Sources of Carbynes 14

I.3 Second Order Rate Constants k, for the Reactions of $CH(X^2\Pi)$ 31

I.4 Second Order Rate Constants k, for the Reactions of $CBr(X^2\Pi)$ and $CCl(X^2\Pi)$ with Saturates and Inorganic Compounds 37

I.5 Second Order Rate Constants k, for the Reactions of $CBr(X^2\Pi)$ and $CCl(X^2\Pi)$ with Alkenes and Benzene 40

I.6 Second Order Rate Constants k, for the Reactions of $CBr(X^2\Pi)$ and $CCl(X^2\Pi)$ with Alkynes 41

II.1 Inorganic Compounds and Alkanes 77

II.2 Alkynes 78

II.3 Silanes 79

II.4 Silanes (continued) 80

II.5 Cyclic Compounds 81

II.6 Heterocyclic Compounds 82

III.1 $\gamma k''$ as a Function of Concentration for the Reaction with Hydrogen 99

III.2 $\gamma k''$ as a Function of Concentration for the Reaction with Ammonia 101

III.3 $\gamma k''$ as a Function of Concentration for the Reaction with Methylchloride 104

III.4 $\gamma k''$ as a Function of Concentration for the Reaction with Propane 105

III.5 $\gamma k''$ as a Function of Concentration for the Reaction with *Iso*butane 107

III.6 $\gamma k''$ as a Function of Concentration for

Table Page

the Reaction with Acetylene 110

III.7 $\gamma k''$ as a Function of Concentration for the Reaction with Acetylene-d_2 114

III.8 $\gamma k''$ as a Function of Concentration for the Reaction with Propyne 116

III.9 $\gamma k''$ as a Function of Concentration for the Reaction with 1-Butyne and 2-Butyne 117

III.10 $\gamma k''$ as a Function of Concentration for the Reaction with 1-Pentyne and 2-Pentyne 118

III.11 $\gamma k''$ as a Function of Concentration for the Reaction with 3,3-Dimethyl-1-butyne and 2,2,5,5-Tetramethyl-3-hexyne 119

III.12 $\gamma k''$ as a Function of Concentration for the Reaction with Phenylacetylene 120

III.13 Second Order Rate Constants k_1 for the Reactions with Alkynes 124

III.14 $\gamma k''$ as a Function of Concentration for the Reaction with Silane 125

III.15 $\gamma k''$ as a Function of Concentration for the Reaction with Monomethylsilane and Dimethylsilane 126

III.16 $\gamma k''$ as a Function of Concentration for the Reaction with Trimethylsilane and Tetramethylsilane 127

III.17 $\gamma k''$ as a Function of Concentration for the Reaction with Silane-d_4 and Monomethylsilane-d_3 128

III.18 $\gamma k''$ as a Function of Concentration for the Reaction with Dimethylsilane-d_2 and Trimethylsilane-d_1 129

III.19 $\gamma k''$ as a Function of Concentration for the Reaction with Diethylsilane and Triethylsilane 130

III.20 $\gamma k''$ as a Function of Concentration for the Reaction with Methyldichlorosilane and Dimethylchlorosilane 135

Table Page

III.21 γk" as a Function of Concentration for the Reaction with Trichlorosilane 136

III.22 γk" as a Function of Concentration for the Reaction with Dichlorosilane and Trimethylchlorosilane 137

III.23 γk" as a Function of Concentration for the Reaction with Trimethylfluorosilane 138

III.24 γk" as a Function of Concentration for the Reaction with Dimethyldifluorosilane 139

III.25 γk" as a Function of Concentration for the Reaction with Methyltrifluorosilane 140

III.26 γk" as a Function of Concentration for the Reaction with Disilane and Disilane-d_6 143

III.27 γk" as a Function of Concentration for the Reaction with Hexamethyldisilane and Hexachlorodisilane 144

III.28 Second Order Rate Constants k_1 for the Reactions with Silanes 146

III.29 Second Order Rate Constants k_1 for the Reactions with Halogenated Silanes 147

III.30 Second Order Rate Constants k_1 for the Reactions with Disilanes 148

III.31 γk" as a Function of Concentration for the Reaction with Cyclopentane and Cyclohexane 150

III.32 γk" as a Function of Concentration for the Reaction with Cyclohexene 151

III.33 γk" as a Function of Concentration for the Reaction with 1,3-Cyclohexadiene and 1,4-Cyclohexadiene 152

III.34 γk" as a Function of Concentration for the Reaction with Benzene and Toluene 153

III.35 γk" as a Function of Concentration for the Reaction with Chlorobenzene and

Table Page

Fluorobenzene 154

III.36 $\gamma k''$ as a Function of Concentration for the Reaction with Tetrahydrothiophene and Tetrahydrofuran 157

III.37 $\gamma k''$ as a Function of Concentration for the Reaction with Thiacyclohexane and Pyridine 158

III.38 $\gamma k''$ as a Function of Concentration for the Reaction with Thiophene and Furan 159

III.39 $\gamma k''$ as a Function of Concentration for the Reaction with Pyrrole and 1-Methylpyrrole 160

III.40 Second Order Rate Constants k_1 for the Reactions with Cyclic Compounds 164

III.41 Second Order Rate Constants k_1 for the Reactions with Heterocyclic Compounds 165

IV.1 Second Order Rate Constants k_1 for the Reactions of $CCl(X^2\Pi)$ and $CBr(X^2\Pi)$ with Inorganic Compounds and Some Saturated Compounds 170

IV.2 Second Order Rate Constants for the Reactions of $CBr(X^2\Pi)$, $CCl(X^2\Pi)$, $O(^3P)$ and $S(^3P)$ with Alkynes 175

IV.3 Second Order Rate Constants k_1 for the Reactions of $CCl(X^2\Pi)$, $SiH_2(^1A_1)$, $CH_2(^1A_1)$, CH_3, and H with Silanes 189

IV.4 Second Order Rate Constants, per Si-H Bond, for the Insertion of $CCl(X^2\Pi)$, $SiH_2(^1A_1)$ and $CH_2(^1A_1)$ into Silanes 192

IV.5 Isotope Effects for the Reactions of $CCl(X^2\Pi)$ with Silanes 194

IV.6 Second Order Rate Constants k_1, per Si-H Bond, and Si-H Bond Stretching Frequencies of Silanes 199

List of Figures

Figure Page

I.1 a. Orbital Occupancy of CH b. Back Coordination Effect of Carbyne Substituents 3

I.2 Electron Arrangements Corresponding to the Spectroscopic States Arising from the Ground and the First Excited Electron Configuration of CCl 6

II.1 The Main Vacuum System 55

II.2 The Flash Photolysis System 57

II.3 The Reaction Vessel and the Reflective Housing 59

II.4 The Spectroscopic Flash Lamp 61

II.5 The Littrow Prism and Mounting 65

II.6 The Flash Photolysis System: Circuit Diagram 66

II.7 Oscilloscope Trace 69

II.8 The Baratron Pressure Meter 70

II.9 Schematic Diagram of the Microdensitometer 72

III.1 Absorption Spectrum of $CCl(X^2\Pi)$ 84

III.2 Peak Height of Full Cell Length *versus* Peak Height of Half Cell Length 89

III.3 Ln (Peak Height) *versus* Ln (Cell Length) 90

III.4 Determination of the Background Decay Rate Constant k' 92

III.5 k' *versus* Flash Energy 94

III.6 k' *versus* Pressure of $CHClBr_2$ 95

III.7 Ln PH *versus* Time Delay t for Ammonia 100

III.8 $\gamma k''$ *versus* Concentration for Ammonia 102

III.9 Ln PH *versus* Time Delay t for *Iso*butane 106

Figure Page

III.10 γk" *versus* Concentration for *Iso*butane 108

III.11 Ln PH *versus* Time Delay t for Acetylene 109

III.12 γk" *versus* Concentration for Acetylene 111

III.13 Ln PH *versus* Time Delay t for Acetylene-d_2 113

III.14 γk" *versus* Concentration for Acetylene-d_2 115

III.15 γk" *versus* Concentration for Propyne 121

III.16 γk" *versus* Concentration for (A) 1-Butyne (B) 2-Butyne (C) 1-Pentyne (D) 2-Pentyne 122

III.17 γk" *versus* Concentration for (A) 3,3-Dimethyl-1-butyne (B) 2,2,5,5-Tetramethyl-3-hexyne (C) Phenylacetylene 123

III.18 γk" *versus* Concentration for (A) Silane (B) Monomethylsilane (C) Dimethylsilane (D) Trimethylsilane 132

III.19 γk" *versus* Concentration for (A) Silane-d_4 (B) Monomethylsilane-d_3 (C) Dimethylsilane-d_2 (D) Trimethylsilane-d_1 133

III.20 γk" *versus* Concentration for (A) Diethylsilane (B) Triethylsilane 134

III.21 γk" *versus* Concentration for (A) Methyldichlorosilane (B) Dimethylchlorosilane 141

III.22 γk" *versus* Concentration for Dichlorosilane 142

III.23 γk" *versus* Concentration for (A) Disilane (B) Disilane-d_6 (C) Hexamethyldisilane 145

III.24 γk" *versus* Concentration for (A) Cyclohexene (B) 1,3-Cyclohexadiene (C) 1,4-Cyclohexadiene 155

Figure Page

III.25 $\gamma k''$ *versus* Concentration for (A) Benzene (B) Toluene (C) Chlorobenzene (D) Fluorobenzene 156

III.26 $\gamma k''$ *versus* Concentration for (A) Tetrahydrothiophene (B) Tetrahydrofuran (C) Thiacyclohexane (D) Pyridine 162

III.27 $\gamma k''$ *versus* Concentration for (A) Thiophene (B) Furan (C) Pyrrole (D) 1-Methylpyrrole 163

IV.1 Log k_1 *versus* Ionization Potential for $CCl(X^2\Pi)$ and $CBr(X^2\Pi)$ Reactions with Acetylenes. 178

IV.2 Log k_1 (per Si-H bond) *versus* Ionization Potential for the Reactions of $CCl(X^2\Pi)$ with Silanes 198

IV.3 Log k_1 *versus* Si-H Bond Stretching Frequency ν for Trisubstituted Silanes 201

IV.4 Log k_1 *versus* Ionization Potential for the Reactions of $CCl(X^2\Pi)$ with Benzene and Substituted Benzenes 212

I. INTRODUCTION

A carbyne is a monovalent carbon radical intermediate in which the carbon atom is connected to another group by a covalent bond. Carbynes are the least understood carbon radical species, for two reasons: 1) they are difficult to generate in a clean, kinetically defined manner, and 2) they are extremely reactive. CH, the simplest of the carbyne family, was first observed several decades ago in the spectra of stars and comets and has been detected, by means of flash photolysis - kinetic spectroscopy, as a transient intermediate in a number of systems. Until recently, more kinetic data were available on CH reactions than on any other carbyne.

In general, the photochemical decomposition of suitable precursor molecules generates carbynes in very low yields, making product analysis difficult, and the simultaneous production of other highly reactive species renders mechanistic considerations speculative, at best (with the exception of CCO_2Et, the chemical reactivity of which has been well delineated, *vide infra*). For these reasons the vast majority of experimental data reported in the literature consists of rate constant measurements obtained by the flash photolysis - kinetic spectroscopic technique.

The following carbynes have been detected upon photolysis of suitable source compounds: CH, CBr, CCl, CF, and perhaps CCN, all of which have been observed spectroscopically, and CCO_2Et, whose presence was rationalized both in terms of product analysis and the nature of the esr signal generated upon photolysis of the source compound.

Of the above carbynes, CF and CCN have not yet been studied kinetically due to the lack of suitable precursors which would produce transient spectra strong enough for kinetic measurements using conventional photolysis apparatus. CI has totally eluded detection, probably due to a combination of factors which include the instability and high reactivity of the carbyne, or low yield for its generation.

A. CARBYNE CHEMISTRY

1. Nature of Carbynes

The bent sp^2 hybrid has long been regarded as a logical structure for a carbene, although a linear sp hybrid is also possible.[1,2] Therefore, the most reasonable structure for a carbyne is an sp hybrid.

The orbital occupancy on the carbon atom of a carbyne comprises a doubly occupied σ orbital, a half filled π orbital and an empty π orbital (Figure I.1a). This electron deficiency in the π orbitals can be partially compensated in the halomethylidynes, CCN, and CCO_2Et, by the back donation of electrons from the halide, CN, and CO groups to the carbon atom. This phenomenon is possibly

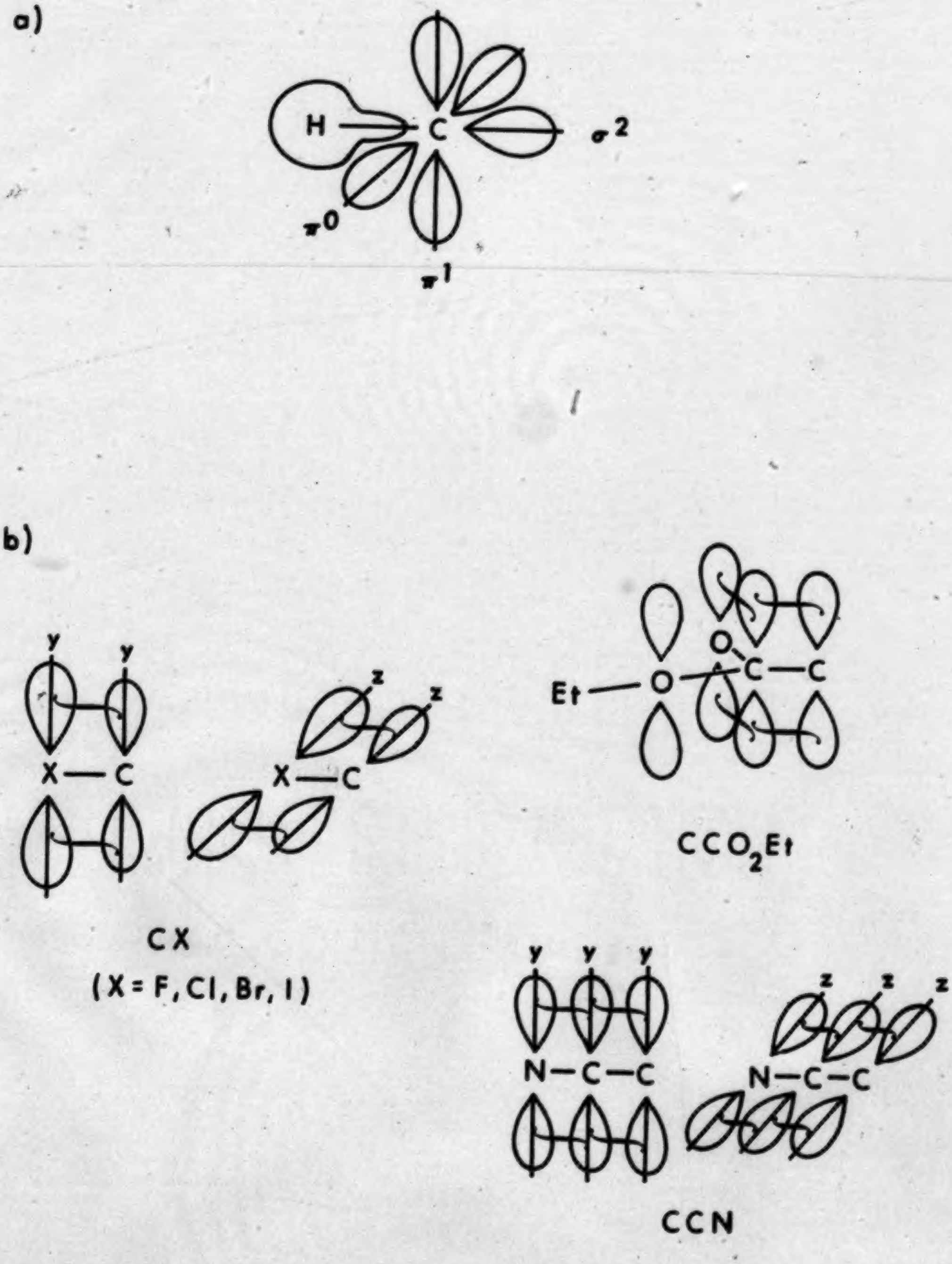
a)
H
C
σ2
π0
π1
b)
y
y
X — C
z
z
X — C
CX
(X = F, Cl, Br, I)
Et — O
O
C — C
CCO2Et
y
y
y
N — C — C
z
z
z
N — C — C
CCN

FIGURE I.1a) Orbital Occupancy of CH b) Back Donation Effect of Carbyne Substituents stronger with the halomethylidynes and CCN, where both pπ orbitals of the carbyne carbon may overlap with those of the halide or with both the CN π molecular orbitals, but weaker with CCO_2Et, where only one pπ orbital of the carbyne carbon can overlap with the CO π molecular orbital (Figure I.1b).

Therefore, although the carbyne carbon becomes more positive as the substituent becomes more electronegative, in the sequence CH, CI, CBr, CCl, CF, there is also an increased transfer of charge back to the carbon atom *via* the pπ orbitals, in going from CI to CF. In general, studies on carbene reactions have indicated that the electrophilic character of the carbene is governed by the population of the pπ orbitals and, but to a much lesser extent, by the total charge, on the carbene carbon. If the carbynes behave similarly, CF would be the least electrophilic carbyne, due to the larger degree of overlap between the pπ orbitals of the carbon and the fluorine atom, while CH, where no back donation occurs, would be the most electrophilic carbyne.

2. Electron Configuration and Term Symbols

In the ground state, the electron configuration of methylidyne CH, the simplest carbyne, is $1\sigma^2 2\sigma^2 3\sigma^2 1\pi^1$. The other carbynes possess analogous configurations: $\ldots w\pi^4 x\sigma^2 v\pi^1$ for the halomethylidynes, $\ldots 3\sigma^2 1\pi^4 4\sigma^2 2\pi^1$ for cyanomethylidyne CCN, and $\ldots 2\pi^2 11\sigma^2 3\pi^1$ for carbethoxymethylidyne CCO_2Et. All of them give rise to a ground state term $X^2\Pi$. Four spectroscopic states, $^4\Sigma^-$, $^2\Delta$, $^2\Sigma^+$ and $^2\Sigma^-$, arise from the first excited configuration $(1\sigma^2 2\sigma^2 3\sigma^1 1\pi^2)$ of CH, the halomethylidynes $(\ldots w\pi^4 x\sigma^1 v\pi^2)$, CCN $(\ldots 3\sigma^2 1\pi^4 4\sigma^1 2\pi^2)$ and CCO_2Et $(\ldots 2\pi^2 11\sigma^1 3\pi^2)$. The quartet state $^4\Sigma^-$ is the lowest lying excited state in all the carbynes. The electron arrangements associated with each of the above symbols are given in Figure I.2 for CCl.

3. Transition Spectra

In kinetic-spectroscopic studies, the attenuation of the carbyne's transition band with time can be used to monitor its concentration. The observed low energy transitions and their corresponding wavelengths for CH, CCl, CBr, CF and CCN are presented in Table I.1.

Methylidyne, CH

CH has been studied most extensively. Three bands are most often seen in the near u.v. region at 430.0 nm, 390.0 nm and 314.3 nm, in decreasing order of emission intensity. In absorption the situation is reversed, with the 314.3 nm band being the most readily observed.[4]

Being one of the most abundant radicals in comets, stellar atmosphere, and interstellar space, CH has been observed in comet emissions and in the absorption spectra of stars for more than half a century.[5] Its emission was also observed in Bunsen flames,[6] in carbon arcs burning in

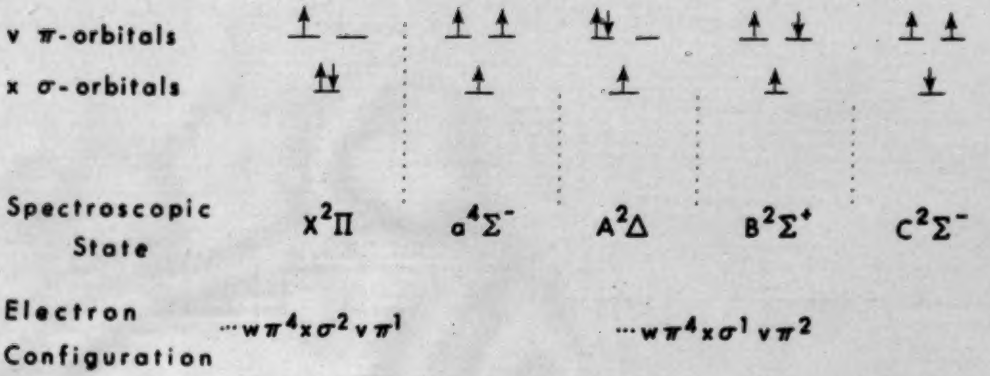
v π-orbitals
x σ-orbitals
Spectroscopic State
$X^2\Pi$
$a^4\Sigma^-$
$A^2\Delta$
$B^2\Sigma^+$
$C^2\Sigma^-$
Electron Configuration
$\cdots w\pi^4 x\sigma^2 v\pi^1$
$\cdots w\pi^4 x\sigma^1 v\pi^2$

FIGURE I.2 Electron Arrangements Corresponding to the Spectroscopic States Arising from the Ground and the First Excited Electron Configuration of CCl

TABLE I.1

Observed Carbyne Transitions and Their Corresponding Wavelengths in the Near U.V.Region[3]

CH		CBr	
Transition	Wavelength (nm)	Transition	Wavelength (nm)
$C^2\Sigma^+ \leftrightarrow X^2\Pi$	314	$B^2\Sigma^+ \leftarrow X^2\Pi$	250
$B^2\Sigma^- \leftrightarrow X^2\Pi$	390	$A^2\Delta \leftarrow X^2\Pi$	305
$A^2\Delta \leftrightarrow X^2\Pi$	430 (vis.)		
$a^4\Sigma^- \leftarrow X^2\Pi$	1674 (i.r.)		

CCl		CF	
Transition	Wavelength (nm)	Transition	Wavelength (nm)
$B^2\Sigma^+ \leftarrow X^2\Pi$	230	$B^2\Delta \rightarrow X^2\Pi$	203
$A^2\Delta \leftrightarrow X^2\Pi$	278	$A^2\Sigma^+ \leftrightarrow X^2\Pi$	240

CCN	
Transition	Wavelength (nm)
$C^2\Sigma^+ \leftarrow X^2\Pi$	470
$B^2\Sigma^- \leftarrow X^2\Pi$	446
$A^2\Delta \leftarrow X^2\Pi$	375

hydrogen,[7] and in electrical discharges through organic vapours e.g. acetylene, methane, benzene.[8] The bands at 430.0 nm, 390.0 nm and 314.3 nm have long been identified as the transitions $A^2\Delta - X^2\Pi$, $B^2\Sigma^- - X^2\Pi$ and $C^2\Sigma^+ - X^2\Pi$ respectively.[7] However, the absorption spectrum had not been seen in the laboratory until 1952, when Norrish *et al.* observed the three characteristic transitions following the oxidation of acetylene initiated by the flash photolysis of a small quantity of nitrogen dioxide.[9]

Kinetic absorption spectroscopy has been used to study the reactions of CH, generated by the photolysis of compounds such as CH_2N_2,[10] C_4H_2[11] and CH_4,[12] by monitoring the $C^2\Sigma^+ \leftarrow X^2\Pi$ absorption band at 314.3 nm. With the advancement of laser technology, recent kinetic measurements were made by monitoring the laser-induced fluorescence (LIF) of the $A^2\Delta \rightarrow X^2\Pi$ band at 430.0 nm.[13,14]

The quartet state $^4\Sigma^-$ has eluded conventional spectroscopy, but was detected recently, in absorption, by laser photoelectron spectroscopy and was estimated to lie 17 kcal mole^{-1} (0.74 eV, 1674 nm) above the ground state,[15] in agreement with an earlier estimate, by *ab initio* calculations, of 0.52 - 0.75 eV.[16]

Herzberg and Johns,[17] following the flash photolysis of CH_2N_2, observed a number of new transitions in the vacuum u.v. region. This included a Rydberg series, starting at 137.0 nm, and some strong absorptions at 300.7, 169.0, 156.0 and 154.0 nm, which were identified by rotational analysis as transitions involving the higher spectroscopic states, $D^2\Pi_i \leftarrow B^2\Sigma^-$, $D^2\Pi_i \leftarrow X^2\Pi$, $E^2\Pi \leftarrow X^2\Pi$ and $F^2\Sigma^+ \leftarrow X^2\Pi$ respectively.

Bromomethylidyne, CBr

The CBr spectrum consists of bands in the region 306 - 300 nm and two diffuse bands at 252.6 nm and 249.6 nm.

Unlike CCl, the emission of which has been observed both in flames and electrical discharge experiments. CBr does not appear to emit, under similar conditions. Emissions around 290 nm, observed in flames containing Br_2,[17,18] and bands in the region 350 - 265 nm, reported in the electrical discharge of carbon tetrabromide vapour,[19] were first believed to be due to CBr, but were later identified as bromine bands.[20]

CBr can be seen in the absorption following the flash photolysis of organic bromides.[21,22] The system near 300 nm was shown to be the $A^2\Delta \leftarrow X^2\Pi$ transition on the basis of the rotational analysis carried out by Dixon and Kroto.[23] Tyerman also observed two diffuse absorption bands at 252.6 nm and 249.6 nm and provisionally assigned them as belonging to the $B^2\Sigma^+ \leftarrow X^2\Pi$ transition.[24]

To date, kinetic absorption spectroscopy has been the only method used to study CBr reactions by monitoring the $(Q_1\ 0,0)$ band of the $A^2\Delta \leftarrow X^2\Pi$ transition at 301.4 nm.[25,26]

Chloromethylidyne, CCl

The transition spectrum of CCl consists of a strong, complex band system near 278 nm and a weaker system near 230 nm.

The emissions near 278 nm obtained in electrical discharges of chlorine-containing hydrocarbons e.g. carbon tetrachloride vapour, were first reported by Asundi and Karim[27] in 1937, and subsequently confirmed by a number of workers.[28,29] This system also occurs in the flame of a cyanogen - chlorine mixture.[18,30] On the basis of rotational analysis, these emissions were identified in 1961 as the $A^2\Delta \rightarrow X^2\Pi$ transition.[31,32] The same system could be observed in absorption following the flash photolysis of some chloromethanes and chloroethylenes.[21,22,33,34]

A band emitting at 244 - 236 nm, first observed by Barrow[39] in the electrical discharge of carbon tetrachloride vapour, was later attributed to chloromethylidyne cation, CCl^+.[35] In 1969, Tyerman[24] studied the flash photolysis of $CF_2CCl_2 + N_2$ mixtures and discovered two new absorption bands at 231.1 nm and 230.4 nm, which were assigned to the $B^2\Sigma^+ \leftarrow X^2\Pi$ system.

The (Q, 0,0) band of the $A^2\Delta \leftarrow X^2\Pi$ transition at 277.7 nm has been used in kinetic absorption spectroscopy for monitoring the CCl concentration.[34]

Most recently, kinetic studies of the CCl reactions have been made by following the laser induced fluorescence (LIF) of the same line.[36]

Asundi and Karim reported that the emission spectrum of CCl_4 also featured strong, wide bands having maxima at 460 nm, 307 nm and 258 nm, and a medium band (maximum at 335 nm), and ascribed these to CCl. However, further investigation is required in order to substantiate this claim.

Fluoromethylidyne, CF

So far, two bands of CF have been observed: one near 240 nm and the other near 203 nm.

The emissions near 240 nm can be observed following the decomposition of CF_4 or other fluorocarbon vapours *via* electrical discharge,[37-40] or shock-heating.[41] They also occur in flames burning in CF_4.[42] The same system in absorption has been observed in electrical discharge experiments[43] and in the carbon-tube furnace decomposition of CF_4.[44]

A rotational analysis done by Andrews and Barrow[37] identified the 240 nm band as the $A^2\Sigma^+ - X^2\Pi$ transition. These authors,[37] and also Carroll and Grennan,[40] assigned the 203 nm system to the $B^2\Delta - X^2\Pi$ transition, which, so far, has only been observed in emission. Both systems have been observed in emission, in electrical discharges through fluorocarbon vapours,[37,38,40] and in the laser photolysis of CF_2Br_2[45] and CF_2Cl_2.[46] The lowest lying $^4\Sigma^-$ state has not been observed, but was estimated to lie about 2.66 eV (60 kcal, 466 nm) above the ground state.[47]

Cyanomethylidyne, CCN

The only report concerning the transition spectrum of CCN is that of Merer and Travis,[44] who flash photolyzed diazoacetonitrile and ascribed a new transient absorption spectrum to CCN. A rotational analysis carried out by the authors indicated that the three bands observed at 470 nm, 446 nm and 375 nm belonged to the $A^2\Delta \leftarrow X^2\Pi$, $B^2\Sigma^- \leftarrow X^2\Pi$ and $C^2\Sigma^+ \leftarrow X^2\Pi$ transitions respectively.

4. Generation of Carbynes

As noted above, carbynes are usually generated in secondary processes: these are little understood and moreover are expected to be influenced by a number of factors such as the wavelength of irradiation and pressure. For example, it will be shown that $CHBr_3$ and $CHCl_3$ generate CBr and CCl respectively upon photolysis; however, the spectral lines attributable to CBr are strong and well defined, whereas under the same conditions, those for CCl are so weak that a vacuum u.v. apparatus must be used.

An additional complicating factor is the simultaneous generation of other reactive species which may interfere with the reaction under study, and/or absorb in the same spectral region as the species being examined.

For the above reasons, and bearing in mind that the transition line(s) being studied should not be masked by absorptions from the source compound, each of the carbynes studied to date has been generated under *ad hoc* conditions.

The methods and sources used are summarized in Table I.2 and will now be described in detail.

Carbethoxymethylidyne, CCO_2Et

The λ < 280 nm photolysis of diethylmercury*bis*diazoacetate in liquid alkanes and alkenes[49-52] leads to the formation of a variety of products which can be rationalized *via* the intervention of carbethoxymethylidyne, CCO_2Et:

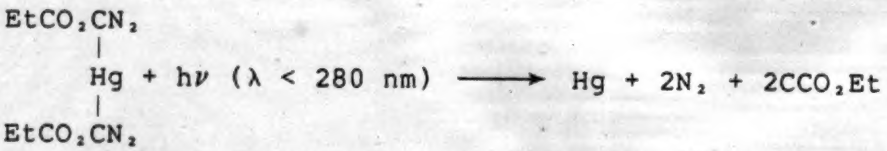

$$\begin{array}{l} EtCO_2CN_2 \\ \quad | \\ \quad Hg + h\nu\ (\lambda < 280\ \text{nm}) \longrightarrow Hg + 2N_2 + 2CCO_2Et \\ \quad | \\ EtCO_2CN_2 \end{array}$$

Moreover, the -196° photolysis of the source compound in a glass matrix generated a single symmetrical esr signal with no hyperfine splitting at $g = 2.001$, indicating the presence of a doublet ground state species containing no protons adjacent to the radical site: $\downarrow\uparrow\downarrow C\text{-}CO_2Et$.

Methylidyne, CH

CH can be generated by the photolysis of a great variety of hydrocarbon precursors. Norrish *et al.*[4] were the first to observe the CH absorption spectrum in the laboratory in 1952, following the oxidation of acetylene initiated by the flash photolysis of a small quantity of nitrogen dioxide. Subsequently, with improved techniques, several groups including Callomon and Ramsay,[11] who flash

TABLE I.2

Potential Photochemical Sources of Carbynes

Carbyne	Source	Method[a)]
CCO_2Et	$EtCO_2CN_2$ Hg $EtCO_2CN_2$	s.s.p.[49–52]
CH	C_4H_2	f.p.[11]
	CH_2N_2	f.p.[10]
	CH_4	f.p.[12]; s.s.p.[53,54]; p.r.[54,77]
	$CHBr_3$	l.p.[13]
	CH_3NH_2	l.p.[59]
	$CHBr_3/M$ ($M=O_2$; SO_2; NO)[b)]	f.p.[55;56;57]
CBr	$\left.\begin{matrix}CHBr_3\\CBr_3CHO\end{matrix}\right\} > \left\{\begin{matrix}CBr_3NO_2\\CHCLBr_2\end{matrix}\right\} > CH_2Br_2*$	f.p.[21,22]
	$CHBr_3$	f.p.[25,26]
CCl	$\left.\begin{matrix}CHCl_2Br\\CHClBr_2\\CCl_2Br_2\end{matrix}\right\} > \left\{\begin{matrix}CCl_3CHO\\CH_2ClBr*\end{matrix}\right\} > \left\{\begin{matrix}CCl_3Br*\\CCl_3NO_2\end{matrix}\right\} > CCl_3CN* > CHCl_3$	f.p.[21,22]
	CCl_3NO	f.p.[33]

Continued...

TABLE I.2 Continued

Carbyne	Source	Method
CCl	CF_2CCl_2 > $CFClCCl_2$ > C_2Cl_4 > $CHClCCl_2$ > CH_2CCl_2 CCl_4	f.p.^{34} l.p.^{56}; s.s.p.^{39,60,61}
CF	$CHFBr_2$* > $CFBr_3$* CF_4, $C_2F_4$$^{b)}$ $CFBr_3$/M* (M=NO; SO_2)$^{b)}$ CF_2Br_2; CF_2Cl_2 $CFCl_3$$^{b)}$	f.p.^{21,22} s.t.^{62} f.p.$^{64;65}$ l.p.$^{45;46}$ s.s.p.^{63}

a) f.p.: flash photolysis
s.s.p.: steady state photolysis
l.p.: laser photolysis
p.r.: pulsed radiolysis
s.t.: shock tube
b) inferred

* vacuum u.v. photolysis

photolyzed diacetylene, and Herzberg and Johns,[18] who flash photolyzed diazomethane, obtained stronger absorption spectra of CH.

However, the first experiment designed to study the rate of CH reactions was done by Braun *et al.*,[12] who flash photolyzed methane and concluded that CH can be formed either by the secondary photolysis of methylene radicals,

$$\begin{tikzcd} CH_4 + h\nu \arrow[r] & H_2 + CH_2 \arrow[d, "h\nu"] \\ & H + CH \end{tikzcd}$$

or *via* the unimolecular decomposition of vibrationally excited CH_2, because at the photolysis wavelength used ($\lambda \geq 105$ nm) the initially produced CH_2 can contain up to 170 kcal mole^{-1} excess energy:

$$\begin{tikzcd} CH_4 + h\nu\ (\lambda \geq 105\ \text{nm}) \arrow[r] & H_2 + CH_2^{\dagger} \arrow[d] \\ & H + CH \end{tikzcd}$$

However, the results of a vacuum u.v. steady state photolysis of methane (λ = 123.6 nm, 106.7 - 104.8 nm, 74.37 - 73.59 nm) studied by Ausloos and coworkers[33,34] indicated that vibrationally excited methyl radicals, which are also produced in the primary processes, could also be the precursors of CH:

$$\begin{tikzcd} CH_4 + h\nu\ (\lambda = 123.6\ \text{nm}) \arrow[r] & H + CH_3^{\dagger} \arrow[d] \\ & {} \end{tikzcd}$$

$$\hookrightarrow CH + H_2 \text{ (or 2H ?)}$$

They also showed that in the pulse radiolysis of methane, CH may arise from the fragmentation of neutral, excited methane molecules formed by electron-impact, instead of *via* an ionic mechanism.

Lin flash photolyzed $CHBr_3/M/SF_6$ systems ($M = O_2$,[55] SO_2,[56] NO[57]) and proposed that CH is generated *via* the sequential absorption of three photons by bromoform and the subsequent primary and secondary fragments:

$$CHBr_3 + h\nu\ (\lambda \geq 165\text{ nm}) \rightarrow Br + CHBr_2$$
$$\xrightarrow{h\nu} Br + CHBr$$
$$\xrightarrow{h\nu} Br + CH$$

The above mechanism differs from the one proposed by Simons and Yarwood[21,22] for the production of CBr from bromoform (*vide infra*). Actually, CH was not observed spectroscopically, but its presence was inferred from the fact that C_2H_2 is a reaction product, probably formed from the recombination of CH radicals.

More recently, CH has been produced by pulsed lasers. Lin and coworkers[13,14] employed a high-power, pulsed ArF excimer laser (193 nm) to photolyze bromoform, under mildly focussed conditions that would allow 2-photon absorption:[58]

$$CHBr_3 + h\nu\ (\lambda = 193\text{ nm}) \longrightarrow \text{virtual state} \xrightarrow{h\nu}$$

$$\longrightarrow 3Br + CH$$

Similarly, Messing *et al.*[20] produced CH from the multiple photon dissociation (MDP) of methylamine CH_3NH_2 induced by a TEA CO_2 laser. Methylamine was chosen since it has well developed P, Q, R branches of the C-N stretching mode in the CO_2 laser region near 10 μm. CH is presumably formed from the secondary MDP of a primary fragment such as CH_2NH_2 or $CHNH_2$, because the formation of CH from CH_3NH_2 in a single step has a prohibitively high energy requirement:

$$CH_3NH_2 + h\nu\ (\lambda = 10\ \mu m) \longrightarrow H + CH_2NH_2$$

$$\xrightarrow{h\nu} NH_3 + CH$$

$$\longrightarrow H_2 + CHNH_2$$

$$\xrightarrow{h\nu} NH_3 + CH$$

The same authors also investigated other compounds such as methanol CH_3OH, ethanol C_2H_5OH, methyl cyanide CH_3CN, ethylene C_2H_4 and ketene CH_2CO, and found these can also be used as sources of CH.

Halomethylidynes

Simons and Yarwood[21,22] investigated potential sources of halomethylidynes extensively by flash photolyzing a number of halogenated compounds, primarily halomethanes, and observed CBr, CCl and CF in absorption. According to their scheme, the halomethylidynes were produced *via* the unimolecular decomposition of vibrationally excited halomethyl radicals:

$$CHX_3 + h\nu \longrightarrow CHX_2^{\dagger} + X$$

$$(CHX_2^{\dagger})_{E \geq E^*} \longrightarrow CX + HX$$

$$\xrightarrow{M} (CHX_2)_{E<E^*}$$

where X = Cl, Br, F, and E^* is the minimum energy required for the unimolecular decomposition.

By varying the energy of photolysis by changing the wavelength of the irradiation, they showed that a large portion of the excess energy available in the primary process ended up in the vibrationally excited halomethyl radicals. When this energy exceeded a minimim required value, E^*, secondary unimolecular decomposition took place to produce the halomethylidynes. Helium was used as a diluent gas to maintain isothermal conditions.

It should be noted that, contrary to Lin's claim,[55-57] neither Simons and Yarwood nor Strausz and coworkers could detect CH following the flash photolysis of CH_2Br_2, CH_2ClBr, and CH_2I_2, with either conventional or vacuum u.v. apparatus, under either adiabatic or isothermal conditions. Simons and Yarwood ascribed this to the relatively high energy requirement for CH generation, and thus, even if sufficient energy resides in the halomethyl radicals for this process, the alternative decomposition to yield halomethylidyne, which requires less energy, would still be more favorable, for example:

Radical Decomposition	Minimum Energy for Decomposition E^* (kcal mole^{-1})
$CH_2Br \longrightarrow CBr + H_2$	65
$CH_2Br \longrightarrow CH + HBr$	101

Bromomethylidyne, CBr:

The only kinetic studies on CBr reactions have been carried out by Strausz and coworkers,[25,26] employing bromoform as the source of CBr. The production scheme, as proposed by Simons and Yarwood,[21,22] is given as:

$$CHBr_3 + h\nu\ (\lambda > 200\ \text{nm}) \longrightarrow CHBr_2^{\dagger} + Br$$

$$(CHBr_2^{\dagger})_{E \geq E^*} \longrightarrow CBr + HBr$$

where E^* = minimum energy for decomposition = 57 kcal mole^{-1}.

Chloromethylidyne, CCl:

Simons and Yarwood[21,22] were the first to observe the absorption spectrum of CCl, which until then had only been reported in emission, by flash photolyzing a series of chloromethanes. They reported that the best sources of CCl are $CHClBr_2$, $CHCl_2Br$ and CCl_2Br_2.

Husain[33] flash photolyzed trichloronitrosomethane and suggested the following mechanism for the production of CCl:

$$CCl_3NO + h\nu\ (\lambda > 190\ \text{nm}) \rightarrow CCl_3^{\dagger} + NO \qquad E \leq 42\ \text{kcal mole}^{-1}$$

$$CCl_3^{\dagger} \rightarrow CCl + Cl_2 \qquad E \sim 107\ \text{kcal mole}^{-1}$$

The CCl concentration was found to depend on the first order of the flash energy, which is indicative of a one-photon process such as the one given above. Since the lower limit of the photolysis flash at 190 nm corresponds to about 150 kcal mole^{-1} energy, Husain concluded that after the primary process, which requires $\leq$ 42 kcal mole^{-1} energy, the excess energy was concentrated in the trichloromethyl radical, so as to meet the energy requirement of approx. 107 kcal mole^{-1} for the unimolecular decomposition to generate CCl. This is supported by the observation that the nitric oxide produced was not vibrationally excited, since only strong (0,0) transitions of the γ-system of NO were seen, while the (0 — 1) transitions were extremely weak.

Tyerman[34] also generated CCl from the flash photolysis of 1,1-dichloroethylenes: CF_2CCl_2, $CFClCCl_2$, C_2Cl_4, $CHClCCl_2$, CH_2CCl_2, in decreasing order in terms of amount of CCl produced. The CCl concentration was found to be dependent on the second order of the flash energy, from which he concluded that the CCl production is a two-photon process:

$$CCl_2CXY + h\nu\ (\lambda > 200\ nm) \longrightarrow CCl_2 + CXY$$

$$X,Y = H,F,Cl$$

$$CCl_2 + h\nu \longrightarrow CCl + Cl$$

Also, the CCl intensity was not affected by the pressure of a foreign gas such as N_2; this rules out the possibility of a vibrationally excited species as being the precursor of the CCl. Furthermore, Tyerman observed vibrationally hot CCl ($v' = 1$) in the absorption spectrum of CCl, but only in the flash photolysis of CF_2CCl_2. His explanation was that since CF_2CCl_2 has no fundamental between 993 and 640 cm^{-1}, it fails to induce rapid vibrational relaxation of the hot CCl ($v' = 1$) (fundamental frequency = 864 cm^{-1}), as the other 1,1-dichloroethylenes would, because they all have fundamental frequencies of the order of 864 ± 50 cm^{-1}. Recently, Wampler and coworkers[34] studied the ArF laser photolysis of CCl_4 and CCl_3F, and discovered that, in both cases, CCl radicals were produced on the average by more than two laser photons. On the basis of the various products formed, they suggested that several different primary processes involving the absorption of one to three photons were actually involved:

$$CCl_4 \longrightarrow CCl_3 + Cl \qquad \Delta H = 71 \text{ kcal mole}^{-1}$$

$$\longrightarrow CCl_2 + Cl_2 \qquad \Delta H = 80 \text{ kcal mole}^{-1}$$

$$\longrightarrow CCl + Cl_2 + Cl \qquad \Delta H = 172 \text{ kcal mole}^{-1}$$

$$CCl_3F \longrightarrow CCl_2F + Cl \qquad \Delta H = 75 \text{ kcal mole}^{-1}$$

$$\longrightarrow CClF + Cl_2 \qquad \Delta H \sim 90 \text{ kcal mole}^{-1}$$

$$\longrightarrow CF + Cl_2 + Cl \qquad \Delta H = 159 \text{ kcal mole}^{-1}$$

$$\longrightarrow CCl + Cl_2 + F \qquad \Delta H = 208 \text{ kcal mole}^{-1}$$

$$\longrightarrow CCl + Cl + ClF \qquad \Delta H = 206 \text{ kcal mole}^{-1}$$

In the steady state photolysis of CCl_4, Rebbert and Ausloos[illegible] suggested that the following primary processes occur, depending on the wavelength:

$$CCl_4 + h\nu \ (\lambda \leq 213.9 \text{ nm}) \longrightarrow CCl_3 + Cl$$

$$(\lambda \leq 163.3 \text{ nm}) \longrightarrow CCl_2 + 2Cl$$

At shorter wavelength, an additional process was believed to be feasible:

$$(\lambda \leq 147\ \text{nm}) \longrightarrow CCl + Cl_2 + Cl\ (\text{or } 3Cl)$$

Although the authors could not obtain any products attributable to the presence of CCl, evidence for the generation of CCl at $\lambda \leq 147$nm, was provided by Davies *et al.*,[61] who postulated that $CClBr_2$, one of the products obtained from the steady-state photolysis of CCl_4 - Br_2 mixtures at 147 nm, arises from the reaction of CCl with Br_2:

$$CCl + Br_2 \longrightarrow CClBr_2$$

$$CClBr_2 + Br_2 \longrightarrow CClBr_3 + Br$$

The above results indicate that chloromethanes, such as CCl_3NO, $CHClBr_2$, $CHCl_2Br$, CCl_3Br, and 1,1-dichloroethylenes, such as CF_2CCl_2 and $CFClCCl_2$ are all good precursors of CCl, using flash photolysis - kinetic spectroscopic techniques. The production of CCl from CCl_4 in sufficient quantities for kinetic studies has not yet been definitely proven, except under laser photolysis conditions, probably due to the high energy requirement for the process.

Fluoromethylidyne, CF:

CF has been observed spectroscopically following the flash photolysis of $CHFBr_2$ and $CFBr_3$ by Simons and Yarwood,[21,22] who used a vacuum u.v. apparatus because the absorption spectrum at 230 nm ($A^2\Sigma^+ \leftarrow X^2\Pi$) overlaps that of the parent compounds. The presence of CF in other systems has also been inferred from a number of other experiments, because its generation is energetically feasible under the conditions employed. For example, shock-heated CF_4 or C_2F_4 in argon diluent was found to decompose to CF_2, some of which may subsequently decompose to CF:[42]

$$CF_2 + Ar \longrightarrow CF + F + Ar$$

By analogy with the proposed production of CCl from the steady-state photolysis of CCl_4 at short wavelength,[40]

$$CCl_4 + h\nu \ (\lambda \leq 147 \text{ nm}) \longrightarrow CCl + Cl_2 + Cl \ (\text{or } 3Cl)$$

CF was believed to be generated in the primary process in the steady-state photolysis of $CFCl_3$ carried out by Rebbert:[43]

$$CFCl_3 + h\nu \ (\lambda \leq 147 \text{ nm}) \longrightarrow CF + Cl_2 + Cl \ (\text{or } 3Cl)$$

The detection of $CFBr_3$, when bromine was added to $CFCl_3$, is evidence for the formation of CF, since it can be formed by the reaction of CF with Br_2:

$$CF + Br_2 \longrightarrow CFBr_2$$

$$CFBr_2 + Br_2 \longrightarrow CFBr_3 + Br$$

Furthermore, in the flash photolyzed systems $CFBr_3/M/SF_6$ ($M = NO$,[44] SO_2[45]), CF was thought to be responsible for the laser emission of CO, which supposedly arises from the reaction:

$$CF + O \longrightarrow CO^{\dagger} + F$$

By analogy with the generation of CH from $CHBr_3$,[56,57] the proposed mechanism of CF production from $CFBr_3$ is a successive photodetachment of Br atoms from $CFBr_3$:

$$\begin{array}{l} CFBr_3 + h\nu\ (\lambda \geq 165\ nm) \longrightarrow Br + CFBr_2 \\ \qquad\qquad\qquad\qquad\qquad\qquad\qquad \xrightarrow{h\nu} Br + CFBr \\ \qquad\qquad\qquad\qquad\qquad\qquad\qquad\qquad\qquad \xrightarrow{h\nu} Br + CF \end{array}$$

Recently, CF emissions were observed by Wampler *et al.*,[45,46] in the laser photolysis of CF_2Br_2 and CF_2CCl_2 using an ArF excimer laser. The energy requirements and the products observed suggested at least a three photon absorption by the parent compounds.

Iodomethylidyne, CI:

The only kinetic study involving CI reported in the literature is that of Refaey and Franklin,[66] who investigated ion-molecular collision processes involving negative ions. The O^- ion detected was proposed to have originated from the reaction $I^- + CO \rightarrow O^- + CI$. Perhaps the only attempt reported in the literature to generate CI was that of Simons and Yarwood,[21,22] who flash photolyzed CHI_3 and CH_2I_2, but failed to detect any transient spectrum attributable to the carbyne.

Cyanomethylidyne, CCN

So far, no kinetic studies have been performed on CCN, which was believed to be generated in the flash photolysis of diazoacetonitrile, and three absorption bands observed in the near u.v. region have been ascribed to it.[68] However, the production scheme was not considered and no further work has been reported.

5. Reactions of Carbynes

Methylidyne, CH

The reactions of CH have been studied since the early sixties. CH has been alluded to many times and suggested as a possible transient in the reactions of carbon atoms with hydrocarbons.[67,69] Wolf,[70] in his study of the reactions of recoil ^{11}C with hydrocarbons, proposed that ^{11}CH was formed by ^{11}C insertion into a C-H bond, followed by the decomposition of the energized radical,

$$^{11}C + HR \longrightarrow [H-^{11}CR]^{\dagger} \longrightarrow {}^{11}CH + R$$

and that the ^{11}CH thus produced was responsible for the subsequent production of ethylene-^{11}C by insertion into a primary C-H bond of the hydrocarbon, followed by C-C bond scission:

$$^{11}\mathrm{CH} + \mathrm{CH_3R} \longrightarrow [\mathrm{H_2{}^{11}C{-}CH_2R}]^{\dagger} \longrightarrow \mathrm{H_2{}^{11}C{=}CH_2} + \mathrm{R}$$

^{11}CH insertion into secondary and tertiary C-H bonds was believed to account for the products 1-butene, in the reaction with butane, and *iso*butylene-^{11}C, in the reaction with *iso*butane, respectively:

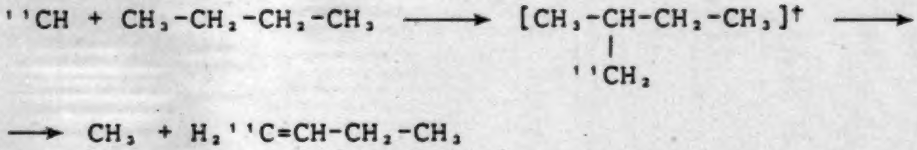

$$^{11}\mathrm{CH} + \mathrm{CH_3{-}CH_2{-}CH_2{-}CH_3} \longrightarrow [\mathrm{CH_3{-}}\underset{\overset{|}{^{11}\mathrm{CH_2}}}{\mathrm{CH}}\mathrm{{-}CH_2{-}CH_3}]^{\dagger} \longrightarrow$$

$$\longrightarrow \mathrm{CH_3} + \mathrm{H_2{}^{11}C{=}CH{-}CH_2{-}CH_3}$$

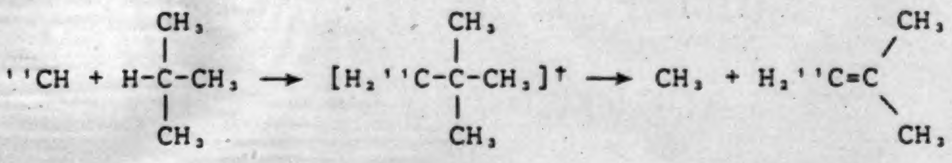

$$^{11}\mathrm{CH} + \mathrm{H{-}}\overset{\mathrm{CH_3}}{\underset{\mathrm{CH_3}}{\mathrm{C}}}\mathrm{{-}CH_3} \rightarrow [\mathrm{H_2{}^{11}C{-}}\overset{\mathrm{CH_3}}{\underset{\mathrm{CH_3}}{\mathrm{C}}}\mathrm{{-}CH_3}]^{\dagger} \rightarrow \mathrm{CH_3} + \mathrm{H_2{}^{11}C{=}C}\begin{array}{l}\diagup \mathrm{CH_3}\\ \diagdown \mathrm{CH_3}\end{array}$$

Furthermore, the reaction with ethane and those hydrocarbons containing an ethyl group gave appreciable yields of propylene-^{11}C. With ethane, the mechanism probably involves C-H bond scission:

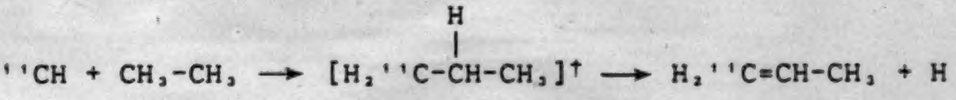

$$^{11}\mathrm{CH} + \mathrm{CH_3{-}CH_3} \rightarrow [\mathrm{H_2{}^{11}}\overset{\overset{\mathrm{H}}{|}}{\mathrm{C}}\mathrm{{-}CH{-}CH_3}]^{\dagger} \rightarrow \mathrm{H_2{}^{11}C{=}CH{-}CH_3} + \mathrm{H}$$

More evidence for the occurrence of CH insertion into C-H bonds was later provided by Wolfgang and coworkers,[71,72] who reacted ^{11}C, produced by nuclear recoil, with $H_2 + C_2H_4$ mixtures. All the products could be assigned to C, CH_2 or CH_3 precursors, except 1-pentene, which apparently arises from ^{11}CH insertion into the C-H bond of C_2H_4:

$$^{11}CH + C_2H_4 \longrightarrow [H_2{}^{11}C\text{-}CH\text{=}CH_2]^{\dagger}$$

The allyl radical may add to ethylene to give a pentenyl radical, which undergoes H-abstraction with another molecule or radical:

$$[H_2{}^{11}C\text{-}CH\text{=}CH_2]^{\dagger} + C_2H_4 \longrightarrow CH_2\text{-}CH_2\text{-}{}^{11}CH_2\text{-}CH\text{=}CH_2 \xrightarrow{RH}$$
$$\longrightarrow CH_3\text{-}CH_2\text{-}{}^{11}CH_2\text{-}CH\text{=}CH_2$$

Alternatively, the allyl radical may combine with an ethyl radical to give 1-pentene:

$$[H_2{}^{11}C\text{-}CH\text{=}CH_2]^{\dagger} + C_2H_5 \longrightarrow C_2H_5\text{-}{}^{11}CH_2\text{-}CH\text{=}CH_2$$

Braun *et al.*[12] were the first to study the kinetics of CH reactions. Until then, the only rate constants reported were those estimated for the reaction of CH with ammonia, deduced from experiments with an acetylene - O_2 - NH_3 flame,[73] and for the reaction of CH with O_2, deduced from C_2H_2 and C_2H_4 flames.[74] In the study done by Braun *et al.*, CH was generated from the flash photolysis of methane, and its decay was followed by monitoring the Q branch of the $C^2\Sigma^+ \leftarrow X^2\Pi$ system at 314.3 nm. The rate constants for the reactions given below were determined relative to the rate constant of recombination of CH, estimated to be 1.2×10^{11} M^{-1} s^{-1}, and are listed in Table I.3:

$$CH + CH_4 \longrightarrow CH_2CH_3^\dagger$$

$$CH + H_2 \longrightarrow CH_3^\dagger$$

$$CH + N_2 \longrightarrow \text{products}$$

They suggested that CH insertion into methane, as proposed earlier by Wolfgang and coworkers,[18] played a dominant role in the formation of ethylene, a major product. This would explain the formation of essentially d_0, d_1, d_3 and d_4, and the non-appearance of d_2 ethylene, in the flash photolysis of a CH_4 - CD_4 mixture:

$$CH + CH_4 \longrightarrow CH_2CH_3^\dagger \longrightarrow CH_2CH_2 + H$$

$$CD + CH_4 \longrightarrow CHDCH_3^\dagger \longrightarrow CHDCH_2 + H$$

$$CH + CD_4 \longrightarrow CHDCD_3^\dagger \longrightarrow CHDCD_2 + D$$

$$CD + CD_4 \longrightarrow CD_2CD_3^\dagger \longrightarrow CD_2CD_2 + D$$

TABLE I.3

Second Order Rate Constants k, for the Reactions of $CH(X^2\Pi)$

Substrate	$k, \times 10^{-9} (M^{-1}s^{-1})$			
	Early estimates	Braun[12]	Bosnali & Perner[77]	Lin[79]
hydrogen H_2		0.62	10.5 ± 1.2	15.7 ± 3.0
nitrogen N_2		0.043	0.61 ± 0.3	0.56 ± 0.06
oxygen O_2	~0.06[73]		424	35.5 ± 4.8 19.8 ± 2.4[59]
ammonia NH_3	>0.06[74]		59 ± 9	
water H_2O			27 ± 5	
carbon monoxide CO			2.9	12.6 ± 1.8
carbon dioxide CO_2				1.14 ± 0.24
nitric oxide NO				175 ± 42
methane CH_4		1.5	20.1 ± 0.5	60.2 ± 18.1
ethane C_2H_6				241 ± 60
propane C_3H_8			82 ± 20	
n-butane n-C_4H_{10}			78 ± 7	349 ± 30
ethylene C_2H_4			69 ± 6	126 ± 48
acetylene C_2H_2			45 ± 9	132 ± 24
propyne C_3H_4				277 ± 90
cyclopropane c-C_3H_6				144 ± 42
cyclohexane c-C_6H_{12}				277 ± 114
benzene c-C_6H_6				47.6 ± 19.3

The insertion reaction of CH with H_2 was inferred from the large increase in the yield of ethane, presumably formed by the recombination of CH_3, upon the addition of hydrogen. *Ab initio* calculations carried out by Brooks and Schaefer[16] yielded very low energy barriers for the insertion reactions of both $CH(X^2\Pi)$ and $CH_2(A^1A_1)$ with H_2,

$$CH(X^2\Pi) + H_2 \longrightarrow CH_3(X^2A_2)$$

$$CH_2(A^1A_1) + H_2 \longrightarrow CH_4(X^1A_1)$$

but substantial barriers for the abstraction reactions.

The above results support the view that, on a spin multiplicity basis, doublet ground state methylidyne may be regarded as the analog of singlet methylene, and quartet, lowest excited methylidyne as that of triplet methylene. Singlet, lowest excited $CH_2(A^1A_1)$ has been shown to insert into C-H bonds and H_2, and it appears that $CH(X^2\Pi)$reacts similarly.

Bosnali and Perner[17] measured rate constants for the reactions of CH with 11 substrates. CH was produced from the pulse radiolysis of methane, and its decay was also followed by monitoring the $C^2\Sigma^+ - X^2\Pi$ system. No product analysis was carried out and the results are summarized in Table I.3.

The reaction of CH with O_2 was studied very recently by Messing *et al.*,[18] who produced CH by the multiple photon dissociation of methylamine using a TEA CO_2 laser. The rate constant, measured by following the laser induced fluorescence (LIF) of the Q branch of the (0,0) band of the $A^2\Delta \rightarrow X^2\Pi$ system at 431.4 nm, was in good agreement with that determined from the chemiluminescence of the $OH(A^2\Sigma^+)$ radical, thus establishing the nature of the reaction as:

$$CH(X^2\Pi) + O_2(X^3\Sigma g^-) \longrightarrow CO(X^1\Sigma^+) + OH(A^2\Sigma^+)$$

$$\Delta H = -56 \text{ kcal mole}^{-1}$$

The measured rate constant, $(19.8 \pm 2.4) \times 10^9 \ M^{-1} \ s^{-1}$, was in agreement with the one determined earlier by Bosnali and Perner. In addition to the above reaction, other channels are possible, such as the ones proposed by Lin,[33] who observed infrared laser emission from both CO (5 nm) and CO_2 (10 nm), following the u.v. ($\lambda > 165$ nm) flash photolysis of a $CHBr_3/O_2/SF_6$ mixture:

$$CH(X^2\Pi) + O_2(X^3\Sigma g^-) \longrightarrow CO(X^1\Sigma^+) + OH(X^2\Pi)$$

$$\longrightarrow CO_2(X^1\Sigma g^+) + H(1^2S)$$

Additional routes yielding $CO(a^3\Pi)$ or HCO are also energetically feasible, but have not been confirmed:

$$CH(X^2\Pi) + O_2(X^3\Sigma g^-) \longrightarrow CO(a^3\Pi) + OH(X^2\Pi)$$

$$\longrightarrow CHO + O(^3P)$$

Lin also investigated other systems, such as $CHBr_3/SO_2/SF_6$[56] and $CHBr_3/NO/SF_6$,[57] and suggested the following reactions as being responsible for the observed CO laser emission:

$$CH(X^2\Pi) + O(^3P) \longrightarrow CO(^1\Sigma^+) + H(^2S)$$

$$CH(X^2\Pi) + NO(^2\Pi) \longrightarrow CO(^1\Sigma^+) + NH(^3\Sigma^-)$$

In this system $O(^3P)$ atoms are formed from the photolysis of SO_2; SO_2 is a good source of $O(^3P)$ because of its high extinction coefficient at $\lambda < 200$ nm and the high quantum yield of production of $O(^3P)$ atoms:

$$SO_2 + h\nu\ (\lambda > 165\text{ nm}) \longrightarrow SO(^3\Sigma^-) + O(^3P)$$

On the basis of product analysis, and the variation of the laser intensity with the flash energy and SO_2 concentration, Lin concluded that the laser emission intensity was limited by the following side reactions:

$$CH + CH \longrightarrow C_2H_2$$

$$CH + SO \longrightarrow \text{products}$$

$$CH + SO_2 \longrightarrow HCSO_2,\ CHO + SO$$

Lin and coworkers[13,14,78,79] have also measured the rates of reaction of CH with a variety of substrates. They photolyzed $CHBr_3$ using a pulsed ArF laser and monitored the LIF of the $A^2\Delta \rightarrow X^2\Pi$ transition at 429.8 nm. Their reported rate constants are presented in Table I.3. Since the rate constants for some substrates such as C_2H_2 amd C_2H_4 were redetermined in their latest paper,[79] only the latter values are presented in Table I.3.

A comparison of the rate constants measured by Braun *et al.*, Bosnali and Perner, and Lin and coworkers indicate that Lin's values are, in general, high. Lin ascribed the lower values reported by Braun to his overestimate of the CH recombination rate, on which the evaluation of the rate constants for H_2, N_2 and CH_4 were based. The values for the rate constants of insertion into primary, secondary and tertiary C-H bonds of saturated hydrocarbons indicate the rather indiscriminate nature of the insertion reaction, being close to collision frequency. Furthermore, a comparison among the rate constants for reactions with CH_4, C_2H_4 and C_2H_2 reveals that CH reacts with the unsaturated bonds as well, probably in a fashion parallel to the well documented concerted cycloaddition of CH_2 to alkenes and alkynes. In fact, *ab initio* molecular orbital calculations carried out by Strausz and coworkers[80] predicted a zero activation energy for the asymmetric concerted cycloaddition of $CH(X^2\Pi)$ to ethylene. In comparison, rate constants for $CH_2(A^1A_1)$ reactions with alkanes and alkenes are of the order of 10^{9} M^{-1} s^{-1}, pointing to the lower reactivity of this species.

Lin and coworkers[illegible] also speculated about the nature of the following reactions of CH with inorganic substrates:

$$CH + N_2 \rightleftharpoons HC{=}N{=}N^{\dagger} \xrightarrow{M} HCN_2$$

$$CH + CO \longrightarrow HC_2O\ ?$$

$$CH + CO_2 \longrightarrow HCO + CO$$

yet product analysis is required to confirm the occurrence of these reactions.

Bromomethylidyne, CBr and Chloromethylidyne, CCl

So far, kinetic studies on CBr and CCl have been restricted to only a few reports. Strausz and coworkers[illegible],[illegible] studied CBr reactions by flash photolyzing $CHBr_3$ and monitoring the $A^2\Delta - X^2\Pi$ absorption at 301.4 nm. Tyerman[illegible] flash photolyzed CF_3CCl_3 to generate CCl and monitored the $A^2\Delta - X^2\Pi$ absorption at 278 nm. Most recently, Wampler and coworkers[illegible] photolyzed CCl_4 with an ArF excimer laser, and followed the CCl concentration *via* the LIF of the 278 nm band.

The great similarity in the reactivity of these two carbynes makes it appropriate to discuss them together. The rate constants measured are summarized in Table I.4. Unlike

TABLE I.4

Second Order Rate Constants k_1 for the Reactions of CBr($X^2\Pi$) and CCl($X^2\Pi$) with Saturates and Inorganic Compounds

Substrate	$k_1 \times 10^{-9}$ ($M^{-1}s^{-1}$)		
	CBr	CCl	
	Strausz''	Tyerman''	Wampler''
methane CH_4	<0.003		≤0.00018
propane C_3H_8		0.10 ± 0.02	≤0.0018
isobutane *iso*-C_4H_{10}	0.018 ± 0.009		≤0.00018
methylchloride $\overline{CH_3}Cl$		0.22 ± 0.01	
chlorotrifluoromethane CF_3Cl		0.075 ± 0.008	
carbon tetrachloride CCl_4			0.018 ± 0.002
ethylchloride C_2H_5Cl		0.22 ± 0.02	
cyclohexane c-C_6H_{12}		0.23 ± 0.03	
hydrogen H_2	<0.003	0.03 ± 0.01	
oxygen O_2	1.3 ± 0.5	2.5 ± 0.3	1.80 ± 0.09
nitrogen N_2	<0.004	<0.0015	
nitric oxide NO	13 ± 2		22.0 ± 1.1
sulphur hexafluoride SF_6			0.014 ± 0.001
argon Ar			≤0.00018

CH, which inserts into C-H bonds indiscriminately at rates approaching collision frequency, CBr, on the other hand, is quite non-reactive towards primary C-H bonds, and the data on *iso*butane suggest a slow insertion into the tertiary C-H bond. Similar studies for CCl are less conclusive, since Tyerman observed slow reactions with propane and cyclohexane, while Wampler reported no measurable reaction with saturated hydrocarbons. Also, values for the halomethanes indicate that the C-F bond is slightly more reactive than the C-Cl bond. This is unusual because the C-F bond is much stronger than the C-Cl bond.

Both O_2 and NO are reactive towards these carbynes, but O_2 reacts at least ten times faster with CH. Furthermore, the reactions of O_2 with CBr, which are highly exothermic,[53] could contribute to the CO and CO_2 laser emission observed by Lin,[55] in the flash photolysis of $CHBr_3/O_2$ mixtures:

$$CBr({}^2\Pi) + O_2({}^3\Sigma g^-) \longrightarrow CO^{\dagger}({}^1\Sigma^+) + BrO({}^2\Pi)$$

$$\Delta H = -117 \text{ kcal mole}^{-1}$$

$$\longrightarrow CO_2^{\dagger}({}^1\Sigma g^+) + Br({}^2P)$$

$$\Delta H = -188 \text{ kcal mole}^{-1}$$

The same could be true for the CO laser emission observed in $CHBr_3/NO$ mixtures,[57] although BrN has not been detected and the exothermicity of this reaction has not been evaluated:

$$CBr(^2\Pi) + NO(^2\Pi) \longrightarrow CO^{\dagger}(^1\Sigma^+) + BrN$$

$$\longrightarrow CN(^2\Pi) + BrO(^2\Pi)$$

$$\Delta H = -11 \text{ kcal mole}^{-1}$$

The lower reactivity of CBr and CCl, compared to CH, is again displayed in the results on alkenes and alkynes (Tables I.5, I.6). For example, CBr and CCl react two orders of magnitude slower (or as much as three orders of magnitude, based on Lin's results) with ethylene, and three orders of magnitude slower with acetylene. Consequently, CBr and CCl display a more selective behaviour in their reactions, which seems to be manifested more with the less reactive alkynes than with the alkenes. For CBr, the rate constants for the methyl-substituted and fluorinated ethylenes, compared with that for ethylene itself, clearly reveal the electrophilic nature of this carbyne which, as suggested earlier, can be attributed to the presence of an empty and a half-filled p orbital on the carbon atom. However, Tyerman reported that the reactivity of CCl with ethylenes increases with increasing halogenation; these results appear to be unusual and warrant further investigation.

Fluoromethylidyne, CF

From studies in shock-tube heating of CF_4 - C_2F_4 mixtures,[62] a value of $k = 6.57 \times 10^{26}\ T^{-2.85}\ ml^2\ mol^{-2}\ s^{-1}$

TABLE I.5

Second Order Rate Constants k_1 for the Reactions of $CBr(X^2\Pi)$ and $CCl(X^2\Pi)$ with Alkenes and Benzene

Substrate	$k_1 \times 10^{-9} (M^{-1}s^{-1})$	
	CBr	CCl
	Strausz and coworkers[25]	Tyerman[81]
ethylene C_2H_4	0.46 ± 0.07	0.33 ± 0.04
propylene C_3H_6	5.5 ± 0.2	2.5 ± 0.25 0.13 ± 0.01[b)]
1-butene $1\text{-}C_4H_8$	9 ± 1	
trans-2-butene *t*-C_4H_8	6 ± 1	9.6 ± 0.8
iso-butene *iso*-C_4H_8		15.5 ± 1.1
tetramethylethylene $(CH_3)_2CC(CH_3)_2$	12 ± 1	
CF_2CCl_2		1.9 ± 0.15
$CFClCCl_2$		8 ± 4
$CHClCCl_2$		4 ± 2
C_2Cl_4		10 ± 5
C_2H_3F	0.18 ± 0.01	
c,*t*-$C_2H_2F_2$	0.12 ± 0.01	
C_2HF_3	side reactions	
C_2F_4	side reactions	
benzene c-C_6H_6	0.22 ± 0.02[a)]	

a) Ruzsicska[84] b) Wampler and co-workers[82]

TABLE I.6

Second Order Rate Constants k_1 for the Reactions of CBr($X^2\Pi$) and CCl($X^2\Pi$) with Alkynes

Substrate	k_1 x 10^{-9}($M^{-1}s^{-1}$)	
	CBr	CCl
	Strausz and coworkers[26]	Tyerman[81]
acetylene	0.081 ± 0.007	0.11 ± 0.01
acetylene-d_2	0.072 ± 0.007	
propyne	4.8 ± 0.6	2.4 ± 0.2
1-butyne	6.2 ± 1.1	
2-butyne	24 ± 5	
1-pentyne	3.6 ± 0.8	
2-pentyne	20 ± 3	
2,2,5,5-tetramethyl-3-hexyne	9.7 ± 1.6	
2-butyne-F_6	0.020 ± 0.002	

was estimated for the reaction CF + F + M, where M = Ar. To date this is the only kinetic measurement on CF reactions reported in the literature.

However, the presence of CF was invoked in order to explain the origin of the CO laser emission observed by Hsu and Lin[45] in the $CFBr_3/SO_2/SF_6$ system,

$$CF(^2\Pi) + O(^3P) \longrightarrow CO^{\dagger}(^1\Sigma^+) + F(^2P)$$

with the possible side reactions postulated to be:

$$CF + CF \longrightarrow C_2F_2$$

$$CF + SO \longrightarrow \text{products } (FCO + S, \text{ etc.})$$

$$CF + SO_2 \longrightarrow \text{products } (FCO + SO, \text{ etc.})$$

Also, in the $CFBr_3/NO/SF_6$ system, examined by Burks and Lin,[44] CF was proposed to be the precursor of $O(^3P)$ atoms:

$$CF(^2\Pi) + NO(^2\Pi) \longrightarrow FCN + O(^3P)$$

$$CF(^2\Pi) + O(^3P) \longrightarrow CO^{\dagger}(^1\Sigma^+) + F(^2P)$$

The following possible side reactions were suggested as limiting the laser output:

$CF + CF \longrightarrow C_2F_2$

$CF + NO \longrightarrow FCO + N$

$CF + N \longrightarrow CN + F$

Carbethoxymethylidyne, CCO_2Et

The liquid phase study on CCO_2Et is, to date, the most comprehensive mechanistic investigation of the nature of carbyne reactions.[49-52] Photolysis of mercury*bis*diazoacetate at $\lambda < 280$ nm produces CCO_2Et, which was found to undergo insertion into the C-H bonds of alkanes, alkenes and alcohols, the O-H bonds of alcohols, and stereospecific cycloaddition to C=C bonds.

On photolysis in cyclohexane, C-H insertion was regarded as being responsible for the formation of the principal products ethyl cyclohexylacetate (I) and diethyl-2,3-dicyclohexylsuccinate (II):

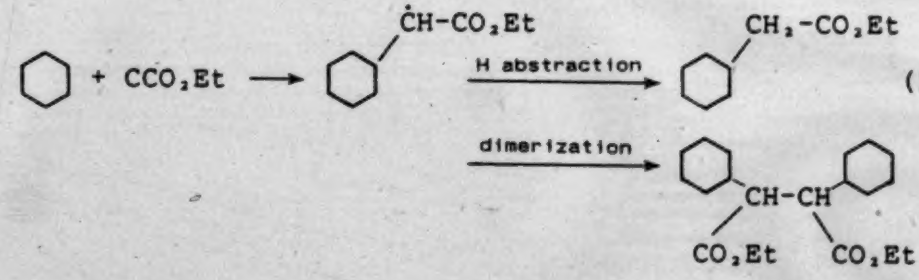

(I)

(II)

Cyclopropyl radical intermediates played an important role in the reactions with alkenes. With cyclohexene, the products ethyl *endo*- (III) and ethyl *exo*-norcarane-7-carboxylate (IV) were ascribed to cycloaddition of the carbyne, followed by H abstraction:

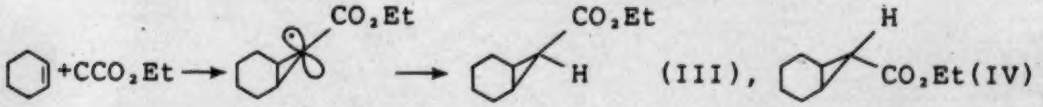

The observation that the less stable *endo* isomer is the predominant product was rationalized on the basis of steric considerations, i.e. radical attack would preferentially take place on the more exposed side of the p orbital, giving rise to the *endo* product. The *endo* - *exo* ratio was found to be dependent on the photolysis wavelength, decreasing from 8.2 to 4.3 with increasing wavelength of irradiation. However, at all wavelengths, the values are considerably higher than those obtained from the reaction of carbethoxymethylene (which is a minor photolysis product) with cyclohexene. Thus the photolysis of ethyl diazoacetate (a precursor of carbethoxymethylene) in cyclohexene leads to the formation of *endo* and *exo* addition products in the ratio of ~ 0.5.[45,46] Therefore the high preponderance of the *endo* isomer in the photolysis of mercury*bis*diazoacetate is a clear indication that the reacting species is definitely the carbyne.

The cyclopropyl radical intermediate can also undergo an addition reaction with cyclohexane and the resulting radical subsequently disproportionates to form ethyl norcarane-7-(3'-cyclohexenyl)-7-carboxylate (V) and ethyl norcarane-7-cyclohexyl-7-carboxylate (VI).

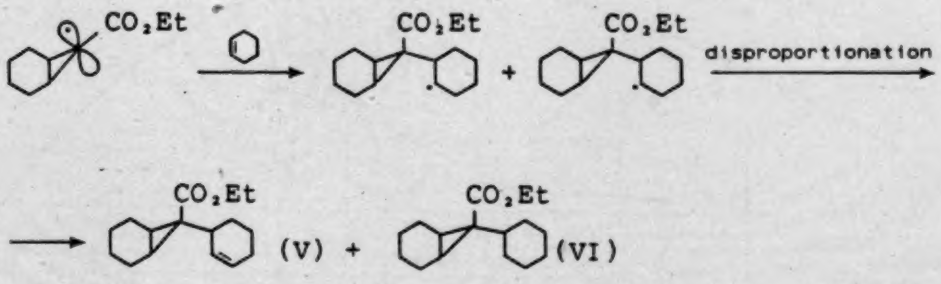
CO₂Et
CO₂Et
CO₂Et
disproportionation
CO₂Et
(V)
CO₂Et
(VI)

CCO_2Et was also shown to insert into the C-H bonds of cyclohexene, and exhibits a slight preference for the weaker allylic C-H bond, as indicated by the relative yields of ethyl (3'-cyclohexenyl)acetate (VII), ethyl (1'-cyclohexenyl)acetate (VIII), and ethyl (4'-cyclohexenyl)acetate (IX):

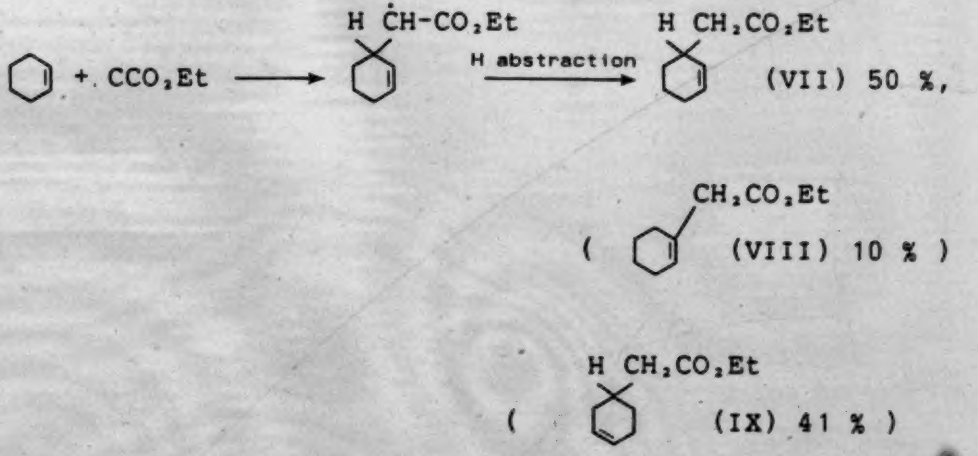
+ CCO₂Et
H ĊH-CO₂Et
H abstraction
H CH₂CO₂Et
(VII) 50 %,
CH₂CO₂Et
((VIII) 10 %)
H CH₂CO₂Et
((IX) 41 %)

Similar results were observed with *cis*- and *trans*-2-butenes. In addition to allylic C-H bond insertion products, cycloaddition led to the formation of ethyl *cis*-2,3-dimethylcyclopropane-*cis*-carboxylate (*endo* isomer) (X) and ethyl *cis*-2,3-dimethylcyclopropane-*trans*-carboxylate (*exo* isomer) (XI) in the reaction with *cis*-2-butene:

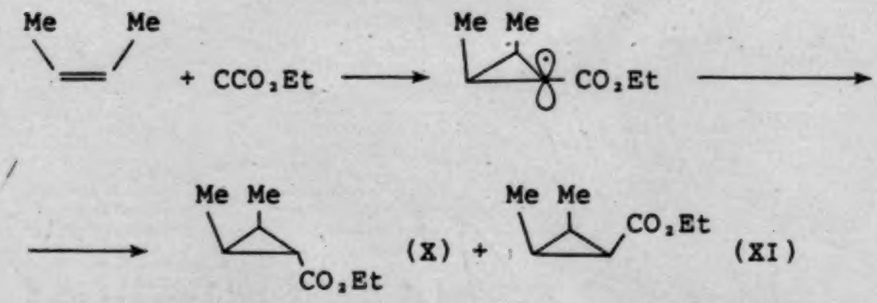

In contrast, only ethyl *trans*-2,3-dimethylcyclopropanecarboxylate (XII) was obtained with *trans*-2-butene:

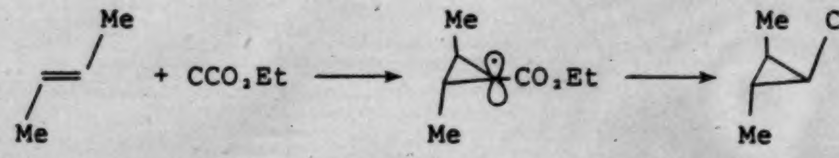

(XII)

These results clearly reveal the stereospecifity of the cyclopropane formation, and strongly suggest that $CCO_2Et(X^2\Pi)$, and most likely all doublet ground state carbynes, undergo concerted, but, as molecular orbital calculations suggest, orbital symmetry forbidden, addition reactions with alkenes. This confirms the hypothesis that, on a spin multiplicity basis, doublet ground state carbyne can be regarded as the analog of singlet carbene, which is known to undergo concerted, asymmetric addition reactions with alkenes.

The reactions with 2-propanol is slightly more complex since insertion into both the O-H and C-H bonds takes place, leading to the formation of the principal products XIII and XIV:

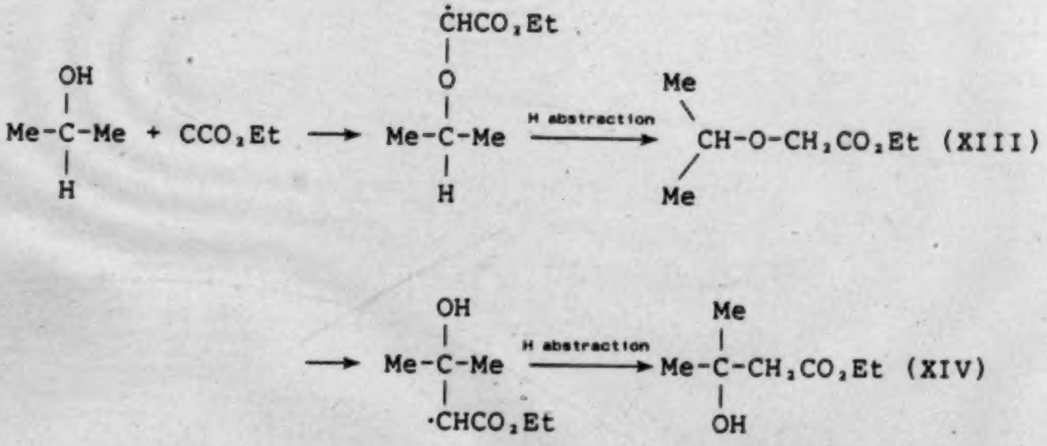
H abstraction
H abstraction
(XIII)
(XIV)

Ethyl 3-methyl-2-butenoate (XV) and *iso*propyl ethoxyacetate (XVI) were also formed. XV was postulated to arise from the dehydration of XIV, whereas the production of XVI was believed to involve a ketene type intermediate formed *via* ethoxy migration:

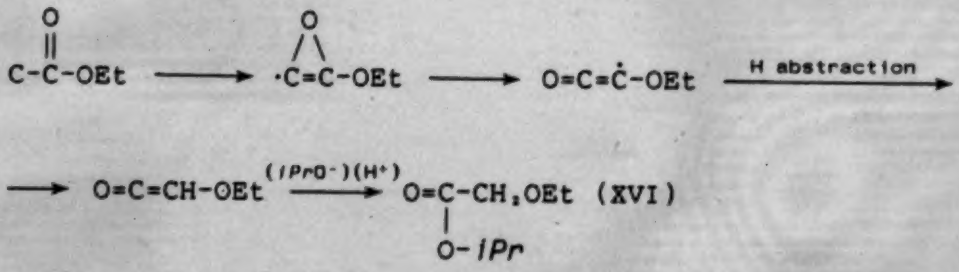
H abstraction
(iPrO⁻)(H⁺)
(XVI)

Kennepohl[53] also investigated the reaction of CCO_2Et with pyrrole and benzene. The prominent feature of the reaction with these substrates was the formation of a cyclopropyl radical intermediate, followed by facile ring expansion.

With pyrrole, the predominant products were ethyl pyridine-3-carboxylate (XVII) and ethyl α-pyrrolacetate (XVIII). XVII was most likely a ring-expansion product,

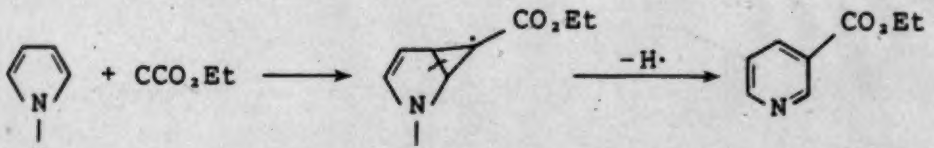

+ CCO₂Et
CO₂Et
-H·
CO₂Et
N
H

(XVII)

while XVIII was probably formed by:

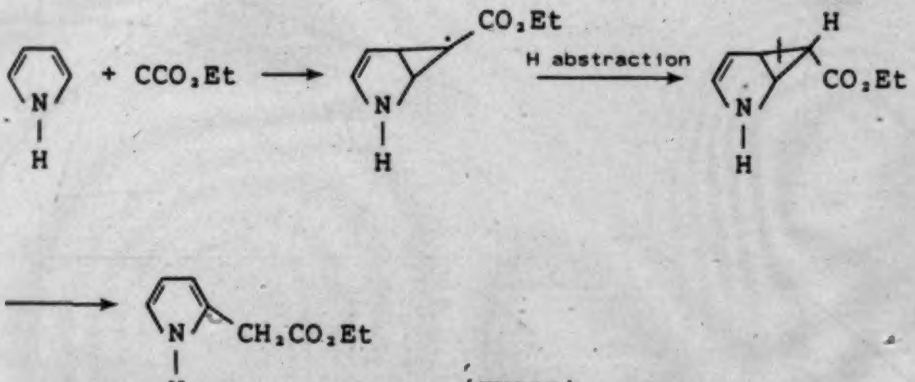

+ CCO₂Et
CO₂Et
H abstraction
H
CO₂Et
CH₂CO₂Et
N
H

(XVIII)

Traces of ethyl pyridine-2-carboxylate (XIX) and dihydropyridines (XX), (XXI) were also detected, and their production schemes were tentatively formulated as:

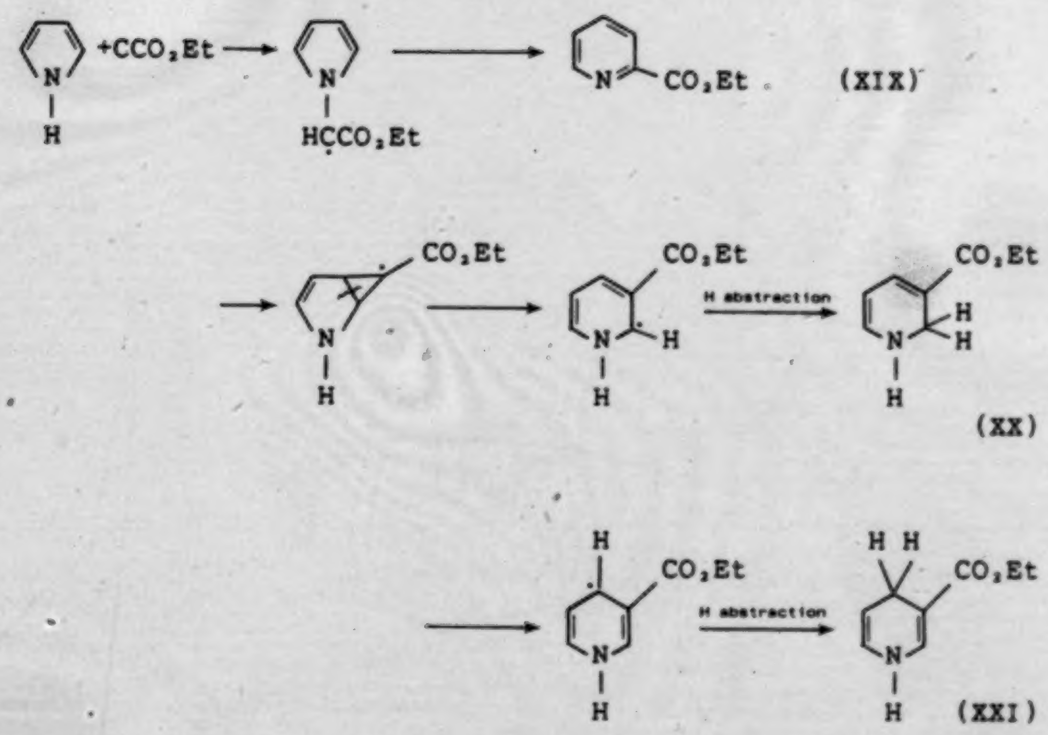
+CCO₂Et
HCCO₂Et
CO₂Et
H abstraction
H abstraction
N
H

(XIX)

(XX)

(XXI)

The photolysis in benzene led to the formation of ethyl cycloheptatriene-carboxylate dimer (XXII) *via* addition of the carbyne across the C=C bond:

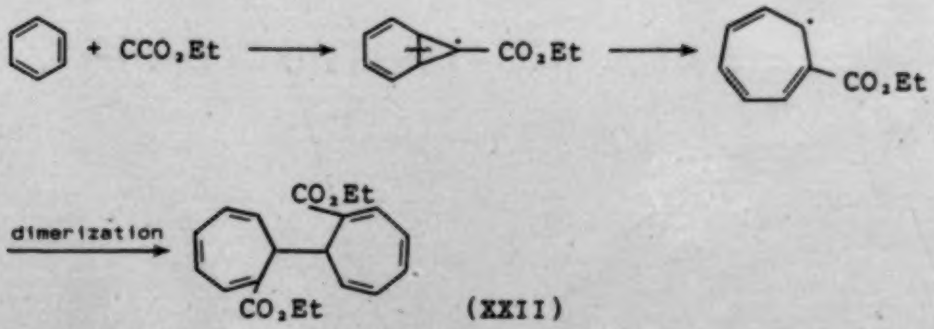
+ CCO₂Et
CO₂Et
dimerization

(XXII)

B. FLASH PHOTOLYSIS

Since the original paper of Norrish and Porter[illegible] appeared thirty years ago, flash photolysis has undergone significant technical refinements, and has become a major implement for photochemical studies of fast reactions. Since flash photolysis is no longer new and many articles have been written on this subject, a brief description of a conventional system here should suffice.

In flash photolysis, a non-equilibrium situation can be created, in a short initiation time of microseconds, and recently, nanoseconds, by a photolysis lamp which produces a high intensity flash. This provides the energy required for the generation of large concentrations of the radical intermediate being studied. Reaction of the radical with an added substrate would alter its decay rate, which can be measured in two ways by kinetic absorption spectroscopy.

1. Flash Spectroscopy

In the first approach the whole absorption spectrum is recorded at a given time. This is accomplished by a monitoring beam from the spectroscopic lamp, fired at a pre-set delay time, which provides essentially a background continuum. After passing through the reaction mixture, the beam is resolved by the spectrograph and recorded on a photographic plate. The procedure is repeated at various delays, so as to obtain a time profile of the chosen absorption band of the transient.

2. Kinetic Spectrophotometry

Here, a single absorption line is monitored as a function of time. This requires the replacement of the spectroscopic flash lamp by a continous light source, and a monochromator to isolate the single wavelength, which is detected by a photomultiplier. The output is stored in a transient recorder and the decay profile of the transient can be displayed on an oscilloscope or on graph paper by using an x-y recorder.

C. AIM OF THE PRESENT INVESTIGATION

The development of improved techniques for the production and detection of radical intermediates in the past two decades has led to a growing body of knowledge concerning the chemistry of carbynes. CH has been well studied, and shown to insert indiscriminately into primary, secondary and tertiary C-H bonds, and also to undergo concerted, asymmetric cycloadditions with alkenes and alkynes. Rate constants have been measured for a variety of substrates: they are all very high, close to collision frequency, and consequently exhibit little variation with the nature of substrates. CCO_2Et also undergoes insertion and concerted cycloaddition, and these reactions appear to be characteristic of carbynes in general.

The early work of Simons and Yarwood has shown that CCl and CBr can be produced by the flash photolysis of a variety of precursors. Although the simultaneous generation of other radical species precludes mechanistic studies by means of product analysis, all these systems are perfectly amenable to kinetic studies.

At the time this project was initiated, some rate constants for the reactions of CCl and CBr with selected alkanes, alkenes and alkynes had been reported (cf Tables I.4 - I.6). In general, they are somewhat lower than those for the analogous CH reactions and in fact the pattern of reactivity towards alkenes and alkynes upon substitution suggests a marked electrophilic character for CCl and CBr. Inspection of the data in Table I.4, however, reveals some inconsistencies:

- Strausz and coworkers[25] reported that CBr is non-reactive towards primary and secondary C-H bonds, and inserts slowly into tertiary C-H bonds, whereas Tyerman[41] reported that CCl, whose reactivity should closely parallel that of CBr, reacts at a measurable rate with propane.
- the rate data for the halomethanes suggest that the rates of reaction with C-F bonds are faster than with C-Cl bonds.[41,42]

It was therefore decided to initiate a kinetic investigation of the reactions of CCl with a variety of substrates, not only in order to resolve the above discrepancies, but to delineate, hopefully on a quantitative basis, the relationship between the reactivity of CCl and the physicochemical properties of the substrates. $CHClBr_2$ was chosen as the precursor of CCl since it is readily available and has been shown to generate CCl in a more or less well defined manner. The following substrates were chosen for study:

- straight chain, branched and cyclic alkanes, in order to assess the effect of the C-H bond strength on the rate of insertion;
- an extensive series of alkynes, to firmly establish the electrophilic nature of CCl;
- silanes, in order to see whether the d-orbitals on the silicon atom would affect the reactivity of CCl; and also to investigate the possibility of insertion into the Si-Si bond;
- halogenated silanes, as a further test of the electrophilic nature of CCl and to see whether the Si-F and Si-Cl bonds are reactive;
- finally, a few selected heterocyclic compounds in order to see whether the site of attack would be shifted to the O, S or N atom.

II. EXPERIMENTAL

A. APPARATUS

1. The Vacuum System

The Main Vacuum System

A conventional high-vacuum system constructed of Pyrex was used for the gas-phase kinetic study. It was completely grease-free, utilizing mainly helium-tested Hoke Valves and Teflon Valves, and consisted of a distillation train and a storage unit (Figure II.1).

The vacuum system was evacuated to a pressure of 10^{-6} torr by means of a mercury diffusion pump backed by a rotary pump (Duo-Seal Vacuum Pump, Model 5KC42 JG14A, W.M. Welch Manufacturing Company). Relative pressures were monitored by Pirani Vacuum Gauges (type GMA140), while absolute measurements were made by mercury manometers and an MKS Baratron Pressure Meter (type 77) capable of measuring absolute pressures in the range 10^{3} to 10^{-2} torr.

The distillation train, consisting of a series of three traps isolated by Teflon Valves, was used for purification of the reagents. The storage system consisted of four 3 - litre bulbs for the temporary storage of reaction mixtures to be used in the flash photolysis.

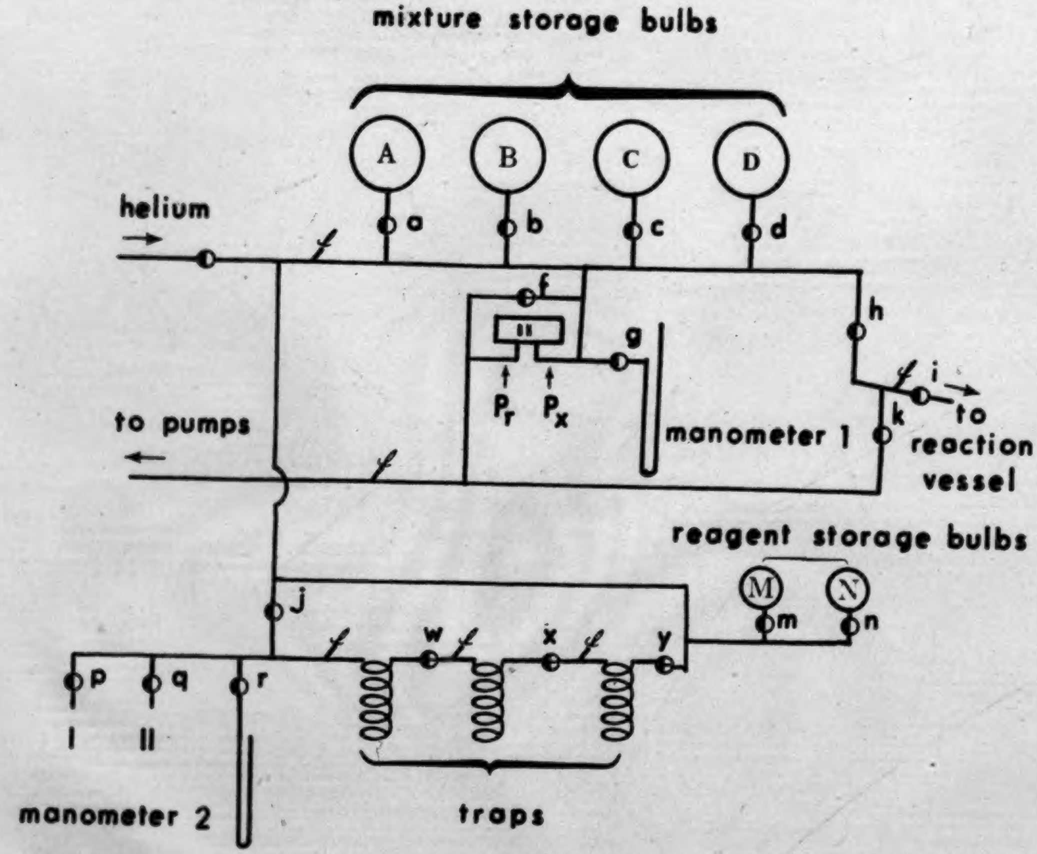
mixture storage bulbs
A
B
C
D
helium
a
b
c
d
f
g
h
i
k
to reaction vessel
P_r
P_x
to pumps
manometer 1
reagent storage bulbs
M
N
m
n
j
w
x
y
p
q
r
I
II
manometer 2
traps

ƒ : Pirani Vacuum Gauge Tube

|| : Baratron Pressure Meter Head

◐ : Hoke Valve

⊖ : Teflon Valve

I : Inlet for the introduction of liquid reagents

II : Inlet for the introduction of gasous reagents

FIGURE II.1 The Main Vacuum System

The Helium Line

Helium was introduced into the main vacuum line after passage through a 30 cm long column of copper turnings (heated to 350°C by heating-ribbons for the removal of oxygen) and a 30 cm long column of molecular sieve (type 5A, for the removal of water vapour).

The Lamp Vacuum System

A separate mercury-free line was used to fill the flash lamps. Vacuum was achieved by a Duo-Seal Vacuum Pump (Model 5KH35KG113E) and the pressure was measured by a mercury manometer with N.R.C. DC 704 pump oil covering the surfaces of the mercury.

2. The Flash Photolysis System

The major components of the flash photolysis system are illustrated in Figure II.2.

The Reaction Vessel and The Reflective Housing

The reaction vessel (Figure II.2) was a quartz cylindrical tube 72 cm long and 21 mm in inner diameter. It was equipped with flat, quartz windows on both ends and a side - arm for the introduction and removal of the reaction mixture. The side-arm was connected to the main vacuum system by a Nupro Valve, which facilitated the detachment of the reaction vessel from time to time for cleaning.

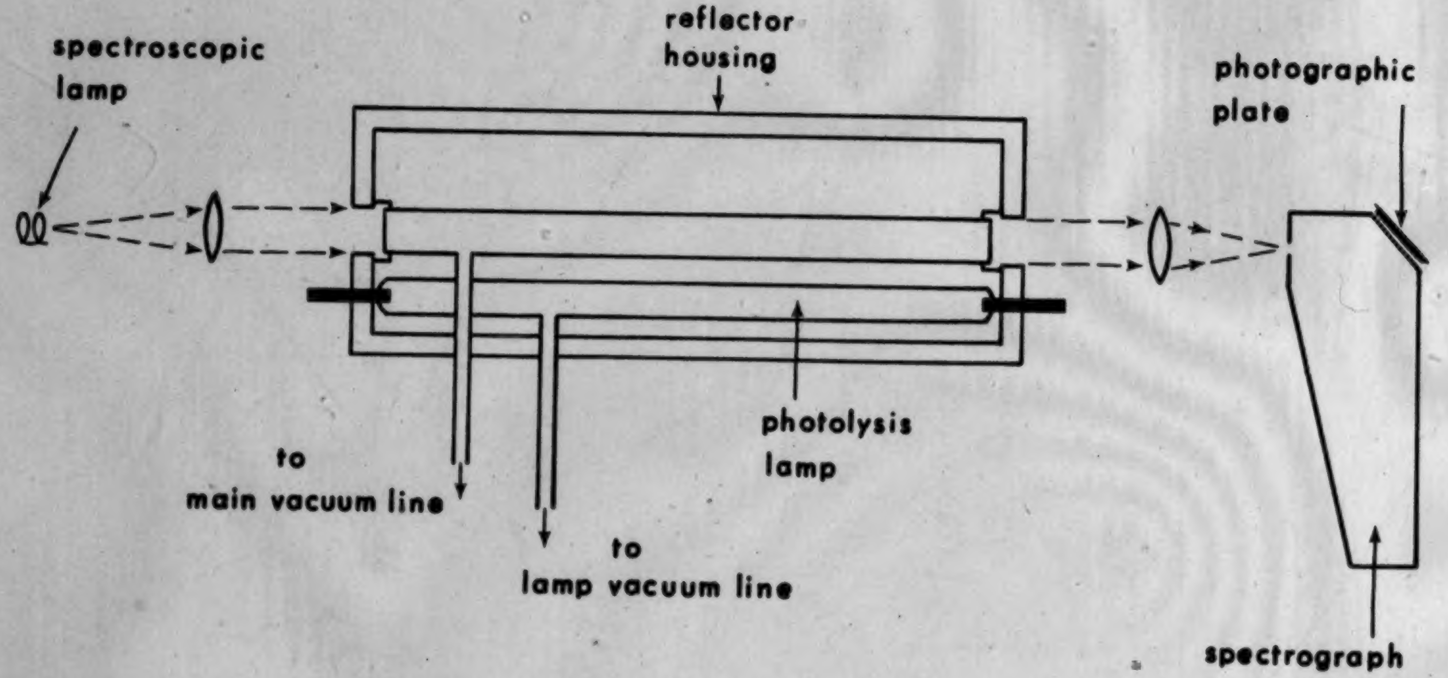
spectroscopic
lamp
reflector
housing
photographic
plate
photolysis
lamp
to
main vacuum line
to
lamp vacuum line
spectrograph

FIGURE II.2 The Flash Photolysis System

The reaction vessel, sitting on two end-supports, was positioned at the centre of a reflective housing assembly lying horizontally along the optical path. Apertures on both ends allowed the passage of light in and out through the reaction vessel.

The housing (Figure II.3) was constructed of aluminum and was cylindrical in shape, 80 cm long and 15 cm in inner diameter. It consisted of two half-cylinders joined together by hinges on one side, so that the upper half could be opened for the removal of the reaction vessel and the photolysis lamp for cleaning. The lower half, upon which the ends of the reaction vessel and the photolysis lamp rested, was mounted by two supports onto the optical bench.

The inner surface of the reflector was coated with MgO which was highly reflective in the visible and quartz u.v. region of the spectrum. Occasional repainting was necessary due to the tendency of the MgO to flake off rather easily.

The Photolysis Lamp

The photolysis lamp (Figures II.2 and II.3) was a quartz tube 19 mm in inner diameter equipped with a side-arm for filling and evacuation. Molybdenum-alloy electrodes (Vitreosil Model T/E7/232) were sealed into each end by standard lead seals able to withstand high thermal shock. The distance between the tips of the electrodes, 73 cm, was about the same as the length of the reaction vessel. The side-arm was connected to the lamp vacuum line through a

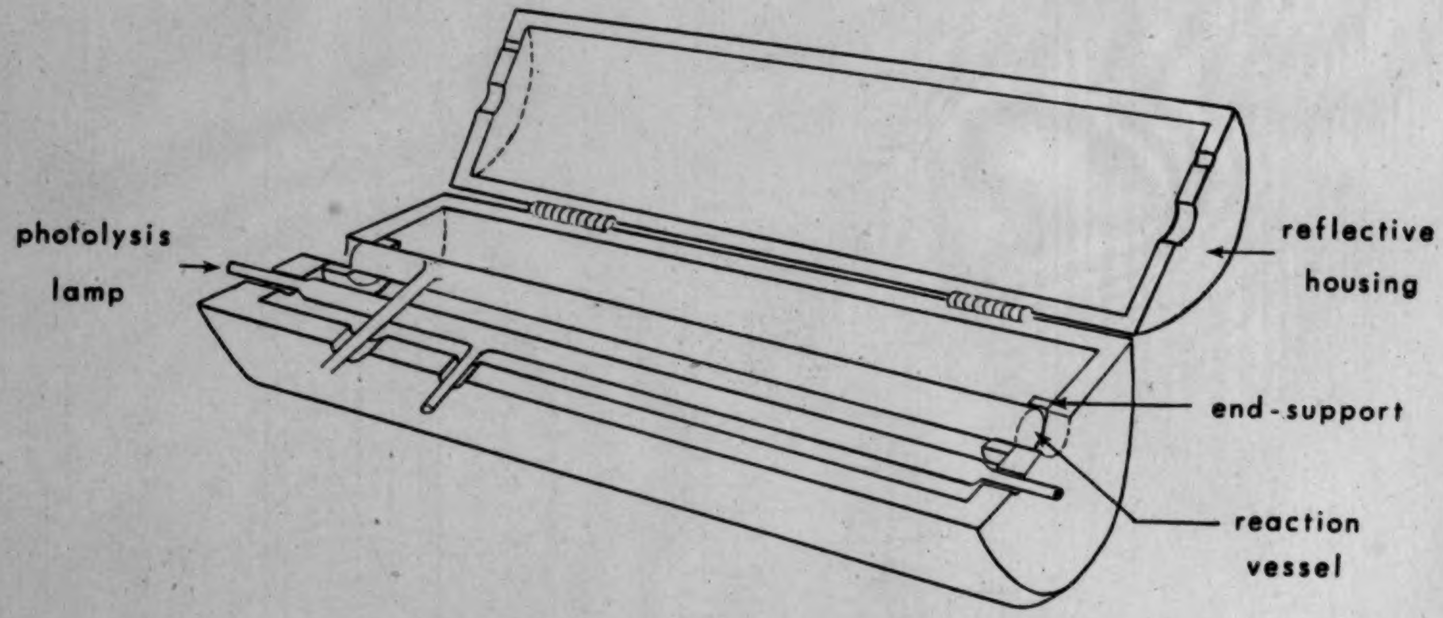
photolysis lamp
reflective housing
end-support
reaction vessel

FIGURE II.3 The Reaction Vessel and the Reflective Housing

high vacuum stopcock (Pyrex V-4) and a detachable ball - joint. The stopcock isolated the lamp from the vacuum line while the ball-joint facilitated the removal of the lamp for cleaning.

The lamp was placed horizontally next to the reaction vessel, with the electrodes resting on the ends of the reflector housing and protruding outside through the end apertures. When filled with 50 torr krypton, the flash reached its maximum intensity in 14 sec and had a half-life of about 22 sec. The lamp circuit included an ignitron (Type NL 7703), which controlled the firing of the lamp, and a G.E. Energy Storage Capacitor (capacitance = 14.5 μF, voltage = 20 kV) which dissipated 2900 kJ per photolysis flash.

To condition a new lamp the following method was used: the lamp was fired initially at a low voltage and the firings were repeated with gradually increasing voltages until the designated voltage (20 kV) was reached. The repeated firings helped to condition the new lamp to the thermal shock of firing at a high voltage, and to degas the electrodes.

The Spectroscopic Lamp

The spectroscopic lamp (Figure II.4) was also made of quartz, and molybdenum alloy electrodes (Vitreosil Model T/E7/232) were sealed into the side-arms by standard lead seals. They were separated by a short capillary tube, 5 cm

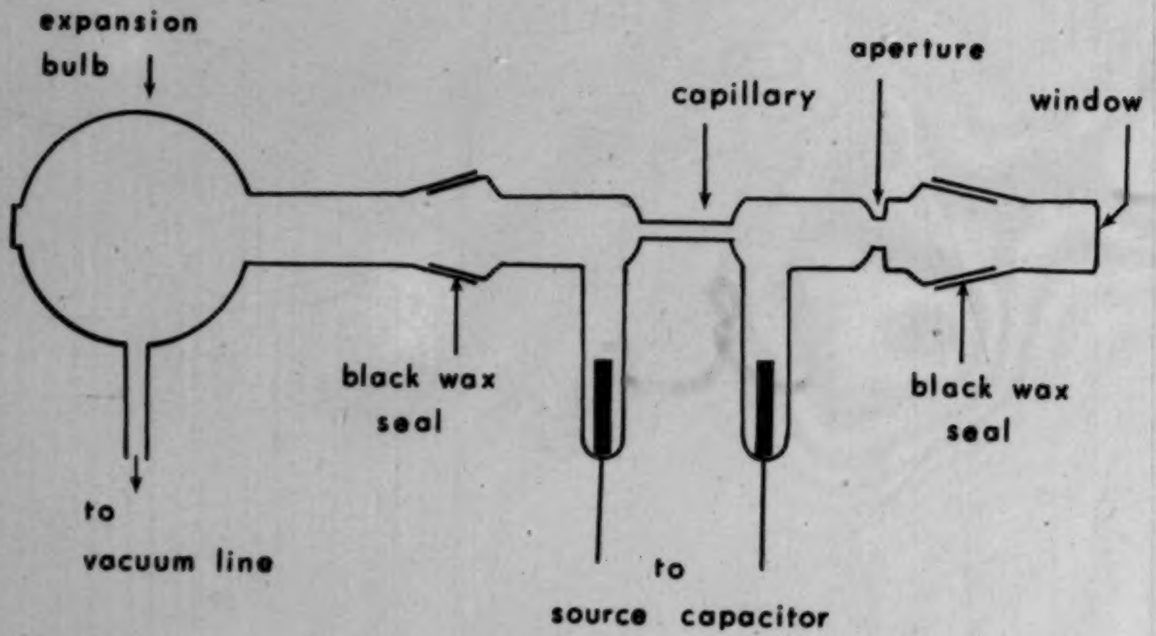
expansion bulb
capillary
aperture
window
black wax seal
black wax seal
to vacuum line
to source capacitor

FIGURE II.4 The Spectroscopic Flash Lamp

long and 3 mm in inner diameter, to ensure high current density and the generation of a plasma. An aperture which was close to the lamp window minimized the passage of silica towards the window, and an expansion bulb was used to accomodate the shock wave which accompanied the flash. The lamp parts were sealed together by black wax to facilitate frequent cleaning, and the lamp was connected to the lamp vacuum line through a high vacuum stopcock (Pyrex V-4) and a detachable ball-joint.

Like the photo-lamp, the spec-lamp was also filled with 50 torr krypton. At this pressure, the spectroscopic flash provided essentially a background continuum. The flash reached its maximum intensity in 6 μsec and had a half-life of about 14 μsec. The lamp circuit also included an ignitron (National Tube NL-7703) and a Tobe Energy Storage Capacitor (Model ESC-357, capacitance = 1.0 μF, voltage = 20 kV) which provided an energy of 200 kJ per flash. The spec-lamp was also conditioned by repeated firings at lower voltages.

The Lenses

Fused quartz lenses were used to collimate the spectroscopic beam during its passage across the reaction vessel and to focus it at the entrance slit of the spectograph. Since the refractive index, n, of the lens changes with light frequency, a small focal length adjustment was necessary.

The focal length f of a lens whose two faces have radii of curvature r_1 and r_2 is given by:

$$\frac{1}{f} = (n - 1)\left(\frac{1}{r_1} + \frac{1}{r_2} \right)$$

This results in the following relationship for the focal lengths of a lens in light of wavelengths $\lambda\alpha$ and $\lambda\beta$:

$$\frac{f(\lambda\alpha)}{f(\lambda\beta)} = \frac{n(\lambda\beta) - 1}{n(\lambda\alpha) - 1}$$

The refractive index n of fused quartz in Na light ($\lambda = 589.3$ nm) is 1.46, and in Cd light ($\lambda = 274.9$ nm), which is close to 280 nm, the region of the u.v. spectrum under investigation here, n = 1.50. Therefore,

$$f_{274.9\,nm} = f_{589.3\,nm}\left(\frac{1.46 - 1}{1.50 - 1}\right)$$

The focal lengths of lens #1 and lens #2 in visible light are 16 cm and 32 cm respectively. Thus,

for lens #1 $$f_{274.9\,nm} = 16\text{ cm}\left(\frac{1.46 - 1}{1.50 - 1}\right) = 14.7\text{ cm}$$

for lens #2 $$f_{274.9\,nm} = 32\text{ cm}\left(\frac{1.46 - 1}{1.50 - 1}\right) = 29.4\text{ cm}$$

Therefore lens #1 was placed 14.7 cm from the spec-lamp and lens #2, 29.4 cm from the spectrographic slit (Figure II.2).

The Spectrograph

The monitoring beam from the spectroscopic lamp entered the spectrograph (Hilger & Watts Model 742.1) through an entrance slit (slit width = 0.010 mm) (Figure II.5). In this Littrow mounting system, utilizing a quartz prism as a dispersion device, each incident ray traversed the prism twice and the resolved spectrum was focussed on a light-sensitive photographic plate (Kodak Spectroscopic Plates ClFO Type 103a-0). The absorption lines in the spectrum were traced out as absorption peaks using a microdensitometer.

The Operation of The Flash Photolysis System

The circuit diagram is illustrated in Figure II.6.

The two lamp capacitors were first charged up to the desired voltages. Pushing the 'start' button supplied the necessary energy for the firing of the photolamp ignitron, which behaved in a similar manner to a spark gap. This closed the lamp circuit and caused the capacitor to discharge through the lamp, producing the photolysis flash. The current generated from the discharge was relayed to the delay generator through the trigger coil. This, after a pre-selected time delay, fired the spectroscopic-lamp ignitron and in turn caused the capacitor to discharge through the lamp. The spectroscopic flash traversed the

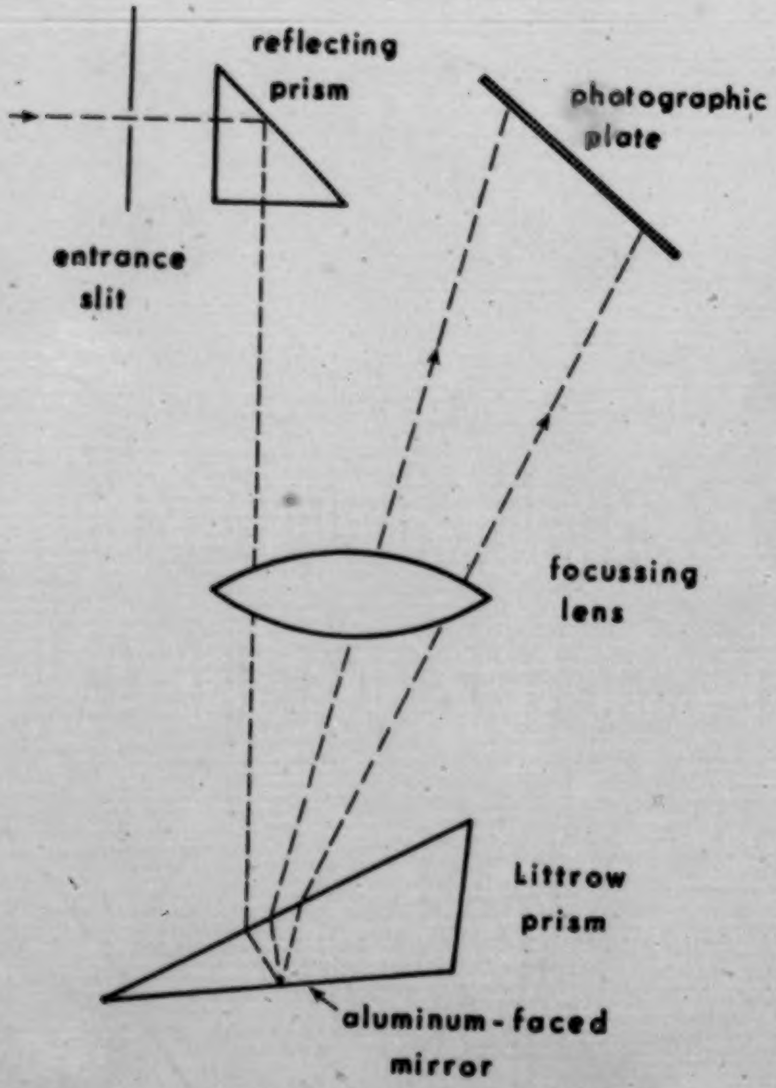
reflecting prism
photographic plate
entrance slit
focussing lens
Littrow prism
aluminum-faced mirror

FIGURE II.5 The Littrow Prism and Mounting

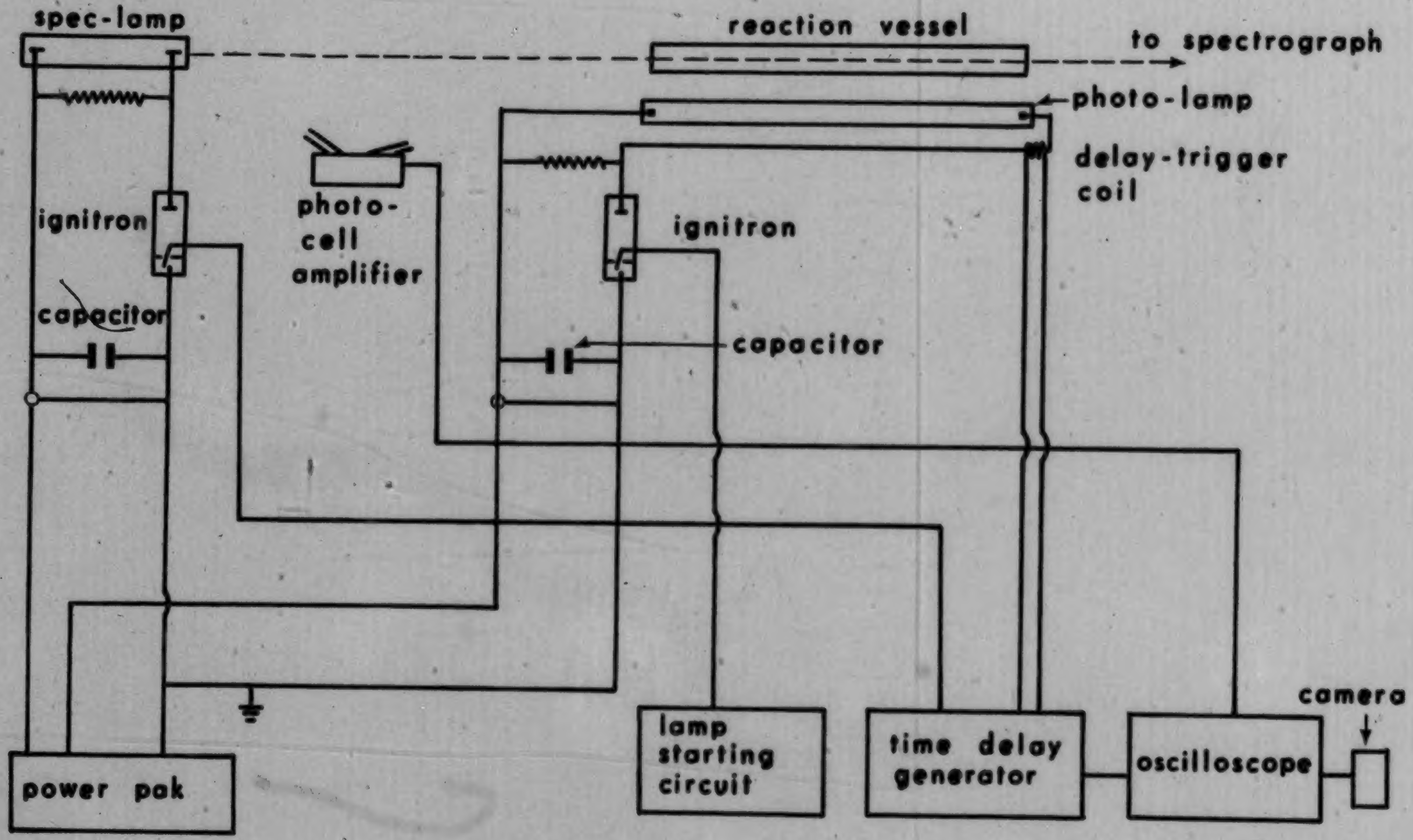
spec-lamp
reaction vessel
to spectrograph
photo-lamp
delay-trigger coil
photo-cell amplifier
ignitron
capacitor
ignitron
capacitor
power pak
lamp starting circuit
time delay generator
oscilloscope
camera

FIGURE II.6 The Flash Photolysis System: Circuit Diagram

reaction vessel axially and was resolved by the spectrograph. The resulting spectrum was recorded on a photographic plate.

The Delay Generator

The delay generator (Type 1217-C General Radio Company) ensured that the spec-lamp was fired at a pre-selected delay time after the photolysis flash. This was accomplished in the following manner: the delay pulse which was relayed from the photo-lamp circuit through the trigger coil entered the output pulse circuit of the Delay Generator and initiated the charging of a capacitor; the rate of charging was dependent on the values of a resistor in the circuit, which was controlled by the settings of a Delay-Time Dial. Once the capacitor was charged up, the voltage in the circuit would be sufficiently strong to turn on a vacuum tube, generating a delayed pulse as an output of the circuit, which eventually reached the spec-lamp circuit and fired the spec-lamp ignitron.

Owing to the limitations of the apparatus (± 5% uncertainty), a means of monitoring the real time delay was necessary. The method was as follows.

Time-Delay Monitoring

When the photo-lamp capacitor discharged across the lamp, but before the high intensity pulse was produced, the current relayed to the delay generator simultaneously activated the horizontal sweep of the oscilloscope (Hewlett-Packard 130C). Moreover, the light pulses from the two flashes were picked up by a photocell (Sylvania, 90CV), amplified, and also displayed on the oscilloscope screen but as vertical signals. The trace was photographed (Hewlett-Packard Oscilloscope Camera, Model 197A) using Polaroid Black and White Films (Type 107 Land Film). The separation between the peak of the photolysis flash signal and that of the following spectroscopic flash signal was taken as the time delay. A typical oscilloscope trace is shown in Figure II.7.

3. Miscellaneous

The Baratron Pressure Meter and the Pressure Meter Head

The MKS Baratron Type 77 Electron Pressure Meter (Figure II.8) was connected to a Pressure Meter Head (Type 77H-300) by a cable. The Head measures absolute pressures by means of a mechanical diaphragm. The sample side Px was separated from the reference side Pr, which was always under vacuum, by closing the valve f (Figure II.1)

The Pressure Readout Dials controlled the amount of pressure applied electronically to the diaphragm on the reference side Pr. If the pressure at Px > Pr, the meter would deflect to the right (positive pressure), whereas if Px < Pr, the meter would move to the left (negative pressure); for Px = Pr the meter would read zero.

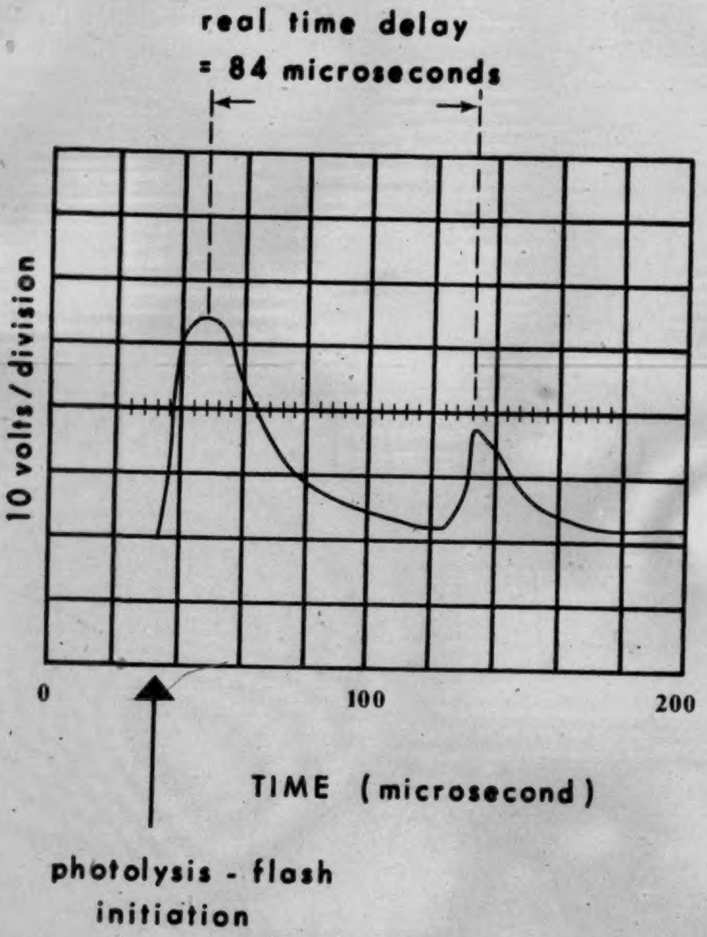

FIGURE II.7 Oscilloscope Trace

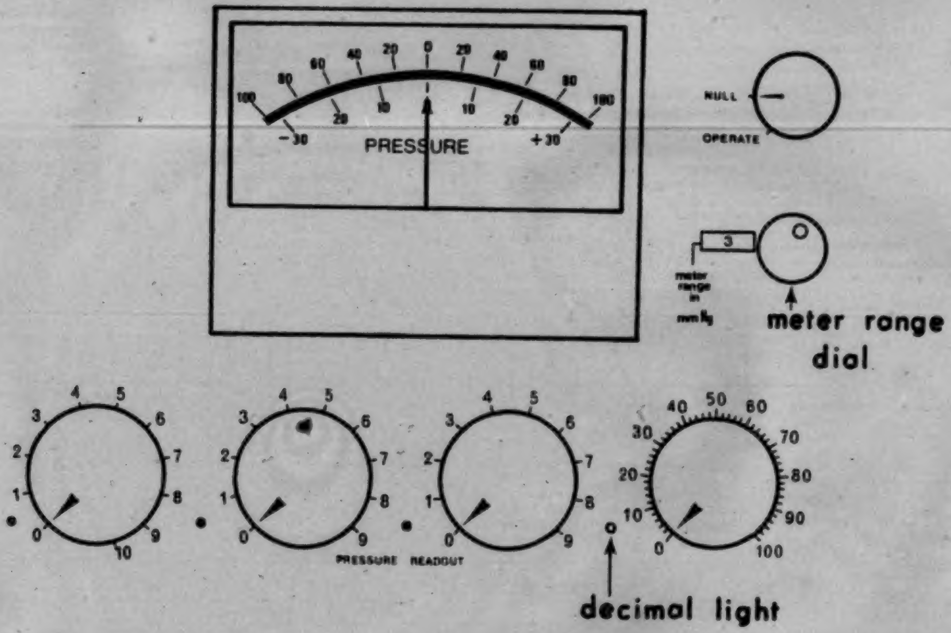
PRESSURE
NULL
OPERATE
3
meter range in mm Hg
meter range dial
PRESSURE READOUT
decimal light
−30
+30

FIGURE II.8 The Baratron Pressure Meter

The pressure of a gas in the vacuum line could be directly read on the Panel Meter. Alternatively, the Pressure Readout Dials could be used to return the meter to the zero reading, in which case the Meter Range Dial should be turned down to a more sensitive scale to ensure that the meter actually returned to zero.

The Microdensitometer

The microdensitometer (Joyce Loebl Model MK11C, Figure II.9) was operated on a double-beam system. A manually adjustable optical density wedge, in the path of the reference beam, was used to establish the baseline. The two beams were alternately fed into the photomultiplier. As the sample spectrum was being scanned, any difference in the intensities of the beams was amplified and the resulting signal activated a servo motor to drive an optical attenuator (another optical density wedge, also placed in the path of the reference beam) so as to nullify the intensity difference. A pen attached to the attenuator traced out the resulting absorption spectrum.

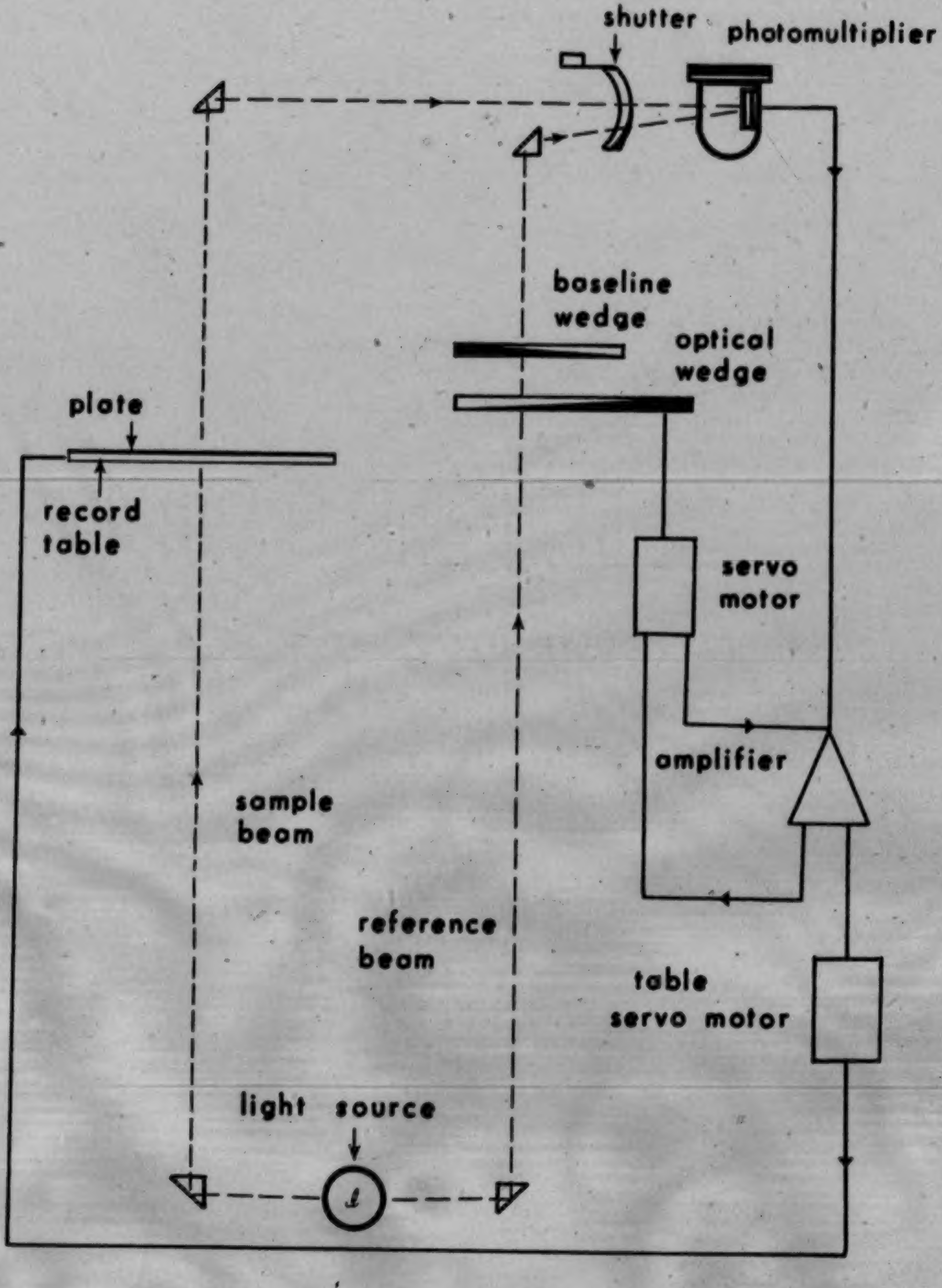
shutter
photomultiplier
baseline
wedge
optical
wedge
plate
record
table
servo
motor
amplifier
sample
beam
reference
beam
table
servo motor
light source

FIGURE II.9 Schematic Diagram of the Microdensitometer

B. OPERATIONAL PROCEDURES

1. The Vacuum System

The reaction mixtures, each containing a different amount of the substrate plus 3 torr $CHClBr_2$ (the source of CCl), in a total pressure of 500 torr helium, were prepared using the 3-litre bulbs A, B, C, and D (Figure II.1). Pressures were monitored by the Baratron Pressure Meter (for pressures below 300 torr) and the mercury manometer #1 (for higher pressures).

The procedure for preparing a mixture (consisting, for example, of 0.3 torr substrate and 3 torr $CHClBr_2$ in a total pressure of 500 torr helium) in the storage bulb A is as follows, assuming that the substrate was stored in bulb M and $CHClBr_2$ was stored in bulb N:

Introduction of The Substrate

The Pressure Readout Dials of the Baratron Pressure Meter were set at 0.3 torr. With all the valves closed except a and k, valve m was slowly opened to expand 0.3 torr substrate into bulb A. The meter on the Baratron Pressure Meter should then return to zero. Valves m and a were closed, and h opened to pump away the substrate in the vacuum line.

Introduction of $CHClBr_2$

Since 0.3 torr substrate was already in bulb A, a total pressure of 3.3 torr needed to be set at the Pressure Readout Dials, and a higher pressure maintained in the vacuum line so that when valve a was opened $CHClBr_2$ would diffuse into bulb A. With all the valves closed (except for k), valve n was slowly opened until the meter on the Pressure Meter moved to the far right. Valve n was then closed. When valve a was slowly opened, $CHClBr_2$ would diffuse into bulb A, as indicated by the gradual leftward movement of the meter. Once the meter was past the zero, valve a was closed, valve n opened again, and the process repeated. As the pressure difference between the vacuum line and the inside of bulb A became smaller, the Pressure Range Dial was turned down gradually until the total pressure in the vacuum line and bulb A was 3.3 torr. Valves a and n were then closed, and valve h opened to pump away the $CHClBr_2$ in the line.

Introduction of Helium

With all the valves closed (except g and k), valve e was opened to admit helium, the pressure of which was monitored by the mercury manometer #1. Valve a was opened, and when 500 torr helium had been admitted into bulb A, valves a and e were closed and valve h was opened to evacuate the excess helium.

The reaction mixtures were stored in bulbs A, B, C, and D for three to four hours to achieve homogeneity. For the flash photolysis of, say, the mixture in bulb A, all the valves were closed except for h and i. Then valve a was slowly opened to fill the line with 50 torr of the mixture. Valves a and i were closed and valve k opened. After firing, valve i was immediately opened to evacuate the reaction vessel, the process being monitored by the Pirani Vacuum Gauge Tubes #2 and #3. Valve k was then closed and valve h opened to introduce a fresh mixture.

After the study of the whole set of reaction mixtures (in bulbs A, B, C, and D) the reaction vessel was cleaned either by flaming or rinsing with 10% hydrofluoric acid. The two lamps were also cleaned with 10% hydrofluoric acid after the study of each substrate was completed.

2. Development of The Plates

The photographic plates were developed in Kodak D-19 Developer for 3 min @24°C, 4 min @20°C, 5 min @16°C. They were then rinsed successively in the Stop Bath (1% Acetic Acid) for 30 sec, Kodak Rapid Fixer for 2 min, and running water at 18 - 21°C for 20 - 30 min. The plates were then air-dried in a dust-free container for a few hours, and finally placed in the microdensitometer for scanning.

C. Materials

All the reagents used in this work were of research grade. Trap-to-trap low temperature vacuum distillation was used for most of the purifications. The substrate placed in trap W (Figure II.1) was first passed through the trap X immersed in a cold slush to retain heavy impurities and was then condensed in the second trap Y, which was immersed in a colder slush at the temperature of which the vapour pressure of the substrate was close to zero. Light impurities having vapour pressures higher than that of the substrate would pass through the second trap Y and be pumped away. The procedure was usually repeated once or twice, and only the middle portion of the distillate was retained for subsequent use and stored in bulb M or N.

The reagents used, their sources, and methods of purification are given in Tables II.1 to II.6. With the exception of helium, hydrogen, ammonia, propane, and phenylacetylene, all materials were degassed at -196°C.

TABLE II.1

Inorganic Compounds and Alkanes

Material	Source	Purification
Chlorodibromomethane	Eastman Organic Chemicals	Distilled at -23°C (Carbon Tetrachloride) and -78°C (Dry Ice/Acetone)
Helium	Linde (Union Carbide Canada, Ltd.)	Passed over Cu at 350°C and then molecular sieve
Hydrogen	Linde (Union Carbide Canada, Ltd.)	Passed over Cu at 350°C and then molecular sieve
Ammonia	Matheson Gas Products	Degassed at -196°C
Chloromethane	Matheson Gas Products	Distilled at -107°C (*I*sooctane) and -131.5°C (*n*-pentane)
Propane	Matheson Gas Products	Degassed at -196°C
2-Methylpropane (*I*sobutane)*	Phillips Petroleum Company	Distilled at -107°C (*I*sooctane) and -131.5°C (*n*-pentane)

* purity checked by gas chromatography

TABLE II.2

Alkynes

Material	Source	Purification
Acetylene	Matheson Gas Products	Distilled at -131.5°C (*n*-pentane) and -160°C (*I*sopentane)
Acetylene-d$_2$	Merck, Sharp and Dohme of Canada, Ltd.	Distilled at -131.5°C (*n*-pentane) and -160°C (*I*sopentane)
Propyne -≡	Matheson Gas Products	Distilled at -107°C (*I*sooctane) and -139°C (Ethylchloride)
1-Butyne --≡	Chemicals Procurement Laboratories	Distilled at -84°C (Ethylacetate) and -131.5°C (*n*-pentane)
1-Pentyne ---≡	Chemicals Procurement Laboratories	Distilled at -64°C (Chloroform) and -107°C (*I*sooctane)
2-Butyne -≡-	Farchan Research Laboratories	Distilled at -64°C (Chloroform) and -107°C (*I*sooctane)
2-Pentyne -≡--	Chemicals Procurement Laboratories	Distilled at -45°C (Chlorobenzene) and -107°C(*I*sooctane)
2,2,5,5-Tetramethyl-3-hexyne +≡+	Chemical Samples Company	Distilled at 0°C (Ice Water) and -64°C (Chloroform)
3,3-Dimethyl-1-butyne +≡	Chemical Samples Company	Distilled at -23°C (Carbon Tetrachloride) and -78°C (Dry Ice/Acetone)
Phenylacetylene 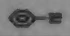	Aldrich Chemical Company, Inc.	Degassed at -23°C (Carbon Tetrachloride)

TABLE II.3
Silanes

Material	Source	Purification
Silane	Petrarch Systems, Inc.	Distilled at -160°C (*Isopentane*) and -196°C (Liquid Nitrogen)
Monomethylsilane	Merck, Sharp and Dohme of Canada, Ltd.	Distilled at -131.5°C (*n*-pentane) and -160°C (*Isopentane*). Further purification by passing through Porapak column at 0°C from a bulb maintained at -64°C (Chloroform). Collected at -196°C (Liquid Nitrogen)
Dimethylsilane	Peninsular Chem. Res., Inc.	Distilled at -131.5°C (*n*-pentane) and -196°C (Liquid Nitrogen)
Trimethylsilane	Chemical Procurement Laboratories	Distilled at -98°C (Methanol) and -131.5°C (*n*-pentane)
Tetramethylsilane	City Chemical Corp.	Distilled at -84°C (Ethylacetate) and -131.5°C (*n*-pentane)
Diethylsilane	Peninsular Chem. Res., Inc.	Distilled at -64°C (Chloroform) and -84°C (Ethylacetate)
Triethylsilane	Peninsular Chem. Res., Inc.	Distilled at -23°C (Carbon Tetrachloride) and -64°C (Chloroform)
Silane-d_4	Merck, Sharp and Dohme of Canada, Ltd.	Distilled at -160°C (*Isopentane*) and -196°C (Liquid Nitrogen)
Monomethylsilane-d_3	Peninsular Chem. Res., Inc.	Same as monomethylsilane
Dimethylsilane-d_2	Merck, Sharp and Dohme of Canada, Ltd.	Distilled at -112°C (Ethanol) and -131.5°C (*n*-pentane)
Trimethylsilane-d_1	Merck, Sharp and Dohme of Canada, Ltd.	Distilled at -98°C (Methanol) and -131.5°C (*n*-pentane)

TABLE II.4
Silanes (Continued)

Material	Source	Purification
Disilane	Merck, Sharp and Dohme of Canada, Ltd.	Distilled at -112°C (Ethanol) and -131.5°C (*n*-pentane)
Disilane-d_6	Merck, Sharp and Dohme of Canada, Ltd.	Distilled at -112°C (Ethanol) and -131.5°C (*n*-pentane)
Hexamethyldisilane	Peninsular Chem. Res., Inc.	Distilled at -23°C (Carbon Tetrachloride) and -64°C (Chloroform)
Trimethylfluorosilane	Peninsular Chem. Res., Inc.	Distilled at -107°C (*I*sooctane) and -160°C (*I*sopentane)
Dimethyldifluorosilane	Peninsular Chem. Res., Inc.	Distilled at -84°C (Ethylacetate) and -131.5°C (*n*-pentane)
Methyltrifluorosilane	Peninsular Chem. Res., Inc.	Distilled at -84°C (Ethylacetate) and -131.5°C (*n*-pentane)
Trichlorosilane	Dow Corning	Distilled at -84°C (Ethylacetate) and -98°C (Methanol)
Methyldichlorosilane	Peninsular Chem. Res., Inc.	Distilled at -78°C (Dry Ice/Acetone) and -98°C (Methanol)
Dimethylchlorosilane	Peninsular Chem. Res., Inc.	Distilled at -64°C (Chloroform) and -84°C (Ethylacetate)
Trimethylchlorosilane	Peninsular Chem. Res., Inc.	Distilled at -64°C (Chloroform) and -107°C (*I*sooctane)
Hexachlorodisilane	Dow Corning	Distilled at 0°C (Ice Water) and -23°C (Carbon Tetrachloride)

TABLE II.5

Cyclic Compounds

Material	Source	Purification
Cyclohexane	BDH Chemicals	Distilled at -23°C (Carbon Tetrachloride) and -98°C (Methanol)
Cyclopentane	American Petroleum Institute	Distilled at -64°C (Chloroform) and -107°C (*Isooctane*)
Cyclohexene	Eastman Organic Chemicals	Distilled at -23°C (Carbon Tetrachloride) and -84°C (Ethylacetate)
1,4-Cyclohexadiene	Chemical Samples Company	Distilled at -23°C (Carbon Tetrachloride) and -78°C (Dry Ice/Acetone)
1,3-Cyclohexadiene	Chemicals Procurement Laboratories	Distilled at -23°C (Carbon Tetrachloride) and -78°C (Dry Ice/Acetone)
Benzene *	Caledon Laboratories, Ltd.	Distilled at -23°C (Carbon Tetrachloride) and -78°C (Dry Ice/Acetone)
Toluene	Caledon Laboratories, Ltd.	Shaken twice with cold conc. H_2SO_4, once with water, once with aq. 5% $NaHCO_3$, again with water; dried successively with $CaSO_4$, P_2O_5. Distilled from P O at 110.6°C
Fluorobenzene	Eastman Organic Chemicals	Dried with P_2O_5. Distilled at 84.7°C
Chlorobenzene	Fischer Scientific Company	Washed successively with conc. H_2SO_4, aq. $NaHCO_3$, water; dried with $CaSO_4$, then P_2O_5. Distilled from P_2O_5 at 132.2°C

* purity checked by gas chromatography

TABLE II.6

Heterocyclic Compounds

Material	Source	Purification
Thiacyclohexane	American Petroleum Institute	Distilled at 0°C (Ice Water) and -78°C (Dry Ice/Acetone)
Thiacyclopentane (Tetrahydrothiophene)	Chemicals Procurement Laboratories	Distilled at -23°C (Carbon Tetrachloride) and -78°C (Dry Ice/Acetone)
Pyrrolidine	American Petroleum Institute	Distilled at -23°C (Carbon Tetrachloride) and -78°C (Dry Ice/Acetone)
Tetrahydrofuran	Fischer Scientific Company	Passed through alumina column; then distilled at -64°C (Chloroform) and -78°C (Dry Ice/Acetone)
Thiophene *	Raylo Chemicals, Ltd.	Gas chromatography: 20% TCP on Chromosorb W (20′) at 60°C
Pyrrole	American Petroleum Institute	Distilled at 0°C (Ice Water) and - 78°C (Dry Ice/Acetone)
1-Methylpyrrole	American Petroleum Institute	Distilled at -23°C (Carbon Tetrachloride) and -78°C (Dry Ice/Acetone)
Furan*	Aldrich Chemical Company, Inc.	Distilled at -78°C (Dry Ice/Acetone) and -98°C (Methanol)
Pyridine	American Petroleum Institute	Distilled at -23°C (Carbon Tetrachloride) and -78°C (Dry Ice/Acetone)

* purity checked by gas chromatography

III. RESULTS

A. SOURCE

Simons and Yarwood[21,22] investigated potential sources of CCl by flash photolyzing a series of chloromethanes. Both CBr_2Cl_2 and $CHClBr_2$, recommended by these authors, were examined for this study. In both cases, a few absorption lines were obtained near 278 nm. $CHClBr_2$ was adopted because it produced a somewhat stronger spectrum (Figure III.1).

B. ABSORPTION SPECTRUM OF $CCl(X^2\Pi)$

The parent compound $CHClBr_2$ was photolyzed in the presence of a large excess of helium to maintain isothermal conditions. However, a vibrationally hot transition, the (Q_1 1,1) band at 277.81 nm, was still observed at a time delay of about 30 μsec.

The assignment of the CCl absorption lines was accomplished on the basis of the rotational analysis carried out by Gordon and King[31] and Verma and Mulliken.[32] The three isothermal transitions observed here were the (Q_1 0,0) band at 277.7 nm, the (Q_2 0,0) band at 278.59 nm, and the (P_2 0,0) band at 278.76 nm, all of which belong to the $A^2\Sigma \leftarrow X^2\Pi$ system. The most intense absorption line at 277.7 nm, which has an atomic line shape, was monitored for this kinetic study.

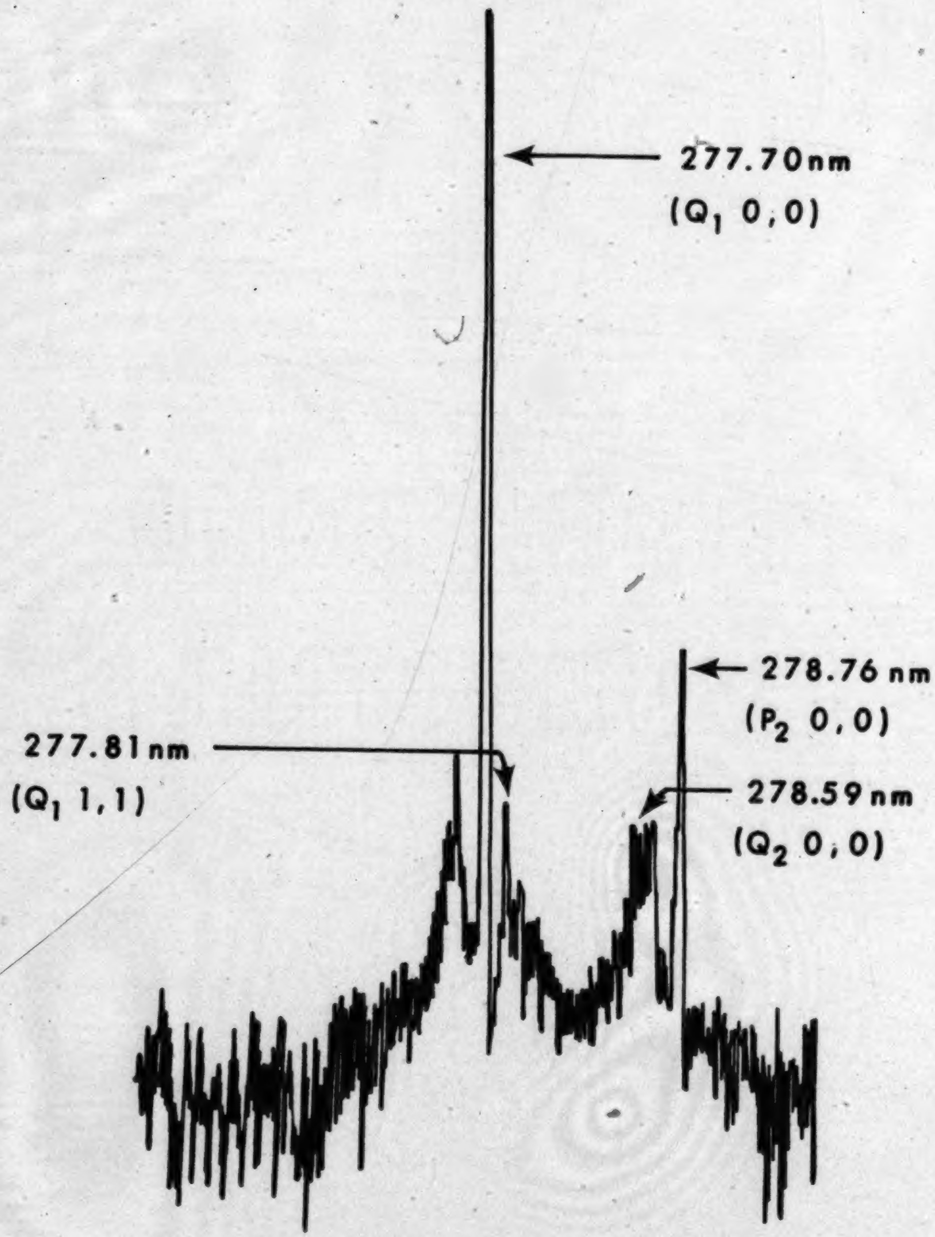

FIGURE III.1 Absorption Spectrum of CCl($X^2\Pi$)

C. RELATIONSHIP BETWEEN THE ABSORPTION PEAK HEIGHT AND THE CCl($X^2\Pi$) CONCENTRATION

The band intensity, or the absorption peak height, is related to the carbyne concentration through a modified form of the Beer-Lambert Law as follows.

The absorption spectrum was recorded on a photographic plate. The density of a photographic image D is related to the exposure E by the expression:

$$D = a.\ln E + b$$

where a and b are constants. Since the exposure E measures the light intensity I falling on the plate,

$$\frac{E_o}{Et} = \frac{I_o}{It}$$

where

E_o = Exposure of the plate with no absorbing species present

Et = Exposure of the plate with absorbing species present at time t

I_o = Light intensity falling on plate with no absorbing species

It = Light intensity falling on plate with absorbing species present at time t

On the other hand, as the absorption band intensity is transformed into the absorption peak by the microdensitometer, the peak height PH should be the difference between the density of image with no absorbing species present, D_0, and that with the absorbing species present at a particular time t, Dt, i.e.:

$$PH = D_0 - Dt = a.\ln (E_0/Et)$$

$$= a.\ln (I_0/It)$$

At this point, it is necessary to introduce a modified form of the Beer-Lambert Law. This is due to the poor resolution of the spectrograph with respect to the fine atomic line structure of the $CCl(X^2\Pi)$ absorption at 277.7 nm; in other words, this deviation from the Beer-Lambert Law occurs when the absorption band is narrow relative to the spectral slit-width. In such cases, the absorbance, $\ln (It/I_0)$, is no longer directly proportional to the concentration of the absorbing species:

$$\ln (It/I_0) = -k(c.l)^{\gamma}$$

The Beer-Lambert Coefficient γ is an empirically determined correction factor whose value is dependent on the type of absorption system. $\gamma = 1$ for broad molecular peaks such as ethylene selenide and well resolved atomic lines. However, γ

approaches 0.5 when the atomic lines are unresolved, such as in Se(4^3P).[44] k is an empirical constant, incorporating the effect of variation of the absorptivity over the spectral band-width.

The relationship between the absorption peak height, PH, and concentration, c, becomes:

$$\begin{aligned} PH &\propto \ln (I_0/It) \\ &\propto k(c.l)^{\gamma} \end{aligned}$$

D. DETERMINATION OF THE BEER-LAMBERT COEFFICIENT γ

The Beer-Lambert Coefficient γ for this absorption system was determined by the Path Length Method, which can be accomplished as follows.

1. Full Cell Length *versus* Half Cell Length

Flash photolysis of a mixture of 0.3 torr $CHClBr_2$ in 50 torr He was carried out, using a fixed set of time delays, with the reaction vessel fully exposed. It was then repeated using the same set of time delays, but with a cardboard tube placed over half of the vessel, thereby reducing the path length l by two:

$$PH(\tfrac{1}{2}\text{-cell}) \propto k(c.\tfrac{1}{2}l)^{\gamma}$$

$$PH(F\text{-cell}) \propto k(c.l)^{\gamma}$$

$$\propto 2^{\gamma}.PH(\tfrac{1}{2}\text{-cell})$$

Therefore, the slope of a plot of PH(F-Cell) *versus* PH($\frac{1}{2}$-Cell), for a given set of time delays, is 2^{γ}. Such a plot is shown in Figure III.2, from which $\gamma = 0.46 \pm 0.13$. The vertical lines accompanying the data points, also shown in all subsequent least square method plots, are the error bars for the root mean square deviations of the y entries.

2. Variation of Cell Length

The mixture was photolyzed here with various portions of the reaction cell covered up, thereby varying the path length l. The concentration of the absorbing species remained constant at a fixed time delay.

$$PH \propto k(c.l)^{\gamma}$$

$$\ln PH \propto [\ln (k.c^{\gamma}) + \gamma.\ln l]$$

Thus a plot of ln PH *versus* ln l at a fixed time delay gives a slope of $\gamma = 0.57 \pm 0.06$ (Figure III.3).

An average value of $\gamma = 0.51 \pm 0.1$ was obtained from the above experiments.

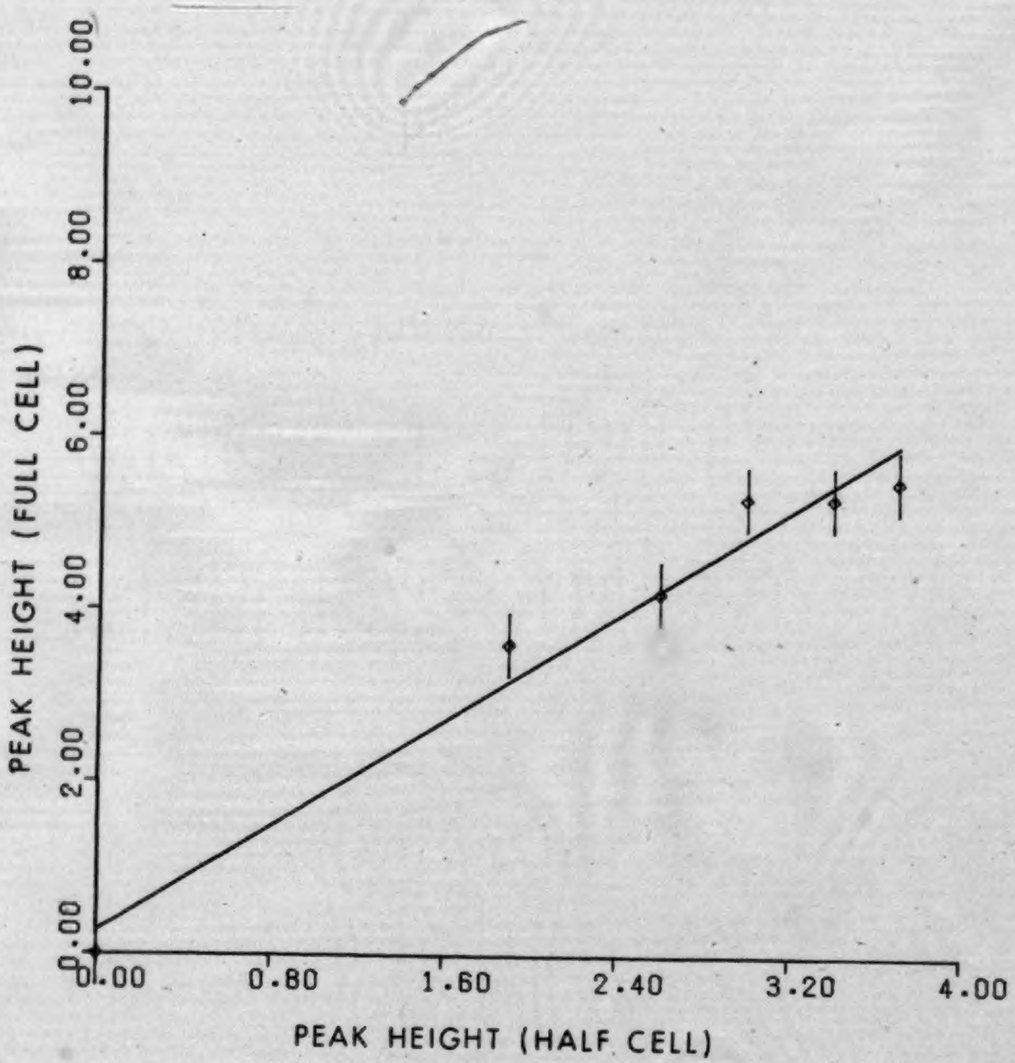

FIGURE III.2 Peak Height of Full Cell Length *versus* Peak Height of Half Cell Length ($CHClBr_2$, 0.3 torr; He, 50 torr; Flash Energy, 2900 kJ)

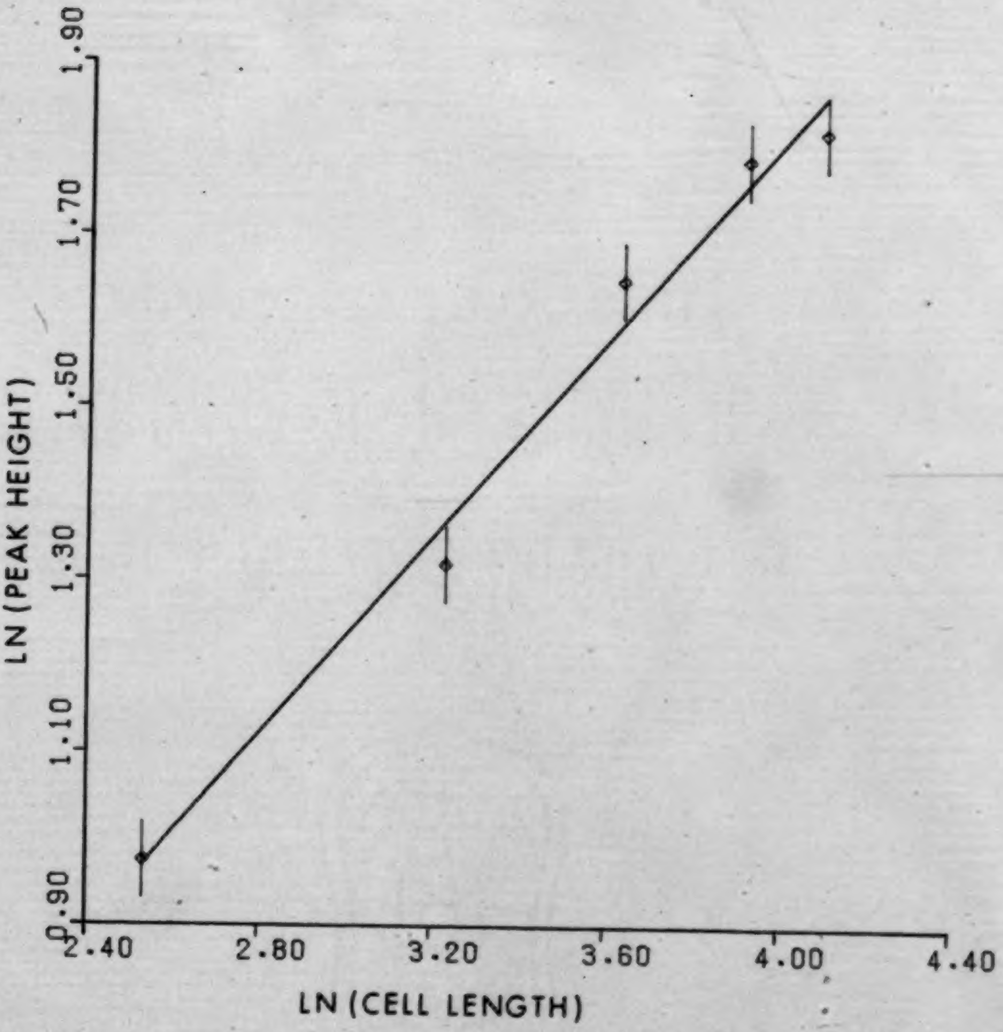

FIGURE III.3 Ln (Peak Height) *versus* Ln (Cell Length) ($CHClBr_2$, 0.3 torr; He, 50 torr; Flash Energy, 2900 kJ)

E. The CCl($X^2\Pi$) DECAY

1. Determination of the Background Decay Rate Constant, k'

A first order CCl decay expression is:

$$-d[CCl]/dt = k'[CCl]$$

$$\ln [CCl] = -k'.t + \text{constant}$$

where [CCl] = concentration of CCl

t = time delay

k'= background decay rate constant of CCl

In such a case, the absorption peak height is related to k' as:

$$PH \propto [CCl]^{\gamma}$$

$$\ln PH \propto \gamma.\ln [CCl]$$

$$= -\gamma.k'.t + \text{constant}$$

The linear proportionality observed between ln PH and time delay t (Figure III.4), for a mixture consisting of 0.3 torr $CHClBr_2$ in 50 torr He photolyzed with an energy of 2900 kJ, indeed indicates a first order decay process. This linear

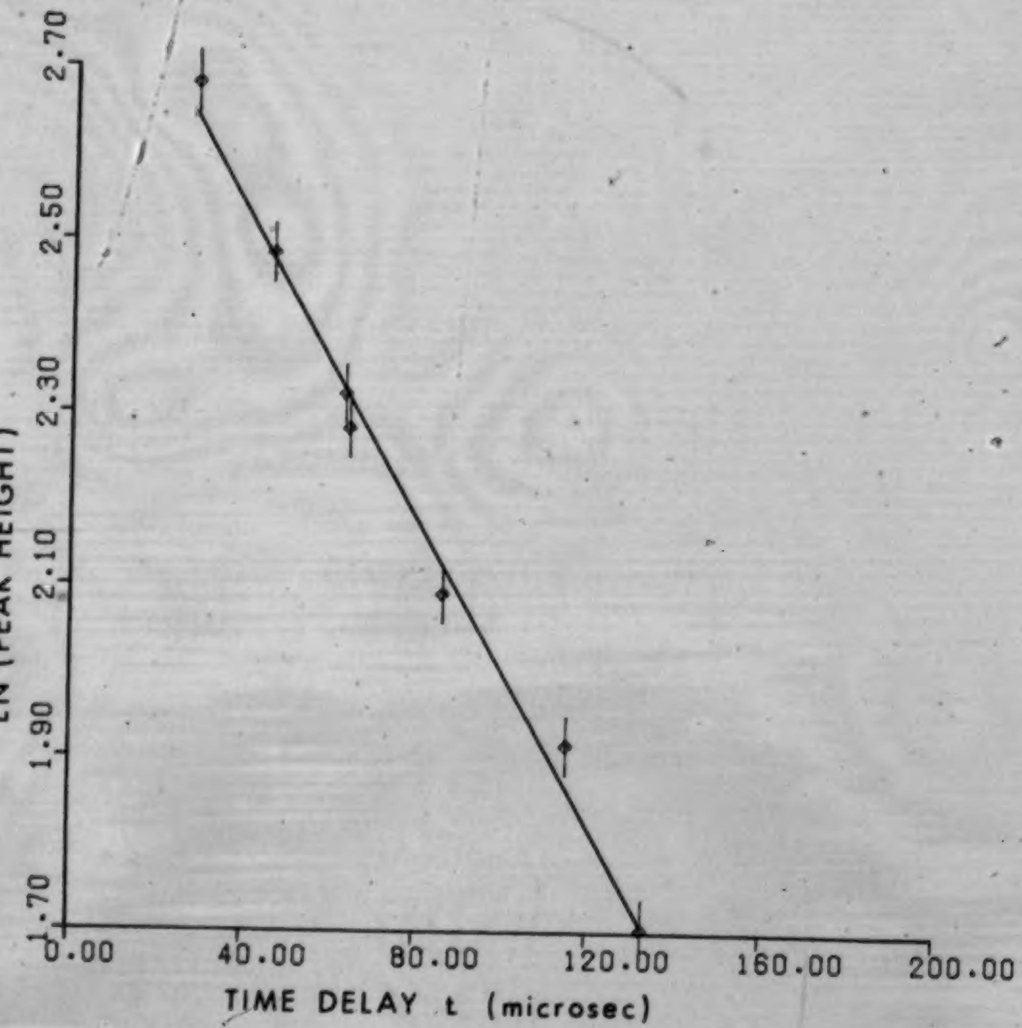

FIGURE III.4 Ln (Peak Height) *versus* Time Delay t
(CHClBr$_2$, 0.3 torr; He, 50 torr; Flash Energy, 2900 kJ)

relationship was still observed upon changing the pressures of $CHClBr_2$ or He, or the flash energy, (*vide infra*).

A mean value of $\gamma k'_m = 8.0 \pm 0.4$ $msec^{-1}$ was obtained under the above conditions (455 measurements). k' is actually a pseudo-first order rate constant measuring the rate of disappearance of CCl in the absence of substrates. However, since the photolysis lamp and reaction vessel were replaced several times during the course of this work, k' varies, due to these slight variations in the experimental conditions, from ~ 12 $msec^{-1}$ to as high as ~ 26 $msec^{-1}$.

2. Effects of Flash Energy, Pressure of $CHClBr_2$ and Pressure of He on The Background Decay Rate Constant k'

The flash energy was varied by changing the photo-lamp capacitor output, using a mixture consisting of 0.3 torr $CHClBr_2$ in 50 torr He. The CCl decay rate was found to increase linearly with the flash energy (Figure III.5), indicating that CCl was removed mainly by reactions with the photolytic products. Thus, for each flash, the energy was kept constant at 2900 kJ, the maximum output for the photo-lamp capacitor, by charging the capacitor to 20 kV.

However, the CCl decay was found to have a non-linear relationship with the pressure of $CHClBr_2$, the CCl parent compound (Figure III.6). Therefore, 0.3 torr $CHClBr_2$, in 50 torr He, was used for each run because k' was found to level off to a constant value of ~ 17 $msec^{-1}$ at this pressure.

Increasing the He pressure from 50 torr (k' = (16.2 ± 1.8) $msec^{-1}$) to 500 torr (k' = (17.4 ± 0.8) $msec^{-1}$),

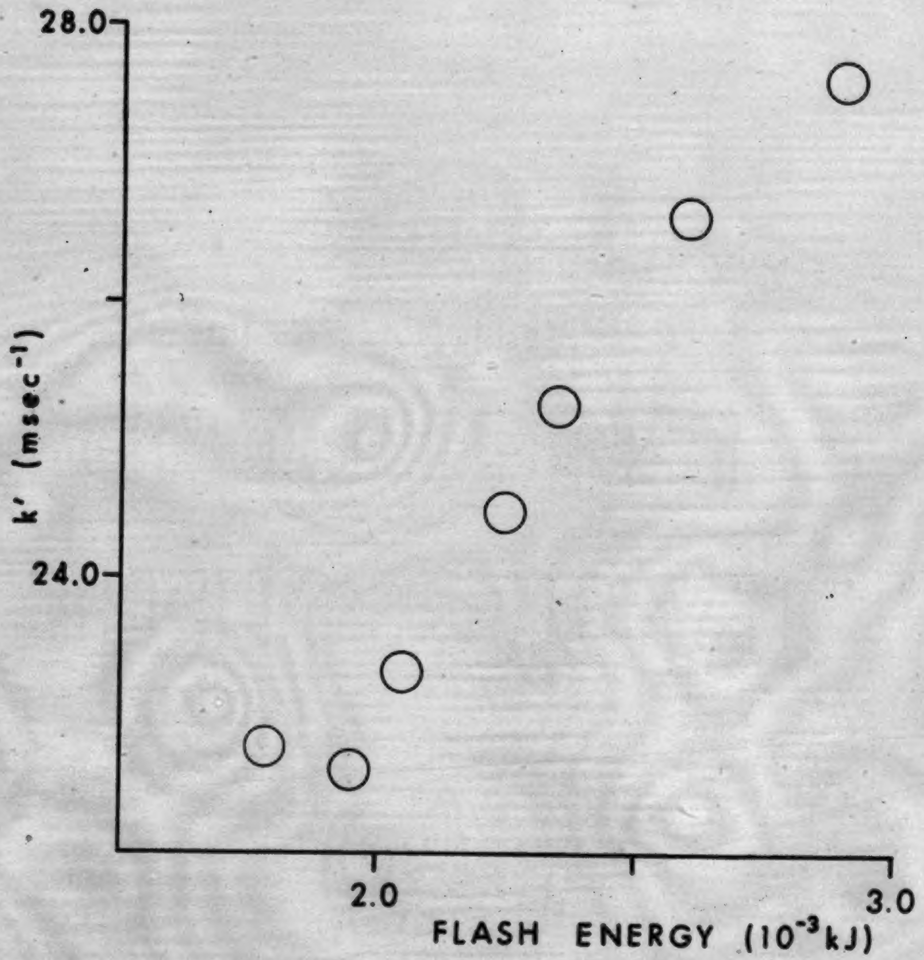

FIGURE III.5 k' *versus* Flash Energy

($CHClBr_2$, 0.3 torr; He, 50 torr)

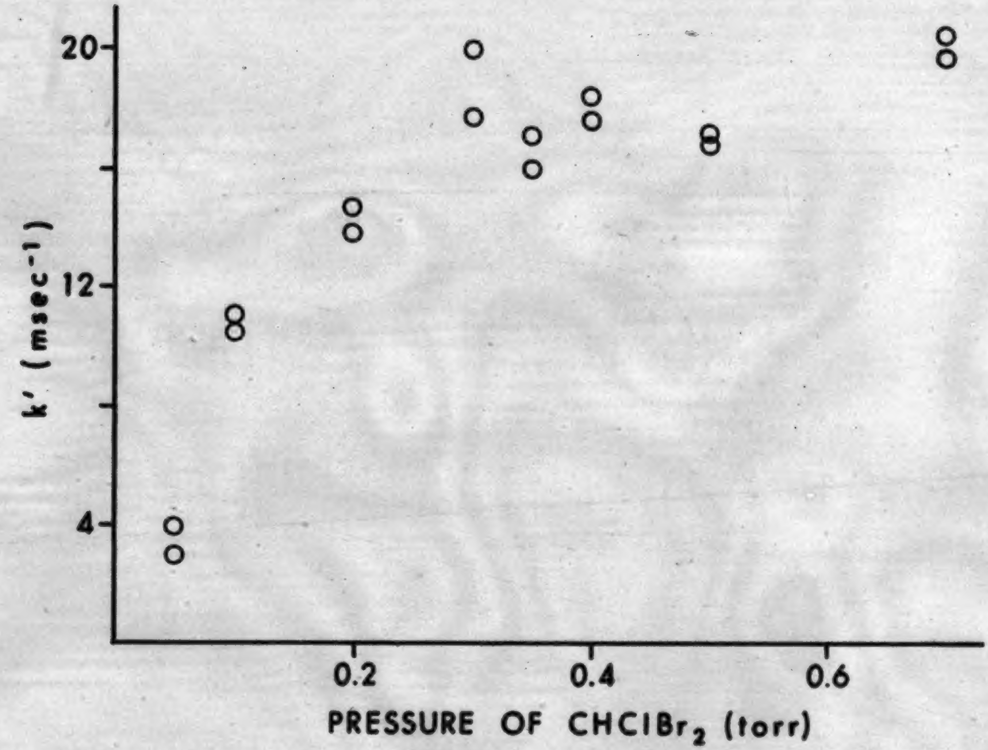

FIGURE III.6 k' *versus* Pressure of $CHClBr_2$
(He, 50 torr; Flash Energy, 2900 kJ)

in the presence of 0.3 torr $CHClBr_3$, had no significant effect on the decay rate of CCl.

3. Determination of the Pseudo-First Order Decay Rate Constant in the Presence of Substrate, k"

In the presence of a reactive substrate:

$$-d[CCl]/dt = k'[CCl] + k_1[CCl][S] = k''[CCl]$$

where

[S] = concentration of the substrate

k_1 = second order rate constant for the reaction of CCl with the substrate

k" = pseudo-first order decay rate constant = $k' + k_1[S]$

The above expression leads to:

$$\ln PH = -\gamma.k''.t + \text{constant}$$

k" can thus be obtained from the slope of the plot of ln PH *versus* t, for a given amount of substrate. Those plots having correlation coefficients < 0.9 were rejected. For the alkynes, which were the first substrates examined, eight measurements were carried out for a given pressure of substrate. Subsequently equally good correlations were obtained for seven measurements at various time delays. In all cases the pressures of $CHClBr_3$ and He were 0.3 and 50 torr, respectively, but when the pressure of the substrate exceeded 50 torr, no He was added to the reaction mixture. The upper limit of the substrate pressure range was either the vapour pressure of the substrate at room temperature, such as in the case of Si_2Cl_6, or the extent where the absorption signals became too weak for meaningful decay plots to be made, due to rapid consumption of CCl.

Determination of the Second Order Rate Constant for the Reaction of CCl with Various Substrates, k_1

k_1 can be obtained from the slope (= γk_1) of the plot of $\gamma k''$ *versus* [S], for a given substrate. The $\gamma k''$ values were given equal weights in the plots, since weighting the $\gamma k''$ entries according to their root mean square (rms) errors, obtained from the ln PH *versus* t plots, does not necessarily improve the correlation coefficients of the plots, as shown by a comparison between the results of the standard and the weighted plots for a few randomly selected substrates (cf Appendix). Similarly, where the $\gamma k''$ values (= $\gamma k'$) were not measured at [S] = 0, no overall improvement in the correlation coefficients could be obtained by including the mean value $\gamma k'_m$, 8.0 ± 0.4 $msec^{-1}$ (*vide supra*), into such plots (cf Appendix). As mentioned earlier, the vertical error bars in such plots indicate the rms deviations of $\gamma k''$. The pressure of a substrate was converted into concentration [S] using the Ideal Gas Equation, PV = nRT.

Inorganic Substrates

Hydrogen:

The ln PH *versus* t plots gave identical slopes in the pressure range 20.0 - 180.0 torr, indicating no measurable reaction with hydrogen. The values of the slopes, or $\gamma k''$, are summarized in Table III.1.

Ammonia:

The plots of ln PH *versus* t for four different concentrations of ammonia (pressure range 0.050 - 12.0 torr) are presented in Figure III.7. The plots are linear and the values of $\gamma k''$ are summarized in Table III.2. The data are somewhat scattered due to the tendency of ammonia to adsorb on the glass surfaces of the apparatus, as evidenced from the slow but gradual decrease in pressures indicated by the Baratron Pressure Meter. The slope of the plot of $\gamma k''$ *versus* concentration (Figure III.8) yielded $k_1 = (4.0 \pm 2.0) \times 10^6$ M^{-1} s^{-1}. A more reliable estimate was obtained as follows.

The reactivity of a substrate can be roughly estimated by comparing the data for substrates in comparable pressure ranges. For ammonia, $\gamma k'' \sim 12$ $msec^{-1}$ at 12 torr, but all the CCl signals were quenched when the pressure was increased to 25 torr. For *iso*butane ($k_1 = (4.5 \pm 0.4) \times 10^6$ M^{-1} s^{-1}), however, the CCl signals were weak but still discernible at 86.5 torr, the maximum pressure used. Thus for ammonia, $k_1 > 4.5 \times 10^6$ M^{-1} s^{-1}. On the other hand, for acetylene ($k_1 = (3.5 \pm 0.4) \times 10^7$ M^{-1} s^{-1}), the maximum pressure used was $\sim$ 11 torr, at which $\gamma k'' \sim 21$ $msec^{-1}$. From this we can imply that ammonia is less reactive than acetylene. Therefore, for ammonia, the estimated rate constant is $(4.5 \times 10^6$ M^{-1} $s^{-1}) < k_1 < (3.5 \times 10^7$ M^{-1} $s^{-1})$.

TABLE III.1

$\gamma k''$ as a Function of Concentration for the Reaction with Hydrogen

Conc (Micromolar)	$\gamma k''$ (1/msec)
1060.3	5.9 ± 0.3
1061.3	5.6 ± 0.2
2648.0	5.9 ± 0.8
2650.6	5.6 ± 0.6
4769.6	6.0 ± 0.5
4769.6	6.1 ± 0.7
9529.7	6.3 ± 0.7
9545.5	5.4 ± 0.2

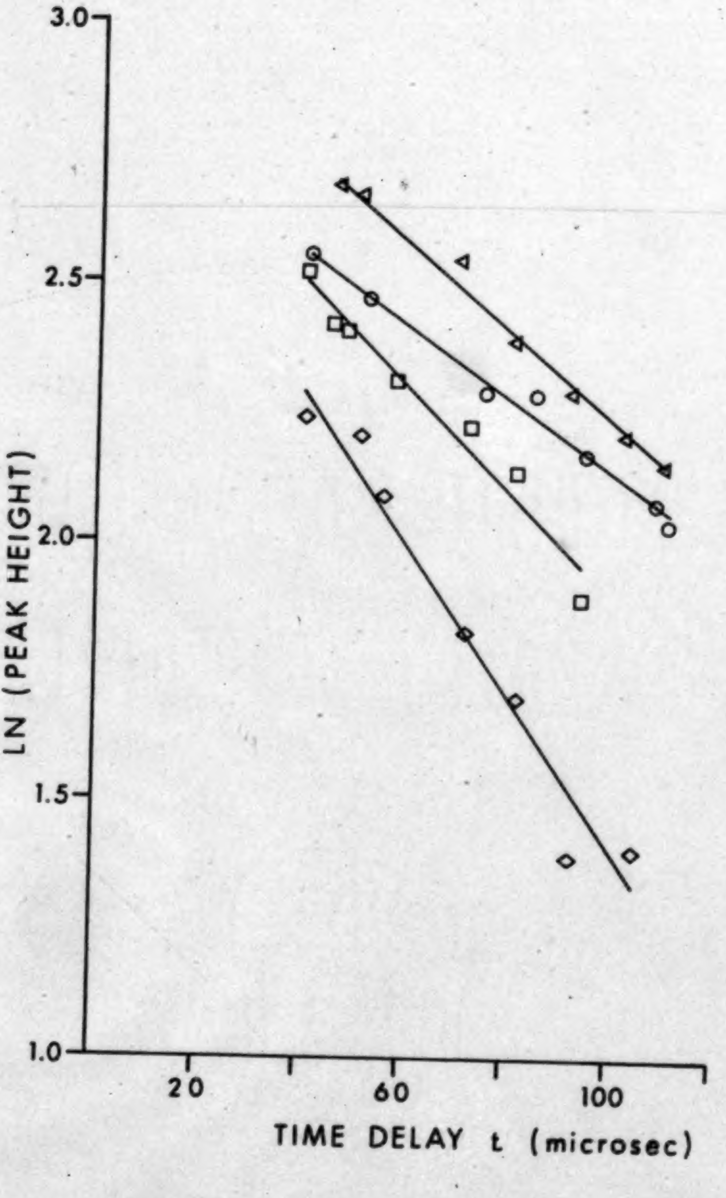

FIGURE III.7 Ln (Peak Height) *versus* Time Delay t for Ammonia (○) 2.66 M; (◁) 21.39 M; (□) 165.65 M; (◇) 272.32 M

TABLE III.2

$\gamma k''$ as a Function of Concentration for the Reaction with Ammonia

Conc (micromolar)	$\gamma k''$ (1/msec)
2.66	7.0 ± 0.2
2.67	7.2 ± 0.5
21.33	8.2 ± 0.5
21.39	8.5 ± 0.2
53.31	9.6 ± 1.2
53.38	9.6 ± 1.7
107.69	7.2 ± 0.8
106.94	9.0 ± 0.5
165.21	8.5 ± 1.8
165.65	10.2 ± 1.0
185.79	10.1 ± 0.5
186.28	9.3 ± 0.3
271.51	9.6 ± 1.2
272.32	14.8 ± 1.4
340.30	8.9 ± 1.7
342.11	11.5 ± 2.1
424.10	9.2 ± 1.2
427.21	8.9 ± 1.2
637.21	9.4 ± 1.5
640.82	11.6 ± 2.5

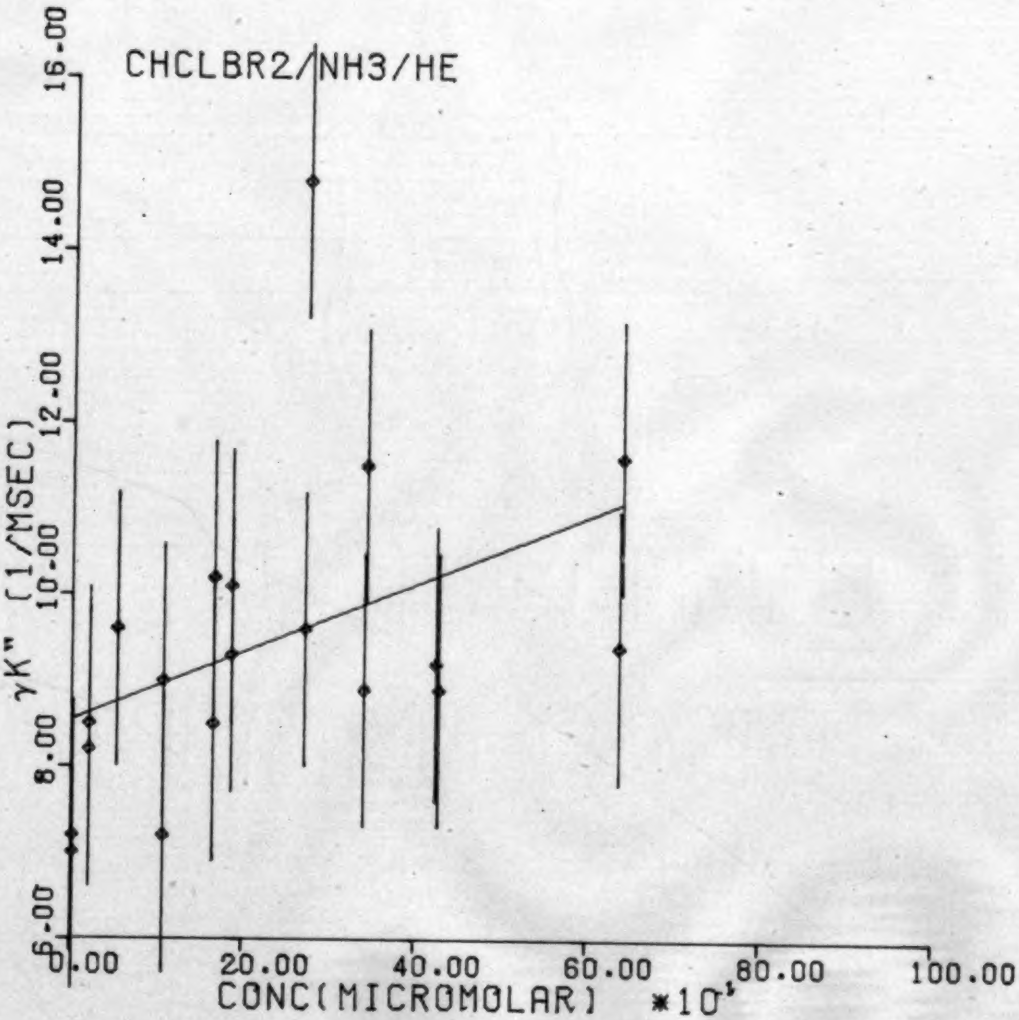

correlation coefficient = 0.44

FIGURE III.8 γk" *versus* Concentration for Ammonia

Alkyl Chlorides and Alkanes

No measurable reaction was observed with methylchloride (Table III.3; pressure range 4.0 - 10.0 torr) and with propane (Table III.4; pressure range, 50 - 250 torr).

*Iso*butane:

In the case of *iso*butane, the enhancement in the values of the pseudo-first order decay rate constant k", with increasing concentrations of the substrate, is apparent from the increase in the slopes of the ln PH *versus* t plots (Figure III.9) Again, the plots indicate first order behaviour and the values of γk" as a function of concentration, summarized in Table III.5 (pressure range 2.0 - 86.48 torr), are plotted in Figure III.10, from the slope of which k_1 was determined to be (4.5 ± 0.4) × 10^4 M^{-1} s^{-1}.

Alkynes

The alkynes examined were acetylene, acetylene-d_2, propyne, 1-butyne, 2-butyne, 1-pentyne, 2-pentyne, 3,3-dimethyl-1-butyne, 2,2,5,5-tetramethyl-3-hexyne and phenylacetylene.

Acetylene:

The plots of ln PH *versus* t, for four concentrations of acetylene, are presented in Figure III.11. The values of γk", obtained from the slopes of such plots, are summarized in Table III.6 (pressure range 0.696 - 10.690 torr), and k_1 was found to be (3.5 ± 0.4) × 10^7 M^{-1} s^{-1} from the slope of the plot of γk" *versus* concentration (Figure III.12).

TABLE III.3

$\gamma k''$ as a Function of Concentration for the Reaction with Methylchloride

Conc (micromolar)	$\gamma k''$ (1/msec)
213.82	6.3 ± 0.5
213.96	5.0 ± 0.4
533.06	5.8 ± 0.3
535.19	5.8 ± 0.3

TABLE III.4

$\gamma k''$ as a Function of Concentration for the Reaction with Propane

Conc (micromolar)	$\gamma k''$ (1/msec)
2669.2	9.1 ± 0.9
2682.6	8.7 ± 0.8
3220.2	7.8 ± 0.4
3220.2	8.1 ± 1.1
4807.7	8.8 ± 1.2
4833.5	6.7 ± 1.1
8050.4	8.3 ± 0.8
8055.8	8.8 ± 0.5
9634.7	12.7 ± 1.3
9676.7	10.4 ± 1.2
13408	8.8 ± 1.4
19911	8.3 ± 0.8

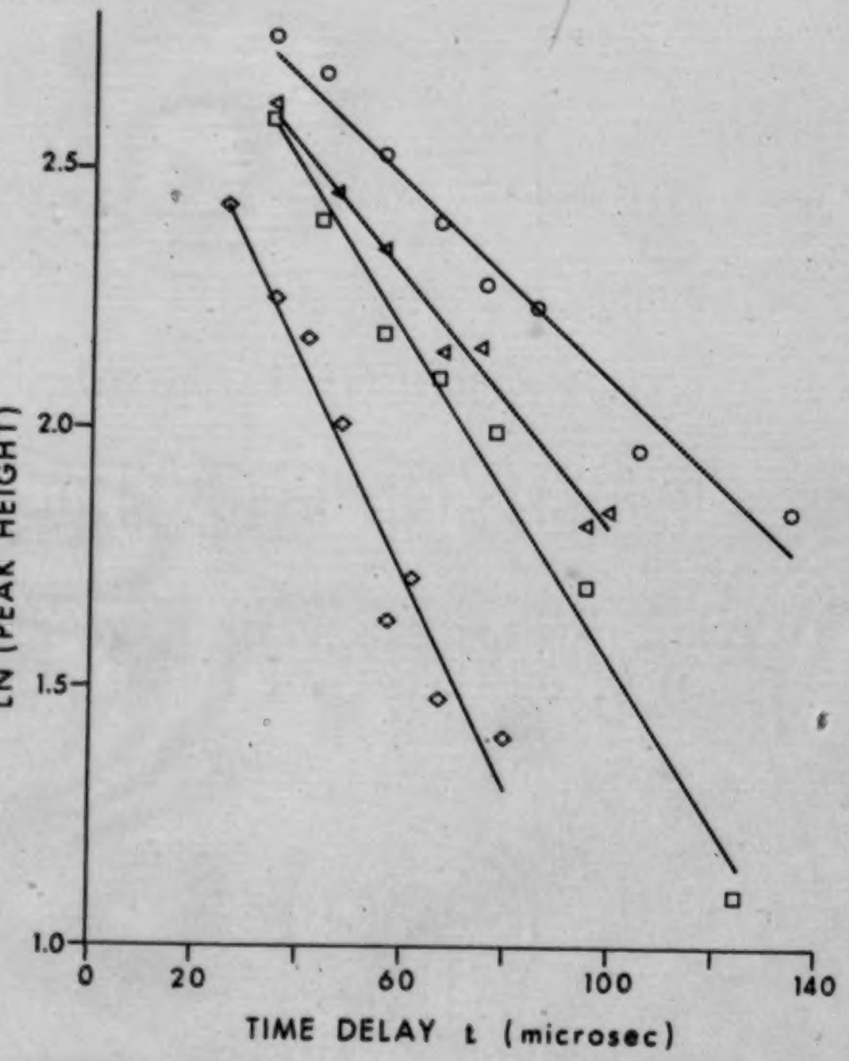

FIGURE III.9 Ln (Peak Height) *versus* Time Delay t for *Iso*butane (○) 214.10 M; (◁) 1863.8 M; (□) 2405.2 M; (◇) 4632.0 M

TABLE III.5

$\gamma k''$ as a Function of Concentration for the Reaction with *Iso*butane

Conc (micromolar)	$\gamma k''$ (1/msec)
107.12	11.3 ± 0.6
107.09	11.3 ± 0.7
214.10	9.6 ± 0.6
214.10	11.1 ± 0.6
321.16	9.5 ± 0.5
321.16	9.6 ± 0.5
428.21	10.0 ± 0.4
428.49	11.6 ± 0.8
1123.6	10.5 ± 0.5
1123.6	10.4 ± 0.6
1863.8	12.1 ± 0.7
1865.0	13.7 ± 0.5
2405.2	13.2 ± 1.0
2405.2	16.0 ± 1.0
4632.0	19.8 ± 1.1
4632.0	21.6 ± 2.1

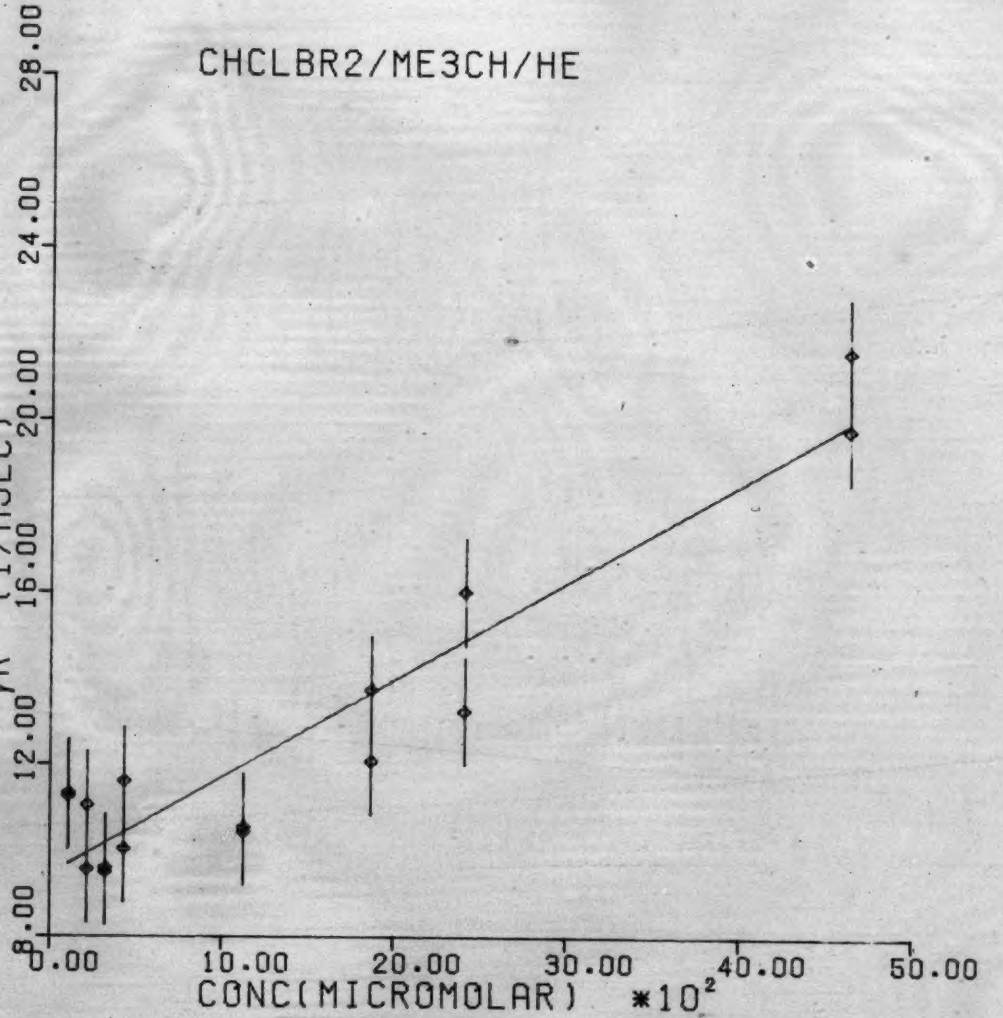

correlation coefficient = 0.94

FIGURE III.10 γk" *versus* Concentration for *Iso*butane

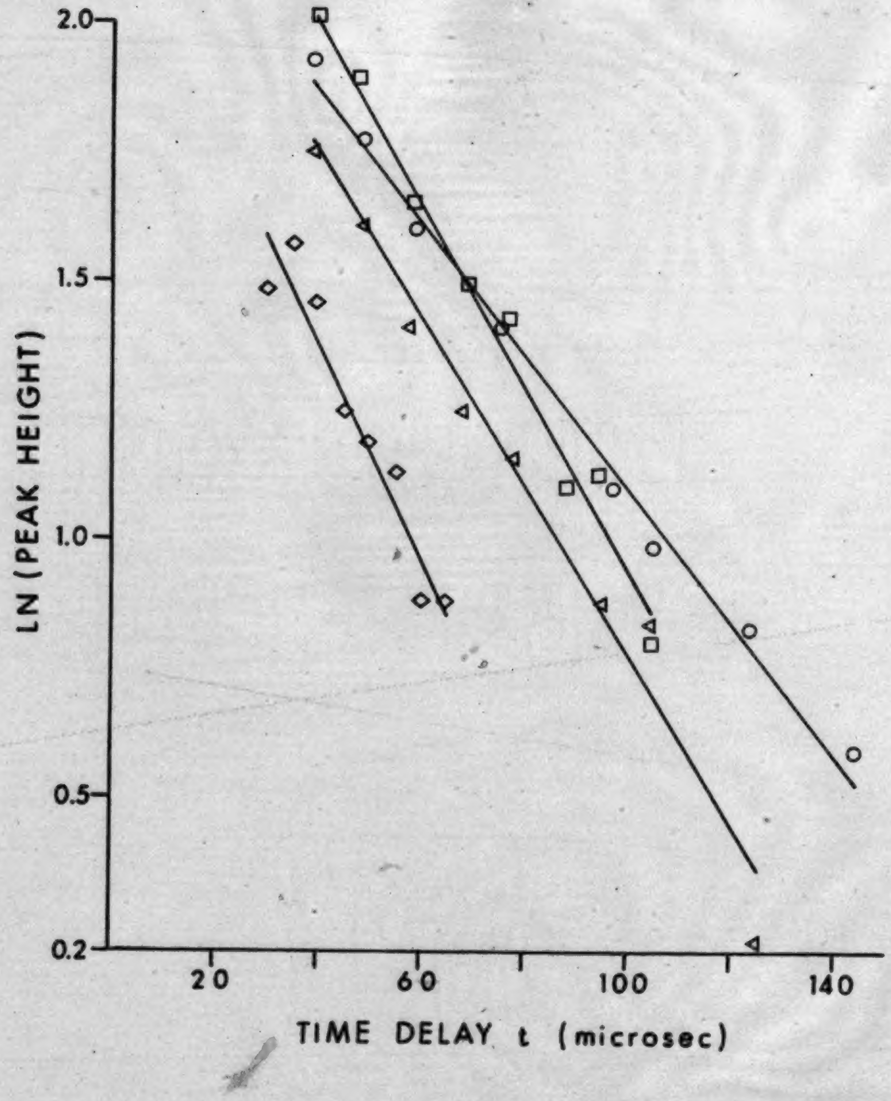

FIGURE III.11 Ln (Peak Height) *versus* Time Delay t for Acetylene (○) 37.33 M; (◁) 78.73 M; (□) 214.03 M; (◇) 571.43 M

TABLE III.6

$\gamma k''$ as a Function of Concentration for the Reaction with Acetylene

Conc (micromolar)	$\gamma k''$ (1/msec)
37.33	12.8 ± 0.5
37.33	14.3 ± 1.2
78.73	13.4 ± 0.4
78.73	16.6 ± 1.6
108.30	15.0 ± 1.7
108.41	12.6 ± 0.9
108.66	14.0 ± 0.9
136.84	16.0 ± 0.9
136.98	15.9 ± 1.4
161.75	16.3 ± 1.0
161.92	15.5 ± 1.3
162.30	13.6 ± 0.7
213.82	18.4 ± 2.0
214.03	17.8 ± 1.2
267.27	17.3 ± 1.9
267.54	15.8 ± 1.1
320.73	17.2 ± 2.0
321.05	15.1 ± 2.2
571.43	20.8 ± 2.4
573.34	21.5 ± 2.2

With no substrate, $\gamma k''=\gamma k'=9.3 \pm 0.6$, 9.6 ± 0.6, 10.1 ± 0.5, 10.3 ± 0.5, 10.5 ± 0.5

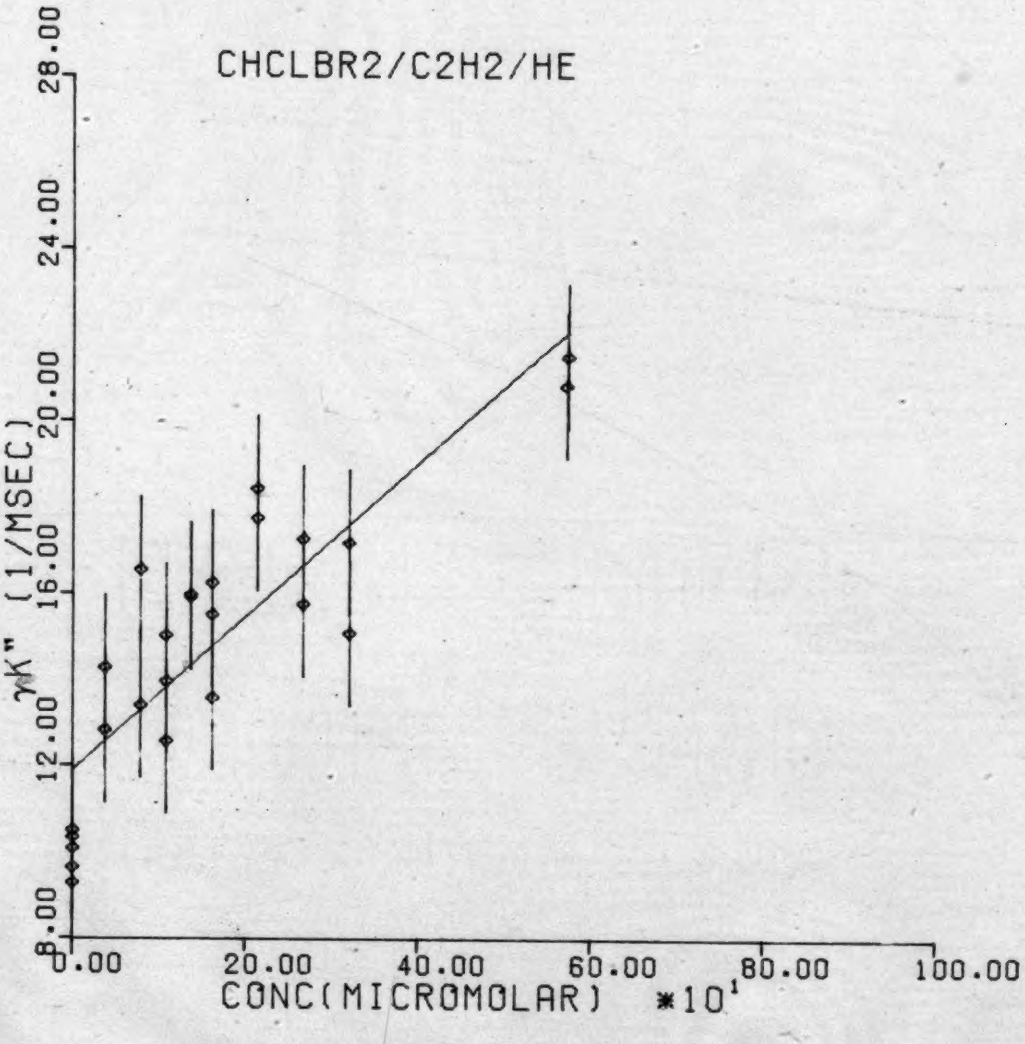

correlation coefficient = 0.86

FIGURE III.12 γk" *versus* Concentration for Acetylene

Acetylene-d_2:

Similarly, ln PH was plotted against t for various concentrations (Figure III.13). The values of $\gamma k''$ thus obtained are summarized in Table III.7 (pressure range, 0.140 - 2.857 torr) and plotted against concentration in Figure III.14, from the slope of which k_1 was determined to be $(3.1 \pm 1.3) \times 10^7$ M^{-1} s^{-1}. The large uncertainty in the result can be ascribed to the small pressure range studied.

Plots of ln PH *versus* t for the remaining alkynes (as well as all the substrates studied in this work) were linear, and henceforth will be omitted for the sake of brevity. The values of $\gamma k''$ as a function of concentration are listed in Tables III.8 - III.12, and the corresponding plots presented in Figures III.15 - III.17, from which the second order rate constants k_1 were obtained. These, together with the number of measurements and the pressure ranges studied, are summarized in Table III.13.

Silanes, Halogenated Silanes, Disilanes and Halogenated Disilanes

Silanes:

The silanes studied were silane, monomethylsilane, dimethylsilane, trimethylsilane, tetramethylsilane, silane-d_4, monomethylsilane-d_3, dimethylsilane-d_2, trimethylsilane-d_1, diethylsilane and triethylsilane.

The values of $\gamma k''$ as a function of concentration are presented in Tables III.14 - III.19, while the plots of $\gamma k''$

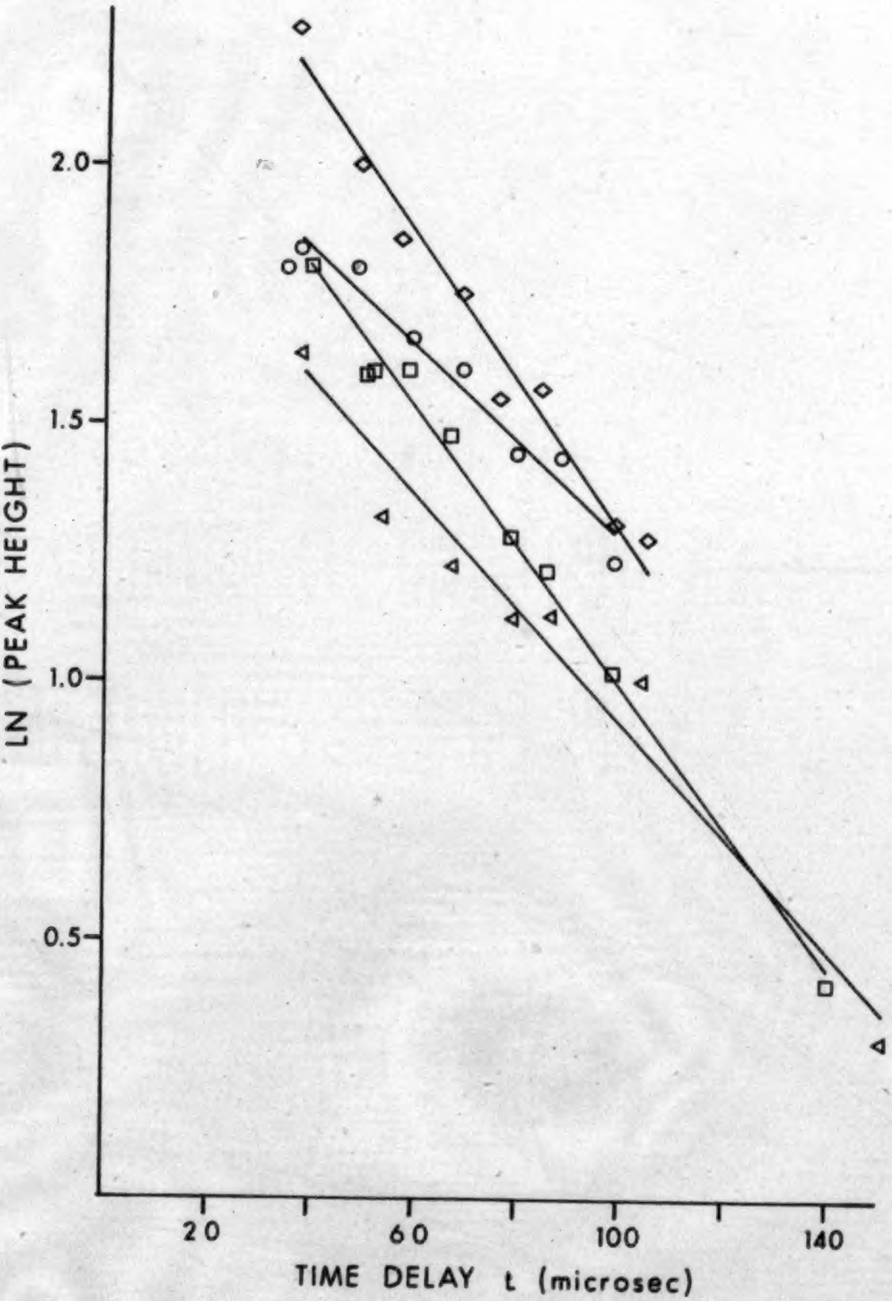

FIGURE III.13 Ln (Peak Height) *versus* Time Delay t for Acetylene-d, (○) 7.534 M; (◁) 52.24 M; (□) 86.511 M; (◇) 110.44 M

TABLE III.7

$\gamma k''$ as a Function of Concentration for the Reaction with Acetylene-d_2

Conc (micromolar)	$\gamma k''$ (1/msec)
7.534	9.2 ± 1.5
7.534	12.2 ± 1.3
22.79	11.0 ± 0.7
22.85	11.1 ± 0.7
52.12	12.5 ± 1.0
52.24	11.7 ± 0.9
60.938	10.9 ± 0.7
60.938	12.0 ± 0.8
86.511	13.3 ± 0.7
86.511	14.7 ± 1.1
106.59	12.6 ± 0.9
106.59	13.4 ± 1.0
110.44	12.4 ± 0.8
110.44	14.3 ± 1.1
125.21	10.7 ± 0.2
125.50	12.8 ± 1.6
125.50	15.2 ± 0.1
152.72	11.8 ± 0.9
152.72	12.7 ± 1.1

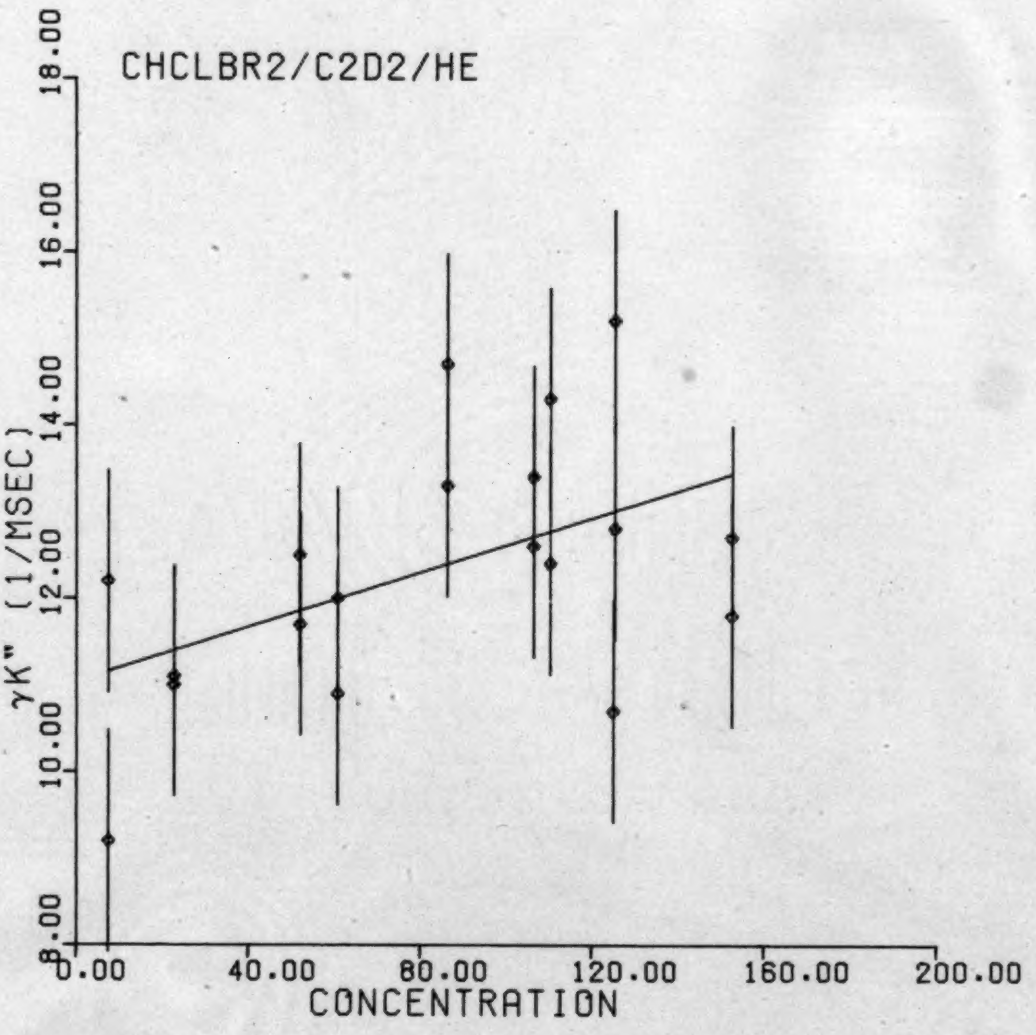

correlation coefficient = 0.50

FIGURE III.14 γk" *versus* Concentration for Acetylene-d,

TABLE III.8

$\gamma k''$ as a Function of Concentration for the Reaction with Propyne

Conc (micromolar)	$\gamma k''$ (1/msec)
0.748	8.3 ± 1.5
2.15	10.1 ± 1.0
2.80	9.1 ± 1.1
2.80	11.3 ± 1.1
3.23	11.1 ± 1.1
3.77	10.0 ± 1.6
3.77	14.3 ± 2.3
4.30	9.4 ± 1.0
4.30	13.1 ± 1.9
4.73	14.4 ± 1.5
4.73	14.6 ± 0.6
5.328	11.3 ± 0.5
5.328	14.0 ± 1.0
6.393	12.9 ± 1.2
6.393	15.0 ± 0.7
7.685	15.6 ± 3.0
7.685	16.0 ± 2.2
9.286	16.4 ± 2.6
9.286	21.1 ± 2.3
10.67	16.5 ± 1.8
10.67	20.5 ± 2.1

With no substrate, $\gamma k'' = \gamma k' = 8.0 \pm 1.0$

TABLE III.9

$\gamma k''$ as a Function of Concentration for the Reaction with 1-Butyne and 2-Butyne

1-Butyne*		2-Butyne**	
Conc (micromolar)	$\gamma k''$ (1/msec)	Conc (micromolar)	$\gamma k''$ (1/msec)
1.07	8.5 ± 0.5	0.21	11.1 ± 2.0
1.61	13.1 ± 1.1	0.21	12.5 ± 1.1
1.61	10.5 ± 0.8	0.21	15.1 ± 2.1
2.20	14.0 ± 1.3	0.32	12.2 ± 0.8
2.20	15.2 ± 2.0	0.32	13.8 ± 1.1
2.68	15.8 ± 1.5	0.43	15.5 ± 1.5
2.68	17.1 ± 1.5	0.43	16.2 ± 2.1
3.43	14.9 ± 1.5	0.538	14.7 ± 1.2
3.44	16.4 ± 1.9	0.540	17.0 ± 5.3
3.75	18.8 ± 1.2	0.700	16.1 ± 2.2
3.76	18.0 ± 2.2	0.702	18.0 ± 1.0
4.23	15.5 ± 2.0	0.861	15.6 ± 3.4
4.88	19.1 ± 1.8	0.861	17.0 ± 1.2
4.88	19.8 ± 1.3	0.861	17.9 ± 1.8
5.417	18.0 ± 0.9	0.969	17.1 ± 2.2
5.421	19.8 ± 1.1	0.969	18.3 ± 2.2
		0.969	22.7 ± 2.2

* With no substrate, $\gamma k'' = \gamma k' = 8.4 \pm 0.8, 10.4 \pm 1.1$

** With no substrate, $\gamma k'' = \gamma k' = 8.0 \pm 1.0$

TABLE III.10

$\gamma k''$ as a Function of Concentration for the Reaction with 1-Pentyne and 2-Pentyne

1-Pentyne		2-Pentyne*	
Conc (micromolar)	$\gamma k''$ (1/msec)	Conc (micromolar)	$\gamma k''$ (1/msec)
1.12	8.9 ± 1.0	0.32	10.6 ± 0.5
2.45	11.7 ± 1.1	0.32	12.9 ± 0.6
2.90	10.9 ± 1.4	0.43	17.2 ± 0.8
2.90	15.0 ± 1.8	0.43	16.0 ± 1.0
3.24	11.9 ± 1.5	0.536	17.9 ± 0.7
3.24	13.4 ± 1.2	0.590	11.7 ± 0.9
3.63	14.7 ± 1.8	0.644	18.2 ± 1.4
3.63	15.3 ± 2.5	0.644	18.6 ± 2.1
4.24	15.2 ± 0.9	0.697	18.3 ± 1.1
4.24	15.2 ± 1.6	0.698	17.9 ± 1.1
5.739	15.6 ± 2.3	0.751	19.0 ± 1.3
5.739	17.0 ± 2.1	0.751	16.9 ± 1.7
		0.803	22.8 ± 1.1
		0.804	14.9 ± 0.9
		0.804	21.3 ± 1.1
		0.858	24.3 ± 3.0
		0.859	19.9 ± 1.5
		1.07	19.0 ± 1.6

* With no substrate, $\gamma k''=\gamma k'=8.3 \pm 0.4,\ 8.6 \pm 0.7,\ 9.4 \pm 1.6$

TABLE III.11

$\gamma k''$ as a Function of Concentration for the Reaction with 3,3-Dimethyl-1-butyne and 2,2,5,5-Tetramethyl-3-hexyne

3.3-Dimethyl-1-butyne*		2,2,5,5-Tetramethyl-3-hexyne**	
Conc (micromolar)	$\gamma k''$ (1/msec)	Conc (micromolar)	$\gamma k''$ (1/msec)
0.21	8.0 ± 0.3	0.53	8.6 ± 1.2
0.27	8.4 ± 0.9	0.53	9.7 ± 0.8
0.27	8.6 ± 0.4	0.53	12.5 ± 1.5
0.42	8.5 ± 1.1	0.799	10.5 ± 1.1
0.43	7.9 ± 0.5	0.799	10.6 ± 0.6
0.532	9.1 ± 0.5	0.799	8.6 ± 0.8
0.540	10.0 ± 1.3	1.06	10.8 ± 2.1
0.748	9.0 ± 0.4	1.07	11.4 ± 1.0
0.750	9.0 ± 0.6	1.16	15.2 ± 2.3
0.846	9.5 ± 0.5	1.17	12.6 ± 1.2
0.847	9.7 ± 0.3	1.33	11.2 ± 1.3
0.961	7.9 ± 0.7	1.34	10.5 ± 1.5
1.18	9.6 ± 0.4	1.60	13.6 ± 1.7
1.18	8.7 ± 0.8	1.60	12.8 ± 1.6
1.39	9.0 ± 0.4	1.60	16.9 ± 1.8
1.38	9.4 ± 0.4	1.61	19.4 ± 1.7
1.53	10.3 ± 0.5	1.86	13.1 ± 1.1
1.53	10.6 ± 0.4	1.87	10.2 ± 0.4
1.71	9.9 ± 0.5	2.13	11.2 ± 1.5
1.88	12.3 ± 0.3	2.14	17.6 ± 3.1
1.89	12.6 ± 0.9	2.14	17.5 ± 1.8
1.93	10.3 ± 0.9	2.40	16.6 ± 2.5
1.93	11.5 ± 1.0	2.41	19.4 ± 1.3
1.94	9.3 ± 0.6	2.66	19.9 ± 3.1
2.11	11.5 ± 0.7	2.67	21.7 ± 1.8
2.11	9.8 ± 0.6	2.68	22.5 ± 1.6
2.42	11.8 ± 1.0	3.15	18.0 ± 1.3
2.42	12.9 ± 1.3	3.18	21.3 ± 2.7
2.50	9.9 ± 0.8	3.71	22.1 ± 3.8
2.69	13.1 ± 1.0	4.31	19.7 ± 4.1
2.68	11.2 ± 1.4	4.35	25.8 ± 2.4
3.22	12.2 ± 1.0		
3.23	11.5 ± 1.3		
3.69	12.7 ± 0.7		
3.70	12.3 ± 0.4		

* With no substrate, $\gamma k'' = \gamma k' = 8.5 \pm 1.2, 8.8 \pm 0.5$

** With no substrate, $\gamma k''=\gamma k'=7.4 \pm 1.4, 8.4 \pm 0.4, 8.9 \pm 1.0$

TABLE III.12

$\gamma k''$ as a Function of Concentration for the Reaction with Phenylacetylene

Conc (micromolar)	$\gamma k''$ (1/msec)
1.07	12.2 ± 1.8
1.07	12.8 ± 1.1
1.71	12.4 ± 0.4
1.71	16.4 ± 1.4
2.14	14.2 ± 1.8
2.14	15.1 ± 1.1
2.78	15.4 ± 1.0
2.79	18.3 ± 1.3
3.20	16.9 ± 2.0
3.21	15.4 ± 0.7

With no substrate, $\gamma k'' = \gamma k' = 9.3 \pm 0.6, 10.3 \pm 0.5$

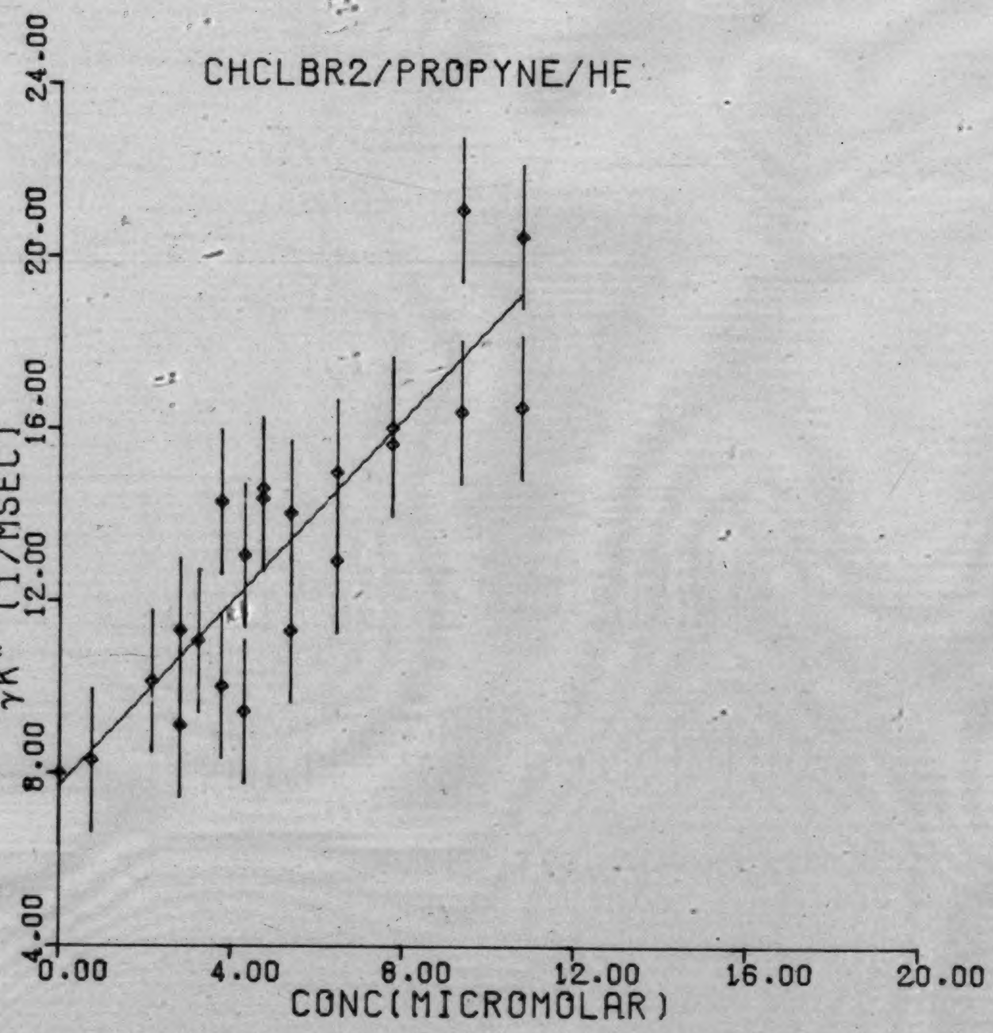

correlation coefficient = 0.90

FIGURE III.15 γk" *versus* Concentration for Propyne

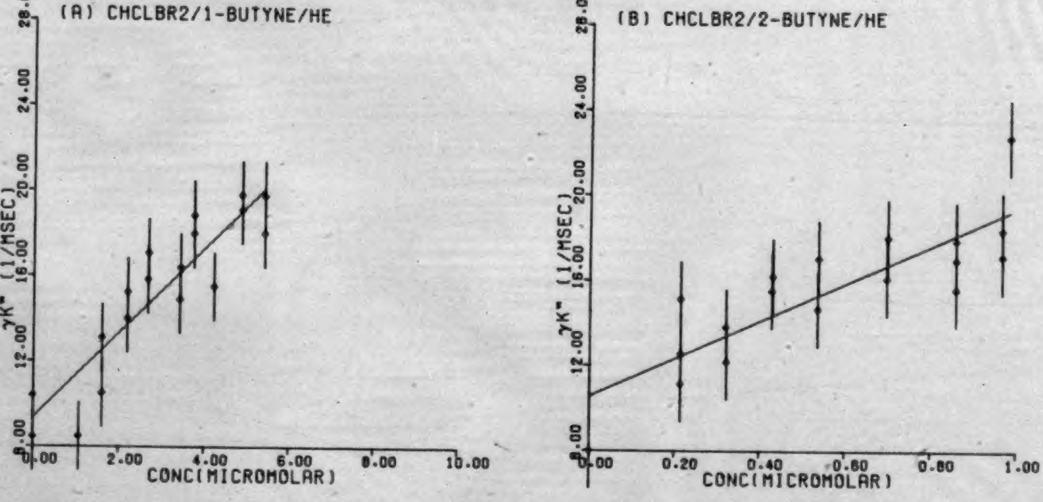

correlation coefficient = 0.87

correlation coefficient = 0.84

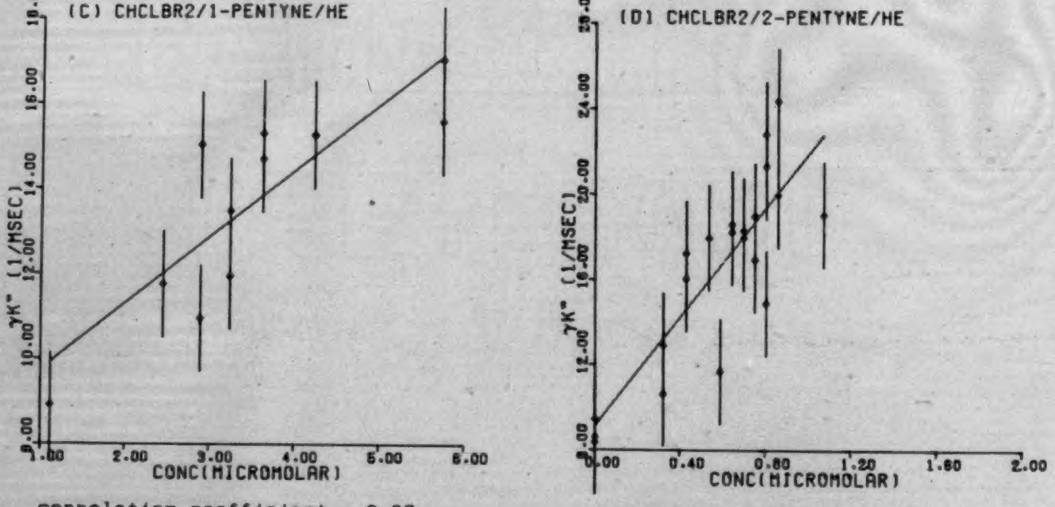

correlation coefficient = 0.87

correlation coefficient = 0.81

FIGURE III.16 γk" *versus* Concentration for (A) 1-Butyne (B) 2-Butyne (C) 1-Pentyne (D) 2-Pentyne

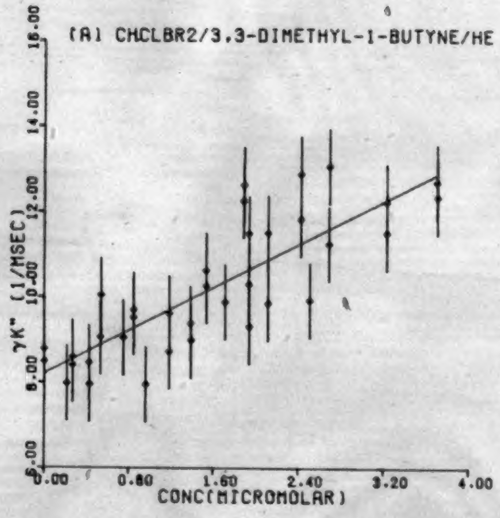

correlation coefficient = 0.83

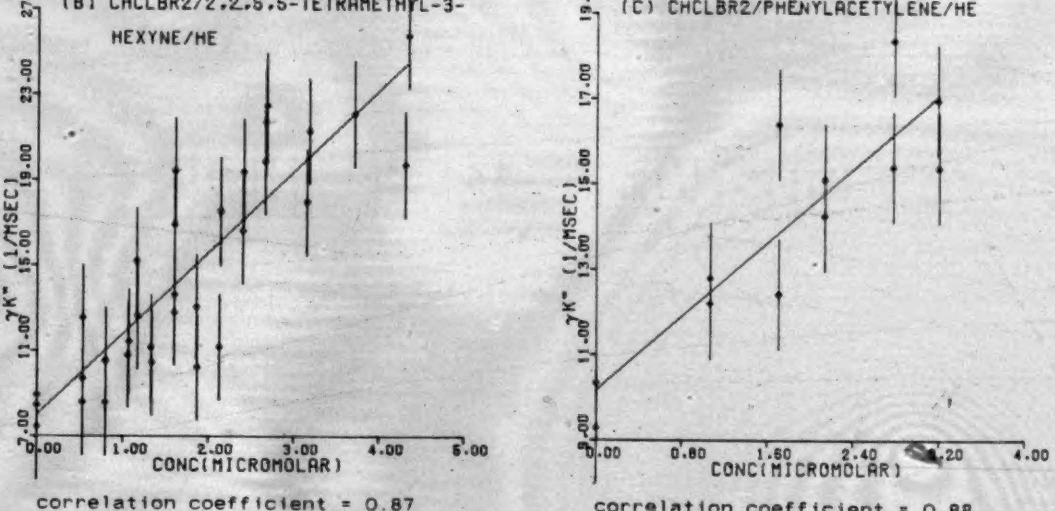

correlation coefficient = 0.87

correlation coefficient = 0.88

FIGURE III.17 γk" *versus* Concentration for (A) 3,3-Dimethyl-1-butyne (B) 2,2,5,5-Tetramethyl-3-hexyne (C) Phenylacetylene

TABLE III.13

Second Order Rate Constants k_1 for the Reactions with Alkynes

Substrate		k_1 ($M^{-1}s^{-1}$)	Number of measurements	Pressure range of substrate (torr)
acetylene	C≡C	(3.5 ± 0.4) X 10^7	200	0.696 - 10.690
acetylene-d_2	DC≡CD	(3.1 ± 1.3) X 10^7	152	0.140 - 2.857
propyne	-≡	(2.2 ± 0.2) X 10^8	176	0.014 - 0.200
1-butyne	--≡	(3.7 ± 0.5) X 10^8	144	0.020 - 0.101
2-butyne	-≡-	(1.8 ± 0.3) X 10^{10}	144	0.004 - 0.018
1-pentyne	---≡	(4.3 ± 0.7) X 10^9	96	0.021 - 0.107
2-pentyne	-≡--	(2.5 ± 0.4) X 10^{10}	168	0.006 - 0.020
3,3-dimethyl-1-butyne	+≡	(2.4 ± 0.3) X 10^9	296	0.004 - 0.070
2,2,5,5-tetra-methyl-3-hexyne	+≡+	(7.6 ± 0.7) X 10^9	272	0.010 - 0.082
phenylacetylene	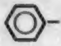-C≡	(4.3 ± 0.7) X 10^9	96	0.020 - 0.060

TABLE III.14

$\gamma k''$ as a Function of Concentration for the Reaction with Silane

Conc (micromolar)	$\gamma k''$ (1/msec)
1.07	9.9 ± 0.9
1.07	11.7 ± 0.4
3.21	11.6 ± 1.0
3.21	11.9 ± 0.5
5.362	13.8 ± 0.7
5.372	14.3 ± 0.4
10.70	13.7 ± 0.5
10.70	15.5 ± 0.6
21.35	15.5 ± 0.8
21.40	16.2 ± 1.2
26.83	17.8 ± 1.3
26.89	20.7 ± 0.7
34.77	17.7 ± 0.7
34.83	20.0 ± 1.4
43.21	22.1 ± 1.1

TABLE III.15

$\gamma k''$ as a Function of Concentration for the Reaction with Monomethylsilane and Dimethylsilane

Monomethylsilane*		Dimethylsilane**	
Conc (micromolar)	$\gamma k''$ (1/msec)	Conc (micromolar)	$\gamma k''$ (1/msec)
0.21	9.2 ± 1.1	0.11	9.9 ± 0.5
0.21	10.2 ± 0.6	0.11	10.1 ± 0.3
0.32	10.5 ± 0.5	0.27	9.2 ± 0.4
0.32	10.6 ± 0.4	0.27	10.4 ± 0.6
0.43	9.3 ± 0.7	0.43	9.2 ± 0.6
0.43	8.8 ± 0.7	0.43	11.1 ± 1.0
0.534	12.2 ± 1.0	0.538	11.3 ± 0.8
0.535	11.0 ± 0.5	0.538	11.3 ± 0.8
0.643	11.2 ± 1.5	0.806	10.9 ± 0.5
0.644	12.2 ± 0.7	0.806	11.7 ± 0.4
0.750	12.8 ± 2.9	1.07	12.1 ± 0.4
0.751	10.2 ± 1.1	1.07	12.3 ± 0.6
0.855	12.5 ± 0.7	1.34	13.3 ± 1.4
0.858	10.6 ± 0.6	1.34	12.4 ± 0.5
0.961	13.2 ± 0.9	1.61	10.6 ± 1.0
0.963	12.4 ± 0.7	1.61	11.4 ± 0.6
1.07	10.8 ± 0.3	1.88	12.4 ± 0.6
1.07	12.4 ± 0.6	1.88	13.6 ± 1.2
1.49	10.1 ± 0.4	2.15	12.8 ± 0.8
1.49	10.9 ± 0.6	2.15	14.3 ± 1.2
2.14	13.4 ± 0.8	2.68	14.1 ± 0.5
3.22	13.8 ± 0.4	2.68	14.7 ± 0.5
3.22	11.9 ± 0.9	3.02	13.7 ± 1.7
4.29	12.8 ± 0.9	3.02	13.6 ± 1.0
4.30	15.2 ± 0.5	3.66	13.1 ± 1.4
5.362	14.7 ± 1.0	3.66	14.1 ± 1.1
5.369	16.7 ± 0.6	4.31	17.6 ± 1.3
6.447	14.9 ± 1.1	5.388	19.3 ± 1.6
7.511	17.4 ± 1.2	5.392	18.8 ± 1.5
8.573	15.0 ± 1.5	6.462	18.5 ± 1.5
8.573	19.1 ± 2.2	7.541	17.8 ± 1.1
		7.541	21.1 ± 2.1
		8.622	24.4 ± 3.1
		8.607	20.4 ± 2.0
		9.703	23.2 ± 2.5

* With no substrate, $\gamma k'' = \gamma k' = 8.6 \pm 0.5, 9.4 \pm 0.4$

** With no substrate, $\gamma k'' = \gamma k' = 8.8 \pm 0.2, 8.6 \pm 0.4$

TABLE III.16

$\gamma k''$ as a Function of Concentration for the Reaction with Trimethylsilane and Tetramethylsilane

Trimethylsilane*		Tetramethylsilane	
Conc (micromolar)	$\gamma k''$ (1/msec)	Conc (micromolar)	$\gamma k''$ (1/msec)
1.61	10.7 ± 0.7	5.326	9.3 ± 0.4
1.61	12.5 ± 0.7	5.342	10.7 ± 0.6
2.68	14.0 ± 0.9	26.57	9.7 ± 0.9
2.68	14.4 ± 0.3	26.61	9.2 ± 0.7
4.27	14.0 ± 0.7	54.429	9.3 ± 0.3
4.29	16.6 ± 1.4	54.465	8.4 ± 0.4
5.363	17.9 ± 0.8	106.27	9.0 ± 0.6
5.369	16.0 ± 0.8	106.34	9.1 ± 0.3
6.427	17.4 ± 0.8	123.39	6.6 ± 0.5
6.434	18.6 ± 1.0	123.72	11.5 ± 1.0
7.504	18.3 ± 1.4	132.62	6.7 ± 0.5
7.506	21.7 ± 1.6	132.93	9.3 ± 0.8
8.570	22.0 ± 1.5	212.53	8.0 ± 0.3
8.578	20.8 ± 2.0	213.23	9.4 ± 0.5
		329.15	7.7 ± 0.9
		330.14	9.9 ± 0.4

* With no substrate, $\gamma k'' = \gamma k' = 8.3 \pm 0.5, 9.1 \pm 0.6$

TABLE III.17

$\gamma k''$ as a Function of Concentration for the Reaction with Silane-d_4 and Monomethylsilane-d_3

Silane-d_4	
Conc (micromolar)	$\gamma k''$ (1/msec)
1.08	10.0 ± 0.5
1.08	10.0 ± 0.7
2.15	10.5 ± 0.7
2.16	11.8 ± 0.6
4.31	11.0 ± 0.8
4.31	11.2 ± 0.9
6.460	11.3 ± 0.1
6.462	12.0 ± 0.9
6.468	11.9 ± 1.1
8.072	12.8 ± 0.6
8.088	11.5 ± 0.5
9.686	12.9 ± 0.4
9.703	13.0 ± 0.8
12.92	13.4 ± 0.7
12.95	13.1 ± 0.5
27.40	13.1 ± 1.0
27.43	15.0 ± 0.9
44.36	15.4 ± 1.0
44.36	16.9 ± 1.2

Monomethylsilane-d_4	
Conc (micromolar)	$\gamma k''$ (1/msec)
0.11	9.1 ± 0.3
0.11	8.4 ± 0.2
0.16	10.2 ± 0.7
0.16	9.3 ± 0.2
0.27	10.0 ± 0.5
0.27	9.3 ± 0.7
0.27	8.5 ± 0.5
0.37	9.7 ± 0.8
0.38	9.2 ± 0.2
0.48	9.7 ± 0.2
0.48	9.7 ± 0.7
0.535	10.0 ± 0.4
0.539	9.6 ± 0.6
0.693	10.3 ± 0.7
0.694	10.4 ± 0.6
0.754	9.4 ± 0.2
0.755	10.5 ± 0.6
0.805	9.4 ± 0.6
0.812	10.1 ± 0.6
1.07	10.4 ± 0.2
2.15	9.9 ± 0.4
2.15	10.8 ± 0.5
4.28	11.3 ± 1.5
4.29	11.5 ± 1.3
6.436	12.8 ± 0.5
6.438	13.0 ± 0.5
8.558	13.6 ± 0.7
8.587	13.6 ± 0.6
7.526	13.9 ± 1.1
10.75	14.1 ± 0.6
10.78	14.4 ± 0.8
12.90	15.1 ± 0.7
12.93	15.7 ± 1.0
15.05	16.0 ± 1.0
15.09	17.6 ± 1.1

TABLE III.18

$\gamma k''$ as a Function of Concentration for the Reaction with Dimethylsilane-d_2 and Trimethylsilane-d_1

Dimethylsilane-d_2*		Trimethylsilane-d_1**	
Conc (micromolar)	$\gamma k''$ (l/msec)	Conc (micromolar)	$\gamma k''$ (l/msec)
0.32	8.8 ± 0.7	0.537	9.3 ± 0.5
0.32	10.1 ± 0.3	0.538	10.4 ± 0.6
0.43	8.8 ± 1.2	0.806	7.5 ± 0.8
0.43	10.2 ± 0.5	0.807	8.4 ± 0.5
0.534	9.3 ± 0.4	1.09	9.8 ± 0.8
0.537	9.4 ± 0.4	1.09	12.7 ± 0.4
0.642	9.8 ± 0.4	1.61	12.3 ± 1.3
0.642	8.3 ± 0.3	1.61	12.0 ± 0.5
0.756	8.9 ± 0.7	2.17	12.7 ± 0.7
0.756	9.1 ± 0.6	3.23	12.5 ± 1.6
0.961	9.5 ± 0.3	3.23	14.3 ± 1.4
0.961	9.9 ± 0.8	4.30	14.5 ± 1.8
1.28	9.6 ± 0.5	4.30	15.5 ± 0.7
1.28	10.1 ± 0.4	5.370	17.6 ± 1.0
1.51	9.9 ± 1.1	5.383	16.5 ± 0.6
1.52	10.4 ± 1.0	6.506	18.7 ± 0.7
1.60	11.3 ± 0.8	7.253	18.8 ± 1.5
1.89	11.9 ± 1.0	7.262	18.8 ± 1.1
1.89	11.1 ± 0.5	7.610	20.4 ± 1.9
2.13	11.8 ± 0.5	8.140	22.1 ± 0.8
2.14	11.7 ± 0.8	8.593	18.4 ± 1.6
2.15	11.0 ± 0.6	8.613	20.4 ± 2.1
2.15	10.1 ± 0.8		
3.23	11.3 ± 0.5		
4.30	14.0 ± 1.4		
4.30	12.8 ± 1.5		
5.387	13.7 ± 0.9		
5.387	15.2 ± 1.9		
6.455	14.8 ± 1.2		
7.519	15.0 ± 1.5		
7.539	14.5 ± 0.8		
8.641	16.3 ± 1.5		

* With no substrate, $\gamma k'' = \gamma k' = 7.4 \pm 0.5, 8.2 \pm 0.5$

**With no substrate, $\gamma k'' = \gamma k' = 8.4 \pm 0.6, 8.4 \pm 0.7$

TABLE III.19

$\gamma k''$ as a Function of Concentration for the Reaction with Diethylsilane and Triethylsilane

Diethylsilane*	
Conc (micromolar)	$\gamma k''$ (1/msec)
2.14	13.8 ± 0.9
2.14	12.5 ± 0.8
4.27	14.1 ± 1.4
4.28	17.9 ± 0.9
5.321	17.9 ± 0.7
5.360	17.2 ± 2.2
6.415	19.3 ± 0.8
6.430	16.3 ± 1.2
6.910	21.1 ± 1.5
6.947	18.9 ± 1.2
8.018	22.2 ± 0.8
9.576	21.2 ± 3.0
9.648	23.9 ± 1.4

Triethylsilane**	
Conc (micromolar)	$\gamma k''$ (1/msec)
0.27	10.4 ± 0.3
0.27	11.6 ± 0.6
0.37	11.9 ± 0.3
0.37	11.4 ± 0.2
0.535	10.4 ± 1.5
0.535	10.3 ± 1.0
0.801	10.2 ± 0.8
0.801	12.6 ± 1.7
1.07	14.2 ± 0.7
1.07	12.3 ± 1.1
1.33	11.6 ± 0.8
1.34	14.7 ± 0.4
1.60	11.7 ± 1.4
1.61	13.5 ± 1.3
2.14	14.2 ± 1.0
2.14	13.2 ± 1.2
3.10	17.8 ± 1.7
3.11	18.3 ± 0.7
3.21	16.8 ± 0.9
3.21	14.1 ± 1.1
4.28	20.0 ± 0.4
5.354	22.0 ± 1.6
6.423	26.2 ± 2.4
6.425	22.8 ± 1.2
7.484	25.9 ± 2.3
7.501	28.4 ± 3.3
8.561	27.6 ± 2.3
8.564	29.0 ± 3.0

---

* With no substrate, $\gamma k'' = \gamma k' = 7.3 \pm 0.4, 9.8 \pm 0.4$

** With no substrate, $\gamma k'' = \gamma k' = 7.3 \pm 0.7, 8.7 \pm 0.3$

versus concentration are given in Figures III.18 - III.20.

Halogenated Silanes:

Trichlorosilane, dichlorosilane, methyldichlorosilane, dimethylchlorosilane, trimethylchlorosilane, methyltrifluorosilane, dimethyldifluorosilane, trimethylfluorosilane were studied.

The values of $\gamma k''$ as a function of concentration are presented in Tables III.20 - III.25. No measurable reaction was obtained with trichlorosilane, trimethylchlorosilane and the methylfluorinated silanes. The plots of $\gamma k''$ *versus* concentration for the other halogenated silanes are given in Figures III.21 and III.22. The data for dichlorosilane are quite scattered, probably due to the occurrence of side reactions.

Disilanes and Halogenated Disilanes:

Disilane, disilane-d_6, hexamethyldisilane and hexachlorodisilane were studied. The values of $\gamma k''$ as a function of concentration are presented in Tables III.26 and III.27. No measurable reaction was obtained with hexachlorodisilane. The plots of $\gamma k''$ *versus* concentration for the other disilanes are given in Figure III.23.

The values of k_1 for silanes, halogenated silanes, disilanes and halogenated disilanes were determined from the slopes of the $\gamma k''$ *versus* concentration plots and are summarized in Tables III.28 - III.30.

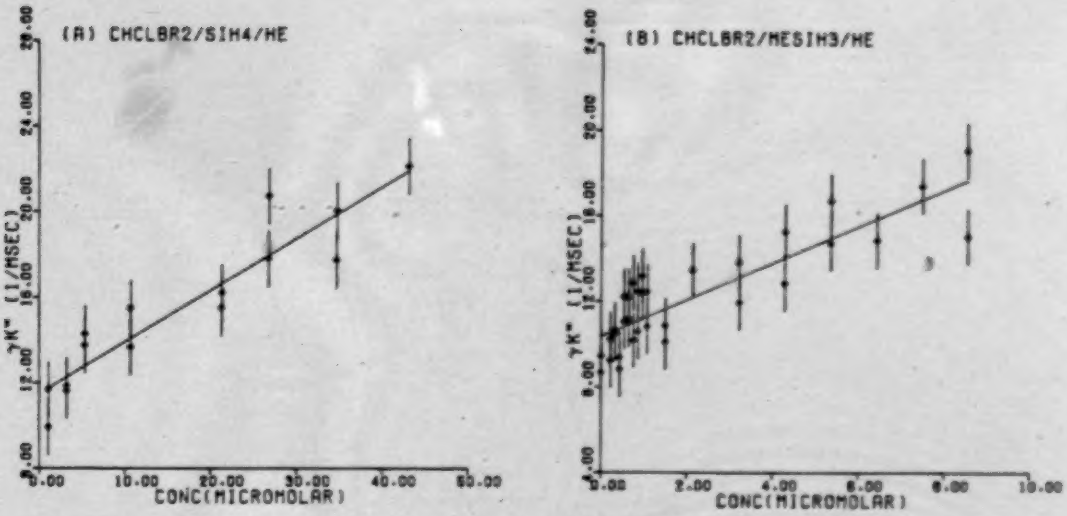

correlation coefficient = 0.94

correlation coefficient = 0.87

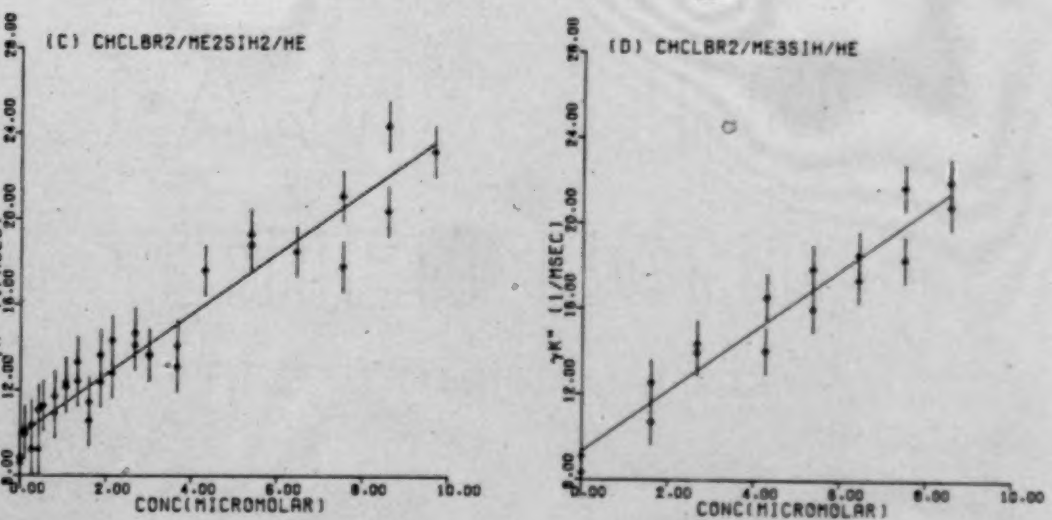

correlation coefficient = 0.96

correlation coefficient = 0.97

FIGURE III.18 γk" *versus* Concentration for (A) Silane (B) Monomethylsilane (C) Dimethylsilane (D) Trimethylsilane

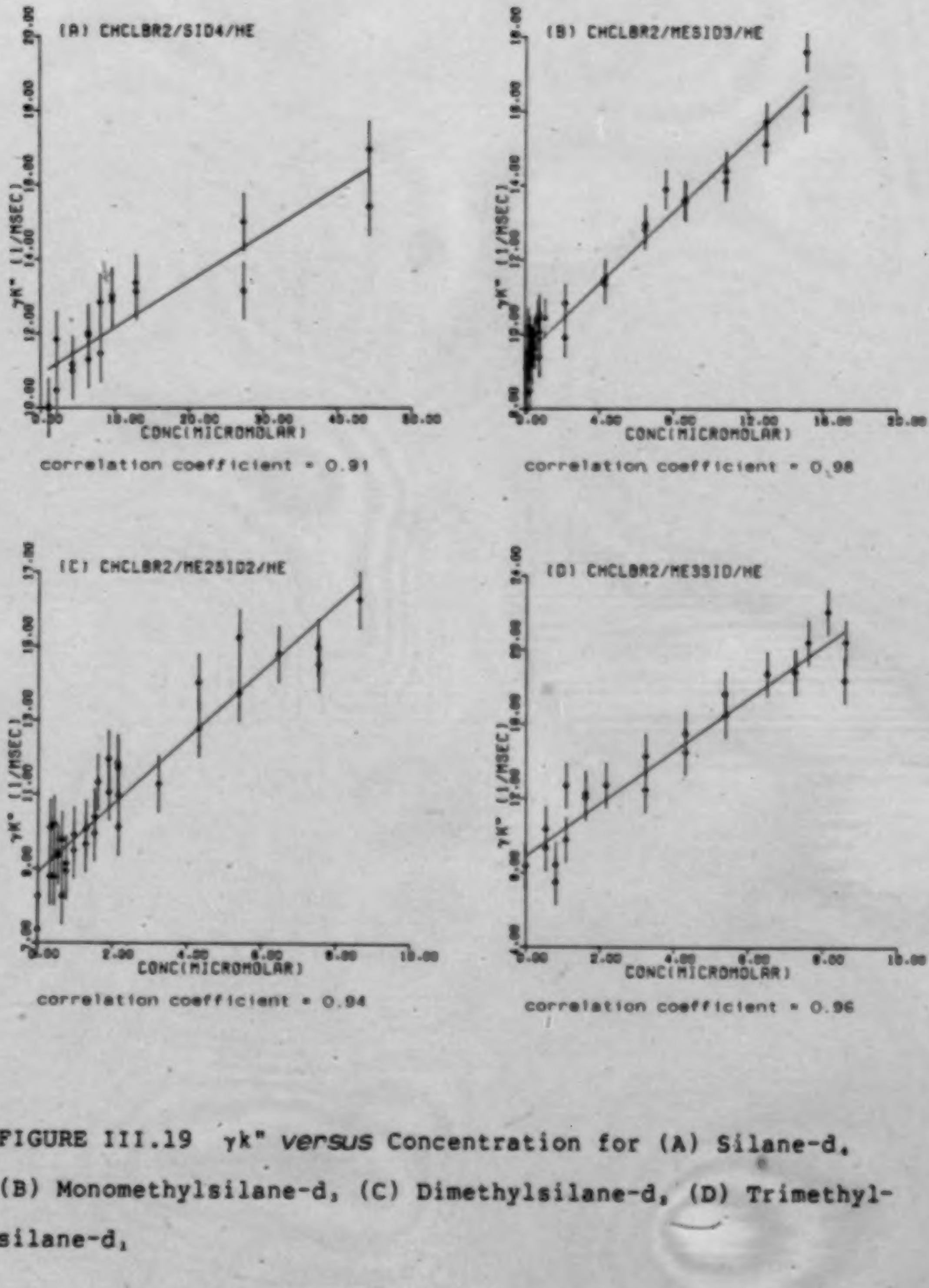

FIGURE III.19 γk" *versus* Concentration for (A) Silane-d, (B) Monomethylsilane-d, (C) Dimethylsilane-d, (D) Trimethylsilane-d,

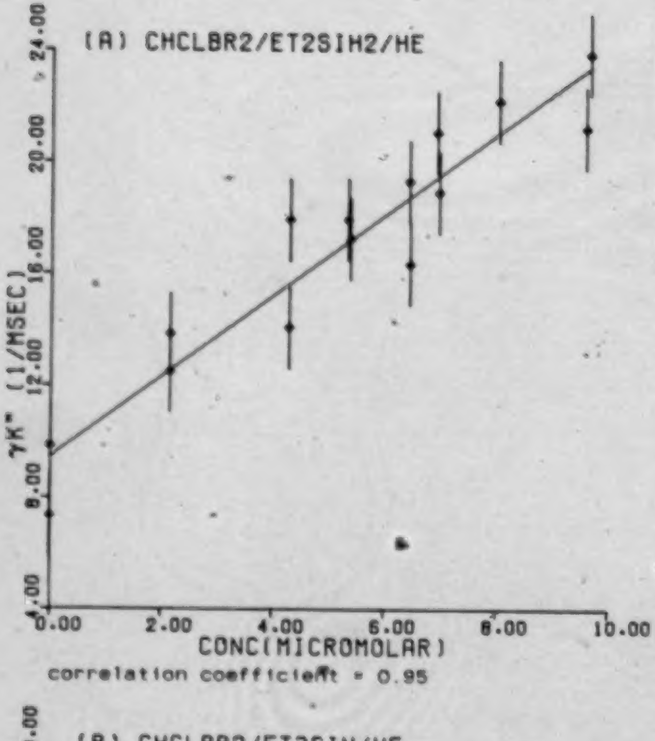

correlation coefficient = 0.95

correlation coefficient = 0.98

FIGURE III.20 γk" *versus* Concentration for (A) Diethylsilane (B) Triethylsilane

TABLE III.20

γk" as a Function of Concentration for the Reaction with Methyldichlorosilane and Dimethylchlorosilane

Methyldichlorosilane* Dichloromethylsilane		Dimethylchlorosilane**	
Conc (micromolar)	γk" (1/msec)	Conc (micromolar)	γk" (1/msec)
2.69	9.4 ± 0.5	2.69	9.6 ± 0.3
2.69	9.8 ± 0.2		
10.73	9.6 ± 0.8	2.69	9.4 ± 0.5
10.78	10.3 ± 0.6		
26.77	9.4 ± 0.7	10.74	12.4 ± 0.6
26.84	8.7 ± 0.7		
42.99	8.9 ± 0.5	10.75	11.9 ± 0.6
43.05	11.3 ± 0.5		
54.028	9.6 ± 0.6	21.41	16.0 ± 0.8
54.265	9.1 ± 0.7		
85.300	10.0 ± 0.3	21.58	16.5 ± 1.2
85.585	11.0 ± 0.4		
113.22	11.0 ± 0.7	37.48	18.9 ± 1.5
134.31	10.6 ± 0.7		
134.99	10.1 ± 1.0	37.85	17.9 ± 1.3
161.44	10.7 ± 0.7		
161.66	10.8 ± 1.0	42.98	17.0 ± 1.0
188.03	10.7 ± 1.3		
188.98	13.0 ± 1.0	42.98	18.1 ± 0.7
203.34	12.2 ± 0.4		
215.40	11.4 ± 1.0	58.997	22.2 ± 1.7
215.47	13.6 ± 0.8		
242.99	13.2 ± 0.4	59.514	23.6 ± 1.7
244.22	13.7 ± 0.3		
293.12	12.1 ± 0.4	107.41	29.6 ± 0.9
294.20	13.5 ± 0.9		
		107.59	29.4 ± 3.1

* With no substrate, γk" = γk' = 8.3 ± 0.4, 8.8 ± 0.3

**With no substrate, γk" = γk' = 7.9 ± 0.6, 8.6 ± 0.5

TABLE III.21

$\gamma k''$ as a Function of Concentration for the Reaction with Trichlorosilane

Conc (micromolar)	$\gamma k''$ (1/msec)	Conc (micromolar)	$\gamma k''$ (1/msec)
0.27	9.8 ± 0.6	8.024	8.5 ± 0.5
0.27	9.0 ± 0.2	8.029	8.9 ± 0.5
0.533	8.5 ± 0.4	10.70	9.6 ± 0.5
0.536	8.4 ± 0.3	10.75	9.2 ± 0.5
0.743	9.3 ± 0.7	16.03	8.2 ± 0.6
0.747	9.1 ± 0.5	16.05	9.2 ± 0.7
1.06	8.7 ± 0.3	21.32	9.2 ± 0.6
1.07	8.3 ± 0.4	21.41	7.9 ± 0.4
1.48	9.3 ± 1.0	26.75	9.6 ± 0.7
1.49	9.4 ± 0.2	26.76	8.6 ± 0.8
1.70	9.3 ± 0.2	32.17	8.0 ± 0.5
1.71	8.9 ± 0.4	32.32	9.3 ± 0.7
2.12	9.6 ± 0.5	37.44	8.6 ± 1.1
2.14	8.1 ± 0.6	55.466	7.9 ± 0.7
2.54	9.1 ± 0.2	55.503	8.4 ± 0.5
2.55	9.8 ± 0.6	168.77	8.6 ± 0.7
3.18	8.8 ± 0.2	169.79	10.0 ± 0.4
3.24	9.7 ± 0.6	267.86	8.6 ± 0.4
4.20	8.2 ± 0.8	269.76	9.7 ± 0.6
4.26	9.7 ± 0.3	371.03	8.8 ± 0.9
4.80	8.0 ± 0.5	371.27	8.6 ± 0.4
4.83	8.1 ± 0.7	482.16	8.8 ± 1.0
5.317	8.5 ± 0.5	485.08	8.5 ± 0.6

With no substrate, $\gamma k'' = \gamma k' = 8.0 \pm 0.5, 8.9 \pm 0.5$

TABLE III.22

$\gamma k''$ as a Function of Concentration for the Reaction with Dichlorosilane and Trimethylchlorosilane

Dichlorosilane*		Trimethylchlorosilane	
Conc (micromolar)	$\gamma k''$ (1/msec)	Conc (micromolar)	$\gamma k''$ (1/msec)
26.37	8.0 ± 1.2	209.69	6.0 ± 0.7
26.57	10.0 ± 0.6	209.90	6.8 ± 0.4
52.908	11.5 ± 0.8	429.73	7.5 ± 0.5
53.153	11.8 ± 0.7	429.87	7.2 ± 0.6
80.155	18.2 ± 1.9		
80.370	16.9 ± 0.4		
105.57	15.2 ± 1.2		
105.96	19.3 ± 1.3		
131.88	18.0 ± 1.2		
132.88	16.2 ± 2.7		
160.26	25.3 ± 2.1		
160.58	26.6 ± 1.8		
268.27	19.0 ± 1.6		
359.10	19.1 ± 2.1		
359.94	26.5 ± 5.7		
1089.6	16.8 ± 1.4		
2717.3	13.3 ± 2.9		
2721.8	17.4 ± 2.0		

* With no substrate, $\gamma k'' = \gamma k' = 6.6 \pm 0.3, 7.3 \pm 0.7$

TABLE III.23

γk" as a Function of Concentration for the Reaction with Trimethylfluorosilane

Conc (micromolar)	γk" (1/msec)
1.06	7.1 ± 0.8
1.07	7.6 ± 0.8
2.66	7.8 ± 1.4
3.08	8.2 ± 0.8
3.08	10.5 ± 1.6
5.374	7.0 ± 0.7
8.032	7.6 ± 0.5
8.061	8.1 ± 1.3
37.00	7.9 ± 0.6
37.08	8.0 ± 0.6
42.77	9.5 ± 1.4
47.59	7.5 ± 1.5
47.76	8.6 ± 0.5
63.721	9.1 ± 0.9

TABLE III.24

$\gamma k''$ as a Function of Concentration for the Reaction with Dimethyldifluorosilane

Conc (micromolar)	$\gamma k''$ (1/msec)
21.27	10.2 ± 0.7
21.30	8.9 ± 0.8
42.55	9.8 ± 0.9
42.61	10.3 ± 0.5
69.335	11.0 ± 0.3
69.427	9.3 ± 0.9
95.740	8.9 ± 0.6
95.740	10.5 ± 1.2
160.15	9.6 ± 0.6
160.20	9.1 ± 0.3
240.20	8.6 ± 0.4
240.28	9.0 ± 0.9

TABLE III.25

$\gamma k''$ as a Function of Concentration for the Reaction with Methyltrifluorosilane

Conc (micromolar)	$\gamma k''$ (1/msec)
5.299	8.3 ± 1.5
10.68	7.4 ± 0.6
10.69	8.3 ± 0.6
21.37	7.3 ± 0.8
21.39	8.6 ± 0.4
23.13	9.1 ± 0.9
23.19	10.6 ± 0.3
23.24	10.2 ± 0.6
26.55	9.7 ± 0.7
37.39	8.1 ± 1.0
37.41	9.3 ± 0.4
42.42	9.3 ± 0.4
42.47	7.8 ± 1.3
53.455	8.1 ± 1.0
53.455	8.6 ± 0.4
63.679	8.4 ± 1.4
63.721	7.2 ± 0.6
95.803	10.7 ± 0.5
95.899	10.3 ± 1.1

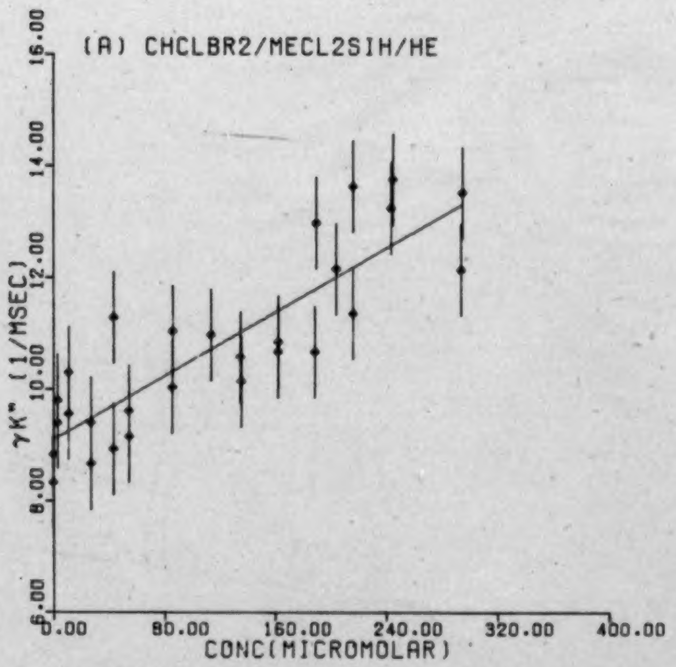

correlation coefficient = 0.86

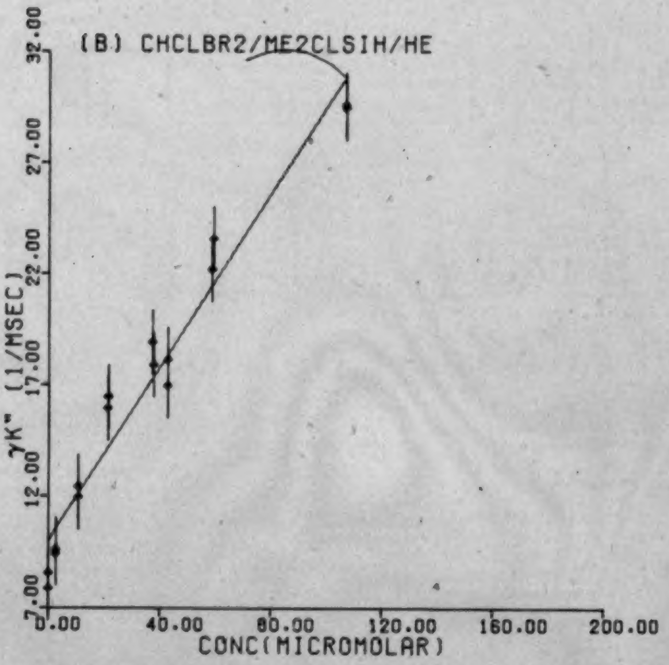

correlation coefficient = 0.98

FIGURE III.21 γk" *versus* Concentration for (A) Methyl dichlorosilane (B) Dimethylchlorosilane

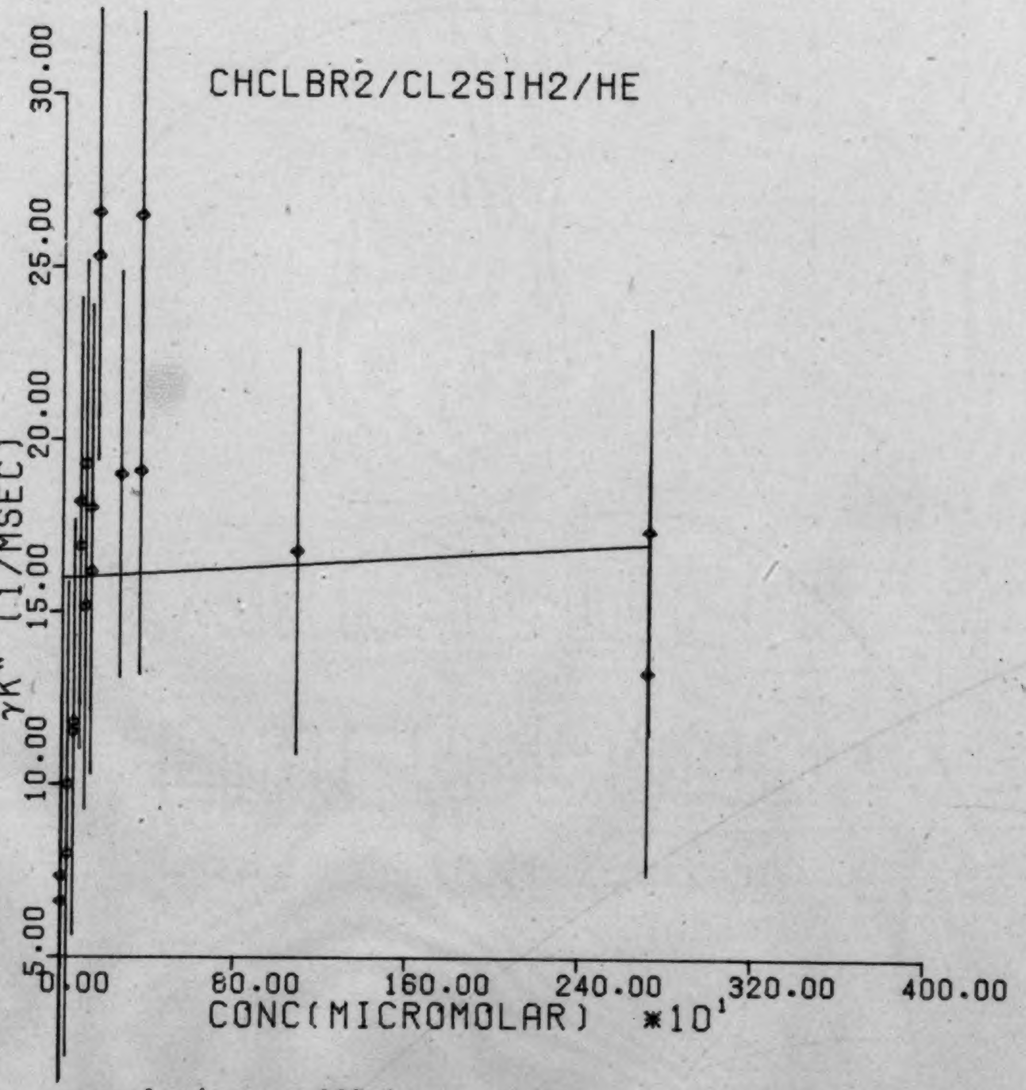

correlation coefficient = 0.53

FIGURE III.22 γk" *versus* Concentration for Dichlorosilane

TABLE III.26

γk" as a Function of Concentration for the Reaction with Disilane and Disilane-d_6

Disilane		Disilane-d_6*	
Conc (micromolar)	γk" (1/msec)	Conc (micromolar)	γk" (1/msec)
0.21	7.4 ± 0.5	0.533	8.1 ± 0.5
0.21	6.3 ± 0.4	0.535	7.0 ± 0.5
0.43	7.5 ± 0.4	1.34	8.3 ± 0.2
0.43	7.9 ± 0.3	1.33	8.9 ± 0.6
0.43	7.7 ± 0.4	2.14	12.1 ± 0.8
0.642	6.5 ± 0.5	2.67	14.4 ± 1.2
0.643	6.5 ± 0.3	2.67	12.1 ± 1.5
1.07	10.0 ± 0.6	3.46	15.4 ± 1.9
1.07	8.1 ± 0.5	3.48	15.9 ± 1.4
1.61	9.7 ± 0.9	4.81	21.5 ± 1.3
1.61	9.9 ± 0.5	4.81	17.4 ± 4.0
2.68	14.1 ± 1.1	6.961	26.1 ± 4.1
2.68	14.4 ± 1.0		
3.48	17.8 ± 0.7		
3.49	17.5 ± 0.9		
4.29	19.1 ± 3.5		

* With no substrate, γk" = γk' = 6.8 ± 0.3, 6.9 ± 0.1

TABLE III.27

$\gamma k''$ as a Function of Concentration for the Reaction with Hexamethyldisilane and Hexachlorodisilane

Hexamethyldisilane*		Hexachlorodisilane	
Conc (micromolar)	$\gamma k''$ (1/msec)	Conc (micromolar)	$\gamma k''$ (1/msec)
1.63	9.1 ± 0.6	21.41	8.8 ± 0.7
1.63	10.0 ± 0.7	21.47	9.8 ± 0.8
5.524	9.6 ± 0.6	32.18	7.8 ± 0.6
43.50	10.4 ± 0.4	32.23	8.0 ± 0.6
44.24	10.8 ± 0.3		
97.585	11.9 ± 1.2		
98.016	10.8 ± 1.0		
128.38	11.0 ± 0.4		
128.68	10.3 ± 0.2		
235.97	12.1 ± 1.0		
236.20	12.4 ± 0.8		
299.85	13.5 ± 0.5		
300.25	14.4 ± 0.5		

* With no substrate, $\gamma k'' = \gamma k' = 8.3 \pm 0.2, 8.8 \pm 0.4$

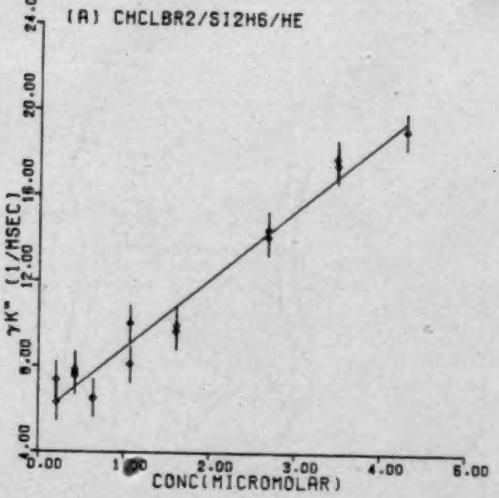

correlation coefficient = 0.98

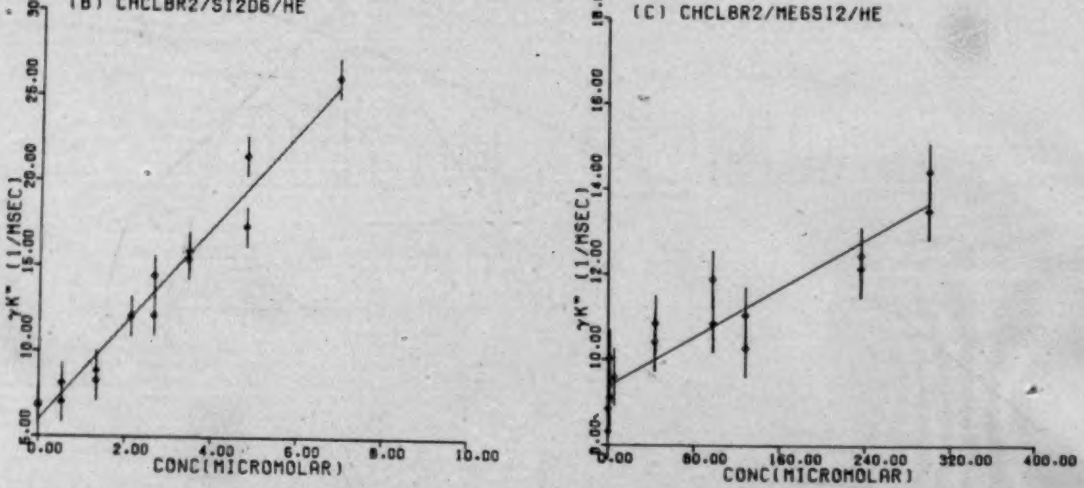

correlation coefficient = 0.98

correlation coefficient = 0.92

FIGURE III.23 γk" *versus* Concentration for (A) Disilane (B) Disilane-d, (C) Hexamethyldisilane

TABLE III.28

Second Order Rate Constants k_1 for the Reactions with Silanes

Substrate		k_1 ($M^{-1}s^{-1}$)	Number of measurements	Pressure range of substrate (torr)
silane	SiH_4	$(4.8 \pm 0.5) \times 10^8$	105	0.020 - 0.806
monomethylsilane	$MeSiH_3$	$(1.7 \pm 0.2) \times 10^9$	231	0.004 - 0.160
dimethylsilane	Me_2SiH_2	$(2.8 \pm 0.1) \times 10^9$	252	0.002 - 0.180
trimethylsilane	Me_3SiH	$(2.8 \pm 0.2) \times 10^9$	112	0.030 - 0.160
tetramethylsilane	Me_4Si	no reaction	112	0.100 - 6.211
silane-d_4	SiD_4	$(2.5 \pm 0.3) \times 10^8$	133	0.020 - 0.826
monomethylsilane-d_3	$MeSiD_3$	$(9.8 \pm 0.4) \times 10^8$	245	0.002 - 0.280
dimethylsilane-d_2	Me_2SiD_2	$(1.8 \pm 0.1) \times 10^9$	238	0.006 - 0.161
trimethylsilane-d_1	Me_3SiD	$(2.8 \pm 0.2) \times 10^9$	161	0.010 - 0.160
diethylsilane	Et_2SiH_2	$(2.9 \pm 0.3) \times 10^9$	105	0.040 - 0.180
triethylsilane	Et_3SiH	$(4.5 \pm 0.1) \times 10^9$	210	0.005 - 0.160

TABLE III.29

Second Order Rate Constants k_2 for the Reactions with Halogenated Silanes

Substrate		k_2 ($M^{-1}s^{-1}$)	Number of measurements	Pressure range of substrate (torr)
trichlorosilane	Cl_3SiH	no reaction	336	0.005 - 9.002
dichlorosilane	Cl_2SiH_2	side reactions?	140	0.500 - 50.800
trimethylchlorosilane	$ClMe_3Si$	no reaction	35	4.000 - 8.200
dimethylchlorosilane	$ClMe_2SiH$	$(3.9 \pm 0.2) \times 10^8$	112	0.050 - 2.000
methyldichlorosilane	Cl_2MeSiH	$(2.9 \pm 0.3) \times 10^7$	196	0.050 - 5.500
trimethylfluorosilane	FMe_3Si	no reaction	112	0.020 - 1.200
dimethyldifluorosilane	F_2Me_2Si	no reaction	84	0.400 - 4.501
methyltrifluorosilane	F_3MeSi	no reaction	154	0.100 - 1.800

TABLE III.30

Second Order Rate Constants k_1 for the Reactions with Disilanes

Substrate		$k_1 (M^{-1}s^{-1})$	Number of measurements	Pressure range of substrate (torr)
disilane	Si_2H_6	$(6.5 \pm 0.3) \times 10^9$	112	0.004 - 0.080
disilane-d_6	Si_2D_6	$(5.6 \pm 0.3) \times 10^9$	98	0.010 - 0.130
hexamethyldisilane	Me_6Si_2	$(2.5 \pm 0.3) \times 10^7$	105	0.030 - 5.600
hexachlorodisilane	Cl_6Si_2	no reaction	28	0.400 - 0.600

Cyclic Compounds and Heterocyclic Compounds

Cyclic Compounds:

Cyclohexane, cyclopentane, cyclohexene, 1,3-cyclohexadiene, 1,4-cyclohexadiene, benzene, toluene, chlorobenzene and fluorobenzene were studied.

The values of $\gamma k''$ as a function of concentration are presented in Tables III.31 - III.35. No measurable reaction was observed with cyclohexane and cyclopentane. Only seven measurements were made for cyclopentane at 26.52 torr due to insufficient amount of pure substrate. The plots of $\gamma k''$ *versus* concentration for the remaining cyclic compounds are given in Figures III.24 and III.25.

Heterocyclic Compounds:

Thiacyclohexane, tetrahydrothiophene, pyrrolidine, tetrahydrofuran, thiophene, pyrrole, 1-methylpyrrole and pyridine were examined.

Pyrrolidine, like ammonia, exhibited a great affinity towards glass surfaces and no determination of $\gamma k''$ was made for this substrate, since the CCl signals were quenched completely at a substrate pressure of only one torr. A comparison with silane ($k_1 = (4.8 \pm 0.5) \times 10^8\ M^{-1}\ s^{-1}$), in which the signals were very weak at the maximum pressure used, 0.806 torr, suggests that for pyrrolidine, $k_1 > 4.8 \times 10^8\ M^{-1}\ s^{-1}$.

For the other heterocyclic compounds, the values of $\gamma k''$ as a function of concentration are presented in Tables III.36 - III.39, while the plots of $\gamma k''$ *versus* concentration

TABLE III.31

$\gamma k''$ as a Function of Concentration for the Reaction with Cyclopentane and Cyclohexane

Cyclopentane		Cyclohexane	
Conc (micromolar)	$\gamma k''$ (1/msec)	Conc (micromolar)	$\gamma k''$ (1/msec)
1416.3	10.0 ± 0.8	53.580	8.4 ± 0.5
		53.669	9.4 ± 0.3
		267.54	8.1 ± 0.4
		268.35	8.9 ± 0.5
		547.24	7.3 ± 1.0
		547.24	8.4 ± 1.0
		1929.3	8.9 ± 0.7

TABLE III.32

$\gamma k''$ as a Function of Concentration for the Reaction with Cyclohexene

Conc (micromolar)	$\gamma k''$ (1/msec)
0.533	7.7 ± 0.8
0.536	8.3 ± 0.4
1.60	10.2 ± 0.7
1.60	10.3 ± 0.6
2.67	12.8 ± 0.9
2.67	13.4 ± 0.2
3.73	14.7 ± 1.1
3.73	15.4 ± 0.4
5.331	21.4 ± 0.5
5.333	19.9 ± 1.0
8.050	22.6 ± 1.9
10.67	24.0 ± 1.4
10.67	25.6 ± 2.2
13.33	27.7 ± 3.5
13.38	28.3 ± 2.3

TABLE III.33

$\gamma k''$ as a Function of Concentration for the Reaction with 1,3-Cyclohexadiene and 1,4-Cyclohexadiene

1,3-Cyclohexadiene		1,4-Cyclohexadiene	
Conc (micromolar)	$\gamma k''$ (1/msec)	Conc (micromolar)	$\gamma k''$ (1/msec)
0.27	5.9 ± 0.4	0.27	6.9 ± 0.4
0.27	7.1 ± 0.6	0.27	7.3 ± 0.3
0.43	6.3 ± 0.6	0.799	8.5 ± 0.4
0.43	5.3 ± 0.3	0.801	6.8 ± 1.0
1.29	6.4 ± 0.6	2.13	9.5 ± 0.7
1.29	8.1 ± 0.9	2.14	9.0 ± 0.3
2.69	8.2 ± 0.9	2.67	9.7 ± 0.7
2.70	9.0 ± 1.4	2.67	10.7 ± 0.6
3.77	9.0 ± 1.1	3.74	11.7 ± 0.7
3.78	8.9 ± 1.3	4.80	14.9 ± 1.1
4.58	7.0 ± 0.7	5.858	16.6 ± 2.2
4.58	7.6 ± 0.6	5.870	17.9 ± 2.3
5.385	11.1 ± 2.0	8.530	22.6 ± 1.2
5.390	8.5 ± 1.2	8.536	21.4 ± 1.6
6.475	9.2 ± 2.0		
6.475	10.6 ± 1.2		
7.541	13.1 ± 2.3		
7.544	11.9 ± 1.0		

TABLE III.34

γk" as a Function of Concentration for the Reaction with Benzene and Toluene

Benzene*		Toluene	
Conc (micromolar)	γk" (1/msec)	Conc (micromolar)	γk" (1/msec)
2.67	7.4 ± 0.3	5.370	10.1 ± 0.3
2.68	9.4 ± 0.5	5.387	9.4 ± 0.8
5.349	9.0 ± 0.2	17.66	9.3 ± 0.9
5.353	10.8 ± 1.1	17.68	12.0 ± 0.8
10.67	10.0 ± 0.9	21.48	12.9 ± 0.8
10.71	8.0 ± 0.1	21.54	13.8 ± 0.5
16.01	10.8 ± 0.7	32.21	12.6 ± 0.7
16.04	10.4 ± 0.4	32.29	13.4 ± 0.7
26.73	9.5 ± 1.4	35.11	14.6 ± 0.5
26.74	10.4 ± 0.6	35.19	15.6 ± 1.7
34.78	11.5 ± 0.6	42.95	16.9 ± 0.7
34.78	11.5 ± 0.9	42.99	15.7 ± 0.3
42.73	12.2 ± 2.4	64.596	19.3 ± 1.3
42.78	10.1 ± 0.9	64.705	18.4 ± 1.0
58.761	10.1 ± 0.8	91.775	24.4 ± 1.7
58.898	11.1 ± 0.8		
107.79	11.8 ± 0.6		
108.04	13.1 ± 1.2		
161.11	14.9 ± 1.8		
186.10	17.0 ± 0.7		
223.39	18.4 ± 0.8		
223.47	16.4 ± 0.7		
298.86	18.2 ± 1.1		
299.15	17.5 ± 1.0		

* With no substrate, γk" = γk' = 6.9 ± 0.2, 7.3 ± 0.5

TABLE III.35

$\gamma k''$ as a Function of Concentration for the Reaction with Chlorobenzene and Fluorobenzene

Chlorobenzene		Fluorobenzene	
Conc (micromolar)	$\gamma k''$ (1/msec)	Conc (micromolar)	$\gamma k''$ (1/msec)
3.86	9.6 ± 0.4	10.72	8.3 ± 0.5
3.86	9.4 ± 0.8	10.72	8.8 ± 0.2
10.72	12.9 ± 0.6	28.84	7.9 ± 0.3
10.73	11.0 ± 0.4	28.84	9.4 ± 0.3
26.88	15.1 ± 0.8	36.57	8.8 ± 0.2
26.89	14.4 ± 0.8	36.60	10.6 ± 0.9
40.32	14.3 ± 1.0	66.769	9.7 ± 0.6
40.33	13.2 ± 1.2	66.791	10.7 ± 0.8
54.651	17.4 ± 1.1	107.39	12.7 ± 0.5
54.724	14.9 ± 1.3	107.46	12.0 ± 0.9
67.128	17.1 ± 2.9	125.94	12.8 ± 1.0
87.496	17.4 ± 2.5		
87.525	16.9 ± 1.5		
107.16	22.8 ± 2.0		
107.23	16.8 ± 2.2		

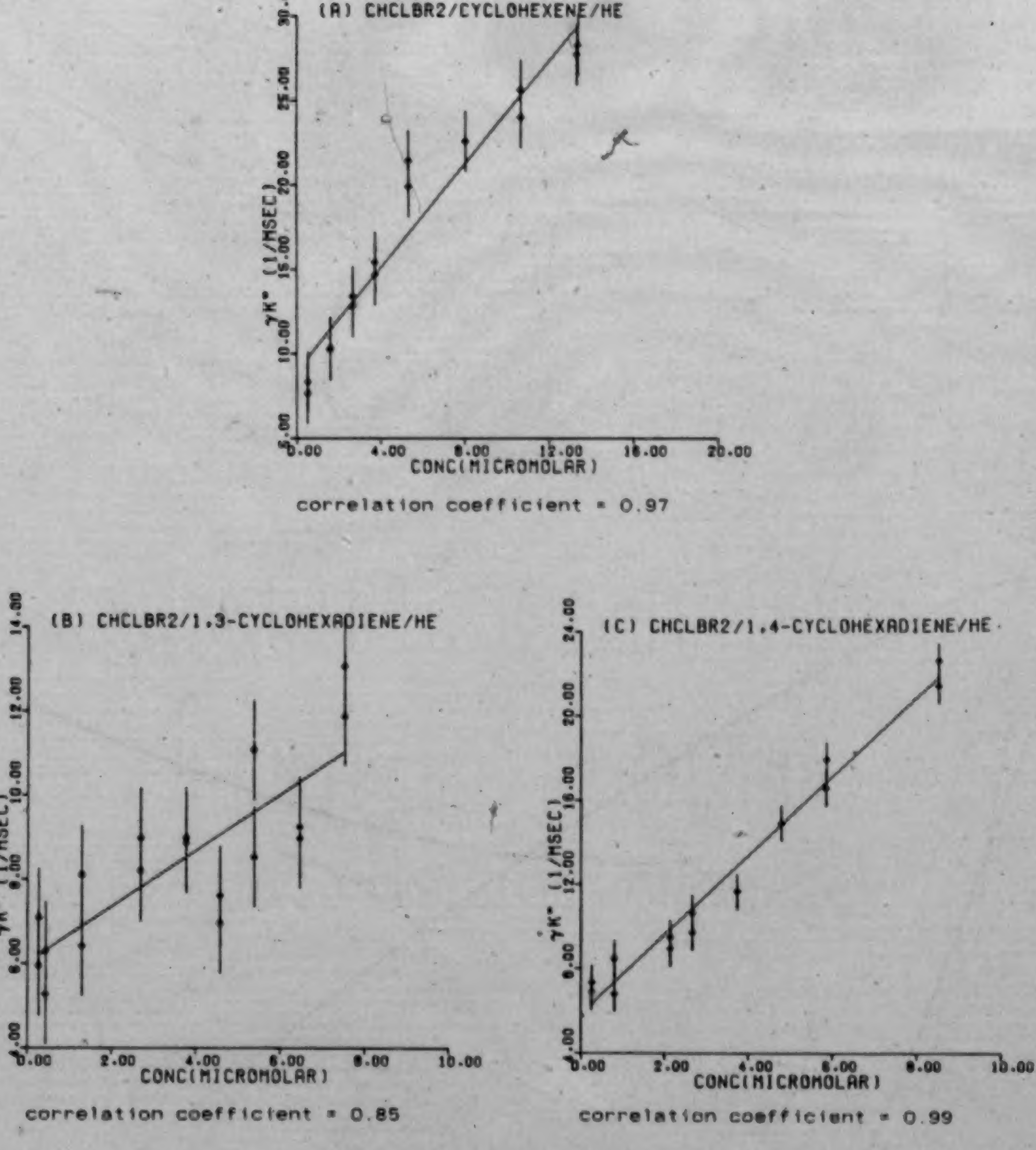

correlation coefficient = 0.97

correlation coefficient = 0.85

correlation coefficient = 0.99

FIGURE III.24 γk" *versus* Concentration for (A) Cyclohexene (B) 1,3-Cyclohexadiene (C) 1,4-Cyclohexadiene

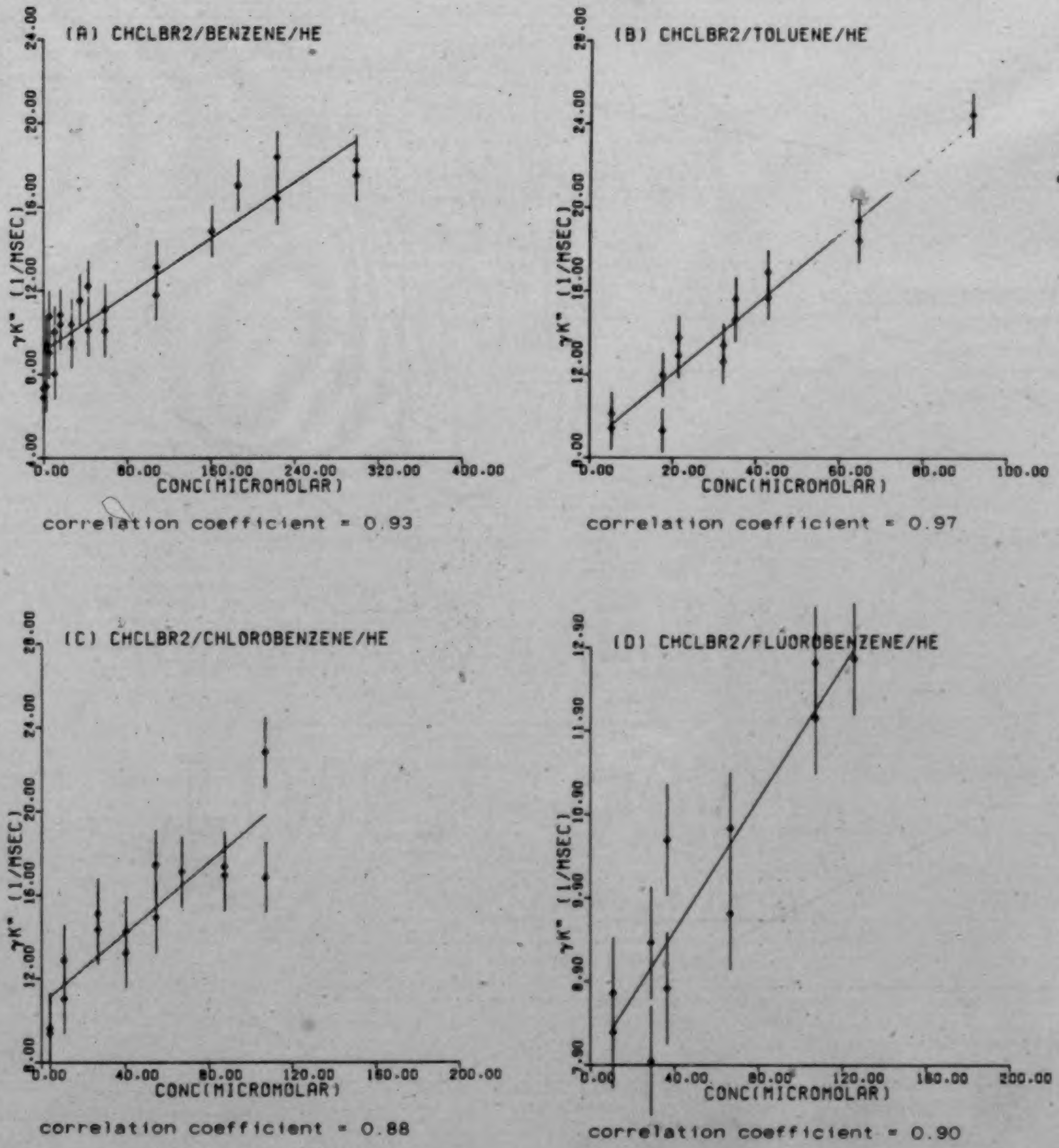

correlation coefficient = 0.93

correlation coefficient = 0.97

correlation coefficient = 0.88

correlation coefficient = 0.90

FIGURE III.25 γk" *versus* Concentration for (A) Benzene (B) Toluene (C) Chlorobenzene (D) Fluorobenzene

TABLE III.36

$\gamma k''$ as a Function of Concentration for the Reaction with Tetrahydrothiophene and Tetrahydrofuran

Tetrahydrothiophene		Tetrahydrofuran	
Conc (micromolar)	$\gamma k''$ (1/msec)	Conc (micromolar)	$\gamma k''$ (1/msec)
0.27	6.9 ± 0.9	22.92	12.9 ± 1.1
0.27	8.1 ± 0.8	22.93	15.6 ± 0.6
0.540	10.1 ± 0.8	54.547	17.0 ± 0.4
0.541	9.2 ± 0.8	54.621	15.6 ± 0.5
1.08	17.1 ± 0.9	64.779	14.7 ± 1.2
1.08	15.6 ± 0.7	64.801	17.7 ± 0.9
1.62	18.1 ± 1.5	107.59	19.2 ± 0.8
1.62	14.6 ± 2.3	107.63	16.8 ± 0.6
2.43	20.3 ± 2.1	134.87	15.7 ± 2.2
2.43	20.0 ± 1.4	135.05	18.0 ± 1.7
3.23	16.4 ± 1.8	150.68	20.8 ± 3.1
3.24	15.6 ± 2.0	190.78	20.6 ± 1.6
4.31	30.6 ± 7.2	190.97	24.1 ± 0.7
4.32	24.5 ± 4.7	288.26	21.6 ± 1.3
5.390	28.2 ± 3.9		

TABLE III.37

$\gamma k''$ as a Function of Concentration for the Reaction with Thiacyclohexane and Pyridine

Thiacyclohexane		Pyridine*	
Conc (micromolar)	$\gamma k''$ (1/msec)	Conc (micromolar)	$\gamma k''$ (1/msec)
0.43	10.5 ± 0.9	0.42	6.5 ± 0.7
0.43	10.1 ± 0.3	2.13	10.5 ± 0.6
0.800	14.8 ± 1.2	2.13	9.2 ± 0.5
0.800	13.4 ± 0.5	3.19	8.5 ± 0.8
1.33	14.8 ± 1.1	4.76	16.7 ± 1.3
1.33	15.3 ± 1.0	4.77	13.1 ± 1.4
1.33	19.3 ± 1.6	7.449	20.2 ± 1.5
1.33	21.2 ± 2.3	7.456	21.7 ± 3.5
2.13	17.3 ± 1.3	7.454	22.0 ± 2.9
2.13	21.5 ± 1.5	9.530	24.5 ± 1.7
2.14	20.7 ± 0.8	9.539	21.4 ± 1.7
2.93	25.7 ± 2.0	12.75	28.7 ± 4.5
2.94	24.7 ± 1.4	12.79	25.2 ± 3.9
3.47	22.3 ± 2.0	15.89	28.8 ± 3.8
3.47	29.6 ± 1.5	15.94	26.3 ± 2.4
4.27	27.6 ± 0.8		
4.28	26.8 ± 1.5		
5.03	30.9 ± 2.1		

* With no substrate, $\gamma k'' = \gamma k' = 10.8 \pm 1.2$

TABLE III.38

$\gamma k''$ as a Function of Concentration for the Reaction with Thiophene and Furan

Thiophene*		Furan	
Conc (micromolar)	$\gamma k''$ (1/msec)	Conc (micromolar)	$\gamma k''$ (1/msec)
0.43	7.5 ± 0.6	1.07	8.2 ± 0.6
0.43	8.5 ± 0.6	1.08	7.7 ± 0.4
1.07	10.8 ± 0.6	2.68	8.5 ± 0.4
1.07	10.2 ± 0.9	2.69	8.0 ± 0.2
1.87	13.7 ± 1.1	4.83	9.2 ± 0.5
2.69	16.0 ± 1.7	4.84	8.3 ± 0.6
2.70	14.9 ± 0.6	7.526	10.0 ± 0.4
3.75	16.7 ± 1.3	7.529	10.5 ± 0.8
5.372	21.7 ± 1.6	16.20	15.8 ± 0.8
5.379	22.9 ± 0.8	32.36	19.5 ± 3.2
		32.42	22.4 ± 1.3
		48.53	27.2 ± 1.0
		48.56	25.9 ± 2.1
		75.440	28.3 ± 3.3
		75.542	30.6 ± 2.9

* With no substrate, $\gamma k'' = \gamma k' = 6.2 \pm 0.2, 6.7 \pm 0.4$

TABLE III.39

$\gamma k''$ as a Function of Concentration for the Reaction with Pyrrole and 1-Methylpyrrole

Pyrrole		1-Methylpyrrole	
Conc (micromolar)	$\gamma k''$ (1/msec)	Conc (micromolar)	$\gamma k''$ (1/msec)
0.43	7.3 ± 0.8	0.27	5.5 ± 0.4
0.43	8.7 ± 0.5	0.27	7.4 ± 0.2
1.07	8.7 ± 0.7	0.539	8.7 ± 0.5
1.07	8.8 ± 0.4	0.541	7.9 ± 0.7
1.71	10.9 ± 0.8	1.08	8.0 ± 0.5
1.72	10.5 ± 0.6	1.08	8.8 ± 0.8
2.68	13.7 ± 1.2	1.62	10.0 ± 1.8
2.68	14.2 ± 1.2	1.62	13.4 ± 1.8
3.22	16.4 ± 0.7	2.43	9.5 ± 1.2
3.49	14.8 ± 0.8	2.43	10.8 ± 1.9
3.49	16.0 ± 1.2	3.23	10.8 ± 1.5
4.28	13.3 ± 1.0	3.24	12.8 ± 1.3
4.29	12.7 ± 0.6	3.77	18.7 ± 4.3
4.82	17.4 ± 1.5	3.78	15.3 ± 2.1
4.84	16.0 ± 1.1	4.04	16.1 ± 3.0
5.356	16.0 ± 2.0	4.06	18.4 ± 2.0
5.369	16.4 ± 1.1	4.31	16.8 ± 2.3
6.427	17.3 ± 1.0	5.398	19.0 ± 1.1
6.438	15.4 ± 1.2		
8.045	21.6 ± 1.9		

are given in Figures III.26 and III.27.

The second order rate constants k, determined from the slopes of the $\gamma k''$ *versus* concentration plots for the cyclic and heterocyclic compounds are summarized in Tables III.40 and III.41 respectively.

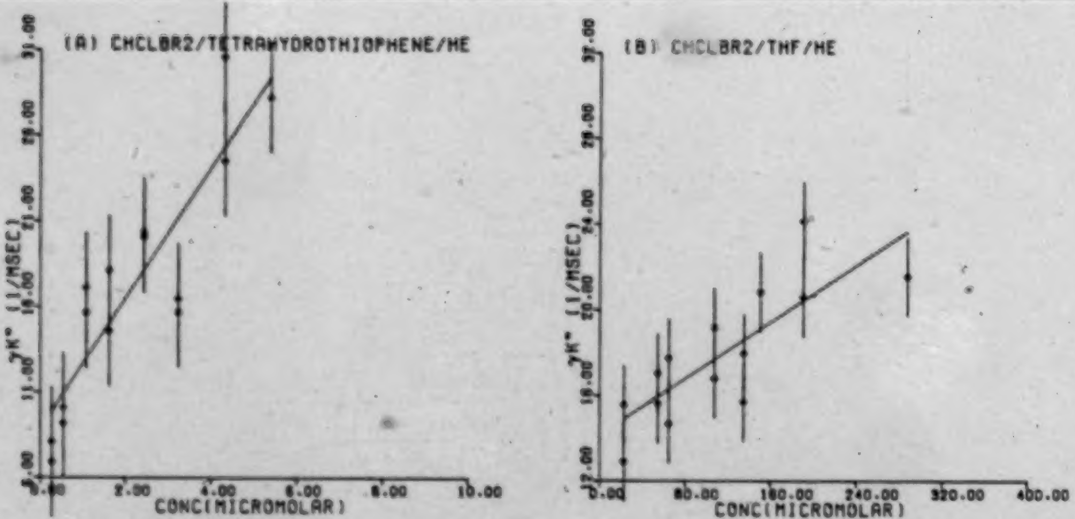

correlation coefficient = 0.89

correlation coefficient = 0.80

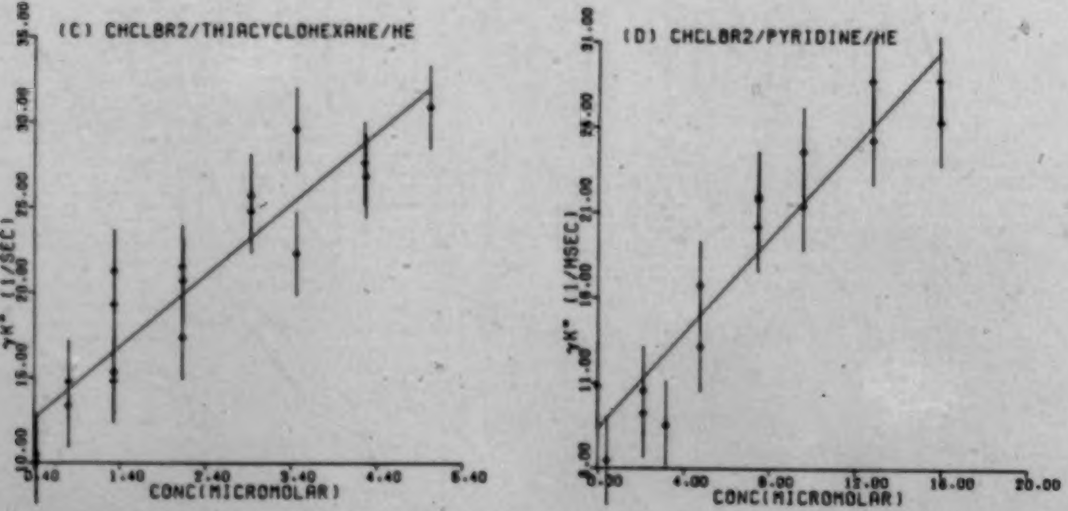

correlation coefficient = 0.93

correlation coefficient = 0.94

FIGURE III.26 γk" *versus* Concentration for (A) Tetrahydrothiophene (B) Tetrahydrofuran (C) Thiacyclohexane (D) Pyridine

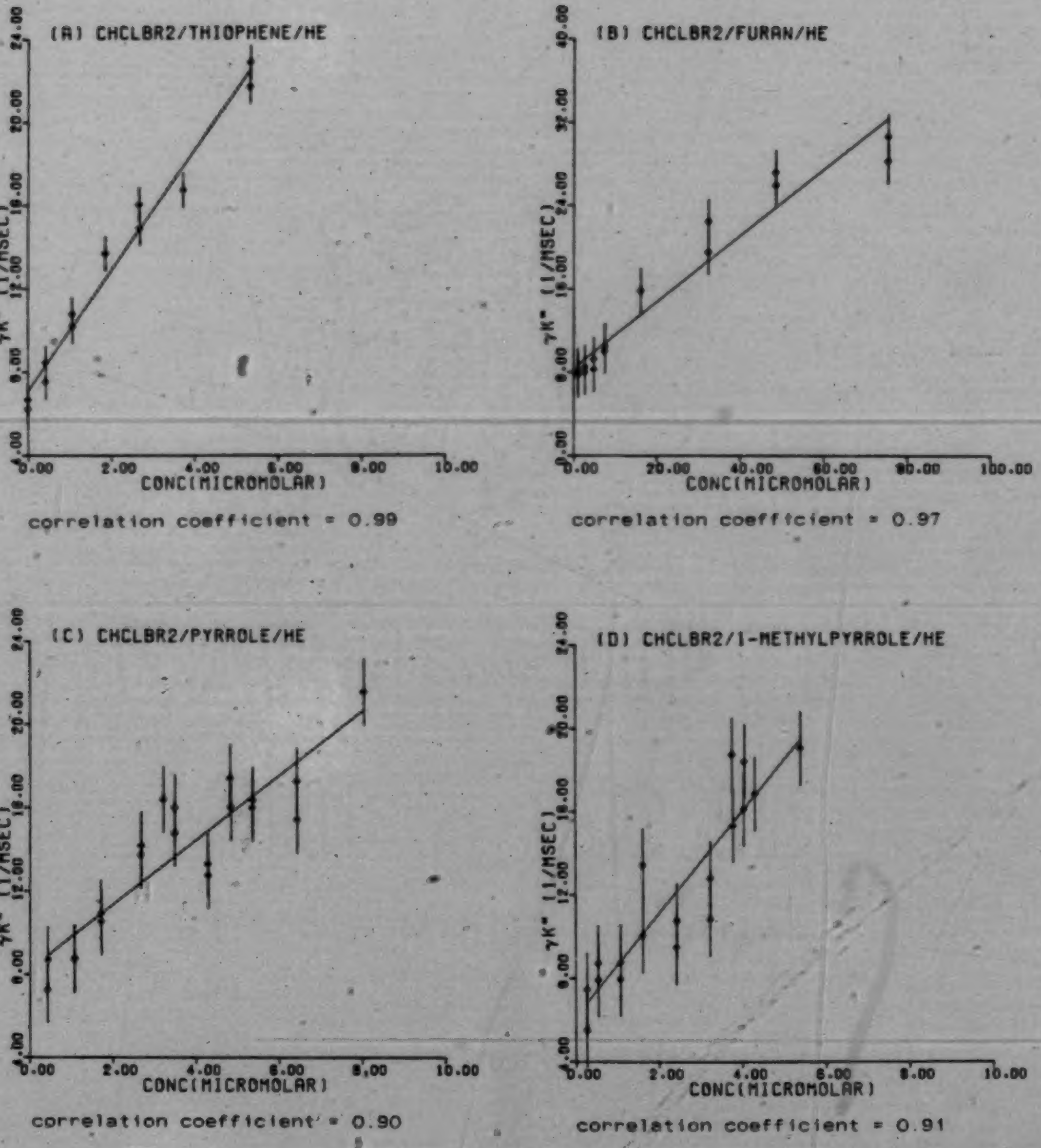

correlation coefficient = 0.99

correlation coefficient = 0.97

correlation coefficient = 0.90

correlation coefficient = 0.91

FIGURE III.27 γk" *versus* Concentration for (A) Thiophene (B) Furan (C) Pyrrole (D) 1-Methylpyrrole

TABLE III.40

Second Order Rate Constants k, for the Reactions with Cyclic Compounds

Substrate		k, ($M^{-1}s^{-1}$)	Number of measurements	Pressure range of substrate (torr)
cyclopentane		no reaction	56	1.000 - 36.020
cyclohexane	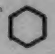	no reaction	7	26.520
cyclohexene		(3.1 ± 0.2) X 10^9	105	0.010 - 0.250
1,3-cyclohexadiene		(1.4 ± 0.2) X 10^9	126	0.005 - 0.140
1,4-cyclohexadiene		(3.7 ± 0.2) X 10^9	98	0.005 - 0.160
benzene		(6.7 ± 0.5) X 10^7	182	0.050 - 5.630
toluene	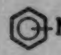Me	(3.3 ± 0.2) X 10^8	105	0.100 - 1.710
chlorobenzene	Cl	(1.7 ± 0.2) X 10^8	105	0.072 - 2.000
fluorobenzene	F	(6.1 ± 0.9) X 10^7	77	0.200 - 2.349

TABLE III.41

Second Order Rate Constants k_1 for the Reactions with Heterocyclic Compounds

Substrate	$k_1 (M^{-1}s^{-1})$	Number of measurements	Pressure range of substrate (torr)
thiacyclohexane 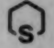	$(8.3 \pm 0.8) \times 10^9$	126	0.008 - 0.094
tetrahydrothiophene	$(7.6 \pm 1.1) \times 10^9$	105	0.005 - 0.100
pyrrolidyne 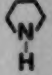	$> 4.8 \times 10^8$	42	1.000 - 30.000
tetrahydrofuran 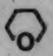	$(6.6 \pm 1.4) \times 10^7$	98	0.426 - 5.371
thiophene	$(5.7 \pm 0.2) \times 10^9$	84	0.008 - 0.100
pyrrole 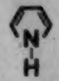	$(3.1 \pm 0.3) \times 10^9$	140	0.008 - 0.150
furan	$(6.3 \pm 0.4) \times 10^8$	105	0.020 - 1.400
1-methylpyrrole 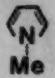	$(4.9 \pm 0.5) \times 10^9$	126	0.005 - 0.100
pyridine	$(2.8 \pm 0.3) \times 10^9$	112	0.008 - 0.300

IV. DISCUSSION

A. GENERATION OF CCl($X^2\Pi$)

Simons and Yarwood[21,22] have proposed a general scheme for the production of carbynes from the flash photolysis of halomethanes. Accordingly, the irradiation of dibromochloromethane, $CHClBr_2$, the CCl parent compound used for this study, in the absorption continuum from 200 to 240 nm produces a vibrationally excited bromochloromethyl radical following cleavage of the weakest C-Br bond. If the excess energy in the excited radical exceeds the minimum value, E^*, required for unimolecular decomposition, CBr and CCl will be generated:

$$CHClBr_2 + h\nu \longrightarrow CHClBr^\dagger + Br$$

$$(CHClBr^\dagger)_{E\geq E^*} \longrightarrow CCl + HBr$$

$$\longrightarrow CBr + HCl$$

$$_{E<E^*} \xrightarrow{M} CHClBr$$

This mechanism is substantiated by the following observations:

- photolysis of $CHClBr_2$ in excess O_2 produced an intense BrO spectrum, but no ClO spectrum was detected. This is strongly indicative of C-Br bond breakage as being the sole primary process.
- on the basis of the endothermicities of the various unimolecular decomposition reactions with respect to the irradiation energies, they concluded that a large proportion of the energy, in excess of that required to promote C-Br cleavage, is concentrated in the vibrationally excited halomethyl radicals.
- the overall energy requirements for the proposed mechanism are consistent with the nature of the carbyne products observed. For example, $CHClBr_2$ yielded both CCl and CBr (the overall energy required, E(tot), is > 102 kcal $mole^{-1}$ for CCl production, and ~ 106 kcal $mole^{-1}$ for CBr production), while CCl_2Br_2 yielded only CCl (E(tot) > 115 kcal $mole^{-1}$ for CCl production, but ~ 128 kcal $mole^{-1}$ for CBr production).
- the alternative route for the production of HBr and HCl by hydrogen abstraction from the parent compound is not favored under conditions of high light intensity and low concentration of the parent compound. Also, as mentioned before, no transient production of Cl atoms was detected, based on the non-appearance of ClO spectrum in the photolysis of $CHClBr_2$ in excess O_2.

- the concentrations of CCl and CBr were found to be linearly proportional to the flash energies, thereby implying a one-photon process.
- a linear relationship exists between the reciprocal concentration of CCl or CBr and the pressure of N_2. This indicates that the unimolecular decomposition of the energized radicals, by analogy with the fluorescence of an excited species, follows a Stern-Volmer Law in competition with collisional deactivation by a foreign gas. Furthermore, the slope, which reflects the mean lifetime of the energized radicals, increases as the wavelength of irradiation increases, indicating a decrease in the rate of decomposition due to less available energy.

Since the proposed mechanism of Simons and Yarwood appears to be well substantiated, no further investigation concerning the production mechanism of CCl from $CHClBr_2$ was carried out for this work. It should be noted that the CCl signals were weak but still discernible in the presence of 250 torr propane, suggesting the possibility that other channels, such as secondary photolysis of CHClBr to generate CCl, may occur. Even so, secondary photolysis of CHClBr must be relatively insignificant compared to unimolecular decomposition of the radical, since Simons and Yarwood observed a linear relationship between CCl concentration and flash energy, implying that the major mode of production of CCl is a one-photon process.

B. REACTION WITH INORGANIC COMPOUNDS AND SOME SATURATED COMPOUNDS

Since only a few inorganic compounds, alkanes and one alkylchloride were examined, they will be discussed together here. The rate constants measured in this work, and those obtained by Tyerman[81] and by Wampler and coworkers,[82] along with comparable results on CBr,[28] are summarized in Table IV.1. For the sake of comparison, rough estimates for the upper limits of reactivity were carried out for hydrogen, methylchloride and propane, for all of which no reaction was detectable, as follows.

No measurable reaction was observed with up to 180 torr hydrogen and 250 torr propane. Since, for *iso*butane ($k_1 = (4.5 \pm 0.4) \times 10^4\ M^{-1}\ s^{-1}$), the CCl signals were almost completely quenched at 86.5 torr, the maximum pressure used, it can be concluded that for both hydrogen and propane, $k_1 < 4.5 \times 10^4\ M^{-1}\ s^{-1}$. Similarly, since the maximum pressures used for methylchloride and acetylene ($k_1 = (3.5 \pm 0.4) \times 10^7\ M^{-1}\ s^{-1}$) were both 10 torr, we can infer that $k_1 < 3.5 \times 10^7\ M^{-1}\ s^{-1}$ for methylchloride.

Tyerman[81] reported very high rate constants for the reactions of CCl with hydrogen, methylchloride and propane, whereas, under similar experimental conditions, no detectable reaction could be observed here. Since, however,

TABLE IV.1

Second Order Rate Constants k, for the Reactions of CCl($X^2\Pi$) and CBr($X^2\Pi$) with Inorganic Compounds and Some Saturated Compounds

Substrate	k, ($M^{-1}s^{-1}$)			
	CCl			CBr
	this work	Tyerman''	Wampler and coworkers''	Strausz and coworkers''
hydrogen H_2	no reaction (≤ 4.5 × 10^6)	(3 ± 1) × 10^7		<3 × 10^6
ammonia NH_3	>4.5 × 10^6 <3.5 × 10^7			
methylchloride CH_3Cl	no reaction (≤ 3.5 × 10^7)	(2.2 ± 0.1) × 10^8		
propane C_3H_8	no reaction (≤ 4.5 × 10^6)	(1.0 ± 0.1) × 10^6	≤ 1.8 × 10^6	
isobutane *iso*-C_4H_{10}	(4.5 ± 0.4) × 10^6		≤ 1.8 × 10^6	(1.8 ± 0.9) × 10^7

Wampler and coworkers[43] and Strausz and coworkers[25] have shown that CCl and CBr are relatively inert with respect to reactions with propane and hydrogen, it must be concluded that Tyerman's results are in error.

The lack of reactivity of CCl with H_2 is in sharp contrast to CH which rapidly inserts into hydrogen to form methane at a rate ~ 10^{10} M^{-1} s^{-1}.[77,79]

The result for propane indicates that the reactions of CCl with primary and secondary C-H bonds are relatively insignificant. Similarly, no reaction was observed with the CBr + CH_4 system ($k_1 < 3 \times 10^6$ M^{-1} s^{-1}),[25] demonstrating the inertness of primary C-H bonds towards CBr. Therefore, the observable reactions measured for CCl and CBr with *iso*butane can be construed as a clear indication of interactions with the weaker tertiary C-H bond. In contrast, CH inserts into primary, secondary and tertiary C-H bonds indiscriminately at rates close to collision frequencies.

The nature of the interaction of singlet carbenes with C-H bonds has been examined in a number of experimental and theoretical studies[1,2] and the results point to a concerted insertion mechanism which is stereospecific and involves a three-centre transition state:

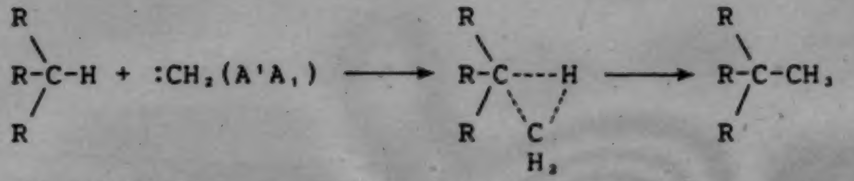

$$R_3C{-}H + {:}CH_2(^1A_1) \longrightarrow R_3C \cdots H\,(CH_2) \longrightarrow R_3C{-}CH_3$$

The alternative mechanism proposed involves abstraction of a hydrogen atom, followed by recombination of the radical intermediates:

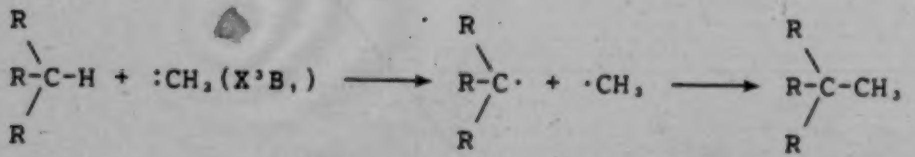

However, generally speaking, the concerted route and the abstraction route are viewed as the most likely for singlet and triplet carbenes, respectively.

On the basis of spin multiplicity, ground state doublet methylidyne may be regarded as the analog of singlet methylene, and quartet methylidyne, as that of triplet methylene. Thus CH($X^2\Pi$) was predicted to undergo concerted insertion into C-H bonds, and this has been proven to be so by many experiments.[70-73,75] CCO_2Et insertion into C-H bonds has also been observed but unlike CH, which inserts indiscriminately, CCO_2Et shows a marked preference in the series primary < secondary < tertiary C-H bonds.[44] CCl and CBr, on the other hand, react only extremely slowly, if at all, with primary and secondary C-H bonds, and the rate of reaction of CCl with tertiary C-H bonds is very slow. The reason for this is unclear, but it may be that electronic states and/or steric effects exert a crucial influence on the reactivity of carbynes, in the same way as carbenes are affected. Thus singlet CH_2 inserts very rapidly into C-H bonds, showing a slight preference for tertiary C-H bonds.

However, CCl_2 does not react with CH_4, reacts very slowly with secondary C-H bonds, and moderately fast with tertiary C-H bonds. This preference for tertiary C-H bonds and the rare examples of insertions of CCl_2 into allylic or benzylic C-H bonds leading to racemization at the asymmetric carbon centres can be explained by the abstraction - recombination process:[3]

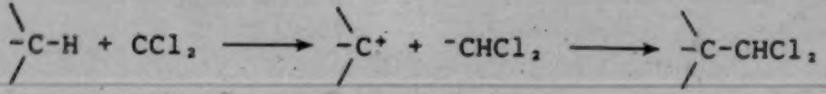

$$\rangle C\text{-}H + CCl_2 \longrightarrow \rangle C^+ + {}^-CHCl_2 \longrightarrow \rangle C\text{-}CHCl_2$$

To rationalize the preference of substituted singlet carbenes for tertiary C-H bonds, on the basis of the concerted mechanism, Doering[44] proposed a polarized transition state which would favor the formation of carbonium ions:

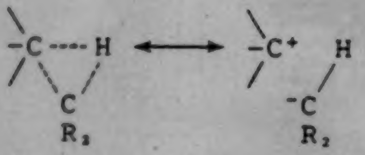

where CR_2 denotes a substituted singlet carbene. Analogously, for the carbyne reactions, CCl or CBr probably stabilizes the anion more than CH, and this may contribute to the higher selectivity exhibited by the halocarbynes.

CCl was observed to react with ammonia at a rate of about three orders of magnitude slower than that of CH (k_1 =

(5.9 ± 0.9) × 10^{10} M^{-1} s^{-1}).[77] The nature of the reaction has not been studied, but it may be insertion, by analogy with the insertion reactions of carbenes into N-H, O-H, S-H and C-N bonds which possibly involve an initial electrophilic attack on the heteroatom.[3]

Carbenes are also known to insert into C-Cl bonds and on this basis, as well as from the above observations, one might expect CCl to react with the C-Cl bond of methylchloride, CH_3Cl. No observable reaction ($k_1 < 3.5 \times 10^7$ M^{-1} s^{-1}) was detected, however, in contrast to Tyerman's value of $k_1 = (2.2 \pm 0.1) \times 10^8$ M^{-1} s^{-1}.[81] Interestingly, Wampler and coworkers[82] measured $k_1 = 1.8 \times 10^8$ M^{-1} s^{-1} for the reaction of CCl with CCl_4. Therefore, the upper limit of $k_1 < 3.5 \times 10^7$ M^{-1} s^{-1} estimated for the reaction with methylchloride is not entirely unreasonable.

C. REACTIONS WITH ALKYNES

CCl closely resembles CBr and other electrophilic species such as $S(^3P)$[83] and $O(^3P)$[84-86] whose reactions with alkynes have been extensively studied (Table IV.2), in that the reactivity, in general, increases with the degree of alkyl substitution on the acetylenic bond. Branching of the alkyl chain results in a lower reactivity, as indicated by 3,3-dimethyl-1-butyne being 50% less reactive than 1-butyne. Since the study on alkanes has shown that the reactions of CCl with primary and secondary C-H bonds are relatively

TABLE IV.2

Second Order Rate Constants k, for the Reactions of $CBr(X^2\Pi)$, $CCl(X^2\Pi)$, $O(^3P)$ and $S(^3P)$ with Alkynes

Substrate	k, × 10^{-9} ($M^{-1}s^{-1}$)				
	CH	CCl[c]	CBr[e]	$O(^3P)$	$S(^3P)$[l]
acetylene	45 ± 9[a] 130 ± 20[b]	0.035 ± 0.004 0.11 ± 0.01[d]	0.081 ± 0.007	0.079[f] 0.094[g]	0.23 ± 0.05
acetylene-d_2		0.031 ± 0.013	0.072 ± 0.017	0.079[h]	0.23 ± 0.03
propyne	280 ± 90[b]	2.2 ± 0.2 2.4 ± 0.2[d]	4.8 ± 0.6	0.54[i]	4.8 ± 0.2
1-butyne		3.7 ± 0.5	6.2 ± 1.1	1.2[i]	3.3 ± 0.2
2-butyne		18 ± 3	24 ± 5	2.9[j]	16 ± 2
1-pentyne		4.3 ± 0.7	3.6 ± 0.8	0.49 ± 0.06[k]	
2-pentyne		25 ± 4	20 ± 3		18 ± 3
3,3-dimethyl-1-butyne		2.4 ± 0.3			
2,2,5,5-tetramethyl-3-hexyne		7.6 ± 0.7	9.7 ± 1.6		
phenylacetylene		4.3 ± 0.7			
2-butyne-F_6			0.020 ± 0.002		0.21 ± 0.04

a) Bosnali and Perner
b) Lin and coworkers
c) This work
d) Tyerman
e) Strausz and coworkers
f) Stuhl and Niki
g) Herron and Huie
h) Arrington and Cox
i) Herbrechtsmeir and Wagner
j) Herbrechtsmeir and Wagner
k) Lin and coworkers
l) Strausz and coworkers

insignificant, the rate constants measured and the trend observed here thus refer to the interaction of the carbyne with the acetylenic bonds. The increase in the reactivity of CCl with increasing alkyl substitution therefore reflects the electrophilic nature of the interaction, and can be ascribed to the increase in the π electron density of the triple bonds.

The rate constant for propyne is in good agreement with the value reported by Tyerman,[81] while his value for acetylene is three times higher than the current measurement. CCl is less reactive towards the simple alkynes than its close carbyne analog, CBr,[34] but the difference gradually diminishes with increasing complexity of the alkynes and even appears to be reversed with the pentynes.

Rate parameters for the reaction of CH with acetylene, reported by Bosnali and Perner[77] (k_1 = $(4.5 \pm 0.9) \times 10^{10}$ M^{-1} s^{-1}) and Lin and coworkers[78] (k_1 = $(1.3 \pm 0.2) \times 10^{11}$ M^{-1} s^{-1}), and with propyne, reported by Lin and coworkers[78] (k_1 = $(2.8 \pm 0.9) \times 10^{11}$ M^{-1} s^{-1}), show that CH is about two to three orders of magnitude more reactive than CCl and CBr. This is not unexpected, since the back - donation of electrons from the halogens to the carbon atom would diminish the electron deficiency of the carbon π orbitals, and, consequently, lower the electrophilicity of the halocarbynes. This phenomenon could also be responsible for the lower reactivity of CCl, compared to CBr, towards the smaller alkynes, due to a greater degree of overlap between the p_π orbitals of C and Cl, as compared to C and Br, resulting in a higher degree of back donation of electrons and lower electrophilicity. However, the reason for the trend reversal with the pentynes is, at this point, still unclear, even though it is difficult to decide whether CCl is definitely more reactive than CBr towards the pentynes, given the limitations of the error of the measurements. Furthermore, accompanying the lower reactivity is a manifestation of a greater selectivity towards the substrates: propyne is only three times more reactive than acetylene towards CH, according to Lin's values, but 59 times more reactive with CBr and 63 times with CCl.

Additional evidence for the electrophilic nature of these reactions is revealed in the linear corelation between log k_1 and the ionization potential of the substrates, a relationship which was also found earlier for CBr[24] (Figure IV.1). The ionization potential measures the energy required for the removal of electron from the highest occupied orbital of the molecule, which in this case is in the acetylenic bond, and therefore can be correlated with the activation energy of the reaction. Therefore, since the reaction rate constant k_1 is related to the activation energy E_a by the following expressions:

$$k_1 = A.e^{-\frac{E_a}{RT}}$$

$$\log k_1 = \log A - 2.303(E_a/RT)$$

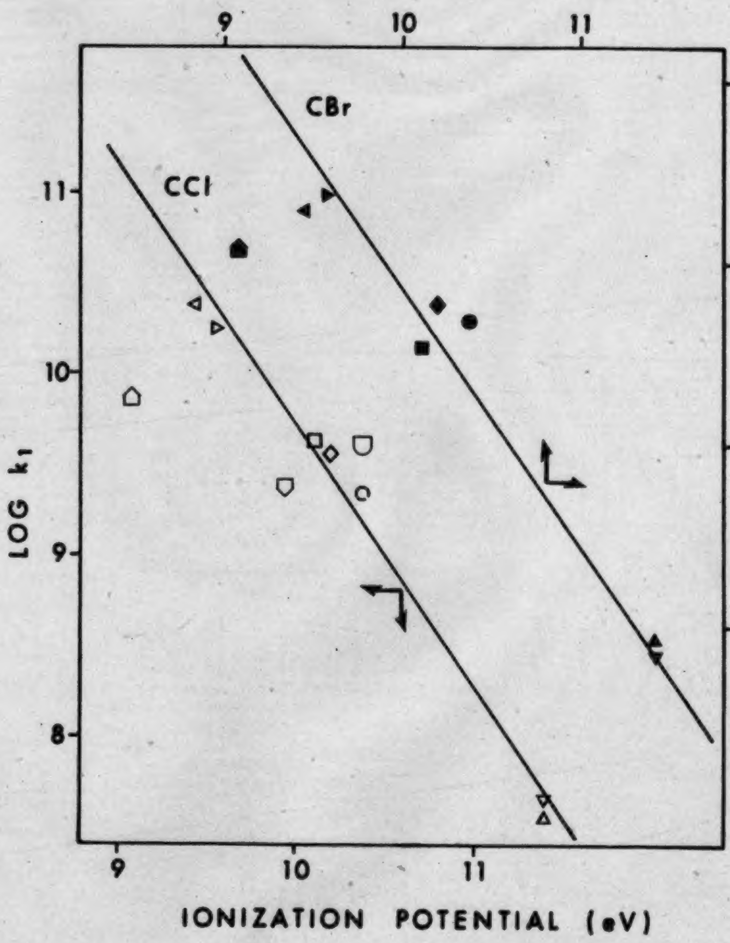

FIGURE IV.1 Log k_1 *versus* Ionization Potential for $CCl(X^2\Pi)$ (open symbols) and $CBr(X^2\Pi)$ (closed symbols) Reactions with Acetylenes. △ HC≡CH; ▽ DC≡CD; ○ -≡; ◇ --≡; □ ---≡; ▷ -≡-; ◁ --≡-; ⛉ ≡+; ⌂ +≡+; ⊔ ≡-⌬

a linear relationship between log k_1 and ionization potential implies essentially constant A-factors for the reactions. Similar linear correlations were shown to exist in the reactions of $S(^3P)$ atoms with simple alkynes[18] and alkenes,[17] and for those few cases with the alkynes where slight deviations from linearity were noted, the A-factors were shown to be smaller.

Some deviations from linearity were also observed for the reactions of CBr with alkenes,[26] while the correlations for the reactions of CCl or $S(^3P)$ with alkenes are linear.[26] Thus for the substrates examined, CBr exhibited an obvious curvature in the log k_1 versus ionization potential plot,[26] due to the lower than expected reactivities of *t*-2-butene and tetramethylethylene. This was ascribed to the large size of CBr, which renders it more susceptible to steric hindrance created by the alkyl groups, thus limiting the access of the carbyne to the unsaturated bonds under attack. This appears to be the major factor in causing smaller A-factor values for the highly alkyl substituted substrates.

Therefore, by analogy, in the reactions of CCl or CBr with alkynes, the lower reactivities of those substrates having branched substituents, which are clearly displayed as negative deviations from the linearity of the log k_1 *versus* ionization potential plots, can be ascribed to steric interference. This is most severe with 2,2,5,5-tetramethyl-3-hexyne, which possesses an additional t-butyl substituent as compared to 3,3-dimethyl-1-butyne.

On the other hand, phenylacetylene displayed a positive deviation from linearity. Since CBr has been shown to react with benzene (k_1 = $(2.2 \pm 0.2) \times 10^8$ M^{-1} s^{-1}),[84] CCl is expected to behave likewise. This, together with the electron - releasing property of the benzene ring towards the triple bonds, may account for the higher reactivity observed with phenylacetylene.

The reactivity trend observed for the reactions of the electrophilic species CCl, CBr, O(^3P) and S(^3P) atoms with alkynes is very similar to that found with the alkenes, in that the reactivity of the substrates increases with the degree of alkyl substitution but decreases with halogen substitution. The results of Tyerman[81] on the reactions of CCl with haloethylenes are anomalous because they do not reflect the electrophilic nature of CCl as revealed by the other investigations; thus remeasurements of his rate constant values would be highly desirable. In general, alkynes appear to be somewhat less reactive than alkenes. This is most pronounced in acetylene, which is, for example, about 100 times less reactive than ethylene towards CCl. Consequently, a greater selectivity was observed for the reactions of CCl with the alkynes: the increase in reactivity from the least reactive acetylene to the most reactive, 2-pentyne, in the alkyne series studied here, is about 100-fold, as compared to an increase of 50-fold from the least reactive ethylene to the most reactive *iso*butene in the alkene series studied by Tyerman.

The addition reactions of O(^{3}P) and S(^{3}P) atoms with alkenes and alkynes have been thoroughly investigated, both from the experimental and theoretical points of view. It would be constructive at this point to summarize briefly the salient features of these reactions.

The primary adducts formed in the reactions of O(^{3}P)[98] and S(^{3}P)[99] with alkenes are triplet biradicals, $>\dot{C}\overset{\dot{O}}{C}<$, and triplet thiiranes, $>\overset{S}{\overbrace{C-C}}<$, respectively; with alkynes, theoretical and experimental results point to the intermediacy of the triplet carbenes $R\ddot{C}\overset{O}{\overset{\|}{C}}R$ and $R\ddot{C}\overset{S}{\overset{\|}{C}}R$.

In general, theoretical calculations on the reaction paths for the additions of divalent species to unsaturated bonds concordantly predict an asymmetrical approach towards the bond under attack. Thus the primary step of the reaction of O(^{3}P) with alkyne appears to involve the formation of vibrationally excited ketocarbenes, which can undergo 1,2 hydrogen shift to form unsaturated ketones, or rearrange to form ketenes. The ketene could further undergo fragmentation to produce CO and alkenes; for example :[100]

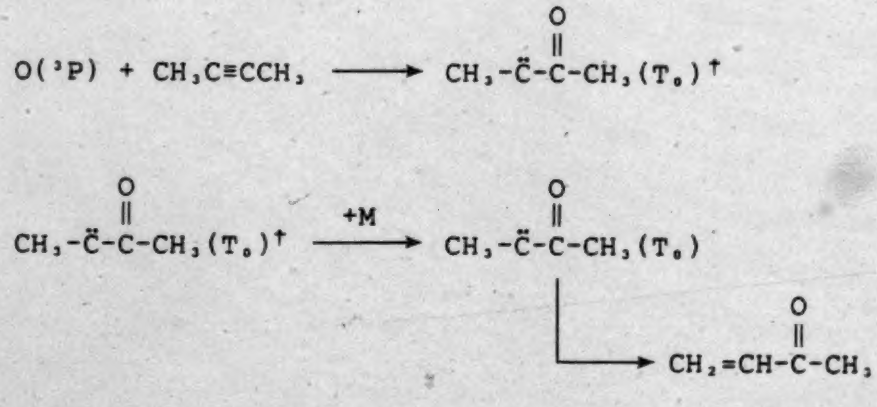

$$O(^3P) + CH_3C{\equiv}CCH_3 \longrightarrow CH_3\text{-}\ddot{C}\text{-}\overset{O}{\overset{\|}{C}}\text{-}CH_3(T_0)^{\dagger}$$

$$CH_3\text{-}\ddot{C}\text{-}\overset{O}{\overset{\|}{C}}\text{-}CH_3(T_0)^{\dagger} \xrightarrow{+M} CH_3\text{-}\ddot{C}\text{-}\overset{O}{\overset{\|}{C}}\text{-}CH_3(T_0)$$

$$\longrightarrow CH_2{=}CH\text{-}\overset{O}{\overset{\|}{C}}\text{-}CH_3$$

$$\longrightarrow (CH_3)_2C{=}C{=}O(T_1)$$

$$(CH_3)_2C{=}C{=}O(T_1) \longrightarrow CO + (CH_3)_2\ddot{C}$$

$$\hookrightarrow CH_3CH{=}CH_2$$

where † denotes a vibrationally excited species. Avery and Heath[101] proposed that the methyl vinyl ketone is formed *via* a carbene - enol - ketone rearrangement:

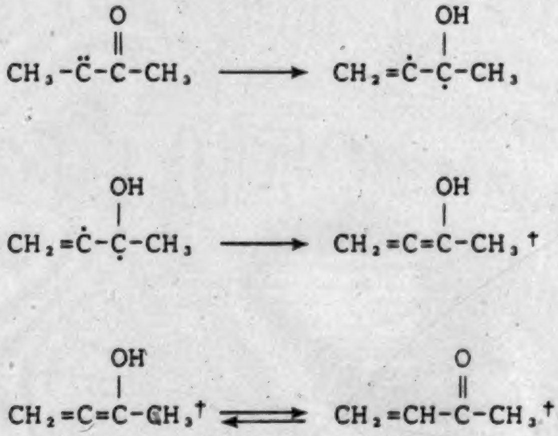

$$CH_3\text{-}\ddot{C}\text{-}\overset{\overset{O}{\|}}{C}\text{-}CH_3 \longrightarrow CH_2{=}\dot{C}\text{-}\overset{\overset{OH}{|}}{\underset{\cdot}{C}}\text{-}CH_3$$

$$CH_2{=}\dot{C}\text{-}\overset{\overset{OH}{|}}{\underset{\cdot}{C}}\text{-}CH_3 \longrightarrow CH_2{=}C{=}\overset{\overset{OH}{|}}{C}\text{-}CH_3^{\dagger}$$

$$CH_2{=}C{=}\overset{\overset{OH}{|}}{C}\text{-}CH_3^{\dagger} \rightleftharpoons CH_2{=}CH\text{-}\overset{\overset{O}{\|}}{C}\text{-}CH_3^{\dagger}$$

However, the intervention of the enol has not been proven experimentally.

Furthermore, the rate constants measured for the reactions of O(^{3}P) with selected alkynes (Table IV.2) indicate that except for acetylene, O(^{3}P) is three to ten times less reactive than CCl. The increase in reaction rate with increasing alkylation of the alkyne reveals the electrophilic nature of the O(^{3}P) atom.

On the other hand, the reactions of $S(^3P)$ with alkynes are much more complicated due to the high reactivities of the primary S + alkyne adducts. On the basis of spin conservation rules and molecular orbital calculations,[102,103] $S(^3P)$ reacts analogously to $O(^3P)$ with alkynes to form ground state triplet thioketocarbene as the primary adduct, which subsequently leads to a variety of products, including thiophene products which are common to all S + alkyne reactions.[104]

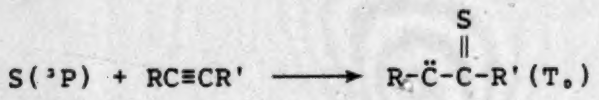

$$S(^3P) + RC\equiv CR' \longrightarrow R\text{-}\ddot{C}\text{-}\overset{\overset{\displaystyle S}{\|}}{C}\text{-}R'(T_0)$$

$$R\text{-}\ddot{C}\text{-}\overset{\overset{\displaystyle S}{\|}}{C}\text{-}R'(T_0) \longrightarrow \text{products}$$

The rate constants for the alkyne reactions indicate that except for acetylene, with which $S(^3P)$ is ~ ten times more reactive than CCl, the reactivities of $S(^3P)$ and CCl are of the same order of magnitude, with CCl perhaps being slightly more reactive.

At this point it is interesting to point out that unlike $O(^3P)$ and $S(^3P)$ atoms, $O(^1D_2)$ and $S(^1D_2)$ atoms probably react with alkynes to form the corresponding cyclic antiaromatic adducts oxirenes and thiirenes. Unfortunately rate constant measurements for these reactions have not been reported in literature.

Singlet methylenes[1,2] undergo concerted cycloaddition reactions with alkenes and alkynes to form cyclopropanes and cyclopropenes, respectively, and relative rate studies on different substrates have also indicated the electrophilic nature of carbenes. By analogy, CCl[81] and CBr[28] were postulated to undergo cycloaddition reactions with alkenes to form cyclopropyl radicals, which can undergo hydrogen abstractions, combine with other radicals, R, or rearrange to allyl radicals:

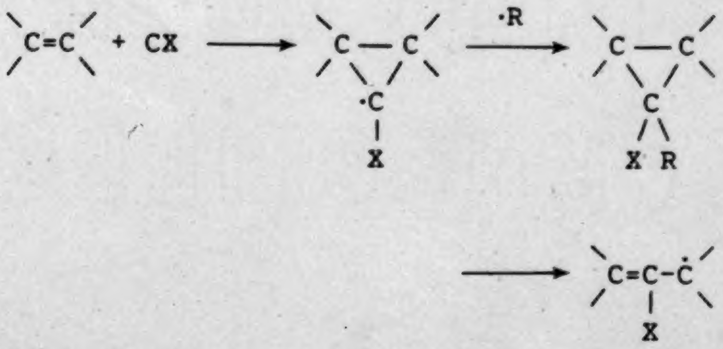

In the liquid - phase study of the reactions of CCO_2Et with alkenes, the corresponding cyclopropyl adducts have been detected.[51] In their studies of $S(^3P)$ reactions with alkenes and alkynes, Strausz and coworkers[90,105] found that the activation energies are higher for the alkynes than for the alkenes, and proposed that this may be related to the ionization potential differences of the substrates.[104] On the other hand, the A-factors were also found to be higher for the alkynes. Owen *et al.*[107] observed the same trend in the reactions of CF_3 radicals with alkynes, and attributed this to the gain in entropy in going from a linear acetylenic molecule to a non-linear activated complex. Thus the higher A-factors observed for the $S(^3P)$ + alkyne reactions may partially compensate for the higher activation energies, but this probably would not be sufficient to render them more reactive than the alkenes.

It is likely that the Arrhenius parameters for the CCl + alkyne reactions follow the same trend; and it is equally possible to rationalize the lower reactivities of the alkynes, as compared to the alkenes, on the basis of a cycloaddition mechanism. *Ab initio* molecular orbital calculations on the reaction of CH with acetylene[108] predicted an asymmetric, concerted mechanism, with zero activation energy, to form a vibrationally excited cyclopropenyl radical,

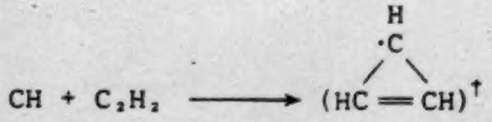

and CCO_2Et was shown to add stereoselectively to alkenyl bonds to form cyclopropyl radicals; therefore, there is no reason why halocarbynes should behave differently, it is thus probable that CCl undergoes cycloaddition reactions with alkynes to form the corresponding cyclopropenyl radicals, which may undergo hydrogen abstractions, combine with other radicals, R', or rearrange to allenyl radicals:

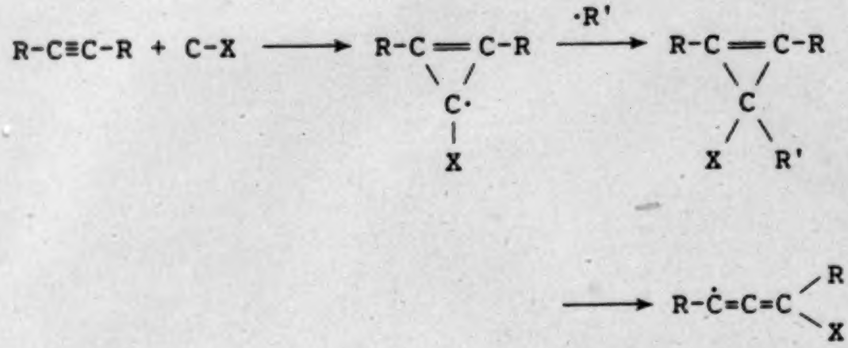

Unfortunately, no product analysis has been performed to substantiate the above proposal. Doering and Henderson[109] suggested that the transition state for the cycloaddition of CCl_2 or CBr_2 to an alkene, in liquid solution, could be represented by:

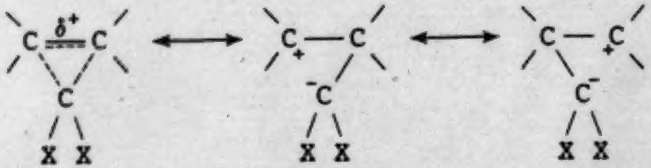

where X = Cl or Br. By analogy, a somewhat similar polar structure can be envisioned for the transition state for the cycloaddition of CCl to an alkene or perhaps an alkyne; the lower reactivity of the alkyne would then be due to the fact that the carbocation formed from the alkyne is less stable than that formed from the alkene, because it cannot attain the sp^2 hybrid orbital configuration, which is generally regarded as the most stable configuration for a carbocation.

No secondary isotope effect was observed for the CCl + acetylene system; as with the CBr, $S(^3P)$ and $O(^3P)$ reactions, k_H/k_D is equal to unity within experimental error, indicating that the new vibrational frequencies created in going from acetylene to the activated complex are not sensitive to deuterium substitution and therefore do not generate an isotope effect.

D. REACTION WITH SILANES

Studies on the CCl + alkane reactions have revealed that, unlike CH which inserts into primary, secondary, and tertiary C-H bonds indiscriminately with rates close to collision frequencies, CCl, on the other hand, is much more selective. It does not react with primary or secondary C-H bonds, but perhaps undergoes a slow insertion (k_1 = $(4.5 \pm 0.4) \times 10^4$ M^{-1} s^{-1}) into the tertiary C-H bond of *iso*butane. The reactions of CCl with some silanes were examined, because it was felt that the weaker Si-H bond may be more amenable than the C-H bond to attack by the halocarbyne. Thus, since $SiH_2(^1A_1)$, which does not react with C-H bonds, inserts into Si-H bonds very rapidly,[118] CCl may behave likewise. The valence electronic structures of $Si(3s^2 3p^2)$ and $C(2s^2 2p^2)$ are similar, however Si may utilize the 3d orbitals for bonding. Thus Si can be pentacoordinate, thereby providing reaction pathways distinctly different from carbon systems.

Previous to this study, no other work on carbyne reactions with silane had been reported in literature. Therefore, for the sake of comparison, the rate constants measured for CCl are presented in Table VI.3, along with data for other well studied radical species such as $SiH_2(^1A_1)$,[111,112] $CH_2(^1A_1)$,[113,114] CH_3[115] and H.[116]

The most prominent feature of the results presented in Table VI.3 is that, in general, CCl reactions with silanes are quite rapid, and in the case of disilane, the reaction is 1/40 that of the collision frequency.[*1] Comparatively, they are of the same order of magnitude as those for $SiH_2(^1A_1)$ and $CH_2(^1A_1)$, slightly faster than H, and up to six orders of magnitude more rapid than CH_3 reactions. Since it is known that both singlet SiH_2 and CH_2 react with silanes mainly by insertion into Si-H bonds, while H and CH_3 undergo hydrogen abstraction, it can be concluded that the reaction of CCl with silane is mainly Si-H bond insertion.

It is not surprising to find no measurable reaction with tetramethylsilane, because the C-H bonds are non - reactive towards CCl. However, provided steric hindrance created by the methyl groups was not the deciding factor in

---

[*1] collision frequencies at 25°C were calculated to be 2.56×10^{11} (Si_2H_6); 2.26×10^{11} (SiH_4); 2.40×10^{11} ($MeSiH_3$); 2.59×10^{11} (Me_2SiH_2); 2.82×10^{11} (Me_3SiH) in M^{-1} s^{-1} units. $\sigma(CCl) = 4.065$ Å,[117] $\sigma(Si_2H_6) = 6.50$ Å, $\sigma(SiH_4) = 5.04$ Å, $\sigma(MeSiH_3) = 5.80$ Å, $\sigma(Me_2SiH_2) = 6.54$ Å, $\sigma(Me_3SiH) = 7.22$ Å.[118]

TABLE IV.3

Second Order Rate Constants k_1 for the Reactions of CCl($X^2\Pi$), SiH ($^1A_1$), CH_2($^1A_1$), CH_3, and H with Silanes

Substrate	$k_1 \times 10^{-9}$ ($M^{-1}s^{-1}$)				
	CCl$^{a)}$	SiH_2	$CH_2$$^{d)}$	$CH_3$$^{f)}$	H$^{h)}$
SiH_4	0.48 ± 0.05	0.57$^{b)}$		6.0 × 10^{-8}	0.26
$MeSiH_3$	1.7 ± 0.2	6.44$^{c)}$	8.4	2.1 × 10^{-8}	0.37
Me_2SiH_2	2.8 ± 0.1	3.03$^{c)}$	8.1	9.6 × 10^{-9}	0.40
Me_3SiH	2.8 ± 0.2	4.46$^{c)}$	7.1	4.0 × 10^{-9}	0.34
Me_4Si	no reaction	no reaction$^{c)}$	6.9	1.9 × 10^{-8}	<0.006
Et_2SiH_2	2.9 ± 0.3				0.78
Et_3SiH	4.5 ± 0.1				0.60
SiD_4	0.25 ± 0.03			9.5 × 10^{-9}	0.09
$MeSiD_3$	0.98 ± 0.04		7.3$^{e)}$	3.1 × 10^{-9}	0.14
Me_2SiD_2	1.8 ± 0.1			2.8 × $10^{-9}$$^{g)}$	
Me_3SiD	2.8 ± 0.2				
Si_2H_6	6.47 ± 0.34	3.69$^{b)}$		6.6 × 10^{-8}	2.23
Si_2D_6	5.61 ± 0.32			1.2 × 10^{-8}	0.90
Me_6Si_2	0.025 ± 0.003				
Cl_6Si_2	no reaction				
Cl_3SiH	no reaction (<0.03)				
$ClMe_3Si$	no reaction				
$ClMe_2SiH$	0.39 ± 0.02				

Continued...

TABLE IV.3 Continued

Cl_2MeSiH	0.029 ± 0.003
FMe_2Si	no reaction
F_2Me_2Si	no reaction
F_3MeSi	no reaction

---

a) This work.

b) John and Purnell[111]; Arrhenius parameters for SiH_2 insertion calculated from co-pyrolysis data and thermochemical information.

c) Cox and Purnell[112]; based on co-pyrolysis data with Si_2H_6 and the calculated value for SiH_2 insertion into Si_2H_6.

d) Marzac and Simons[113], Hase and Simons[114]; values for overall rate constant for CH_2 insertion into both Si-H and C-H bonds. Absolute values calculated from data for CH_2 insertion into silanes relative to CH_2 insertion into CH_4. $CH_2(^1A_1) + CH_4 \longrightarrow C_2H_6$, $k_1 = 1.1 \times 10^8\ M^{-1}s^{-1}$.

e) Calculated from the isotope effect of 1.15.

f) Strausz and coworkers[115]; room temperature data calculated from the Arrhenius parameters.

g) Abstraction by CD_3 radicals.

h) Austin and Lampe[116]; values for H abstraction relative to $H + C_2H_4 \longrightarrow C_2H_5$. Value for k_H taken as $5.1 \times 10^8\ M^{-1}s^{-1}$.

causing this lack of reaction, the result may have another implication, in that the Si-C bonds are inert as well. If this is the case, CCl closely resembles $SiH_2(^1A_1)$, which does not react with either C-H or Si-C bonds, but readily inserts into Si-H bonds. On the other hand, $CH_2(^1A_1)$, like CCl and $SiH_2(^1A_1)$, readily inserts into Si-H bonds and does not react with Si-C bonds, but does react with tetramethylsilane by inserting into the primary C-H bonds.

The effects of alkyl substitution in the silanes on the rates of the CCl reaction do not follow those observed for $SiH_2(^1A_1)$ and $CH_2(^1A_1)$. For example, with increasing alkylation of silane, an increase in reaction rate was observed for CCl, yet $SiH_2(^1A_1)$ does not display any particular trend, while a decrease in rate was observed with $CH_2(^1A_1)$.

Perhaps a more meaningful comparison of the rate constants is one carried out on the basis of rates per Si-H bond (Table IV.4). CCl and SiH_2 react with the alkylated monosilanes primarily by insertion into Si-H bonds. However, $CH_2(^1A_1)$ also inserts into C-H bonds at rates seven to nine times slower than insertion into the Si-H bonds of the same substrate. Therefore, the rates of reaction of $CH_2(^1A_1)$ with silanes on the basis of per Si-H bond insertion, listed in Table IV.4, were determined by converting the C-H bonds into the equivalent number of Si-H bonds using the known values for the relative rates of C-H and Si-H bond insertion.

TABLE IV.4

Second Order Rate Constants k_1, per Si-H bond, for the Insertion of $CCl(X^2\Pi)$, $SiH_2(^1A_1)$ and $CH_2(^1A_1)$ into Silanes

Substrate	k_1 (per Si-H bond) $\times 10^{-9}(M^{-1}s^{-1})$		
	CCl [a)]	SiH_2 [b)]	CH_2 [c)]
SiH_4	0.12	0.14	
$MeSiH_3$	0.57	2.15	2.51
Me_2SiH_2	1.4	1.52	2.82
Me_3SiH	2.8	4.46	3.13
Si_2H_6	1.1	0.61	
SiD_4	0.06		
$MeSiD_3$	0.33		
Me_2SiD_2	0.9		
Me_3SiD	2.8		
SiD_6	0.93		

a) This work.

b) Purnell and coworkers[111,112]

c) Per Si-H bond values calculated from the data given in Table IV.3 and the relative rates of $CH_2(^1A_1)$ insertion into C-H and Si-H bonds[113,114]: SiH/CH = 8.9 for $MeSiH_3$, 6.9 for Me_2SiH_2 and 7.1 for Me_3SiH. Hence the equivalent number of Si-H bonds are: for $MeSiH_3$, 3 + 3 × 1/8.8 = 3.34; for Me_2SiH_2, 2 + 6 × 1/6.9 = 2.87; for Me_3SiH, 1 + 9 × 1/7.1 = 2.27

In this case, better correlations between reactivity and structure of the substrate can be found for all these species, in that the reaction rate obviously increases with the degree of alkylation of the silane. However, the value for the SiH_2 + $MeSiH_3$ reaction reported by Purnell and coworkers does not appear to follow the general pattern and its redetermination may be desirable. The reactivity of the Si-H bond is, therefore, in the order, tertiary > secondary > primary. A comparison of the rate constants for trimethylsilane (k_1 = $(2.8 \pm 0.2) \times 10^9$ M^{-1} s^{-1}) and *iso*butane (k_1 = $(4.5 \pm 0.4) \times 10^6$ M^{-1} s^{-1}) indicates that for CCl, there is a tremendous preference for the tertiary Si-H bond over the tertiary C-H bond. Although $CH_2(^1A_1)$ also shows some selectivity, as mentioned before, the insertion rate ratio Si-H/C-H observed, ~ 7-9, is much smaller.

Upon deuteration of the silanes, a primary isotope effect was observed, the magnitude of which is dependent on the reactivity of the Si-H bond (Table IV.5). The effect is negligible in the case of tertiary Si-H bonds, but increases, as reactivity decreases, to a factor of 1.9 with the Si-H bond of monosilane. Comparatively, the isotope effect is smaller, 1.15, for $CH_2(^1A_1)$ insertion into primary Si-H bonds, and larger, ~ 2.7, for the CH_3 abstraction reaction with monomethylsilane.

An examination of the results with the halomethylsilanes shows that progressive replacement of the methyl groups of trimethylsilane with chlorine atoms results in a

TABLE IV.5

Isotope Effects for the Reactions of $CCl(X^2\Pi)$ with Silanes

Substrate	$k_1 \times 10^{-9}(M^{-1}s^{-1})$		k_{1H}/k_{1D}
	X = H	X = D	
Me_3SiX	2.8 ± 0.2	2.8 ± 0.2	1.0
Me_2SiX_2	2.8 ± 0.1	1.8 ± 0.1	1.5
$MeSiX_3$	1.7 ± 0.2	0.98 ± 0.04	1.7
SiX_4	0.48 ± 0.05	0.25 ± 0.03	1.9

systematic reduction in the rate constant for reaction with CCl. Each successive replacement leads to an order of magnitude decrease in the rate constant, so that the rate of reaction with trichlorosilane is at least two orders of magnitude slower than the rate of reaction with trimethylsilane. For the sake of comparison, the upper limit of the reactivity of trichlorosilane was estimated as follows.

No reaction was detected with up to nine torr trichlorosilane. Since, for acetylene (k_1 = $(3.5 \pm 0.4) \times 10^7$ M^{-1} s^{-1}), the CCl signals were almost completely quenched at ~ ten torr, the maximum substrate pressure used, it can be estimated that for trichlorosilane, $k_1 < 3.5 \times 10^7$ M^{-1} s^{-1}.

The lack of reaction with methyltrifluorosilane and dimethyldifluorosilane supports earlier observations that reactions with primary C-H bonds are insignificant, and furthermore confirms the inertness of the Si-C bond towards CCl, because the methyl groups here should impose less hindrance than the four methyl groups in tetramethylsilane to the accessibility of the Si-C bond, and hence should not be responsible for the non-reaction with the substrates. However, variation of the Si-C bond strength with the substituents on either side should not be ignored.[118] Even so, the observation that the reactivity of the methylsilanes follows the same order as that of the Si-H bond parameters (*vide infra*) is a good indication that reaction with the Si-C bond, if at all operative, is relatively insignificant compared to insertion into the Si-H bond.

If the hydrogen atom of trimethylsilane is replaced by a chlorine or fluorine atom, no measurable reaction can be detected between CCl and trimethylchlorosilane or trimethylfluorosilane. This is not too surprising, since the results with CH_3Cl have indicated that reaction of CCl with the C-Cl bond is rather insignificant ($k_1 < 3.5 \times 10^7$ M^{-1} s^{-1}). Moreover, Si-halide bonds are even more ionic than the corresponding C-halide bonds, a factor which will no doubt contribute to the low reactivity of silicon halides towards electrophilic reagents. The higher electronegativities of F and Cl atoms would confer a high partially positive charge on Si, causing a stabilization of the 3d orbitals of Si, which can thus interact with the lone pairs of electrons of the halogens. This results in double-bond character and higher bond energies for the Si-F and Si-Cl bonds. Indeed, the results with the trimethylhalogenosilanes indicate that both Si-F and Si-Cl bonds are non-reactive towards CCl, whose reactions with the monosilanes can thus be restricted solely to insertion into Si-H bonds.

The order of reactivity established for the Si-H bonds, tertiary > secondary > primary, along with the observation that replacement of the methyl groups with chlorine atoms results in reduced rates of Si-H bond insertion, strongly points to the electrophilic nature of the insertion reaction. The correlation between log k_1 and ionization potential[117] of the substrates has already been recognized as evidence of such behaviour. This relationship was found earlier for the reactions of CCl with alkynes, and is now observed here for silanes as well (Figure IV.2). The displacement of the graph for the ethylsilanes seems to indicate a different homologous silane series. The ionization potentials for hydrogenated and deuterated silanes were assumed to be identical, but in fact could differ by 0.1 - 0.2 eV; in that case it is possible that the two plots for methylated silanes would superimpose. The linearity of these plots indicates constant A-factors for the reactions, suggesting that steric hindrance caused by the alkyl groups on the insertion reactions is insignificant.

Given our previous observations concerning the electrophilic nature of CCl, correlations between the rate of insertion and other molecular parameters of the Si-H bond would be expected. The Si-H bond stretching frequencies for a series of silanes with various degrees of methyl and chloro substitution have been discussed by Hollandsworth and Ring,[128] who observed an increase in the stretching frequency of the Si-H bond when the methyl substituents are successively replaced by chlorine atoms. This correlates well with the observed decrease in reactivity of the Si-H bond with decreasing alkyl substitution or increasing chloro substitution (Table IV.6).

This variation in stretching frequencies can be predicted on the basis of the s and p character of the

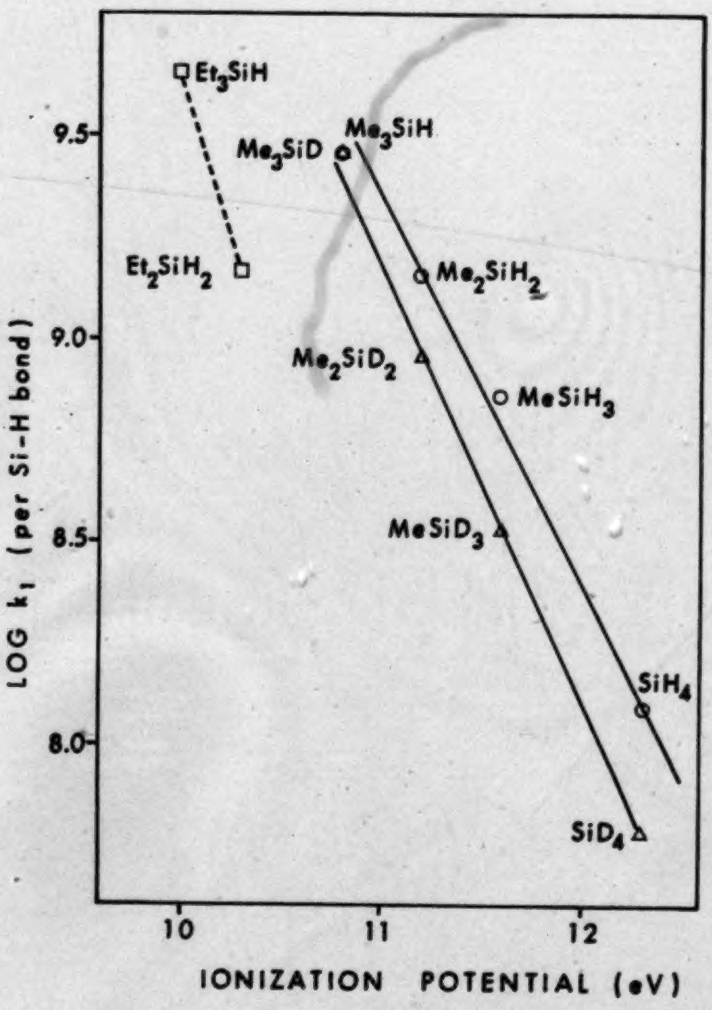

FIGURE IV.2 Log k$_1$ (per Si-H bond) *versus* Ionization Potential for the Reactions of CCl($X^2\Pi$) with Silanes

TABLE IV.6

Second Order Rate Constants k_1, per Si-H Bond, and Si-H Bond Stretching Frequencies ν of Silanes

Substrate	k_1 (per Si-H bond) $\times 10^{-9}$ ($M^{-1}s^{-1}$)	cm^{-1}
SiH_4	0.12	2182$^{a)}$
$MeSiH_3$	0.85	2167$^{b)}$
Me_2SiH_2	1.40	2143$^{c)}$
Me_3SiH	2.80	2125$^{d)}$
Et_3SiH	4.50	2105$^{e)}$
Me_2ClSiH	0.39	2174$^{e)}$
$MeCl_2SiH$	0.029	2214$^{e)}$
Cl_3SiH	<0.03	2257$^{e)}$

a) Meal and Wilson[121]

b) Wilde[122]

c) Ebsworth *et al.*[123]

d) Hollandsworth and Ring[120]

e) Webster[124]

silicon orbital bonded to the hydrogen in the Si-H bond. The above observations suggest that the bond strength increases correspondingly with increasing bond stretching frequency. Although there are large discrepancies in the values of the Si-H bond energies reported in literature, in general they do seem to decrease with increasing number of methyl groups on the silicon; for example, Austin and Lampe[114] showed that the Si-H bond strength, in kcal mole^{-1} units, decreases in the order, SiH_4, 93; $MeSiH_3$, 90; Me_2SiH_2, 88; Me_3SiH, 85.

The trisubstituted silanes were investigated more closely in order to examine the relationship between reactivity and stretching frequency, under the constant environment that all the substrates possess only one Si-H bond. The upper limit was log $k_1 < 7.5$ for Cl_3SiH, although no observable reaction was detected. The plot of log k_1 *versus* Si-H bond stretching frequency (Figure IV.3) suggests a somewhat curved relationship, possibly due to the fact that the double bond character of the Si-Cl bond would return electrons to the silicon, which acts as an electron sink, thereby reducing the negative inductive effect of replacing the methyl groups by the chlorine atoms in the silicon series. Furthermore, the above correlation also agrees with the amount of hydridic character of the Si-H bond (*vide infra*).

Since C-H bonds are non-reactine towards CCl, the reaction observed with hexamethyldisilane is strongly indicative of reaction with the Si-Si bond. However, on the

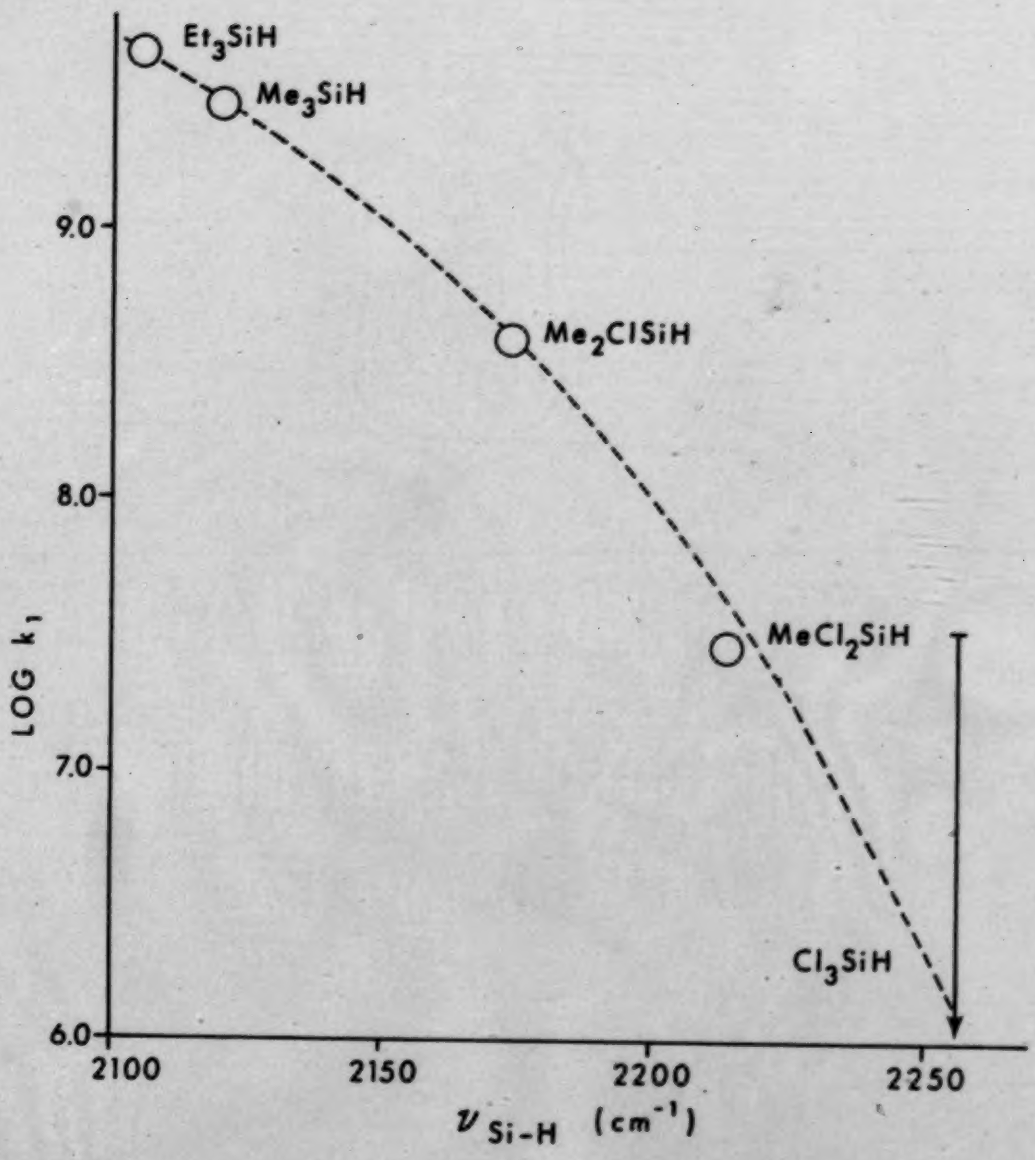

FIGURE IV.3 Log k_1 *versus* Si-H Bond Stretching Frequency νSi-H for Trisubstituted Silanes

basis of the low Si-Si bond energy, ~ 67 kcal mole^{-1},[128] a much faster reaction would be anticipated. The rather low rate constant observed, (2.5 ± 0.3) × 10^7 M^{-1} s^{-1}, may therefore be caused by steric hindrance, created by the six methyl groups, which limits the availability of the Si-Si bond. However, it does not appear that the much larger rate constant, (6.5 ± 0.3) × 10^8 M^{-1} s^{-1}, for the reaction with disilane, Si_2H_6, is due to enhanced reactivity with the Si-Si bond because, as will be shown below, the reactivity correlates well with the rate of Si-H bond insertion in monosilanes. Therefore, it can be concluded that the reaction of CCl with the Si-Si bond of disilane is slow and does not make a significant contribution towards the overall reaction rate.

Sefcik and Ring[124] observed that, on the basis of Si-H bond stretching frequencies, the hydridic character of the hydrogen atom attached to silicon increases with increasing methylation. This was confirmed by recent molecular orbital calculations performed by Perkins *et al.*,[127] who obtained values for the negative charge density on the hydrogen of the Si-H bond ranging from ~ -0.03 to ~ -0.11 in going from SiH_4 to Me_3SiH. The reactivity of the silanes towards CCl, compared on a per Si-H bond basis, thus follows the order of the hydridic character of the Si-H bond,

$$Me_3SiH > Me_2SiH_2 > Si_2H_6 > MeSiH_3 > SiH_4$$

However, this trend was not observed in the study of the reactions of $SiH_2(^1A_1)$ with silanes carried out by Sefcik and Ring,[134] who found that disilane is more reactive than dimethylsilane,

$$Me_3SiH > Si_2H_6 > Me_2SiH_2 > MeSiH_3 > SiH_4$$

They attributed this anomaly to the occurrence of $SiH_2(^1A_1)$ insertion into the Si-Si bond, the product of which is indistinguishable from that formed by Si-H bond insertion. For the CCl reaction, however, disilane follows the same order of reactivity as the order of hydridic character of the Si-H bond; this constitutes additional evidence to the effect that reaction with the Si-Si bond must be relatively insignificant compared to insertion into the Si-H bond.

When the methyl groups in hexamethyldisilane are replaced with chlorine atoms, no measurable reaction could be detected. This suggests that the reaction with the Si-Si bond is also electrophilic in nature, and that the low rate constant associated with the hexamethyldisilane reaction is solely due to an inefficient reaction with the Si-Si bond itself, rather than to steric hindrance created by the methyl groups, because this interference may be compensated by the positive inductive effect of the methyl substituents.

The observation that the increasing reactivity of the silanes can be correlated with increasing hydridic character of the Si-H bond may shed some light on the mechanism of the insertion reaction. Since the hydridic character of a Si-H bond reflects the negative charge density on the hydrogen, a reasonable transition state would involve an electrophilic attack by CCl on the hydrogen, resulting in a hydride ion transfer with more or less simultaneous back donation of the lone pair of electrons on the carbon of the carbyne to the silicon,

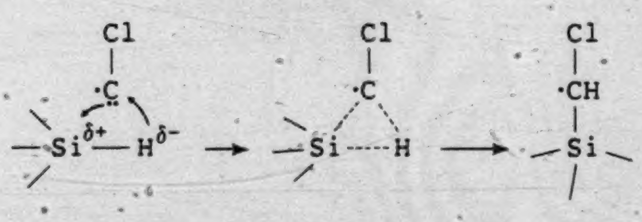

The empty d orbitals of the silicon may take part in the back donation process during the formation of the transition state, and this may contribute to the relative ease of Si-H bond insertion compared to C-H bond insertion, since silicon's capability of being pentacoordinate would doubtless enhance the stability of the transition state.

The reactivities of CCl($X^2\Pi$), SiH$_2$($^1A_1$) and CH$_2$($^1A_1$) with respect to silanes can be summarized as follows:

- C-H bonds:
  neither CCl nor SiH$_2$ react with C-H bonds, while CH$_2$ inserts readily.
- Si-H bonds:
  all three species undergo insertion reactions with Si-H bonds; CH$_2$ shows a slight preference towards Si-H bonds over the corresponding C-H bonds (insertion rate ratio

~ 7-9)

- Si-C bonds:

  CCl, SiH_2 and CH_2 are all non-reactive towards Si-C bonds.

- Si-Si bonds:

  SiH_2 inserts into Si-Si bonds,[126] while the reaction of CCl with the Si-Si bond is relatively slow; no products attributable to Si-Si bond insertion could be obtained in the CH_2 + Me_6Si_2 system,[128] the only study of the reaction of CH_2 with disilane reported in literature.

E. REACTION WITH CYCLIC AND HETEROCYCLIC COMPOUNDS

Carbynes undergo electrophilic cycloadditions with alkynes, alkenes and unsaturated cyclic compounds. Kinetic studies on the reactions of carbynes with alkenes and alkynes have suggested that the behaviour of $^2\Pi$ carbynes parallels that of $^1A_1$ carbenes, therefore CCl was also expected to undergo cycloadditions with unsaturated cyclic compounds.

No measurable reaction was detected with cyclohexane and cyclopentane; this is compatible with earlier observations that CCl is non-reactive towards primary or secondary C-H bonds, and strongly suggests that the rate constants measured for the unsaturated compounds are due to cycloadditions of CCl to C=C bonds.

A comparison of the rate constant values for cyclohexene ($k_1 = (3.1 \pm 0.2) \times 10^9\ M^{-1}\ s^{-1}$) and ethylene ($k_1 = (3.3 \pm 0.4) \times 10^8\ M^{-1}\ s^{-1}$), reported by Tyerman,[81] indicates that the presence of four methylene groups greatly enhances the electron density of the double bond, and results in an increased reactivity of an order of magnitude. The rate constant measured for 1,4-cyclohexadiene, $(3.7 \pm 0.2) \times 10^9\ M^{-1}\ s^{-1}$, is almost comparable with that for cyclohexene.It is quite surprising to measure an even slower reaction with 1,3-cyclohexadiene ($k_1 = (1.4 \pm 0.2) \times 10^9\ M^{-1}\ s^{-1}$) because this compound is generally more reactive than 1,4-cyclohexadiene towards an electrophile. This discrepancy can be ascribed to the lower electron density of the double bonds in 1,3-cyclohexadiene due to conjugation and subsequent delocalization, thus retarding the initial rate of electrophilic attack; the enhanced reactivity of 1,3-cyclohexadiene with respect to electrophilic substitution can be rationalized in terms of the stability of the ionized intermediate, for which resonance structures can be written:

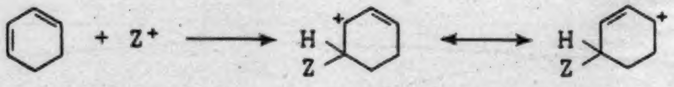

For the cycloaddition reaction with carbynes, however, no such stabilizing structures can be envisioned for the cyclopropyl radical intermediate.

The ionization potentials of cyclohexene, 1,3- and 1,4-cyclohexadiene, and benzene have been determined by many workers using different techniques[129],[130] and the correlation between reactivity and ionization potential of the substrates, found in previous studies on alkenes, alkynes and silanes, was not observed for these four substrates. Moreover, the data for all of these compounds deviate significantly from the linear graph of the log k_1 *versus* ionization potential plot for the alkenes, studied by Tyerman; this was expected because they do not belong to the same homologous series of alkenes.

The relatively high ionization potential of benzene, 9.24 eV,[129] compared to, for example, cyclohexene, 8.72 eV,[129] is indicative of extra stability of the benzene ring due to resonance effects. Thus the slow reaction observed with benzene ($k_1 = (6.7 \pm 0.5) \times 10^7\ M^{-1}\ s^{-1}$) can be ascribed to the low availability of the π electrons due to a high degree of delocalization. In fact, this slower rate with benzene is compatible with the slow rate measured for the reaction of CBr with benzene ($k_1 = (2.2 \pm 0.2) \times 10^8\ M^{-1}\ s^{-1}$),[84] and was also observed in a recent study of CH reactions by Lin and coworkers.[79] In the reaction with benzene, both CH insertion into C-H bonds and cycloaddition to the C=C bonds were expected to occur; however, despite the fact that the statistical factor for the attack on π bonds is six times larger in benzene than in acetylene, and the strength of the C-H bonds in both molecules are comparable (~ 112 kcal mole^{-1}),[79] the rate constant measured for the reaction of CH with benzene ($k_1 = (4.8 \pm 1.9) \times 10^{10}$ M^{-1} s^{-1}) turned out to be two to three times slower than with acetylene ($k_1 = (1.3 \pm 0.2) \times 10^{11}$ M^{-1} s^{-1}).

The electrophilic substitution reactions of benzene and substituted benzenes[131] have been well studied for many years. However, similar kinetic studies on the rate of cycloadditions of carbenes and carbynes with benzene and substituted benzenes (except for CH,[79] CBr[84] and CCO_2Et[82] + benzene systems) have not yet been reported in the literature. For electrophilic substitution, the reactivity of the substituted benzene was found to depend on the inductive effect of the substituent group: alkyl groups are known to activate, and halide groups deactivate, the benzene ring.

In addition to altering the electron density in the ring by a combination of inductive and mesomeric effects, a substituent group can also induce polarization of the ring π system with the effect of reducing the aromaticity, due to π electrons being localized at certain parts of the ring. Dhingra *et al.*[132] proposed that the dilution shifts of aromatic protons in non-polar, isotropic solvents such as carbon tetrachloride are directly proportional to aromaticity, and estimated the aromaticities of some monosubstituted benzenes from proton resonance data as: benzene and toluene, aromaticity, A = 100%; fluorobenzene, A = 89%; chlorobenzene, A = 98%.

However, the order of reactivity observed here for the reactions of CCl with substituted benzenes does not exactly follow the trend established for electrophilic substitution reactions, which is, toluene > benzene > chlorobenzene > fluorobenzene in decreasing order of reactivity. Instead, the methyl group and, to a lesser extent, the chlorine atom, were found to activate the ring, while the effect on reactivity due to the fluorine substituent is negligible compared to benzene.

Kennepohl[52] studied the reaction of CCO_2Et with benzene, and suggested that the cycloheptatriene radical is the reactive intermediate, on the basis of the detection of its dimers. The cycloheptatriene radical intermediate supposedly arises from the cycloaddition of CCO_2Et with benzene followed by ring expansion:

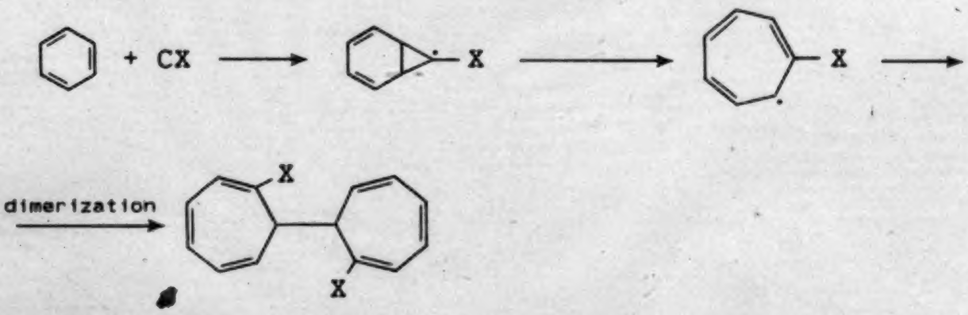

where $X = CO_2Et$. CCl should react in a similar manner. Hence the basic difference between electrophilic substitution and cycloaddition reactions with the benzene ring is that electrophilic substitution involves the carbonium ion intermediate,

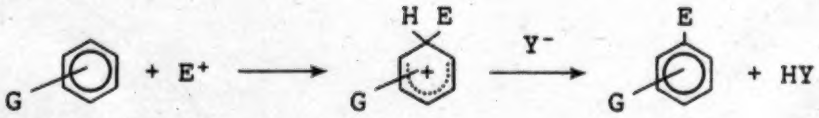

which can be affected by a substituent group, G, already attached to the ring: electron-releasing substituents such as CH_3 stabilize the carbonium ion, leading to a faster reaction than benzene; on the other hand, electron withdrawing substituents such as Cl, F intensify the positive charge of the intermediate, destabilizing it, thus causing a slower reaction. However, since the ring structure is eventually retained, the reactivity of the benzene ring may be less dependent on its aromaticity than in a cycloaddition reaction, which forms cycloaddition products that would destroy the benzene ring system. Although the nature of the rate – determining step in electrophilic substitution reactions may vary according to the reactants and the experimental conditions employed, of crucial importance is the fact that the carbonium ion intermediate can be stabilized by resonance, which does not exist in cyclopropyl radical intermediates. Therefore, in cycloaddition reactions with benzene rings, the aromaticity of the ring may be of comparable significance to the electron-releasing or withdrawing effects of the substituent in determining the reactivity.

In toluene, the positive inductive effect of the methyl group should be mainly responsible for the observed reactivity (k_1 = $(3.3 \pm 0.2) \times 10^8$ M^{-1} s^{-1}) being five times that of benzene (k_1 = $(6.7 \pm 0.5) \times 10^7$ M^{-1} s^{-1}). Particularly interesting is the activation of the ring by Cl in chlorobenzene (k_1 = $(1.7 \pm 0.2) \times 10^8$ M^{-1} s^{-1}) since the aromaticity is not considerably lower than that of benzene (aromaticity: 98% of benzene, from proton resonance data, 93% of benzene, from resonance energy data);[132] yet it appears that the electron-releasing mesomeric effect of Cl, aided by a slightly lower degree of delocalization of the electrons, has more than overcome the electron-withdrawing inductive effect of Cl, resulting in a twofold increase in reactivity over that of benzene towards CCl. With fluorobenzene, the mesomeric effect should be minimal due to the high electronegativity of F, and in this case it seems that the negative inductive effect is neutralized by the effect of a lower aromaticity, and as a result the observed reactivity (k_1 = $(6.1 \pm 0.9) \times 10^7$ M^{-1} s^{-1}) is about the same as that of benzene, within experimental error.

The electrophilic nature of the cycloaddition reactions with benzene and the substituted benzenes is again reflected in the correlation between log k_1 and the ionization potential[133] of the substrates (Figure IV.4). However, the lack of sufficient data makes it difficult to conclude whether there may be slight curvature in the plot.

The results of the study by Kennepohl lend further support to the prediction that carbynes and carbenes behave in an analogous manner, since $CHCO_2Et$ also reacts with

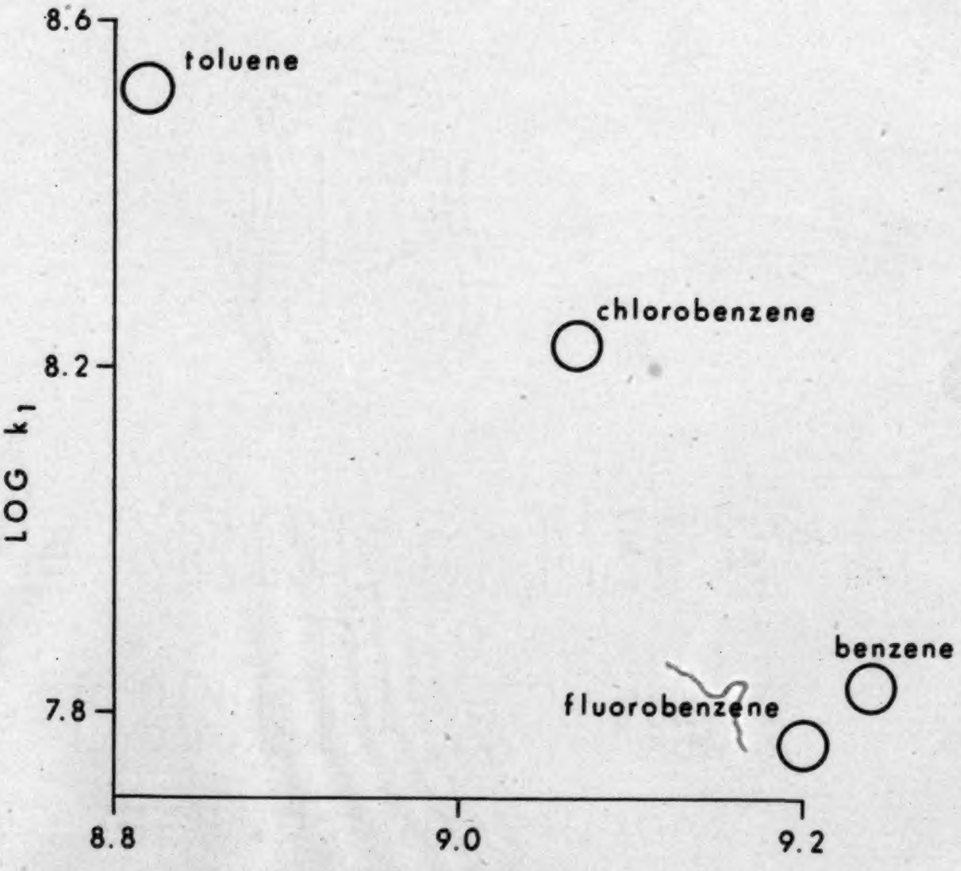

FIGURE IV.4 Log k_1 *versus* Ionization Potential for the Reactions of $CCl(X^2\Pi)$ with Benzene and Substituted Benzenes

benzene to form a norcaradiene ester which subsequently undergoes ring expansion by the Cope rearrangement to give the cycloheptatriene ester:

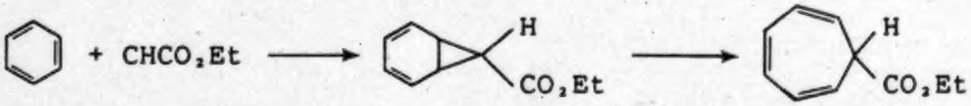

For the carbenes, the expected reduction in reactivity in going from methylene to chlorocarbenes is reflected in the products obtained in their reactions with benzene: CH_2 reacts by insertion into C-H bond to give toluene and by addition to the aromatic ring, followed by ring expansion, to give cycloheptatriene;[134] CHCl gives only the product of ring expansion[138] and CCl_2 does not react.[109]

The insertion reactions of carbenes are not confined only to C-H, Si-H or N-H bonds. Insertion into C-O, C-N, or C-S bonds have also been reported,[1,3] and the mechanisms probably involve initial electrophilic attack on the heteroatoms to form unstable ylides.

The measurable, and in some cases high, rate constants obtained with the saturated heterocyclic compounds thiacyclohexane (k_1 = $(8.3 \pm 0.8) \times 10^9$ M^{-1} s^{-1}), tetrahydrothiophene (k_1 = $(7.6 \pm 1.1) \times 10^9$ M^{-1} s^{-1}), pyrrolidine ($k_1 > 4.8 \times 10^8$ M^{-1} s^{-1}) and tetrahydrofuran (k_1 = $(6.6 \pm 1.4) \times 10^7$ M^{-1} s^{-1}) constitute clear evidence for the occurrence of interactions between CCl and the heteroatoms, although the rate constant for reaction with NH_3 (4.5×10^6

M^{-1} s^{-1} < k_1 < 3.5×10^7 M^{-1} s^{-1}) suggests that reaction with the N-H bond could contribute to the overall reaction observed with pyrrolidine. A comparison of the data for thiacyclohexane and tetrahydrothiophene, which have statistically six and five C-H bonds respectively, shows that they are equally reactive within experimental error, thus implying that insertion into the ring C-H bonds is comparatively insignificant and that reactions are restricted to the heteroatoms. Besides, the introduction of a heteroatom into the ring does not appear to alter the C-H bond strength to a great extent: the C-H bond energy of cyclopentane, which is non-reactive towards CCl, is $\sim$ 95 kcal $mole^{-1}$,[136] while the α C-H bond energy of tetrahydrofuran is $\sim$ 92 kcal $mole^{-1}$.[137]

At this point it is rather difficult to pinpoint the nature of the interactions of CCl with the heteroatoms. By analogy with the behaviour of the carbenes, CCl may undergo electrophilic attack on the heteroatom to form ylides, which may be either stable as in the case of sulphur ylides, or undergo ring expansion as in nitrogen or oxygen ylides, resulting in apparent C-N or C-O bond insertion products:

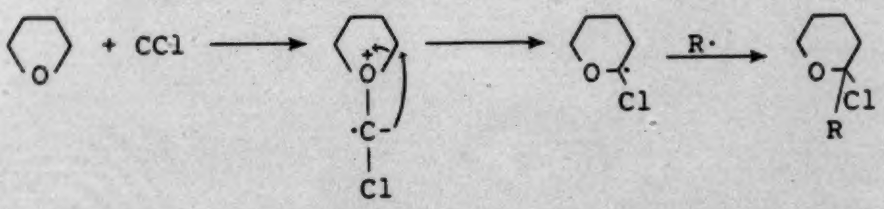

where R denotes a reactive radical present in the system.

The introduction of two double bonds into the heterocyclic ring, as in the case of thiophene, pyrrole and furan, would satisfy the (4n + 2) rule and render the heterocyclic compound aromatic. The aromaticity should be affected by the electronegativity of the heteroatom, which determines the degree the lone pair of electrons from the heteroatom is delocalized into the π system:

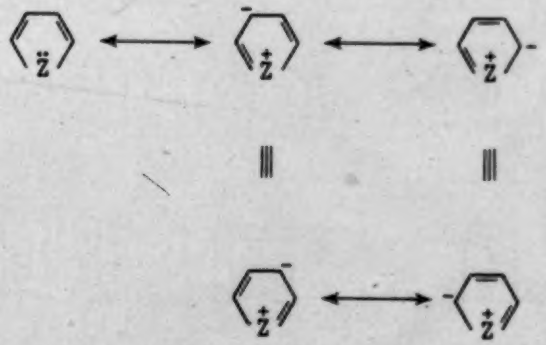

where Z = S, N or O.

However, some controversy exists in assessing the aromaticity of the above compounds. The consensus is benzene > thiophene > pyrrole > furan, although some results based on resonance energy or ring current data reverse the order of thiophene and pyrrole. The % aromaticity based on resonance energy data from Wheland[138] was compiled by Kanekar *et al.*[139] as: benzene, aromaticity, A = 100%; thiophene, A = 78%; pyrrole, A = 63%; furan, A = 44%. The above order correlates well with the order of electronegativity of the heteroatoms, which is, S < N < O, since the π electrons would be more localized on the more electronegative atom such as oxygen, thus reducing the degree of delocalization or the aromaticity of the ring.

Thiophene ($k_1 = (5.7 \pm 0.2) \times 10^9$ M^{-1} s^{-1}) is somewhat less reactive than tetrahydrothiophene ($k_1 = (7.6 \pm 1.1) \times 10^9$ M^{-1} s^{-1}) towards CCl. This may be due to the lone pair of electrons from sulphur in thiophene being delocalized into the ring. Consequently, the rate of attack at the sulphur atom would decrease and this may not be compensated enough by the presence of the two double bonds in thiophene, due to a high degree of delocalization of electrons in the π system. On the other hand, the higher reactivity of furan ($k_1 = (6.3 \pm 0.4) \times 10^8$ M^{-1} s^{-1}) compared to tetrahydrofuran ($k_1 = (6.6 \pm 1.4) \times 10^7$ M^{-1} s^{-1}) may be attributed to the presence of the two extra double bonds and a much lower degree of delocalization of the π electrons. Unfortunately, it is impossible to compare the reactivities of pyrrole and pyrrolidine due to difficulties encountered during the study of the pyrrolidine reaction, as mentioned in Chapter III.

Thiophene and furan yield cyclopropyl 2,3-adducts upon reaction with carbenes.[148] Although with pyrrole,[148] only substitution products (which are sometimes accompanied by ring-expansion products) can be obtained, the formation of cyclopropane was nevertheless proposed as an intermediate step:

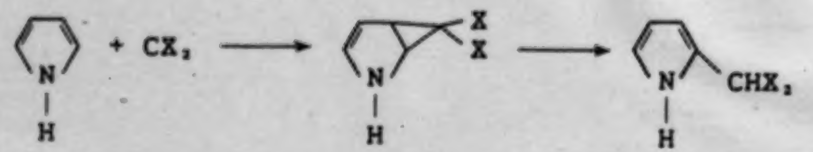

where CX_2 is a general formula for carbenes. By analogy, carbynes should react in the same manner. Thus, Kennepohl[63] studied the reaction of CCO_2Et with pyrrole, and the major product, 3-substituted pyridine, was rationalized in terms of a cyclopropyl radical intermediate formed *via* cycloaddition:

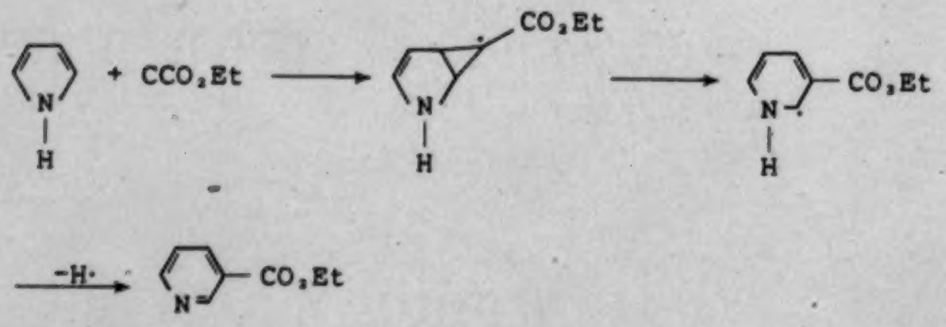

The above result is in agreement with the observation that the π bond orders of the 2,3 or 4,5 bonds are higher than those of the other bonds in thiophene, pyrrole and furan.[141] Although carbene reactions with the heteroatoms in thiophene, pyrrole and furan have not been observed, such a reaction probably occurs with the more electrophilic carbynes. Thus Kennepohl has suggested that reaction of CCO_2Et with the nitrogen atom is the most probable route for the production of pyridine-2-carboxylate, a minor product from the reaction of CCO_2Et with pyrrole. Although he did not speculate further on the mechanistic nature of the reaction, it probably involves the formation of ylide-type radical intermediates. Moreover, the rate constants obtained for the reactions of CCl with ammonia (4.5×10^4 M^{-1} s^{-1} $< k_1 <$ 3.5×10^7 M^{-1} s^{-1}) and pyrrolidine ($k_1 > 4.8 \times 10^8$ M^{-1} s^{-1}) also suggest that insertion into the N-H bond may contribute to the overall rate constant measured with pyrrole.

The order of reactivity observed here, thiophene > pyrrole ≫ furan, is different from the one already established for electrophilic substitutions, pyrrole ≫ furan > thiophene.[142-144] Although the initial step in both reactions involves the breaking-up of the aromatic ring, the ionic intermediate in electrophilic substitution can be stabilized by resonance, which does not occur in cycloaddition:

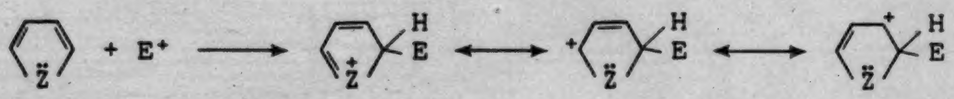

and this partly explains the difference in the reactivities. Also, the former reactions were studied mainly in solution rather than in the gas phase, and solvation can stabilize the ionic intermediates or transition states.

Furthermore, interactions of CCl with the heteroatoms must also contribute to the difference in the order of reactivity as compared to electrophilic substitution. Linda *et al.*[142] found a correlation, not observed here, in that higher reactivity towards electrophilic substitution corresponds to a lower ionization potential of the five-membered heteroaromatic compounds, similar to the relationships established previously for the reaction of CCl with alkynes and silanes. However, these correlations are valid only if the electrons are removed from the π system, and hence if the reaction sites involve both the π electrons and the heteroatoms, the lack of correlation between log k_1 and ionization potential of the substrates in the CCl reactions is not entirely unexpected.

The positive inductive effect of the methyl group is evident from the increased reactivity of 1-methylpyrrole ($k_1 = (4.9 \pm 0.5) \times 10^9\ M^{-1}\ s^{-1}$) compared to pyrrole ($k_1 = (3.1 \pm 0.3) \times 10^9\ M^{-1}\ s^{-1}$). This also points to the electrophilic nature of CCl and suggests that insertion into the N-H bond is relatively insignificant.

Furthermore, the increase in reactivity of two orders of magnitude with pyridine ($k_1 = (2.8 \pm 0.3) \times 10^9\ M^{-1}\ s^{-1}$), compared to benzene ($k_1 = (6.7 \pm 0.5) \times 10^7\ M^{-1}\ s^{-1}$), can be attributed to a lower degree of delocalization of π electrons in pyridine, the aromaticity of which was estimated to be ~ 60% of that of benzene;[139] the possibility of interaction with the nitrogen atom, however, should not be excluded.

Finally it may be of interest to point out that during the investigation of the reaction of CCl with pyridine, the absorption spectrum of pyridine was clearly discernible before photolysis, became extremely weak immediately after the photolysis flash and apparently recovered in intensity when the spectrum was again taken two minutes later.

The above observation may be indicative of pyridine being vibrationally or electronically excited during flash photolysis, and therefore the rate constant measured is that for the reaction of CCl with an excited pyridine molecule. However,

- the spectrum of 1.2 torr pyridine + 6.1 torr cyclohexane, in 50 torr helium, was still barely discernible 500 μs after the photolysis flash, indicating that no vibrational or electronic relaxation by cyclohexane has taken place.
- the rate constant measured with 0.3 torr $CHClBr_2$ + 0.09 torr pyridine in 50 torr helium, $\sigma k_1 \sim 14.9 \times 10^3$ M^{-1} s^{-1}, is somewhat smaller than that with 0.3 torr $CHClBr_2$ + 0.1 torr pyridine + 0.5 torr cyclohexane (used to collisionally relax excited pyridine) in 50 torr helium, $\sigma k_1 \sim 20.2 \times 10^3$ M^{-1} s^{-1}. However, it is actually difficult to ascertain whether this difference is significant, given the error limitations of the experiment.

These results show that:

- either cyclohexane is not an effective quencher of the excited pyridine, or the quantity used was insufficient. In any case, it appears that a fairly long lived metastable state of pyridine must have been formed.
- if there was indeed some relaxation by cyclohexane leading to the increased rate of reaction observed, the conclusion would be that the ground state pyridine is more reactive. However, further investigations on this subject would be highly desirable.

V. CONCLUSIONS

Second order rate constant measurements have been carried out for the reactions of $CCl(X^2\Pi)$ with hydrogen, ammonia, methylchloride, propane, *iso*butane, and representative series of alkynes, silanes, cyclic and heterocyclic compounds.

CCl was produced from $CHClBr_2$ mainly *via* the secondary unimolecular decomposition of vibrationally excited CHClBr radicals formed in the primary process:

$$CHClBr_2 + h\nu\ (\lambda > 200\ nm) \longrightarrow CHClBr^{\dagger} + Br$$

$$CHClBr^{\dagger} \longrightarrow CCl + HBr$$

$$\longrightarrow CBr + HCl$$

The simultaneous production of CBr is regarded to be insignificant, since its absorption line at ~ 301.5 nm was extremely weak although still somewhat discernible. However, the very low yield of CCl under conventional photolysis conditions makes direct mechanistic kinetic investigation impossible. As a result, rate constants for the reactions of CCl with a variety of substrates were measured employing flash photolysis - absorption spectroscopic techniques, by monitoring the CCl absorption line at 277.7 nm which has been assigned to the (Q, 0,0) band of the $A^2\Delta \leftarrow X^2\Pi$ system.

The nature of the reactions of CCl with the various substrates examined was deduced on the basis of:

- the prediction that $CH(^2\Pi)$ should display chemical properties analogous to those of $CH_2(^1A_1)$;
- the known chemistry of CH and CCO_2Et;
- *ab initio* studies on the CH + C_2H_2 and CH + C_2H_4 reaction paths;
- and comparison of the rate constant data among analogous substrates.

The rate constant values measured for the reactions of CH, CCl and CBr with various substrates indicate that CH is the most reactive carbyne, reacting indiscriminately at rates close to collision frequencies. On the other hand, CCl, being less electrophilic, behaves like CBr and is less reactive and, consequently, more selective.

Unlike CH which inserts rapidly into H_2 with a rate constant of $\sim 10^{10}\ M^{-1}\ s^{-1}$, CCl does not react with H_2, but, like CH, it appears to undergo insertion into the N-H bonds of NH_3. CH displays little selectivity in its reactions with alkanes, while CCl does not react with propane, cyclopentane or cyclohexane, and thus is inert with respect to insertion into primary and secondary C-H bonds; however, a slow but measurable reaction with *iso*butane ($k_1 = (4.5 \pm 0.4) \times 10^4\ M^{-1}\ s^{-1}$) was observed, pointing to insertion into the tertiary C-H bond of *iso*butane.

The chemically similar species $CH_2(^1A_1)$ and $CH(X^2\Pi)$ have been shown to undergo concerted insertion with C-H bonds, CCl is expected to behave likewise. The existance of a polarized transition state may explain the higher reactivity of tertiary C-H bonds due to the formation of a stable tertiary carbonium ion:

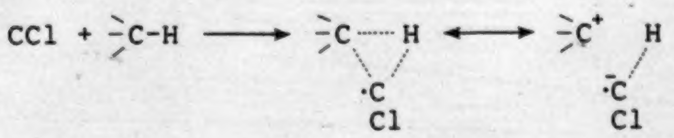

No measurable reaction was detected for the CCl + CH_3Cl system; however, the upper limit estimated for the reaction indicates that a slow insertion into the C-Cl bond may still be possible.

The rate constants for the reactions of CCl with acetylene, acetylene- d_2, propyne, 1-butyne, 2-butyne, 1-pentyne, 2-pentyne, 3,3-dimethyl-1-butyne, 2,2,5,5-tetramethyl-3-hexyne, and phenylacetylene range from 10^7 to 10^{10} M^{-1} s^{-1}. As with the CCl + alkene reactions, higher reactivity corresponds to increasing alkyl substitutions at the C≡C bonds, reflecting the electrophilic nature of the reactions. The mechanism of the reactions with alkynes is postulated to be similar to that with the alkenes, in that CCl undergoes asymmetric, concerted cycloadditions with the unsaturated bonds to form cyclopropenyl radical intermediates. In general, alkynes are less reactive than alkenes, and this may be ascribed to higher activation energies for the alkyne reactions, because the carbocation formed from the alkynes is less stable than that formed from the alkenes, due to its inability to achieve the sp^2 hybrid orbital configuration believed to be the most stable configuration for a carbocation:

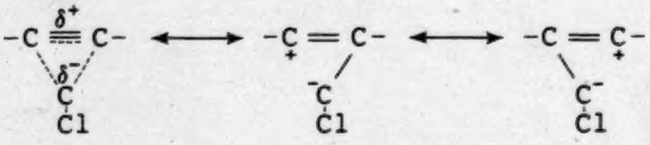

The electrophilic nature of the cycloaddition is further reflected in the linear correlation between log k_1 and ionization potential of the substrates. Negative deviations from the linear relationship in the cases of 3,3-dimethyl-1-butyne and 2,2,5,5-tetramethyl-3-hexyne indicate that steric hindrance plays a role here.

The reactions of CCl with monosilanes are confined to insertion into the Si-H bonds, since Si-F, Si-Cl and Si-C bonds were shown to be non-reactive. The electrophilic nature of the insertion reactions is once again revealed in the increase in reactivity observed with increasing alkyl or decreasing chloro substitution at the silicon atom, and also in the linear relationship found between log k_1 and ionization potential of the substrates. The reactivity of the Si-H bond is in the order tertiary > secondary > primary, with the tertiary Si-H bond being 600 times more reactive than the tertiary C-H bond.

A primary isotope effect was also observed, which ranges from 1.0 with the tertiary Si-H bond, and increases, as the reactivity of the Si-H bond decreases, to a factor of ~ 2 for monosilane.

The reactivity can also be correlated with other bond parameters such as dissociation energy, stretching frequency and hydridic character of the Si-H bond. The observation that higher reactivity corresponds to higher hydridic character of the Si-H bond led to the formulation of a transition state which involves electrophilic attack by CCl on the hydrogen, resulting in a hydride$^-$ ion transfer with more or less simultaneous back donation of the lone pair of electrons from the carbon to the silicon atom,

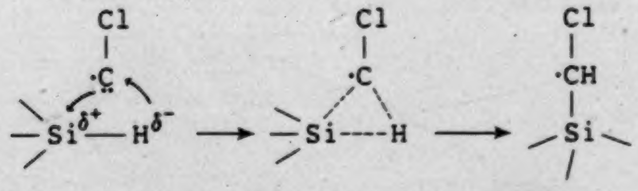

while the empty d orbitals on the silicon may also help in the formation of the cyclopropyl radical intermediate. The ability of silicon to be pentavalent could play a role in the very rapid Si-H bond insertion reactions compared to the slower insertion into C-H bond. Results with the disilanes indicate that CCl also reacts with the Si-Si bond, the reaction is also electrophilic but relatively insignificant compared to Si-H bond insertion.

It is postulated that CCl reacts with cyclic and heterocyclic compounds mainly *via* cycloaddition to the C=C bonds to form cyclopropyl radical intermediates, which may further undergo ring expansion to form e.g., the cycloheptatriene radical in the case with benzene:

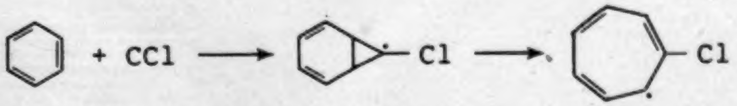

The orders of reactivity observed with benzene and substituted benzenes, toluene > chlorobenzene > benzene ≈ fluorobenzene, and with the heteroaromatic compounds, thiophene > pyrrole ≫ furan, do not exactly follow the trend established for electrophilic substitution reactions; this is not unexpected since the primary adducts and the rate determining steps are quite different in the two systems.

Similarly, the correlation observed between reactivity and ionization potential of the heteroaromatic compounds for electrophilic substitutions was not observed for the cycloaddition reactions here. From this, and also on the basis of comparison of the rate data for heterocyclic compounds with those of analogous paraffinic and alkenic compounds, it is concluded that, in addition to cycloaddition, CCl can also attack heteroatoms.

From the present study it can be concluded that $CCl(X^2\Pi)$ does not react with primary and secondary C-H bonds, but undergoes slow insertion with tertiary C-H bonds and perhaps with the C-Cl bond. It also inserts rapidly into

Si-H bonds, but reacts slowly with the Si-Si bond, and is relatively non-reactive towards Si-C, Si-F and Si-Cl bonds. CCl also undergoes cycloadditions with C=C and C≡C bonds, and in the case of heterocyclic compounds, may react with the heteroatoms as well.

Bibliography

1. W. Kirmse, "Carbene Chemistry", 2nd ed., Academic Press, New York (1971)
2. "Carbenes" vol. I & II, R. A. Moss and M. Jones, Jr., Ed., John Wiley and Sons, New York (1973)
3. R. W. B. Pearse and A. G. Gaydon, "The Identification of Molecular Spectra", 3rd ed., John Wiley and Sons, New York (1976); B. Rosen, "Données Spectroscopiques Relatives aux Molécules Diatomiques", Pergamon Press, Oxford (1970)
4. R. G. W. Norrish, G. Porter and B. A. Thrush, Proc. Roy. Soc. (London), *216A* (1953) 165
5. P. Swings and O. Struve, Phys. Rev., *39* (1932) 142; W. S. Adams, Astrophys. J., *93* (1941) 11; P. Swings, C. T. Elvey and H. W. Babcock, Astrophys. J., *94* (1941) 320
6. K. H. Geib and W. M. Vaidya, Proc. Roy Soc. (London), *178A* (1941) 351; A. G. Gaydon and H. G. Wolfhard, Proc. Roy. Soc. (London), *194A* (1948) 169
7. E. Fagerholm, Arkiv. Mat., Astron. Fysik., *27A (19)* (1940) 18; E. Fagerholm, Naturwissenschaften, *25* (1937) 106
8. H. W. Harkins, Trans. Farad. Soc., *30* (1934) 221
9. L. Gerö, Z. f. Phys., *118* (1941) 27
10. G. Herzberg and J. W. C. Johns, Astrophys. J., *158* (1969) 399
11. J. H. Callomon and D. A. Ramsay, Can. J. Phys., *35*

(1957) 129

12. W. Braun, K. H. Welge and J. R. McNesby, J. Chem. Phys., *45* (1966) 2650; W. Braun, J. R. McNesby and A. M. Bass, J. Chem. Phys., *46* (1967) 2071

13. J. E. Butler, L. P. Goss, M. C. Lin and J. W. Hudgens, Chem. Phys. Letters, *63* (1979) 104

14. J. W. Fleming, G. T. Fugimoto, M. C. Lin and A. B. Harvey, Proc. Int. Conf. on Lasers 1979, STP Press, McLean (1980) 246

15. A. Kasdan, E. Herbst and W. C. Lineberger, Chem. Phys. Letters, *31* (1975) 78

16. G. C. Lie, J. Hinze and B. Liu, J. Chem. Phys., *57* (1972) 625

17. E. H. Coleman and A. G. Gaydon, Farad. Soc. Disc., *2* (1947) 166

18. G. Pannetier and P. Laffitte, Compt. Rend., *226* (1948) 72

19. R. A. Durie and T. Iredale, Trans. Farad. Soc., *44* (1948) 806

20. P. Venkateswarlu, Proc. Ind. Acad. Sci., *25A* (1947) 138; R. D. Verma, Proc. Ind. Acad. Sci., *47A* (1958) 196

21. J. P. Simons and A. J. Yarwood, Trans. Farad. Soc., *57* (1961) 2167

22. J. P. Simons and A. J. Yarwood, Trans. Farad. Soc., *59* (1963) 90

23. R. N. Dixon and H. W. Kroto, Trans. Farad. Soc., *59* (1963) 1484

24. W. J. R. Tyerman, Spectrochimica Acta, *26A* (1970) 1215

25. R. S. McDaniel, R. Dickson, F. C. James, O. P. Strausz and T. N. Bell, Chem. Phys. Letters, *43* (1976) 130

26. F. C. James, B. Ruzsicska, R. S. McDaniel, O. P. Strausz and T. N. Bell, Chem. Phys. Letters, *45* (1977) 449

27. R. K. Asundi and S. M. Karim, Proc. Ind. Acad. Sci., *6A* (1937) 328

28. T. Horie, Proc. Phys. Math. Soc. Japan, *21* (1937) 143; P. Venkateswarlu, Phys. Rev., *77* (1950) 79; Y. Y. Kuzyakov and V. M. Tetevskiĭ, Nauch. Doklady Vyssheĭ Shkoly, Khim. i Khim. Tekhnol., *2* (1959) 233

29. R. F. Barrow, G. Drummond and S. Walker, Proc. Phys. Soc. (London), *67A* (1954) 186

30. W. M. Vaidya, Proc. Roy. Soc. (London), *178A* (1941) 356; G. Pannetier and A. G. Gaydon, Compt. Rend., *225* (1947) 1139

31. R. D. Gordon and G. W. King, Can. J. Phys., *39* (1961) 252

32. R. D. Verma and R. S. Mulliken, J. Mol. Spectroscopy, *6* (1961) 419

33. D. Husain, Nature, *195* (1962) 796

34. W. J. R. Tyerman, Trans. Farad. Soc., *65* (1969) 2948

35. Y. Y. Kuzyakov and V. M. Tetevskiĭ, Izvest. Vysshikh Ucheb. Zavedeniĭ, Khim. i Khim. Tekhnol., *3* (1960) 293

36. J. J. Tiee, F. B. Wampler and W. W. Rice, J. Chem. Phys., *72* (1980) 2925

37. E. B. Andrews and R. F. Barrow, Proc. Phys. Soc.

(London), *64A* (1951) 481

38. J. E. Hesser and K. Dressler, J. Chem. Phys., *45* (1966) 3149

39. Y. Y. Kuzyakov and V. M. Teteyskii, Optika i Spektrosk, *5* (1958) 699

40. R. K. Carroll and T. P. Grennan, J. Phys., *3B* (1970) 865

41. J. A. Harrington, A. P. Modica and D. R. Libby, J. Chem. Phys., *44* (1966) 3380

42. D.E. Mann, H. P. Broida and B. E. Squires, J. Chem. Phys., *22* (1954) 348

43. B. A. Thrush and J. J. Zwolenik, Trans. Farad. Soc., *59* (1963) 582

44. J. L. Margrave and K. Wieland, J. Chem. Phys., *21* (1953) 1552

45. F. B. Wampler, J. J. Tiee, W. W. Rice and R. C. Oldenborg, J. Chem. Phys., *71* (1979) 3926

46. J. J. Tiee, F. B. Wampler and W. W. Rice, Chem. Phys. Letters, *68* (1979) 403

47. T. H. Dunning, Jr., W. P. White, R. M. Pitzer and C. W. Mathews, J. Mol. Spectroscopy, *75* (1979) 297

48. A. J. Merer and D. N. Travis, Can. J. Phys., *43* (1965) 1795

49. T. DoMinh, H. E. Gunning and O. P. Strausz, J. Amer. Chem. Soc., *89* (1967) 6785

50. O. P. Strausz, T. DoMinh and J. Font, J. Amer. Chem. Soc., *90* (1968) 1930

51. O. P. Strausz, G. J. A. Kennepohl, F. X. Garneau, T.

DoMinh, B. Kim, S. Valenty and P. S. Skell, J. Amer. Chem. Soc., *96* (1974) 5723

52. G. J. A. Kennepohl, Ph. D. Thesis, University of Alberta (1972)

53. R. E. Rebbert and P. Ausloos, J. Photochem., *1* (1972/73) 171

54. R. Gordon, Jr. and P. Ausloos, J. Chem. Phys., *46* (1967) 4823

55. M. C. Lin, J. Chem. Phys., *61* (1974) 1835

56. M. C. Lin, Int. J. Chem. Kinetics, *5* (1973) 173; M. C. Lin, Int. J. Chem. Kinetics, *6* (1974) 1

57. M. C. Lin, J. Phys. Chem., *77* (1973) 2726

58. M. C. Lin, private communication

59. I. Messing, C. M. Sadowski and S. V. Filseth, Chem. Phys. Letters, *66* (1975) 95

60. R. E. Rebbert and P. J. Ausloos, J. Photochem., *6* (1976/77) 265

61. D. D. Davis, J. F. Schmidt, C. M. Neeley and R. J. Hanrahan, J. Phys. Chem., *79* (1975) 11

62. A. P. Modica, J. Chem. Phys., *44* (1966) 1585; A. P. Modica and S. J. Sillers, J. Chem. Phys., *48* (1968) 3283

63. R. E. Rebbert, J. Photochem., *8* (1978) 363

64. T. L. Burks and M. C. Lin, J. Chem. Phys., *64* (1976) 4235

65. D. S. Y. Hsu and M. C. Lin, Int. J. Chem. Kinetics, *10* (1978) 839

66. K. M. A. Refaey and J. L. Franklin, Int. J. Mass

Spectry. & Ion Phys., *20* (1976) 19

67. A. P. Wolf, Ann. Rev. Nuclear Sci., *10* (1960) 259

68. E. P. Rack and A. F. Voigt, J. Phys. Chem., *67* (1963) 198

69. C. MacKay and R. Wolfgang, J. Amer. Chem. Soc., *83* (1961) 2399

70. A. P. Wolf, Adv. Phys. Org. Chem., *2* (1964) 201

71. J. Nicholas, C. MacKay and R. Wolfgang, J. Amer. Chem. Soc., *88* (1966) 1065

72. C. MacKay, J. Nicholas and R. Wolfgang, J. Amer. Chem. Soc., *89* (1967) 5758

73. D. R. Safrany, R. R. Reeves and P. Harteck, J. Amer. Chem. Soc., *86* (1964) 3160

74. R. P. Porter, A. H. Clark, W. E. Kaskan and W. E. Browne, Eleventh Symposium (International) on Combustion, Berkeley, California (1966) 907

75. J. Dubrin, C. MacKay and R. Wolfgang, J. Amer. Chem. Soc., *86* (1964) 959

76. B. R. Brooks and H. F. Schaefer III, J. Chem. Phys., *67* (1977) 5146

77. M. W. Bosnali and D. Perner, Z. Naturforsch., *26a* (1971) 1768

78. J. E. Butler, J. W. Fleming, L. P. Goss and M. C. Lin, Laser Probes for Combustion Chemistry, ACS Symposium, series 134, D. R. Crosley, ed. (1980) 397

79. J. E. Butler, J. W. Fleming, L. P. Goss and M. C. Lin, Chem. Phys., *56* (1981) 355

80. R. K. Gosavi, H. E. Gunning and O. P. Strausz, Chem. Phys. Letters, *76* (1980) 159

81. W. J. R. Tyerman, J. Chem. Soc. (A), (1969) 2483

82. J. J. Tiee, F. B. Wampler and W. W. Rice, Chem. Phys. Letters, *73* (1980) 519

83. S. W. Benson, "Thermochemical Kinetics", 2nd ed., John Wiley and Sons, New York (1976)

84. B. Ruzsicska, unpublished data

85. P. S. Skell and R. M. Etter, Proc. Chem. Soc. (London), (1961) 443

86. W. R. Moser, J. Amer. Chem. Soc., *91* (1969) 1135

87. R. G. W. Norrish and G. Porter, Nature, *164* (1949) 658

88. A. B. Callear and W. J. R. Tyerman, Trans. Farad. Soc., *62* (1966) 371

89. T. L. Gilchrist and C. W. Rees, "Carbenes, Nitrenes and Arynes", 2nd ed., Thomas Nelson and Sons, London (1969) 73

90. A. van Roodselaar, I. Safarik, O. P. Strausz and H. E. Gunning, J. Amer. Chem. Soc., *100* (1978) 4068

91. F. Stuhl and H. Niki, J. Chem. Phys., *55* (1971) 3954

92. J. T. Herron and R. E. Huie, J. Phys. Chem. Ref. Data, *2* (1973) 467

93. C. A. Arrington, Jr. and D. J. Cox, J. Phys. Chem., *79* (1975) 2584

94. P. Herbrechtsmeir and H. Gg. Wagner, Ber. Bunsenges. Physik. Chem., *79* (1975) 461

95. P. Herbrechtsmeir and H. Gg. Wagner, Ber. Bunsenges.

Physik. Chem., *79* (1975) 673

96. W. M. Shaub, T. L. Burks and M. C. Lin, Chem. Phys., *45* (1980) 455

97. J. Connor, A. van Roodselaar, R. W. Fair and O. P. Strausz, J. Amer. Chem. Soc., *93* (1971) 560

98. R. J. Cvetanović, Can. J. Chem., *36* (1958) 623

99. K. S. Sidhu, E. M. Lown, O. P. Strausz and H. E. Gunning, J. Amer. Chem. Soc., *88* (1966) 254; O. P. Strausz, Pure Appl. Chem., *4* (1971) 165

100. J. Fenwick, G. Frater, K. Ogi and O. P. Strausz, J. Amer. Chem. Soc., *95* (1973) 124

101. H. E. Avery and S. J. Heath, Trans. Farad. Soc., *68* (1972) 512

102. O. P. Strausz, R. K. Gosavi, A. S. Denes and I. G. Csizmadia, J. Amer. Chem. Soc., *98* (1976) 4784

103. O. P. Strausz, R. K. Gosavi and H. E. Gunning, Chem. Phys. Letters, *54* (1978) 510

104. B. Verkóczy, Ph. D. Thesis, University of Alberta (1981)

105. O. P. Strausz, W. B. O'Callaghan, E. M. Lown and H. E. Gunning, J. Amer. Chem. Soc., *93* (1971) 559

106. P. Carlier, J. E. Dubois, P. Maselet and G. Monview, J. Electron Spectry. Rel. Phenomena, *7* (1975) 55

107. G. E. Owen, J. M. Pearson and M. Szwarc, Trans. Farad. Soc., *61* (1965) 1722

108. R. K. Gosavi and O. P. Strausz, to be published

109. W. von E. Doering and W. A. Henderson, Jr., J. Amer. Chem. Soc., *80* (1958) 5274

110. I. M. T. Davidson, Reaction Kinetics, Specialist Periodical Reports (Chem. Soc., London), *1* (1975) 212

111. P. John and J. H. Purnell, J. Chem. Soc., Farad. Trans. 1, *69* (1973) 1455

112. B. Cox and J. H. Purnell, J. Chem. Soc., Farad. Trans. 1, *71* (1975) 859

113. C. J. Mazac and J. W. Simons, J. Amer. Chem. Soc., *90* (1968) 2484

114. W. L. Hase and J. W. Simons, J. Chem. Phys., *54* (1971) 1277

115. R. E. Berkley, I. Safarik, O. P. Strausz and H. E. Gunning, J. Phys. Chem., *77* (1973) 1741; R. E. Berkley, I. Safarik, H. E. Gunning and O. P. Strausz, J. Phys. Chem., *77* (1973) 1734; O. P. Strausz, E. Jakubowski, H. S. Sandhu and H. E. Gunning, J. Chem. Phys., *51* (1969) 552

116. E. R. Austin and F. W. Lampe, J. Phys. Chem., *81* (1977) 1134

117. R. A. Svehla, NASA Technical Report R132 (1962)

118. H. E. O'Neal and M. A. Ring, Inorg. Chem., *5* (1966) 435

119. R. Roberge, C. Sandorfy, J. I. Matthews and O. P. Strausz, J. Chem. Phys., *69* (1978) 5105

120. R. P. Hollandsworth and M. A. Ring, Inorg. Chem., *7* (1968) 1635

121. J. H. Meal and M. K. Wilson, J. Chem. Phys., *24* (1956) 385

122. R. E. Wilde, J. Mol. Spectroscopy, *8* (1962) 427

123. E. A. V. Ebsworth, M. Oynszchuk and N. Sheppard, J. Chem. Soc., (1958) 1453

124. D. E. Webster, J. Chem. Soc., (1960) 5132

125. I. M. T. Davidson and A. V. Howard, J. Chem. Soc., Farad. Trans. 1, *71* (1975) 69

126. M. D. Sefcik and M. A. Ring, J. Amer. Chem. Soc., *95* (1973) 5168

127. K. A. Perkins, P. G. Perkins and T. N. Bell, unpublished data

128. R. T. Conlin, P. P. Gaspar, R. H. Levin and M. Jones, Jr., J. Amer. Chem. Soc., *94* (1972) 7165

129. M. I. Al-Joboury and D. W. Turner, J. Chem. Soc., (1964) 4434

130. J. L. Franklin and S. R. Carroll, J. Amer. Chem. Soc., *91* (1969) 6564

131. R. T. Morrison and R. N. Boyd, "Organic chemistry", 2nd ed., Allyn and Bacon, Boston (1970); J. A. Hirsch, "Concepts in Therotical Organic Chemistry", Allyn and Bacon, Boston (1975)

132. M. M. Dhingra, G. Govil, C. R. Kanekar and C. L. Khetrapal, Proc. Ind. Acad. Sci., *65A* (1967) 203

133. K. Watanabe, T. Nakayama and J. Mottl, J. Quant. Spectry. Radiat. Transfer (1962) 369

134. W. von E. Doering and L. H. Knox, J. Amer. Chem. Soc., *72* (1950) 2305

135. G. L. Closs and L. E. Closs, Tetra. Letters, *10* (1960) 38

136. K. C. Ferguson and E. Whittle, Trans. Farad. Soc., *67* (1971) 2618; S. H. Jones and E. Whittle, Int. J. Chem. Kinetics, *2* (1970) 479; S. Furuyama, D. M. Benson and S. W. Benson, Int. J. Chem. Kinetics, *2* (1970) 83

137. D. M. Golden and S. W. Benson, Chem. Rev., *69* (1969) 125

138. G. W. Wheland, "Resonance in Organic Chemistry", John Wiley and Sons, New York (1955)

139. C. K. Kanakar, G. Govil, C. L. Khetrapal and M. M. Dhingra, Proc. Ind. Acad. Sci., *64A* (1966) 315

140. Sir D. Barton and W. D. Ollis, "Comprehensive Organic Chemistry", *4* (1979)

141. M. K. Mahanti, Ind. J. Chem., *15B* (1977) 168

142. P. Linda, G. Marino and S. Pignataro, Ric. Sci., *39* (1969) 666

143. P. Linda and G. Marino, J. Chem. Soc., (1968) 392; S. Clementi, F. Genel and G. Marino, Chem. Comm., (1967) 498

144. L. A. P. Kane-Maguire and C. A. Mansfield, J. Chem. Soc., Chem. Comm. (1973) 540

APPENDIX A

Standard and weighted least square plots of $\gamma k''$ *versus* [S] have been carried out for each of the following substrates: 1-butyne, disilane-d_6, hexamethyldisilane, benzene, cyclohexene, 1,4-cyclohexadiene and tetrahydrofuran, using unweighted and weighted entries of $\gamma k''$ respectively.

For the weighted plots, the weight factor = $1/\sigma^2$, where σ is the root mean square error in the slope, $\gamma k''$, of the plot of ln PH *versus* delay time t. For example, $\sigma = 1.2$ msec^{-1} for $\gamma k'' = 10.4 \pm 1.2$ msec^{-1}. The results are as follows.

1-butyne:

```
RESULTS OF ANALYSIS                          STANDARD LINEAR     WEIGHTED LINEAR
*******************                          ***************     ***************

SLOPE                                    =       1.9794              2.2065

Y-INTERCEPT                              =       9.3290              7.8742

ESTIMATE OF RMS ERROR IN SLOPE           =      0.23173             0.28612
ESTIMATE OF RMS ERROR IN INTCP           =      0.78475             0.76560
ROOT MEAN SQUARE DEVIATION               =       1.5714              1.8073
CORRELATION COEFFICIENT                  =      0.90563             0.92233
```

disilane-d_6:

```
RESULTS OF ANALYSIS                          STANDARD LINEAR     WEIGHTED LINEAR
*******************                          ***************     ***************

SLOPE                                    =       2.8073              1.8964

Y-INTERCEPT                              =       5.9520              6.7418

ESTIMATE OF RMS ERROR IN SLOPE           =      0.15800             0.97667E-01
ESTIMATE OF RMS ERROR IN INTCP           =      0.50265             0.25387
ROOT MEAN SQUARE DEVIATION               =       1.1313              2.6741
CORRELATION COEFFICIENT                  =      0.98152             0.90066
```

hexamethyldisilane:

```
RESULTS OF ANALYSIS                      STANDARD LINEAR      WEIGHTED LINEAR
*******************                      ***************      ***************

SLOPE                                =     0.14310E-01          0.15621E-01

Y-INTERCEPT                          =      9.3716               8.8787

ESTIMATE OF RMS ERROR IN SLOPE       =     0.16375E-02          0.34519E-03
ESTIMATE OF RMS ERROR IN INTCP       =     0.24927              0.10658
ROOT MEAN SQUARE DEVIATION           =     0.65502              0.76313
CORRELATION COEFFICIENT              =     0.92441              0.89337
```

benzene:

```
RESULTS OF ANALYSIS                      STANDARD LINEAR      WEIGHTED LINEAR
*******************                      ***************      ***************

SLOPE                                =     0.33620E-01          0.41083E-01

Y-INTERCEPT                          =      9.1012               7.8843

ESTIMATE OF RMS ERROR IN SLOPE       =     0.25969E-02          0.87158E-03
ESTIMATE OF RMS ERROR IN INTCP       =     0.31303              0.12056
ROOT MEAN SQUARE DEVIATION           =      1.2026               1.5402
CORRELATION COEFFICIENT              =     0.93527              0.90431
```

In those cases where values of $\gamma k''$ were not measured in the absence of substrates ($\gamma k'' = \gamma k'$ at $[S] = 0$), the effects of including the mean value $\gamma k'_m = 8.0 \pm 0.4\ \text{msec}^{-1}$, obtained from 455 measurements, in both the standard and the weighted plots of $\gamma k''$ *versus* [S] were examined. The results obtained for cyclohexene, 1,4-cyclohexadiene and tetrahydrofuran are presented as follows.

cyclohexene:

---

without $\gamma k'_m$:

```
RESULTS OF ANALYSIS                        STANDARD LINEAR     WEIGHTED LINEAR
*******************                        ***************     ***************

SLOPE                               =          1.5316              2.0151

Y-INTERCEPT                         =          8.9441              7.8741

ESTIMATE OF RMS ERROR IN SLOPE      =       0.10825             0.14061
ESTIMATE OF RMS ERROR IN INTCP      =       0.76728             0.88202
ROOT MEAN SQUARE DEVIATION          =        1.7615              3.2741
CORRELATION COEFFICIENT             =       0.96903             0.95050
```

$\gamma k''$ (= $\gamma k'_m$) = 8.0 ± 0.4 msec^{-1}:

```
RESULTS OF ANALYSIS                        STANDARD LINEAR     WEIGHTED LINEAR
*******************                        ***************     ***************

SLOPE                               =          1.5473              2.0057

Y-INTERCEPT                         =          8.8027              7.9114

ESTIMATE OF RMS ERROR IN SLOPE      =       0.10020             0.11609
ESTIMATE OF RMS ERROR IN INTCP      =       0.68767             0.70509
ROOT MEAN SQUARE DEVIATION          =        1.7166              3.1282
CORRELATION COEFFICIENT             =       0.97188             0.96000
```

1,4-cyclohexadiene:

---

without $\gamma k'_m$:

```
RESULTS OF ANALYSIS                        STANDARD LINEAR     WEIGHTED LINEAR
*******************                        ***************     ***************

SLOPE                               =          1.8719              1.5891

Y-INTERCEPT                         =          5.8460              6.4380

ESTIMATE OF RMS ERROR IN SLOPE      =       0.81982E-01         0.62192E-01
ESTIMATE OF RMS ERROR IN INTCP      =       0.36411             0.25765
ROOT MEAN SQUARE DEVIATION          =       0.80398              1.2078
CORRELATION COEFFICIENT             =       0.98869             0.96055
```

$\gamma k''$ (= $\gamma k'_m$) = 8.0 ± 0.4 msec^{-1}:

```
RESULTS OF ANALYSIS                        STANDARD LINEAR     WEIGHTED LINEAR
*******************                        ***************     ***************

SLOPE                               =          1.8110              1.4883

Y-INTERCEPT                         =          6.1889              6.7628

ESTIMATE OF RMS ERROR IN SLOPE      =       0.90465E-01         0.66667E-01
ESTIMATE OF RMS ERROR IN INTCP      =       0.38816             0.26683
ROOT MEAN SQUARE DEVIATION          =       0.93748              1.4096
CORRELATION COEFFICIENT             =       0.98416             0.94243
```

---

tetrahydrofuran:

---

without $\gamma k'_m$:

```
RESULTS OF ANALYSIS                          STANDARD LINEAR      WEIGHTED LINEAR
*******************                          ***************      ***************

SLOPE                                    =    0.32990E-01          0.37473E-01

Y-INTERCEPT                              =    14.133               14.279

ESTIMATE OF RMS ERROR IN SLOPE           =    0.70148E-02          0.55744E-02
ESTIMATE OF RMS ERROR IN INTCP           =    0.94422              0.73143
ROOT MEAN SQUARE DEVIATION               =     1.8207               1.9724
CORRELATION COEFFICIENT                  =    0.80516              0.83791
```

$\gamma k''$ (= $\gamma k'_m$) = 8.0 ± 0.4 msec^{-1}:

```
RESULTS OF ANALYSIS                          STANDARD LINEAR      WEIGHTED LINEAR
*******************                          ***************      ***************

SLOPE                                    =    0.40638E-01          0.60053E-01

Y-INTERCEPT                              =    12.914               11.502

ESTIMATE OF RMS ERROR IN SLOPE           =    0.81395E-02          0.61480E-02
ESTIMATE OF RMS ERROR IN INTCP           =     1.0585              0.77934
ROOT MEAN SQUARE DEVIATION               =     2.2871               2.8228
CORRELATION COEFFICIENT                  =    0.81070              0.82971
```

The above results indicate that the method used in this work for the treatment of data is satisfactory, since weighting the $\gamma k''$ entries or including the mean value $\gamma k'_m$ in the plots where the values of $\gamma k''$ were not measured at [S] = 0 does not in general alter the correlation coefficients of the plots.

APPENDIX B

The correlation coefficients for the plots of $\gamma k''$ *versus* [S] for all the substrates studied in this work are presented here, along with the second order rate constants k_1 and the number of measurements. In all, there are 26 plots with correlation coefficients > 0.9, 14 plots with correlation coefficients between 0.8 and 0.9, and 3 plots with correlation coefficients < 0.8.

The correlation coefficients of the plots for ammonia, acetylene-d_2, and dichlorosilane are all < 0.8. For ammonia, $4.5 \times 10^4\ M^{-1}\ s^{-1} < k_1 < 3.5 \times 10^7\ M^{-1}\ s^{-1}$ (160 measurements) and the correlation coefficient was 0.44. For *iso*butane, $k_1 = (3.1 \pm 1.3) \times 10^7\ M^{-1}\ s^{-1}$ (152 measurements) and the correlation coefficient was 0.50. For dichlorosilane, k_1 was not determined although the $\gamma k''$ *versus* [S] plot has been made (140 measurements), with a correlation coefficient of 0.53. Possible explanations for the poor correlations obtained with these compounds have been discussed in Chapter III.

For *iso*butane, the rate constant k_1 was determined to be $(4.5 \pm 0.4) \times 10^4\ M^{-1}\ s^{-1}$ (112 measurements) and the correlation coefficient was 0.94. Data for the other substrates are as follows.

Second Order Rate Constants k, for the Reactions with Alkynes

Substrate	k, $(M^{-1}s^{-1})$	Number of measurements	Correlation coefficient
acetylene	$(3.5 \pm 0.4) \times 10^{7}$	200	0.86
propyne	$(2.2 \pm 0.2) \times 10^{9}$	176	0.90
1-butyne	$(3.7 \pm 0.5) \times 10^{9}$	144	0.87
2-butyne	$(1.8 \pm 0.3) \times 10^{10}$	144	0.84
1-pentyne	$(4.3 \pm 0.7) \times 10^{9}$	96	0.87
2-pentyne	$(2.5 \pm 0.4) \times 10^{10}$	168	0.81
3,3-dimethyl1-butyne	$(2.4 \pm 0.3) \times 10^{9}$	296	0.83
2,2,5,5-tetra-methyl-3-hexyne	$(7.6 \pm 0.7) \times 10^{9}$	272	0.87
phenylacetylene	$(4.3 \pm 0.7) \times 10^{9}$	96	0.88

Second Order Rate Constants k_1 for the Reactions with Silanes

Substrate	$k_1 (M^{-1}s^{-1})$	Number of measurements	Correlation coefficient
silane	$(4.8 \pm 0.5) \times 10^8$	105	0.93
monomethylsilane	$(1.7 \pm 0.2) \times 10^9$	231	0.87
dimethylsilane	$(2.8 \pm 0.1) \times 10^9$	252	0.96
trimethylsilane	$(2.8 \pm 0.2) \times 10^9$	112	0.97
silane-d_4	$(2.5 \pm 0.3) \times 10^8$	133	0.91
monomethylsilane-d_3	$(9.8 \pm 0.4) \times 10^8$	245	0.98
dimethylsilane-d_2	$(1.8 \pm 0.1) \times 10^9$	238	0.94
trimethylsilane-d_1	$(2.8 \pm 0.2) \times 10^9$	161	0.96
diethylsilane	$(2.9 \pm 0.3) \times 10^9$	105	0.95
triethylsilane	$(4.5 \pm 0.1) \times 10^9$	210	0.98
dimethylchlorosilane	$(3.9 \pm 0.2) \times 10^8$	112	0.98
methyldichlorosilane	$(2.9 \pm 0.3) \times 10^7$	196	0.86

Second Order Rate Constants k, for the Reactions with Disilanes

Substrate	k,($M^{-1}s^{-1}$)	Number of measurements	Correlation coefficient
disilane	(6.5 ± 0.3) × 10^9	112	0.98
disilane-d_6	(5.6 ± 0.3) × 10^9	98	0.98
hexamethyldisilane	(2.5 ± 0.3) × 10^7	105	0.92

Second Order Rate Constants k, for the Reactions with Cyclic Compounds

Substrate	k, ($M^{-1}s^{-1}$)	Number of measurements	Correlation coefficient
cyclohexene	$(3.1 \pm 0.2) \times 10^{9}$	105	0.97
1,3-cyclohexadiene	$(1.4 \pm 0.2) \times 10^{9}$	126	0.85
1,4-cyclohexadiene	$(3.7 \pm 0.2) \times 10^{9}$	98	0.99
benzene	$(6.7 \pm 0.5) \times 10^{7}$	182	0.93
toluene	$(3.3 \pm 0.2) \times 10^{8}$	105	0.97
chlorobenzene	$(1.7 \pm 0.2) \times 10^{8}$	105	0.88
fluorobenzene	$(6.1 \pm 0.9) \times 10^{7}$	77	0.90

Second Order Rate Constants k, for the Reactions with Heterocyclic Compounds

Substrate	k, ($M^{-1}s^{-1}$)	Number of measurements	Correlation coefficient
thiacyclohexane	(8.3 ± 0.8) × 10^{9}	126	0.93
tetrahydrothiophene	(7.6 ± 1.1) × 10^{9}	105	0.89
tetrahydrofuran	(6.6 ± 1.4) × 10^{7}	98	0.80
thiophene	(5.7 ± 0.2) × 10^{9}	84	0.99
pyrrole	(3.1 ± 0.3) × 10^{9}	140	0.90
furan	(6.3 ± 0.4) × 10^{8}	105	0.97
1-methylpyrrole	(4.9 ± 0.5) × 10^{9}	126	0.91
pyridine	(2.8 ± 0.3) × 10^{9}	112	0.94